THE UNIVERSITY *of* EDINBURGH

Transcriptomic and proteomic analysis of arbovirus-infected tick cells

Sabine Weisheit

Thesis submitted for the degree of Doctor of Philosophy

The Roslin Institute and Royal (Dick) School of Veterinary Studies, University of Edinburgh

2014

Declaration

I declare that all the work included in this thesis is my own except where otherwise stated. No part of this work has been, or will be submitted for any other degree or professional qualification.

Sabine Weisheit

2014

The Roslin Institute and Royal (Dick) School of Veterinary Studies
University of Edinburgh
Easter Bush
Midlothian EH25 9RG
Scotland, UK

The Pirbright Institute
Ash Road
Pirbright, Woking
Surrey GU24 0NF
England, UK

Acknowledgements

I would like to thank my supervisors **John Fazakerley** and **Lesley Bell-Sakyi** for their guidance during my PhD. Especially **Lesley** was always there for answering questions about ticks and tick cell lines, providing fresh tick cells whenever needed and she also tirelessly read and corrected my thesis - thank you. During my PhD project I had the special opportunity to do TBEV work in the laboratory of **Libor Grubhoffer** at the University of South Bohemia in Budweis, Czech Republic and to do proteomics work in the laboratory of **José de la Fuente** at the University of Castilla-La Mancha in Ciudad Real, Spain. I want to thank them for giving me the opportunity to do essential experiments for my PhD, as well as for their constant support whenever needed. Special thanks also go to members of **Libor's** lab, including **Hana Tykalová** and **Daniel Růžek** who grew wildtype TBEV and to **Marie Vancová** who processed and helped with interpretation of my EM samples. Special thanks go to members of **José's** lab, including **Margarita M Villar Rayo** and **Marina Popara** for training me in processing samples for MS analysis, as well as to **Margarita** for conducting the MS experiments and analysing the 2D-DIGE images. Thanks go to **Ulrike Munderloh** for the provision of the IDE8 cell line, **Franz X. Heinz** for TBEV NS1 antibody and plasmids encoding TBEV and TBEV replicons, **Andres Merits** for SFV reporter viruses, **Sonja Best** for LGTV NS5 antibodies, **Mayuri Sharma** and **Richard Kuhn** for the LGTV replicon, **Steve Mitchell** for preparing SFV EM samples, **Houssam Attoui** for training me to work in the CL3 facility, **Jan Kim** and **Mick Watson** for advice concerning bioinformatics, **Claudia Rückert** for sharing her LGTV data, **Gerald Barry** and **Claire Donald** for propagating SFV reporter viruses, **Rennos Fragkoudis** for the SFV4(3F)-ZsGreen plasmid and **Esther Schnettler** for all her invaluable input. Thanks also go to the POSTICK project in the **Marie Curie FP7- PEOPLE-ITN programme** for funding. Thank you to the other current and previous members of our lab: **Mhairi Ferguson**, **Karen Sherwood**, **Stacey Human**, **Julio Rodriguez**, **Joana Ferrolho** and **Adrian Zagrajek**. On a more personal note I want to thank my family **Michael, Gunda**, **Stefanie**, **Markus**, **Tim** and **Ben** without whose support and love I would not have achieved as much as I have. Lastly I also want to thank the amazing student community at the Pirbright Institute and my friends, who have helped me through the last year of my PhD - I do not know what I would have done without your constant encouragement.

Abstract of Thesis

Ticks are important vectors of a wide variety of pathogens including protozoa, bacteria and viruses. Many of the viruses transmitted by ticks are of medical or veterinary importance including tick-borne encephalitis virus (TBEV) and Crimean-Congo hemorrhagic fever virus causing disease in humans, and African swine fever virus and Nairobi sheep disease virus affecting livestock. Although several studies have elucidated tick antimicrobial mechanisms including cellular immune responses such as nodulation, encapsulation and phagocytosis and humoral immune responses such as the JAK/STAT pathway, complement-like proteins, antimicrobial peptides, lectin like pattern-recognition molecules and lysozymes, very little is known about the innate immune response of ticks towards viral infection. This study therefore aimed to identify molecules that might be involved in the response of ticks to viral infection. The hypothesis was that TBEV infection leads to changes in the expression of immunity-related transcripts and proteins in *Ixodes* spp. tick cells and that at least some of these might be antiviral. *Ixodes scapularis*-derived cell lines IDE8 and ISE6 were chosen since *I. scapularis* is currently the only tick species with a sequenced genome and an *Ixodes ricinus*-derived cell line, IRE/CTVM19, was used because *I. ricinus* is the natural vector of TBEV. Basic parameters required to study the responses of tick cells to infection were determined, including levels of virus infection, kinetics of virus replication and production, formation of replication complexes and uptake of dsRNA or siRNA. The cell lines IDE8, ISE6 and IRE/CTVM19 were infected with either of two tick-borne flaviviruses, TBEV and Langat virus (LGTV), or with the mosquito-borne alphavirus Semliki Forest virus (SFV). Infection was characterised using techniques including plaque assay, luciferase assay, immunostaining and conventional, confocal and electron microscopy. Two time points for transcriptomics and proteomics analysis of TBEV-infected IDE8 and IRE/CTVM19 cells were selected: day 2 post-infection (p.i.) when virus production was increasing and day 6 p.i. when virus production was decreasing. RNA and protein were isolated from TBEV-infected and mock-infected tick cells at

days 2 and 6 p.i. and RNA-Seq and mass spectrometric technologies were used to identify changes in, respectively, transcript and protein abundance. Differential expression of transcripts was determined using the data analysis package DESeq resulting in a total of 43 statistically significantly differentially expressed transcripts in IDE8 cells and 83 in IRE/CTVM19 cells, while differential protein representation using X^2 test statistics with Bonferroni correction in IDEG6 software resulted in 76 differentially represented proteins in IDE8 cells and 129 in IRE/CTVM19 cells. These included transcripts and proteins which could affect stages of the virus infection, including virus entry, replication, maturation and protein trafficking, and also innate immune responses such as phagocytosis, RNA interference (RNAi), the complement system, the ubiquitin-proteasome pathway, cell stress and the endoplasmic reticulum (ER) stress response. After verification of sequencing data by qRT-PCR, the ability of several of the identified transcripts or proteins to affect virus infection was determined by knockdown experiments in IDE8 and IRE/CTVM19 cells using wild type LGTV, LGTV replicons or TBEV replicons. Knockdown of genes encoding proteins including the ER chaperone gp96 and the heat-shock protein HSP90 resulted in increased virus production in both cell lines, hinting at an antiviral role. In contrast, knockdown of calreticulin, another ER chaperone, resulted in a decrease in virus production in IRE/CTVM19 cells but not in IDE8 cells, implying a requirement for virus production. This functional genomics approach has identified possible novel genes/proteins involved in the interaction between flaviviruses and tick cells and also revealed that there might be antiviral innate immune pathways present in ticks additional to the exogenous RNAi pathway.

List of Figures

List of Tables

Abbreviations

6K	6 kilodalton protein
AcN	Acetonitrile
Ago	Argonaute
AHFV	Alkhumra haemorrhagic fever virus
Alix/AIP2	Programmed cell death 6 interacting protein
AMP	Antimicrobial peptide
AP-2	Adaptor protein-2
APS	Ammonium persulphate
Arf	ADP ribosylation factor
ASFV	African swine fever virus
BCA	Bicinchoninic acid
BFV	Barmah Forest virus
BHK	Baby hamster kidney cells
BSA	Bovine serum albumin
BTV	Bluetongue virus
C	Capsid
CCD	Charge coupled device
CCHFV	Crimean-Congo haemorrhagic fever virus
Cdc42	Cell division cycle 42
cDNA	Complementary DNA
CHIKV	Chikungunya virus
CL	Containment level
CMC	Carboxymethyl cellulose
CNS	Central nervous system
Coomassie	Coomassie Brilliant Blue R-250
CPV	Cytopathic vacuole(s)
CrPV	Cricket paralysis virus
Ct	Threshold cycle
DAPI	4’,6-diamidino-2-phenylindole
Dcr	Dicer
DCV	*Drosophila* C virus
DENV	Dengue virus
Dif	Dorsal-related immune factor
DIGE	Difference in gel electrophoresis
DMEM	Dulbecco’s Modified Eagle’s Medium
DMSO	Dimethylsulphoxide
DNA	Deoxyribonucleic acid
dNTP	Deoxy-nucleoside triphosphate
Dome	Domeless
DRG	Developmentally-regulated GTP-binding protein
Dscam	Down syndrome cell adhesion molecule
dsRNA	Double-stranded RNA

DTT	Dithiothreitol
E	Envelope
EEEV	Eastern equine encephalitis virus
EF	Elongation Factor
eGFP	Enhanced green fluorescent protein
eIF	Eukaryotic translation initiation factor
EMCV	Encephalomyocarditis virus
ER	Endoplasmic reticulum
EST	Expressed sequence tag(s)
FACS	Fluorescence-activated cell sorting
FCS	Foetal calf serum
FDR	False discovery rate
FHV	Flock house virus
Fluc	Firefly luciferase
FMDV	Foot-and-mouth disease virus
Fth	Ferritin heavy chain
GFAP	Glial fibrillary acidic protein
GMEM	Glasgow's Minimal Essential Medium
Gp96	Tumor rejection antigen
Grp170	Hypoxia up-regulated protein
Hes	Hairy enhancer of split
HSP	Heat-shock protein(s)
IFN	Interferon
Ig	Immunoglobulin
Illumina	Illumina Solexa sequencing
IMD	Immune deficiency
INSIG	Insulin induced protein
IPG	Immobilised pH gradient
IRES	Internal ribosomal entry site
IκB	Inhibitor κB
JAK	Janus kinase
JEV	Japanese encephalitis virus
kb	Kilobase(s)
kDA	Kilodalton
KFDV	Kyasanur Forest disease virus
L-15	L-15 (Leibovitz) medium
LACV	La Crosse virus
LB medium	Luria-Bertani medium
LC-MS/MS	Liquid chromatography-tandem mass spectrometry
LGTV	Langat virus
LIV	Louping ill virus
LPS	Lipopolysaccharide
MDA-5	Melanoma differentiation-associated protein 5
MEB	Midgut escape barrier
MIB	Midgut infection barrier
miRISC	MiRNA-induced silencing complex

miRNA	Micro-RNA
MOI	Multiplicity of infection
mRNA	Messenger RNA
MS	Mass spectrometry
MUC	Mucin
MYD88	Myeloid differentiation primary response gene
NBCS	Newborn calf serum
NCR	Non-coding region
NFAT	Nuclear factor of activated t-cells
NFκB	Nuclear factor κB
NS	Non-structural
nsP	Non-structural protein
NT	Nucleotide
NTPase	Nucleoside triphosphatase
OHFV	Omsk haemorrhagic fever virus
ONNV	O'nyong-nyong virus
ORF	Open reading frame
p.i.	Post-infection
p.t.	Post-transfection
PACS	Phosphofurin acidic cluster sorting protein
PAF-AH	Platelet-activating factor acetylhydrolase
PAMP	Pathogen-associated molecular pattern
PAP	Prophenoloxidase activating
PARP	Poly(ADP-ribose) polymerase
PBS	Phosphate buffered saline
PBSA	Phosphate buffered saline and 0.75% albumin
PCR	Polymerase chain reaction
PEG	Polyethylene glycol
pen/strep	100 U/ml penicillin and 100 µg/ml streptomycin
PFU	Plaque-forming units
PI3K	Phosphoinositide3-kinase
piRISC	PiRNA-induced silencing complex
piRNA	PIWI-interacting RNA
PIWI	P-element induced wimpy testis
PO	Phenoloxidase
Poly(A) tail	Polyadenylated tail
POWV	Powassan virus
pre-miRNA	Precursor micro-RNA
PRGP	Peptidoglycan-recognition protein
pri-miRNA	Primary micro-RNA
prM/M	Precursor membrane/membrane glycoprotein
proPO	Prophenoloxidase
PRR	Pattern-recognition receptor
PS cells	Porcine kidney stable cells
qPCR	Quantitative PCR
qRT-PCR	Quantitative Real-Time polymerase chain reaction

Rab	Ras-related protein
RdRP	RNA-dependent RNA polymerase
REL	Relish
RIG-I	Retinoic acid-inducible gene 1
RIN	RNA integrity number
RISC	RNA-induced silencing complex
Rluc	*Renilla* luciferase
RNA	Ribonucleic acid
RNAi	RNA interference
rRNA	Ribosomal RNA
RRV	Ross River virus
RTPase	RNA triphosphatase
RT-PCR	Reverse transcription PCR
RVFV	Rift Valley fever virus
SCRV	St Croix River virus
SDS	Sodium dodecyl sulphate
SDS-PAGE	Sodium dodecyl sulphate – polyacrylamide gel electrophoresis
SEB	Salivary gland escape barrier
sfRNA	Subgenomic flaviviral RNA
SFV	Semliki Forest virus
SHA	Subviral particles
SIB	Salivary gland infection barrier
SIGMAV	Sigma virus
SINV	Sindbis virus
siRNA	Small interfering RNA
SOC	Super Optimal broth with Catabolite repression
Spp	Species
ssRNA	Single-stranded RNA
STAT	Signal transducers and activators of transcription
TAB1	TAK-1 binding protein
TAK1	Transforming growth factor β activated kinase-1
TAV	Thosea asigna virus
TBE buffer	Tris-borate buffer
TBE	Tick-borne encephalitis
TBEV	Tick-borne encephalitis virus
TE buffer	Tris-EDTA buffer
TEM	Transmission electron microscope
TEMED	Tetramethylethylenediamine
TEP	Thioester-containing proteins
TFA	Trifluoroacetic acid
TGN	Trans-Golgi network
TLR	Toll-like receptor
TOR	Target of rapamycin
TPB	Tryptose phosphate broth
Tudor-SN	4SNc Tudor-SN

UPR	Unfolded protein response
UTR	Untranslated region
UV	Ultra-violet
v-ATPase	Vacuolar ATPase
VEEV	Venezuelan equine encephalitis virus
viRNA	Virus-derived small interfering RNA
VP	Vesicle packets
VSV	Vesicular stomatitis virus
WEEV	Western equine encephalitis virus
WNV	West Nile virus
WSSV	White spot syndrome virus
YFV	Yellow fever virus

1 Chapter 1 Introduction

Ticks are considered to be second only to mosquitoes as vectors of diseases of medical and veterinary importance. They transmit an enormous variety of pathogens including the medically important arboviruses Crimean-Congo haemorrhagic fever virus (CCHFV) and tick-borne encephalitis virus (TBEV); however very little is known about the antiviral defence response in ticks compared to that of mosquitoes. The present study was carried out to identify novel defence mechanisms in tick cells in response to TBEV infection. In this chapter current knowledge of arboviruses, including a more detailed report about the virus families *Flaviviridae* and *Togaviridae*, of ticks and tick-borne diseases and of the innate immune responses of arthropods and ticks will be reviewed.

1.1 Arthropod-borne viruses

Arthropod-borne viruses, or arboviruses, are viruses transmitted biologically between vertebrate hosts by haematophagous, blood feeding arthropod vectors such as midges, mosquitoes, biting flies and ticks (Ciota & Kramer, 2010; Coffey et al., 2013; Go, Balasuriya & Lee, 2014; Hollidge, González-Scarano & Soldan, 2010; Weaver & Reisen, 2010). As the term biological transmission implies, arboviruses have to be able to replicate in both the arthropod vector and the vertebrate host species to sufficiently high titres to ensure transmission and are not simply transmitted mechanically by contaminated mouthparts (Weaver, 1997). The most common form of virus transmission is horizontal, in which the virus is taken up by the vector through a blood meal from a viraemic animal. In the vector the virus then has to overcome the midgut barrier, disseminate to and replicate in the salivary glands before being injected with saliva into the next host during blood feeding (Weaver & Barrett, 2004; Weaver & Reisen, 2010). Other modes of transmission, which are less common but important for the maintenance of some arboviruses in nature, include venereal horizontal transmission from a vertically infected male to a female vector and vertical transmission from female to offspring (transovarial) or between different developmental stages (transstadial) (Go, Balasuriya & Lee, 2014; Weaver & Reisen, 2010). In order to replicate efficiently to high enough titres for maintaining these complex transmission cycles, arboviruses have to overcome two different immune systems, the vertebrate immune system, with its innate and

adaptive immune responses, and the innate defence responses of the arthropod vector. The antiviral innate defence response of arthropod vectors plays an important role in controlling virus infection which will be discussed later (Section 1.3.1).

Arboviruses are almost exclusively RNA viruses found in a number of different virus families, including *Togaviridae* (genus *Alphavirus*), *Flaviviridae* (genus *Flavivirus*), *Bunyaviridae* (genera *Nairovirus*, *Phlebovirus*, *Orthobunyavirus*, and *Tospovirus*), *Orthomyxoviridae* (genus *Thogotovirus*), *Rhabdoviridae* (genus *Vesiculovirus*) and *Reoviridae* (genera *Orbivirus* and *Coltivirus*) (Go, Balasuriya & Lee, 2014; Weaver & Reisen, 2010). There is however one exception, a single DNA arbovirus African swine fever virus (ASFV) in the family *Asfarviridae* (genus *Asfivirus*) (Dixon et al., 2012). The lack of DNA arboviruses is thought to correlate with the fact that RNA viruses show higher mutation rates and genetic plasticity compared to DNA viruses, making DNA viruses less flexible for replicating alternatively in vertebrate and invertebrate hosts (Holland & Domingo, 1998). Several arboviruses, with a majority transmitted by mosquitoes or ticks, are of medical and veterinary importance causing severe disease and death. A list of the most important arboviruses including their primary vectors are listed in Table 1.1.

Table 1.1 Arboviruses of medical and veterinary importance, their primary vectors and disease caused

Genus	Virus spp	Primary Vector	Disease
Flavivirus	Dengue virus	*Aedes aegypti*	Human: haemorrhagic fever
	West Nile virus	Various mosquito species	Human and horses: encephalitis
	Yellow fever virus	*Aedes* and *Haemagogus* spp	Human: pantropic
	Japanese encephalitis virus	*Culex tritaeniorhynchus*	Human and horses: encephalitis
	St. Louis encephalitis virus	*Culex* spp	Human: encephalitis
	Murray Valley fever virus	*Culex annulirostris*	Human: encephalitis
	Tick-borne encephalitis virus	*Ixodes* spp	Human: encephalitis
	Kyasanur Forest disease virus	*Haemaphysalis spinigera*	Human: haemorrhagic fever
	Alkhumra haemorrhagic fever virus	*Mosquitoes? Ticks?*	Human: haemorrhagic fever
	Omsk haemorrhagic fever virus	*Dermacentor spp*	Human: haemorrhagic fever
	Louping ill virus	*Ixodes ricinus*	Sheep: encephalitis
	Powassan virus	*Ixodes* spp	Human: encephalitis
Alphavirus	Chikungunya virus	*Aedes spp*	Human: arthralgia and encephalitis
	Venezuelan equine encephalitis virus	*Aedes spp*	Human and horses: encephalitis
	Eastern equine encephalitis virus	*Culex* spp	Human and horses: encephalitis

	O'nyong nyong virus	*Anopheles spp*	Arthralgia
Vesiculovirus	Vesicular stomatitis virus	*Phlebotominae*	Horses, cattle and pigs: Vesiculation, ulceration Humans: flu-like illness
	Chandipura virus	*Phlebotomus spp*	Humans: encephalitis
	Bovine ephemeral fever virus	*Culicoides spp*	Cattle: fever, lameness
Orthobunyavirus	La Crosse virus	*Aedes triseriatus*	Human: encephalitis
	Oropouche virus	*Culicoides spp*	Human: fever
	Schmallenberg virus	*Culicoides spp*	Ruminants: abortion, birth defects
Phlebovirus	Rift Valley fever virus	*Aedes and Culex spp*	Human: encephalitis, haemorrhagic fever Domestic ruminants: abortion, haemorrhage, necrotic hepatitis
	Heartland virus	*Amblyomma spp ?*	Human: fever, fatigue, anorexia, diarrhoea
	Severe fever with thrombocytopenia syndrome virus	*Haemaphysalis spp ?*	Human: acute fever, thrombocytopaenia
Nairovirus	Crimean-Congo haemorrhagic fever virus	*Hyalomma* spp	Human: haemorrhagic fever
	Nairobi sheep disease virus	*Rhipicephalus appendiculatus*	Sheep, goats: fever, haemorrhagic gastroenteritis, abortion
Thogotovirus	Thogoto virus	*Rhipicephalus spp, Amblyomma variegatum, Hyalomma spp*	Sheep: fever, abortion Cattle: leucopenia Human: encephalitis
Orbivirus	Bluetongue virus	*Culicoides* spp	Ruminants: fever, swelling of the tongue
	African horse sickness virus	*Culicoides* spp	Horses: pyrexia, lesions, haemorrhages
	Tribeč virus	*Ixodes ricinus*	Human: encephalitis
Coltivirus	Colorado tick fever virus	*Dermacentor andersoni*	Human: fever, rarely encephalitis and haemorrhagic fever
Asfivirus	African swine fever virus	*Ornithodorus* spp	Domestic pigs: pantropic

In nature arboviruses are usually maintained in an enzootic cycle between the invertebrate vector and vertebrate reservoir hosts which are typically rodents, birds or non-human primates (Hollidge, González-Scarano & Soldan, 2010; Weaver & Barrett, 2004). Spillover transmission to humans or domestic animals can occur, resulting in disease in the so-called dead-end hosts. For some viruses such as chikungunya (CHIKV), dengue (DENV) and yellow fever (YFV), an urban epidemic cycle in which humans have become reservoir hosts has been described (Barrett & Higgs, 2007; Singh & Unni, 2011; Weaver & Barrett, 2004), whereas domestic animals in a rural epizootic cycle serve as reservoir hosts for Japanese encephalitis

virus (JEV) and Venezuelan equine encephalitis virus (VEEV) (van den Hurk, Ritchie & Mackenzie, 2009; Weaver & Barrett, 2004; Weaver et al., 1999). In addition to adaptation of viruses to new hosts, the geographic distribution and frequency of epidemic outbreaks has increased worldwide (Gubler, 1996; Weaver & Reisen, 2010). Possible explanations for the expansion of arboviruses are thought to be environmental changes and globalisation which allow vectors such as mosquitoes, ticks, sandflies and midges to invade new territories, bringing with them the threat of arboviruses (Charrel, de Lamballerie & Raoult, 2007).

1.1.1 Flaviviruses

Flaviviruses belong to the family *Flaviviridae*, which comprises the genera *Flavivirus*, *Pestivirus*, *Hepacivirus* and *Pegivirus* (Stapleton et al., 2011), but only virus species of the genus *Flavivirus* are known to be transmitted by arthropods. The genus *Flavivirus* consists of more than 70 viruses which can be grouped into no known vector, insect-specific, mosquito-borne and tick-borne flaviviruses (Cook et al., 2012; Kuno et al., 1998). The latter two are the most important groups with virus species causing disease in animals and humans ranging from encephalitis (e.g. West Nile virus (WNV), JEV, TBEV and louping ill virus (LIV), see Table 1.1) to haemorrhagic fever (e.g. Alkhumra haemorrhagic fever virus (AHFV), DENV, Kyasanur Forest disease virus (KFDV) and Omsk haemorrhagic fever virus (OHFV) see Table 1.1) (Gould & Solomon, 2008; Gritsun, Nuttall & Gould, 2003; Pastorino et al., 2010). Both mosquito- and tick-borne viruses can be further categorised into antigenic complexes and subcomplexes or into clusters according to their phylogenetics (Calisher & Gould, 2003). Flaviviruses of medical and veterinary importance and their vector species are shown in Table 1.1.

Mosquito-borne flaviviruses are transmitted by a variety of mosquito species and can infect numerous vertebrates. However, some of them such as YFV show a limited host and vector range whereas others like WNV replicate in a wide range of vector and host species (Gould & Solomon, 2008; Gubler, 2007; Weissenböck et al., 2010). For many of the mosquito-borne flaviviruses, birds are important in the enzootic cycle as reservoir hosts and, in some cases (e.g. JEV), domesticated animals take that role in an epizootic cycle (Go, Balasuriya & Lee, 2014; Schweitzer, Chapman &

Iwen, 2009; Weaver & Barrett, 2004). In contrast, humans are considered dead-end hosts which do not play a role during the virus transmission cycle, with the exception of DENV and YFV for which humans are possible reservoir hosts developing high viraemia sufficient for virus transmission in an urban transmission cycle (Weaver & Barrett, 2004).

The tick-borne flaviviruses form the tick-borne encephalitis serocomplex within the family *Flaviviridae* and, in contrast to mosquito-borne flaviviruses, none of the tick-transmitted viruses have humans as reservoir hosts (Dobler, 2010; Robertson et al., 2009). The main reservoir hosts are considered to be rodents, insectivores or seabirds. Depending on their host-preference, tick-borne flaviviruses can be grouped into the mammalian- and seabird-subgroups, which include viruses such as Langat virus (LGTV), LIV, OHFV, Powassan virus (POWV), KFDV and TBEV in the first group and Meaban, Tyulyeni and Kadam viruses in the second group (Go, Balasuriya & Lee, 2014; Gritsun, Nuttall & Gould, 2003). Most of the tick-borne flavivirus infections of humans are associated with encephalitis but, as mentioned above, AHFV, KFDV and OHF viruses can also result in haemorrhagic fever (Holbrook, 2012; Madani, 2005; Růžek et al., 2010). Two members of the tick-borne flavivirus group, LGTV and TBEV, will be briefly introduced in 1.1.1.3 and 1.1.1.2 respectively.

1.1.1.1 Flavivirus genome organisation and life cycle

Flaviviruses are small enveloped viruses with a single-stranded non-segmented RNA genome of positive sense of approximately 11 kb. They contain a 5' type I cap ($m^7GpppAmpN_2$) (Cleaves & Dubin, 1979; Wengler, Wengler & Gross, 1978) but lack, in contrast to cellular messenger RNA (mRNA), a 3' polyadenylated tail (poly(A) tail) (Wengler, Wengler & Gross, 1978) (Figure 1.1). Some TBEV isolates, however, have been shown to contain a poly(A) sequence in the variable region of the 3' non-coding region (NCR) (Wallner et al., 1995). The single long open reading frame (ORF) encoded within the flavivirus genome is flanked by 5' and 3' NCRs of 100 nt and 400-800 nt respectively, which play important roles during virus replication, translation and genome packaging and also appear to influence neuroinvasiveness (Mandl, 2005; Markoff, 2003). The 5' NCR sequence is not well

conserved between different flaviviruses but similar secondary structures form within this region (Brinton & Dispoto, 1988; Thurner et al., 2004) which influence the translation of the genome as well as initiation of replication and host range. Similarly, the 3' NCR differs greatly between mosquito- and tick-borne flaviviruses but similar patterns of conserved sequences and structures have been identified which play a role during replication, translation and possibly selection of RNA templates for either replication or translation (Lindenbach, Thiel & Rice, 2007; Markoff, 2003).

The genomic RNA is infectious (Peleg, 1969) and once it enters a cell it can be translated into a single long polyprotein of approximately 3,400 amino acids which is cleaved by viral and host cell proteases co- and post-translationally into three structural and seven non-structural (NS) proteins (Murray, Jones & Rice, 2008; Rice et al., 1985), as indicated in Figure 1.1, which are required for replication and assembly. The main functions of each viral protein are depicted and briefly described in Figure 1.1. The most well-characterised proteins are the multifunctional NS proteins NS3 and NS5. NS3 serves together with its cofactor NS2B as a serine protease necessary for the processing of the polyprotein. Additionally its helicase/NTPase activity (Gorbalenya et al., 1989; Wengler & Wengler, 1991) is required for unwinding of the double-stranded RNA (dsRNA) intermediate (Warrener, Tamura & Collett, 1993), whereas its RNA triphosphatase (RTPase) activity is needed for capping of the newly produced RNA genome (Wengler & Wengler, 1993). The NS5 protein exhibits S-adenosyl methyltransferase (Egloff et al., 2002; Koonin, 1993) and RNA-dependent RNA polymerase (RdRP) activity (Ackermann & Padmanabhan, 2001; Guyatt, Westaway & Khromykh, 2001; Tan et al., 1996), which are involved in 5' cap modification and RNA replication, respectively. Furthermore it was shown that TBEV and LGTV NS5 antagonise interferon (IFN) signalling (Best et al., 2005; Werme, Wigerius & Johansson, 2008).

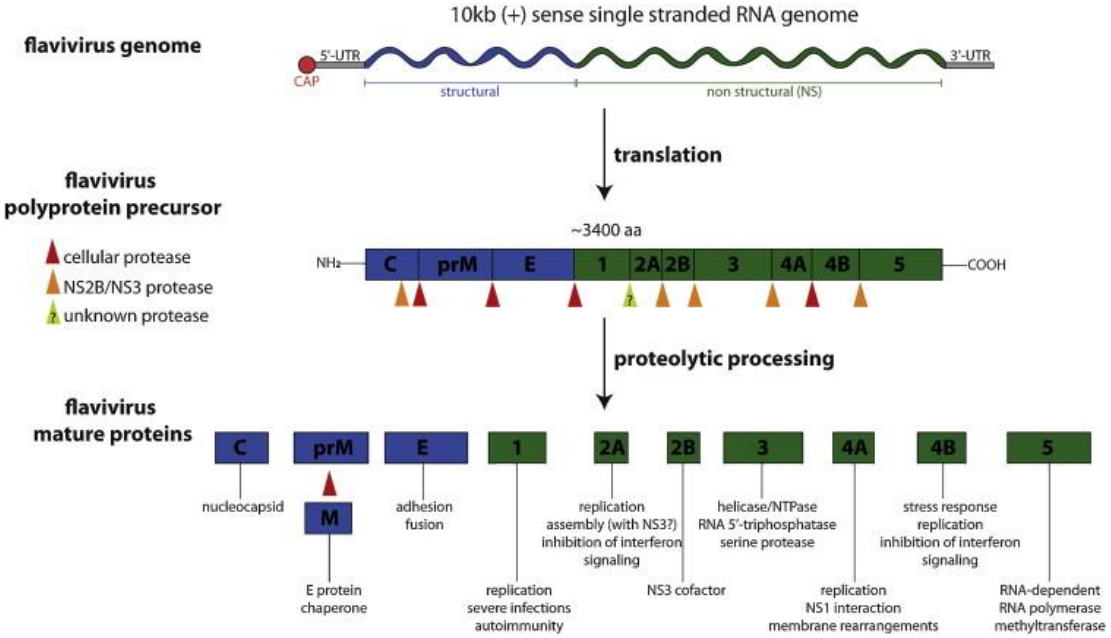

Figure 1.1 Organisation of the flavivirus genome and polyprotein

The flavivirus positive sense single-stranded (ssRNA) genome is approximately 11 kb long with a 5' cap and no 3' poly(A) tail. Its single ORF, flanked by 5' and 3' untranslated region (UTRs; also referred to as NCRs), encodes an approximately 3400 amino acid long single polyprotein which is co- and post-translationally cleaved into 3 structural proteins (blue) and 7 non-structural proteins (green). Cleavage sites for cellular proteases, between C/prM prM/E, E/NS1 and NS4A/NS4B, are indicated with ▲, whereas cleavage by the viral protease NS3 with its cofactor NS2B, between NS2A/NS2B, NS2B/NS3, NS3/NS4A, NS4B/NS5 and carboxy terminus of capsid (C), is indicated by ▲. The protease responsible for cleavage between NS1 and NS2A is currently unknown. Putative functions of each viral protein are as follows. Structural proteins: Capsid (C) interacts with viral RNA to form nucleocapsid; precursor membrane/membrane glycoprotein (prM/M) prevents premature cleavage of the envelope (E) glycoprotein during transit through the secretory pathway; E mediates receptor binding and membrane fusion during virus entry. Non-structural (NS) proteins: NS1 is required for flavivirus replication possibly during negative strand RNA synthesis early in infection and provokes an immune response when it is secreted from the cells; NS2A is a transmembrane protein involved in virus assembly possibly coordinating the shift between virus replication and RNA packaging; NS2B is membrane-associated and serves as cofactor for NS3; NS3 is a multifunctional protein with serine protease, NTPase/helicase and RTPase activity required for replication and polyprotein processing; NS4A interaction with NS1 is required for membrane rearrangements and it co-localises with RNA replication complexes; NS4B co-localises with NS3 and viral dsRNA in replication complexes; NS5 is a multifunctional protein with methyltransferase and RdRP activity. The image was taken from Pastorino et al., 2010.

The life cycle of flaviviruses including infection, replication and release of infectious virions is depicted in Figure 1.2. Vertebrate host cells targeted by flaviviruses include monocytes, macrophages and dendritic cells (Plekhova et al., 2011). The virus attaches to the surface of its target cell mediated by the E protein, and is internalised by receptor-mediated endocytosis in clathrin-coated pits (e.g. (Acosta,

Castilla & Damonte, 2011; Chu & Ng, 2004; Gollins & Porterfield, 1985; Krishnan et al., 2007)). The acidic pH in endosomes causes reorganisation of the E protein triggering fusion of the viral and host cell membranes and leading to the release of the nucleocapsid and viral RNA into the cytoplasm (Rey et al., 1995; Stiasny & Heinz, 2006). In the cytoplasm the viral RNA serves three functions: as mRNA for translation into a single long polyprotein, as template for RNA replication and as genetic material which is packaged into new virus particles. The polyprotein is cleaved, as mentioned above, by viral and host cell proteases into structural and NS proteins required for replication and assembly. RNA replication takes place in replication complexes that are associated with perinuclear membranes, where replicase proteins associate with viral RNA, and possibly host factors (Mackenzie, 2005; Miller & Krijnse-Locker, 2008; Welsch et al., 2009), leading to the synthesis of negative-sense complementary RNA, which in turn serves as template for positive-strand RNA synthesis. In mammalian cells, RNA synthesis starts as early as 3 h post-infection (p.i.) (Lindenbach & Rice, 1997) and is asymmetric with approximately ten times more positive strand RNA than negative strand RNA (Chu & Westaway, 1985; Cleaves, Ryan & Schlesinger, 1981; Muylaert et al., 1996). New immature virions are assembled by interaction of the C protein with viral RNA in the cytoplasm and subsequent budding through the endoplasmic reticulum (ER) to acquire an envelope containing E and prM in heterodimeric association (Mandl, 2005). These virus particles are transported through the late *trans*-Golgi network (TGN) in acidic vesicles where cleavage of prM into M by furin initiates the reorganisation of E into fusion-competent homodimers (Heinz et al., 1994; Stadler et al., 1997; Yu et al., 2008). The mature infectious virions are then released by fusion of the transport vesicle membrane with the host cell membrane.

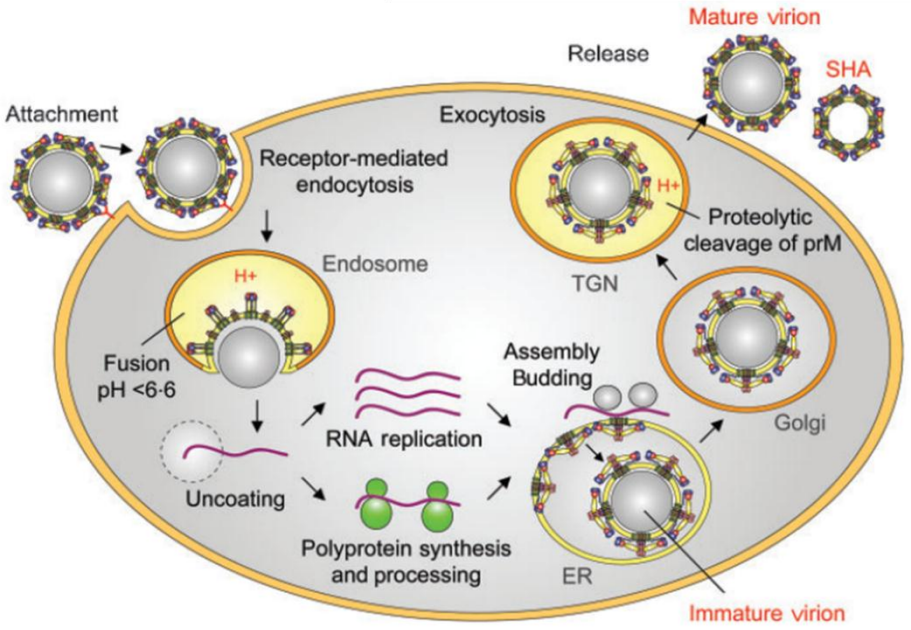

Figure 1.2 Diagram of the flavivirus life cycle in vertebrate cells

Flaviviruses enter the cell by receptor-mediated endocytosis in clathrin-coated pits. The acidic environment in endosomes triggers reorganisation of the envelope (E) protein which leads to membrane fusion and release of the nucleocapsid and viral RNA into the cytoplasm. In the cytoplasm, viral RNA is translated into a single long polyprotein which is cleaved by viral and host-cell proteases into individual viral proteins required for replication and assembly. Viral RNA is asymmetrically replicated close to the ER leading to new positive-strand RNA via the production of full length negative-strand RNA. During polyprotein processing, the precursor membrane protein (prM) and E are translocated to the ER and the capsid (C) protein interacts with viral RNA to form the nucleocapsid which, upon budding through the ER, acquires its envelope consisting of prM and E. Immature virions are then transported through the Golgi apparatus along the exocytic pathway during which acidic pH and cleavage of prM to M by furin results in reorganisation of the envelope protein leading to mature, fusion-competent virions. The mature virions are released by exocytosis. A natural by-product of flavivirus infection is the production of subviral particles (SHA) which lack the nucleocapsid and only contain the viral envelope. TGN: trans-Golgi network. Image was taken from Stiasny & Heinz, 2006.

Virus replication starts as early as 3 - 6 h p.i. and production of infectious virions takes approximately 12 h (Chambers et al., 1990). In mammalian cells it is often accompanied by cytopathic effect whereas in arthropod cells it more commonly leads to persistent infection (Bell-Sakyi et al., 2007, 2012).

Some studies comparing the maturation process of flaviviruses in arthropod and mammalian cells did not find any marked differences, either in the distribution of viral proteins determined by immunofluorescence or in the formation of virus-induced structures as seen by electron microscopy (Barth, 1999; Hase et al., 1987;

Offerdahl et al., 2012; Rahman et al., 1998), suggesting a similar maturation process in arthropod and mammalian cells. However, ultrastructural changes observed within these studies were generally more pronounced in mammalian cells which showed signs of cytopathic effect that did not occur in arthropod cells. In contrast, other studies suggest differences in the maturation of flaviviruses between vertebrate and arthropod cells. One study comparing changes in tick and porcine kidney stable (PS) cells upon TBEV infection observed differences in the localisation of virus particles, which were, respectively, in the cytoplasm and in the rough ER and Golgi, suggesting *cis*- and *trans*-type maturation processes, respectively, for TBEV in these two cell types (Senigl, Grubhoffer & Kopecký, 2006). During *trans*-type maturation of flaviviruses mature virions are assembled intracellularly and are transported through the secretory pathway to the cell membrane where they are exported by exocytosis (Leary & Blair, 1980), whereas during *cis*-type maturation, nucleocapsids are present in the cytoplasm and structural proteins are trafficked, possibly along microtubules (Chu & Ng, 2002), to the cell membrane where viruses egress by budding (Ng, Tan & Chu, 2001). Furthermore, another study suggested that in Vero cells flavivirus replication occurs within vesicle packets, whereas in the mosquito cell line C6/36 virus-induced vacuoles are assumed to be the location for replication (Mackenzie, Jones & Young, 1996). The advancement in technology, with the ability to generate 3D reconstructions of ultrastructural changes, should help to elucidate which of these observations reflect reality. However care needs to be taken when interpreting data from different time-points in comparisons of arthropod and mammalian cells, since arthropods can become persistently infected whereas mammalian cells die upon virus infection and thus acute and persistent infection in these different cell types might be associated with very different ultrastructural changes.

1.1.1.2 Tick-borne encephalitis virus

TBEV is one of the most important tick-borne viruses in Europe, Russia and many parts of Asia, causing tick-borne encephalitis (TBE) in humans with an estimated annual number of up to 10,000 disease cases in Russia and 3,000 in Europe (Charrel et al., 2004; Lindquist & Vapalahti, 2008; Mansfield et al., 2009; Pfeffer & Dobler,

2011). The disease was first described in 1931 as aseptic meningitis which occurred seasonally (Schneider, 1931). Six years later the causative agent, TBEV, was isolated (Zilber, 1939). Based on serological and sequence analysis TBEV can be taxonomically classified into three subtypes, the Western European, Siberian and Far-Eastern subtypes. The Western European subtype is transmitted by *Ixodes ricinus* ticks in Central, Eastern and Northern Europe, whereas the Siberian and Far-Eastern subtypes are transmitted by *Ixodes persulcatus* ticks in Siberia, parts of Russia, Latvia, Finland and the latter subtype additionally in Central and Eastern Asia including China and Japan (Dobler et al., 2012; Dumpis, Crook & Oksi, 1999; Lindquist & Vapalahti, 2008; Mansfield et al., 2009; Süss, 2003). The main vector on the Japanese island of Hokkaido is *Ixodes ovatus*, and other tick genera such as *Haemaphysalis* and *Dermacentor* have been shown to transmit the virus under certain ecological conditions (Dobler et al., 2012). The main reservoir hosts for the transmission of TBEV are the yellow necked mouse, *Apodemus flavicolli*, and the bank vole, *Myodes glareolus* (Dobler, 2010; Franke et al., 2010; Hubálek & Rudolf, 2012), which are thought to become persistently infected and may support virus survival during the winter (Tonteri et al., 2011). A typical transmission cycle for TBEV is shown in Figure 1.6.

The three different virus subtypes differ not only in their vector species and geographical distribution but also in their clinical manifestation and long-term outcome (Dobler et al., 2012; Dumpis, Crook & Oksi, 1999; Gritsun, Lashkevich & Gould, 2003; Lindquist & Vapalahti, 2008; Mandl, 2005; Mansfield et al., 2009). The Western European subtype usually causes a biphasic illness with fever, fatigue, general malaise, headache and myalgia in the first stage and, after a symptom-free period of around one week, may progress in 20 to 30% of patients, by involvement of the central nervous system (CNS), to meningitis, encephalitis or myelitis resulting in a case fatality rate of around 1-2% (Gritsun, Lashkevich & Gould, 2003; Mandl, 2005; Mansfield et al., 2009). The Siberian subtype causes a similar case fatality rate of 2-3% (Atrasheuskaya, Fredeking & Ignatyev, 2003; Mansfield et al., 2009) but has a tendency to become chronic. In contrast, the Far Eastern subtype leads to a more severe disease with a higher rate of CNS disorders and neurological sequelae

causing death in approximately 20-40% of patients (Mandl, 2005; Mansfield et al., 2009).

Reports of TBEV infections in new, formerly unaffected areas, such as new regions and at higher altitude, are increasing and can be attributed to several factors, such as expanding tick populations and longer tick activity due to climatic factors, changes in socioeconomic behaviour and changes in land use and leisure activities (Danielová & Kliegrová, 2008; Dobler et al., 2012; Jaenson et al., 2012; Lindgren & Gustafson, 2001; Randolph, 2004; Süss, 2008)

1.1.1.3 Langat virus

LGTV belongs to the TBE serocomplex of tick-borne flaviviruses and was first isolated from *Ixodes granulatus* ticks in Malaysia (Smith, 1956). According to a recent review, LGTV was also identified in *I. persulcatus* ticks in Siberia and *Haemaphysalis papuana* ticks in Thailand (Dobler, 2010). Since no natural LGTV disease cases were reported, and due to its close antigenic relationship to TBEV, attenuated LGTV strains were tested as possible live vaccines against encephalitis caused by tick-borne flaviviruses (Dobler, 2010). One of these strains, Yelantsev, was tested in a human trial in Russia in which it led to meningoencephalitis in a small number of cases (Smorodincev & Dubov, 1986). Trials in human volunteers and animals with the LGTV strain E5, which exhibits reduced neuroinvasiveness, showed high levels of neutralising antibodies which cross-reacted with TBEV, POWV and KFDV (Price & Thind, 1973; Price et al., 1970). Due to its low pathogenicity, apart from in patients with suppressed immune function (Webb et al., 1966), and lack of naturally-occurring cases of disease in humans and animals (Dobler, 2010), LGTV is a useful model, with a low risk for the researcher, for studying more virulent tick-borne flavivirus infections.

1.1.2 Alphaviruses

Alphaviruses and *Rubiviruses* are the two genera of the family *Togaviridae*, however only the alphaviruses are arboviruses. There are currently 29 alphaviruses (Powers et al., 2012), each of them with several variants and strains, and almost all are

transmitted by mosquitoes apart from the aquatic viruses salmon pancreatic disease virus and southern elephant seal virus which are either water-borne or transmitted by aquatic arthropods such as ectoparasitic lice (Linn et al., 2001; McLoughlin & Graham, 2007). Alphaviruses are distributed world-wide, even in Antarctica (Linn et al., 2001), and are grouped according to their distribution as either New World or Old World alphaviruses (Strauss & Strauss, 1994). New World alphaviruses, which mainly cause encephalitis, include Eastern equine encephalitis virus (EEEV), Western equine encephalitis virus (WEEV) and VEEV, and are distributed across the Americas. In contrast, Old World alphaviruses usually lead to arthralgia, are found in Europe, Asia, Australia and parts of Africa and include Sindbis virus (SINV), CHIKV, O'nyong-nyong virus (ONNV), Ross River virus (RRV), Barmah Forest virus (BFV) and Semliki Forest virus (SFV). Exceptions with respect to the disease outcome are SINV and SFV, as they are associated with encephalitis in mice, and CHIKV and RRV as they can cause encephalitis in humans (Go, Balasuriya & Lee, 2014; Hollidge, González-Scarano & Soldan, 2010; Zacks & Paessler, 2010). Alphaviruses of medical and veterinary importance and their vector species are shown in Table 1.1.

Alphaviruses are able to infect a wide variety of hosts including birds, mammals, reptiles and amphibians, but the main amplifying hosts are birds (SINV, SFV, EEEV and WEEV), rodents (RRV, VEEV, BFV) and monkeys (CHIKV, ONNV) (Go, Balasuriya & Lee, 2014). In humans and equines, which are usually considered dead-end hosts, they can lead to serious epidemics. Of the three equine encephalitis alphaviruses, VEEV is possibly the most important zoonotic pathogen, although EEEV with a case fatality rate in humans of up to 70%, compared to 1% in VEEV cases, is more virulent (Zacks & Paessler, 2010). VEEV is capable of producing epidemics and is more transmissible causing disease in almost all infected humans. Some strains of VEEV are transmitted in an epizootic cycle in which horses are amplifying hosts leading more readily to infection of humans; both hosts develop high viraemia thus possibly becoming a source of infection for mosquitoes (Go, Balasuriya & Lee, 2014; Weaver et al., 1996; Zacks & Paessler, 2010). The ability of alphaviruses to rapidly cause an epidemic was also seen with the outbreak of CHIKV on the island of La Reunion (Enserink, 2006). This was associated with a mutation in

the viral envelope protein which increased the infectivity of CHIKV for *Aedes albopictus* (Vazeille et al., 2007), a vector now widely distributed across southern Europe (Gratz, 2004). The epidemic subsequently spread to India, South-East Asia, some countries in southern Europe and the Americas (Van Bortel et al., 2014; Charrel & Lamballerie, 2008; Pialoux et al., 2007; Rezza et al., 2007), with reports of encephalitis in elderly and infant patients (Robin et al., 2008).

1.1.2.1 Alphavirus genome organisation and life cycle

Alphaviruses are small (~70 nm) enveloped viruses with a positive sense, non-segmented ssRNA genome of 11 to 12 kb in length. The genome contains two distinct ORFs, flanked by 5' and 3' UTRs and has a 5' cap and a 3' poly(A) tail, as indicated in Figure 1.3. The first ORF at the 5' end occupies over two-thirds of the genome and encodes the four non-structural proteins (nsP1- 4) required for replication and polyprotein processing. The 3' ORF, under the control of a subgenomic (26S) promoter (Ding & Schlesinger, 1989; Kuhn, 2007; Strauss & Strauss, 1994), encodes the five structural proteins C, the three E glycoproteins E1, E2 and E3 and the 6 kDa (6K) protein (Kääriäinen et al., 1987).

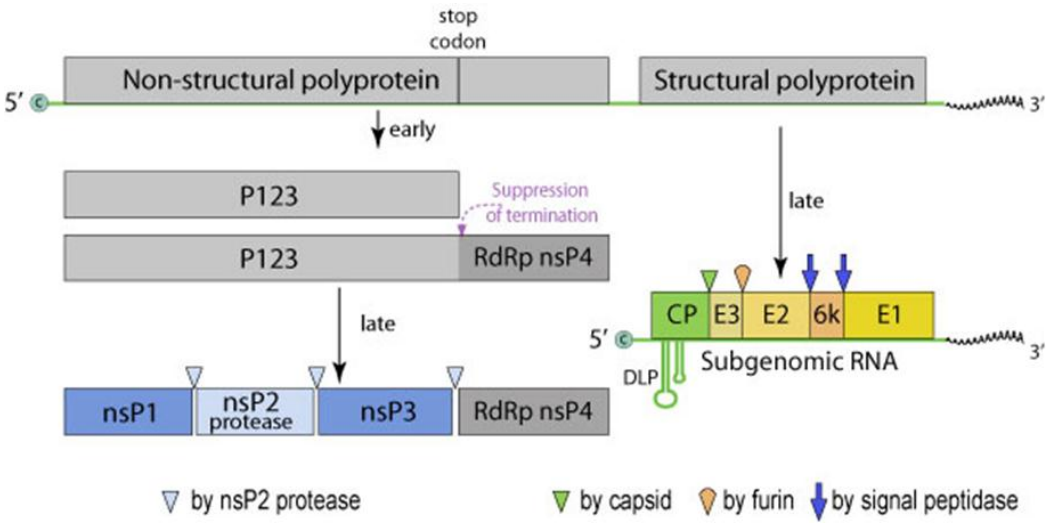

Figure 1.3 Organisation of the alphavirus genome and polyprotein

The alphavirus positive sense single-stranded (ssRNA) genome is approximately 11 - 12 kb long with a 5' cap and 3' poly(A) tail. The first ORF, at the 5' end, encodes the four non-structural proteins nsP1 - nsP4, while the 3' ORF encodes the five structural proteins C, E1, E2, E3 and 6k, under the control of a subgenomic promoter. Early on during infection the non-structural proteins are translated from the viral genomic RNA yielding two different polyproteins, namely P123 and P1234. This is caused by an opal termination codon (UAG) between nsP3 and nsP4. The polyproteins P123 and P1234 are then sequentially cleaved by the viral protease nsP2.
The subgenomic RNA is translated late during infection into a single polyprotein, from which the C protein is autoproteolytically cleaved and cellular proteases are responsible for cleavage of the other structural proteins as indicated.
Image was taken from http://viralzone.expasy.org/all_by_species/625.html.

The life cycle of alphaviruses including genome replication is depicted in Figure 1.4. Alphaviruses enter the cell by receptor-mediated endocytosis in clathrin-coated pits (DeTulleo & Kirchhausen, 1998; Helenius et al., 1980; Marsh & Helenius, 1980; Marsh, Bolzau & Helenius, 1983), with the E2 protein binding possibly to laminin, a receptor present on the surface of a variety of vertebrate cells as well as on arthropod cells (Strauss et al., 1994; Wang et al., 1992). In the cytoplasm the virus-containing clathrin-coated pits fuse with endosomes and subsequently lysosomes (Strous & Govers, 1999), leading to a drop in pH which triggers a conformational change of the E2-E1 heterodimer. This conformational change reveals a fusion loop on E1, which upon insertion into the endosome membrane leads to fusion with the viral envelope and release of the nucleocapsid into the cytoplasm (Ahn et al., 1999; Gibbons et al., 2000, 2003; Hammar et al., 2003; Lescar et al., 2001; Wahlberg et al., 1992). The

nucleocapsid disassembles and releases the mRNA-like virus genome into the cytoplasm (Helenius, Marsh & White, 1982; Marsh & Helenius, 1980).

In the cytoplasm, viral RNA can be directly translated by the cellular translation machinery. Translation begins with the viral genomic RNA yielding two different polyproteins, namely P123 and P1234. This is the case for most alphaviruses and is caused by an opal termination codon (UAG) between nsP3 and nsP4 which results in read-through occurring at a frequency of 10-20% (Jose, Snyder & Kuhn, 2009; Li & Rice, 1993). This read-through leads to predominant production of P123 compared to P1234 and is possibly employed to regulate translation of the RdRp nsP4. However some alphaviruses, such as SFV with the exception of SFV strain A7(74), have no opal termination codon, but instead an arginine leading to production of only P1234 (Strauss, Rice & Strauss, 1983; Takkinen, 1986). The polyprotein P1234 is exclusively cleaved by the viral protease nsP2 (Merits et al., 2001) resulting in the immediate release of nsP4, followed by nsP1, nsP2 and finally nsP3 (Kim et al., 2004).

Once the nsPs have been processed they stay together and form a replicase complex required for genome replication. The replicase complex is thought to associate with endosomal and lysosomal membranes leading to the formation of so-called cytopathic vacuoles (CPV) associated with alphavirus replication (Froshauer, Kartenbeck & Helenius, 1988). CPV I are sites of alphavirus genome replication (Friedman et al., 1972; Grimley, Berezesky & Friedman, 1968; Kujala et al., 2001) and CPV II are associated with virus maturation (Pathak et al., 1976). In CPV I vesicles, the replicase complex formed by P123 and processed nsP4 produces a negative strand RNA antigenome using the complete positive strand as template. This replicase complex is efficient for minus-strand synthesis but not for plus-strand synthesis and further processing of P123 into individual viral proteins decreases the ability to transcribe minus-strand RNA (Kim et al., 2004; Shirako & Strauss, 1994). Thus minus-strand RNA is transcribed early during infection whereas viral RNA genome and subgenomic RNA is produced late during infection. The replicase complex formed from the individual viral nsPs then produces full length plus-strand RNA from the 3’ end or subgenomic RNA from the subgenomic promoter (Kääriäinen et al., 1987; Kim et al., 2004).

All the nsPs have multifunctional roles and are crucial to virus genome replication, which will be briefly described. NsP1 coats the interior of replication complexes and directs the viral genome towards these (Kujala et al., 2001; Spuul et al., 2007). Furthermore it initiates the synthesis of negative-strand RNA (Shirako, Strauss & Strauss, 2000; Wang, Sawicki & Sawicki, 1991) and is responsible, together with nsP2, for capping newly-produced RNA through RTPase, methyl- and guanyl-transferase activity (Vasiljeva et al., 2000). The nsP2 protein contains NTPase, GTPase, ATPase and RNA helicase activity in its N-terminal region (de Cedrón et al., 1999; Rikkonen, 1996; Rikkonen, Peränen & Kääriäinen, 1994). Additionally it is implicated in the termination of the negative-strand replication and in initiating the subgenomic RNA synthesis (Suopanki et al., 1998). The C-terminal domain of nsP2 consists of a papain-like cysteine protease which is responsible for sequential cleavage of the viral polyprotein containing the nsPs (Merits et al., 2001). Furthermore, nsP2 has been shown to be an antagonist of IFN production (Breakwell et al., 2007) and is possibly responsible for the shut-down of host cell protein synthesis in Old World alphaviruses (Garmashova et al., 2006). In contrast to the other nsPs, the function of nsP3 is still unclear. However some studies have suggested a role for nsP3 in negative-strand and subgenomic RNA synthesis (LaStarza, Lemm & Rice, 1994; Wang, Sawicki & Sawicki, 1994), in cleavage of the polyprotein by nsP2 (De Groot et al., 1990) and attaching the replicase complex to membranes (Peränen & Kääriäinen, 1991). As already mentioned above, nsP4 is the RdRP that replicates the alphaviral genome (Keränen & Kääriäinen, 1979). NSP4 also exhibits protease activity contributing to the cleavage of nsP3 from nsP4 during the processing of the nsP polyprotein (Takkinen et al., 1990).

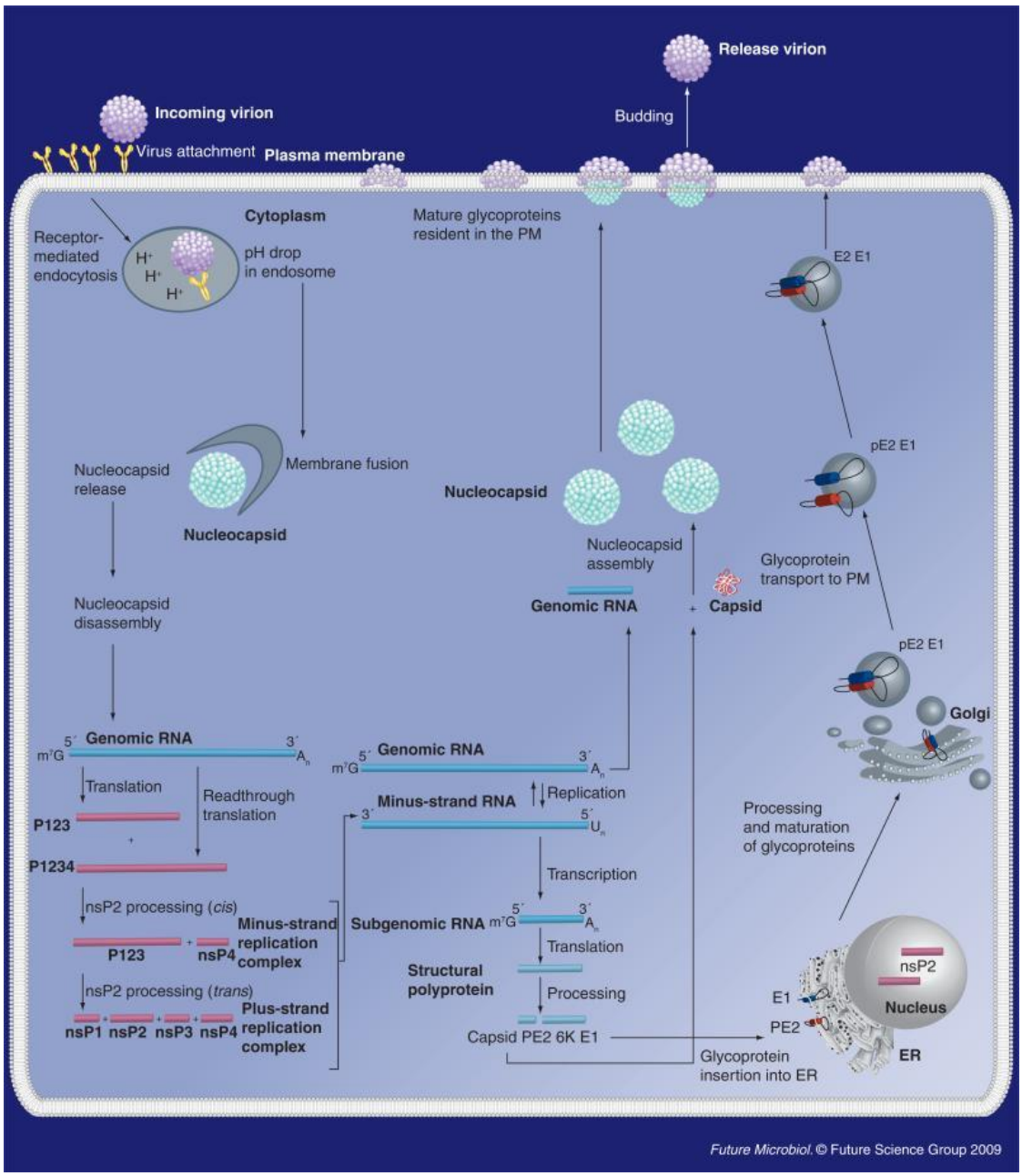

Figure 1.4 Alphavirus life cycle in vertebrate cells

Alphaviruses are taken up by receptor-mediated endocytosis and are released by fusion of the viral membrane with the endosome membrane, mediated by a conformational change of the envelope proteins induced by acidic pH. In the cytoplasm the nucleocapsid disassembles and releases the viral genome. The genomic RNA encoding the non-structural proteins is subsequently translated and processed, enabling genome replication and translation of the subgenomic mRNA into structural proteins. The envelope proteins are translocated to the ER where they are processed and further transported through the TGN to the plasma membrane. The nucleocapsid is assembled by interaction of the viral RNA with the capsid protein, which is transported to the cell membrane where it associates with the envelope proteins and leads to budding.
ER: endoplasmic reticulum, nsP: non-structural protein PM: plasma membrane Image was taken from Jose, Snyder & Kuhn, 2009.

The subgenomic RNA is translated into a single polyprotein, in the order C-pE2-6K-E1, from which the C protein is autoproteolytically cleaved facilitating its rapid release (Aliperti & Schlesinger, 1978). Upon cleavage the N-terminal signal of pE2 is exposed allowing translocation of pE2 and E1 to the ER (Bonatti et al., 1984), where both are anchored via transmembrane domains into the ER membrane (Melancon & Garoff, 1986). In the ER the envelope proteins are modified by addition of carbohydrate chains and fatty acids and are further modified during the transportation through the TGN. From there the envelope proteins are transported to the cell membrane. During transportation the pE2 protein is processed into E2 and E3 which is the final maturation step required for the production of infectious particles. The processed envelope proteins are finally embedded into the cell membrane. In the cytoplasm the C protein interacts with a packaging signal on the viral genome which initiates assembly into a nucleocapsid (Geigenmüller-Gnirke et al., 1991; Weiss et al., 1989), which is subsequently transported to the cell membrane. At the cell membrane the nucleocapsid interacts with the cytoplasmic domain of E2 and initiates the budding of new virions from the cell (Lopez et al., 1994; Suomalainen, Liljeström & Garoff, 1992). The 6K protein is required for correct virion assembly. If absent, virus is still assembled but contains incorrectly structured glycoprotein-spikes reducing infectivity (McInerney et al., 2004).

1.1.2.2 Semliki Forest virus

SFV is a member of the genus *Alphavirus* and was first isolated from an *Aedes abnormalis* mosquito in the Semliki Forest in Uganda (Smithburn, Haddow & Mahaffy, 1946). It circulates in sub-Saharan Africa and is primarily transmitted by *Aedes africanus* and *Aedes aegypti* mosquitoes (Mathiot et al., 1990). The natural hosts of SFV are thought to be monkeys and small mammals but it can also infect equines and humans which are both dead-end hosts. In humans, SFV usually causes a mild febrile illness accompanied by fever, myalgia, arthralgia and headaches, but there is a report of one fatal case of a laboratory-acquired human infection (Willems et al., 1979). This strain of SFV is now no longer used in laboratories. There are several different SFV laboratory strains which can be distinguished into two groups according to their pathogenicity in adult mice. The virus used in the present study

was SFV4 which is a complementary DNA (cDNA) clone derived from the prototype strain (Liljeström & Garoff, 1991; Liljestrom et al., 1991). It exhibits virulence in adult mice upon intranasal or intracerebral but not upon intraperitoneal injection, unless administered at a high dose (Fazakerley, 2002; Glasgow et al., 1991).

SFV4 is widely used in research due to the possibility of manipulating its genome with relative simplicity, including mutation and insertion of foreign genes. Foreign genes such as *Renilla* luciferase (Rluc), ZsGreen and enhanced green fluorescent protein (eGFP) can be inserted in the genomic or subgenomic RNA enabling indirect measurement of SFV4 replication, and even the insertion of a second subgenomic promoter allowing the expression of a foreign gene in large amounts is possible (Tamberg et al., 2007). An example of an SFV reporter virus engineered to express a marker gene is SFV4(3F)-ZsGreen, which contains the marker ZsGreen fused to nsP3 enabling the visualisation of nsP3 and virus replication complexes in cell culture and in the mouse model (Tamberg et al., 2007).

Although SFV is a mosquito-borne virus and is not known to be transmitted by ticks in nature, several studies have shown that SFV can readily infect tick cell lines and produce infectious virus particles (Leake, 1987; Leake, Pudney & Varma, 1980; Pudney, 1987). Interestingly, SFV was recently isolated from ticks in Kenya (Lwande et al., 2013) but their capacity to transmit the virus has not been proven and virus might have been present in the blood taken up by ticks if they had recently fed on SFV-infected, viraemic vertebrate hosts. SFV constructs were used in the present study to characterise viral infection in tick cells.

1.2 Ticks and tick-borne viruses

Ticks are obligate haematophagous ectoparasites belonging to the phylum Arthropoda, subphylum *Chelicerata*, and are grouped quite basally in the phylum Arthropoda. They are thus quite distant evolutionarily from other important arthropod vectors such as mosquitoes, sandflies and midges, which belong to the subphylum Hexapoda, class Insecta, order Diptera (Figure 1.5).

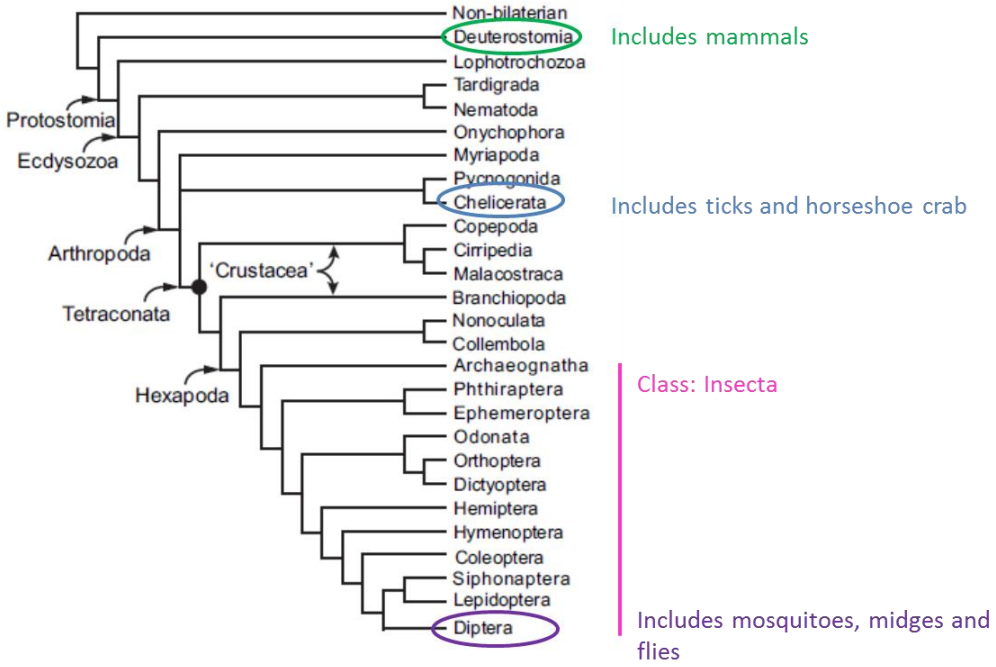

Figure 1.5 Phylogenetic tree of major animal lineages

Phylogenetic tree of major animal lineages inferred from maximum likelihood analysis based on highly conserved regions from orthologous genes present in publicly-available EST data (adapted from Andrew, 2011). Ticks are members of the Chelicerata and are considered basal in the phylum Arthropoda. Most other arthropod vectors, including mosquitoes, midges and sand flies belong to the order Diptera within the class Insecta subphylum Hexapoda and are considered as 'higher insects' with a faster evolution rate.

Within the subphylum *Chelicerata* ticks form part of the class Arachnida, subclass Acari, order Parasitiformes and Suborder Ixodida (Guglielmone et al., 2010). The suborder Ixodida further comprises three families, with over 900 tick species. The three families are the monotypic Nuttalliellidae, the Argasidae and the Ixodidae, with the two latter families referred to as soft and hard ticks respectively (Barker & Murrell, 2004). Soft and hard ticks not only vary in their morphological features, such as larger size and leathery cuticle for the former and a sclerotized dorsal plate called the scutum for the latter, but also in several other biological, physiological and ecological features (Estrada-Peña et al., 2004; Walker et al., 2003). Soft ticks are divided into four genera namely *Argas*, *Carios*, *Ornithodorus* and *Otobius* (Estrada-Peña et al., 2004; Guglielmone et al., 2010; Walker et al., 2003) which are mostly multiple-host parasites. They usually have several nymphal stages which all feed rapidly, for periods of minutes to several hours, on their hosts. Adult soft ticks are

able to feed several times taking up only a small blood meal and females, after mating away from the host, deposit a limited number of eggs (100 to 500) after each meal (Estrada-Peña et al., 2004; Walker et al., 2003). Soft ticks can live for many years and can survive in their nymphal and adult stages for several years without a blood meal.

The majority of tick species belong to the Ixodidae with approximately 702 species described so far in 14 genera (Guglielmone et al., 2010). These 14 genera are split into Prostriata, with *Ixodes* being the only genus comprising 243 species, and the Metastriata containing the other 13 genera (Nava, Guglielmone & Mangold, 2009). In contrast to soft ticks, hard ticks have only three developmental stages – larvae, nymphs and adults – and usually feed slowly for several days to fully engorge. Upon finishing a blood meal the larvae and nymphs moult to the next stage and, after mating and full engorgement within one blood meal, the adult female ticks deposit thousands of eggs and die. The feeding and moulting behaviour of Ixodidae vary depending on the tick species which are referred to as one-, two- or three-host ticks (Estrada-Peña et al., 2004; Walker et al., 2003).

One-host ticks, such as those of the genus *Rhiphicephalus* (*Boophilus*) (Estrada-Peña et al., 2004; Jongejan & Uilenberg, 2004; Walker et al., 2003), feed and remain attached to the same host during all their developmental stages from larva to engorged female, over a period of at least three weeks. Thus moulting and mating occur on the same individual host. After mating and engorgement, female ticks detach from the host to deposit their eggs from which larvae hatch. The two-host life cycle is similar to the one-host life cycle but only larvae and nymphs feed on the same individual (Estrada-Peña et al., 2004; Jongejan & Uilenberg, 2004; Walker et al., 2003). Engorged nymphs drop off, moult away from the host, and the resulting adult finds a second host, which may or may not be of the same species. Two-host ticks include *Hyalomma detritum detritum* and *Rhiphicephalus evertsi* (Estrada-Peña et al., 2004; Jongejan & Uilenberg, 2004; Walker et al., 2003). Most of the hard ticks follow a three-host life cycle, including all *Ixodes*, *Amblyomma*, and *Haemaphysalis* species, and some species of *Dermacentor*, *Rhiphicephalus* and *Hyalomma* (Jongejan & Uilenberg, 2004; Walker et al., 2003). Three host ticks do not moult on the host. Once larvae finish feeding they detach, moult and the resulting nymphs find a second

host. When fully engorged, nymphs detach and moult to the adult stage which searches for a third host. In the Prostriata (*Ixodes* spp) mating usually takes place off-host, before adult attachment, whereas in the Metastriata (all other species) mating usually occurs on the host, after the female has attached and fed for a few days (Kaufman, 2004). The life cycle of three-host ticks is usually long, taking from six months to several years (Estrada-Peña et al., 2004; Walker et al., 2003). In the case of *Ixodes* spp the complete life cycle takes about three years but might be prolonged to 4 - 6 years depending on availability of hosts (Moshkin et al., 2009).

Apart from different life cycles, tick species also exhibit different behaviours in searching for their hosts. Some ticks such as those of the genera *Rhiphicephalus*, *Haemaphysalis* and *Ixodes* climb up onto the vegetation and wait until a suitable host passes by, which is referred to as questing. Others, such as adult ticks of the genera *Amblyomma* and *Hyalomma* exhibit exophilic behaviour in that they hunt and actively run towards a nearby host. Endophilic or nidocolous behaviour can be described as spending the entire life cycle in close proximity to the hosts, in for example nests, burrows, stables or huts. This behaviour is common for argasids and some *Ixodes* spp.

Some tick species prefer to feed on specific vertebrate hosts, such as those of the one-host genus *Rhiphicephalus* (*Boophilus*) which preferentially feed on cattle. Others such as *Ixodes* spp feed on a range of wild and domestic vertebrate hosts. Overall however, the number of species adapted to domestic animals and humans is limited but these are of major importance for transmission of a wide range of pathogens (Jongejan & Uilenberg, 2004).

1.2.1 Ticks as important vectors causing disease in animals and humans

Ticks harm their hosts not only by sometimes causing severe blood loss or induction of paralysis, toxicosis and skin irritation as a result of saliva injection but more importantly by their ability to transmit an enormous variety of pathogens including bacteria, protozoa and viruses (Jongejan & Uilenberg, 2004). They are considered to be second worldwide to mosquitoes as vectors of human disease and the most

important vectors of pathogens causing diseases of veterinary importance (de la Fuente et al., 2008a). The viruses transmitted by ticks belong to the six virus families *Rhabdoviridae*, *Asfarviridae*, *Reoviridae*, *Orthomyxoviridae*, *Bunyaviridae* and *Flavivivridae* and possibly a seventh, *Arenaviridae*, to which as yet unassigned viruses might belong (Hubálek & Rudolf, 2012; de la Fuente et al., 2008a; Labuda & Nuttall, 2004; Nuttall, 2009). Some viruses of medical and veterinary importance transmitted by ticks are listed in Table 1.1.

The ability of a tick to transmit a particular virus and be a competent vector depends on several factors. Firstly, the tick has to be able to acquire the virus by feeding on an infected host; secondly, the virus has to be maintained in the tick from one developmental stage to the next, and thirdly, the virus has to be transmitted to the host upon feeding (Nuttall, 2009). The period between acquisition and transmission of the pathogen is referred to as the extrinsic incubation period during which the pathogen has to overcome several barriers, replicate efficiently and escape the tick immune response before being able to be transmitted to the next host (Nuttall, 2009). In insects, four barriers which restrict either virus entry or exit, the midgut infection barrier (MIB), the midgut escape barrier (MEB), the salivary gland infection barrier (SIB) and the salivary gland escape barrier (SEB) have to be overcome (Hardy et al., 1983). Each of these might play a decisive role in determining vector competence for a certain pathogen. In ticks, evidence for the existence of a MIB was seen in a study determining vector capacity of *Rhiphicephalus appendiculatus* and *Amblyomma variegatum* for the closely-related *Orthomyxoviridae* Thogoto and Dhori viruses (Jones et al., 1989). The authors found that both tick species were competent vectors for Thogoto virus when fed on infected hamsters but both failed to transmit Dhori virus. Dhori virus was only transmitted by both tick species when virus was inoculated into the haemocoel of engorged nymphs, circumventing the midgut, suggesting that the midgut is an important barrier for infection with Dhori virus but not Thogoto virus in both tick species (Jones et al., 1989). Another study investigating the vector competence of *R. appendiculatus* for Dugbe virus found that, in contrast to Dhori virus which only survived in the tick for less than 4 days, Dugbe virus survived for at least 21 days but was not able to survive the moulting period and could not be transmitted by the adult stage (Steele & Nuttall, 1989). However, as

for Dhori virus, Dugbe virus was able to replicate in and be transmitted by *R. appendiculatus* upon inoculation of virus into the haemocoel, suggesting that there is no SIB for either virus in *R. appendiculatus*, but possibly due to the difference in survival dynamics, an MIB for Dhori virus and an MEB for Dugbe virus (Nuttall, 2009).

Once the virus has passed the midgut barrier it has to travel to the salivary glands, possibly by passing through the haemocoel either as free virions or in infected haemocytes. The latter route may for example be used by Dugbe virus and ASFV which have both been observed in haemocytes of their respective tick vectors *A. variegatum* and *Ornithodorus moubata* (Booth, Gould & Nuttall, 1991; Greig, 1972). Upon successful crossing of the salivary gland barrier, including cell penetration, replication to high titres and virus release, the virus can be transmitted to the next host upon feeding (Alekseev & Chunikhin, 1990; Belova, Burenkova & Karganova, 2012; Khasnatinov et al., 2009). Pathogens are injected into the host together with tick saliva, which contains a pharmacopoeia of substances including anti-coagulant, anti-platelet, vasodilatory, anti-inflammatory and immunomodulatory components (Francischetti et al., 2009) allowing the tick to feed on liquid blood and remain attached by preventing the sensation of pain or itching which would possibly result in removal of the tick by the host. Furthermore there is direct and indirect evidence that tick saliva components, possibly by modulating the host response, promote the transmission of pathogens to the host, also referred to as saliva-activated transmission (Nuttall & Labuda, 2004).

The transmission of tick-borne infections can occur either vertically, which includes transstadial or transovarial transmission, or horizontally, including tick to tick transmission by co-feeding and tick to vertebrate or vertebrate to tick transmission. As an example of a transmission cycle of viruses by three host-ticks in nature, the transmission cycle of TBEV, as depicted in Figure 1.2, will be briefly explained.

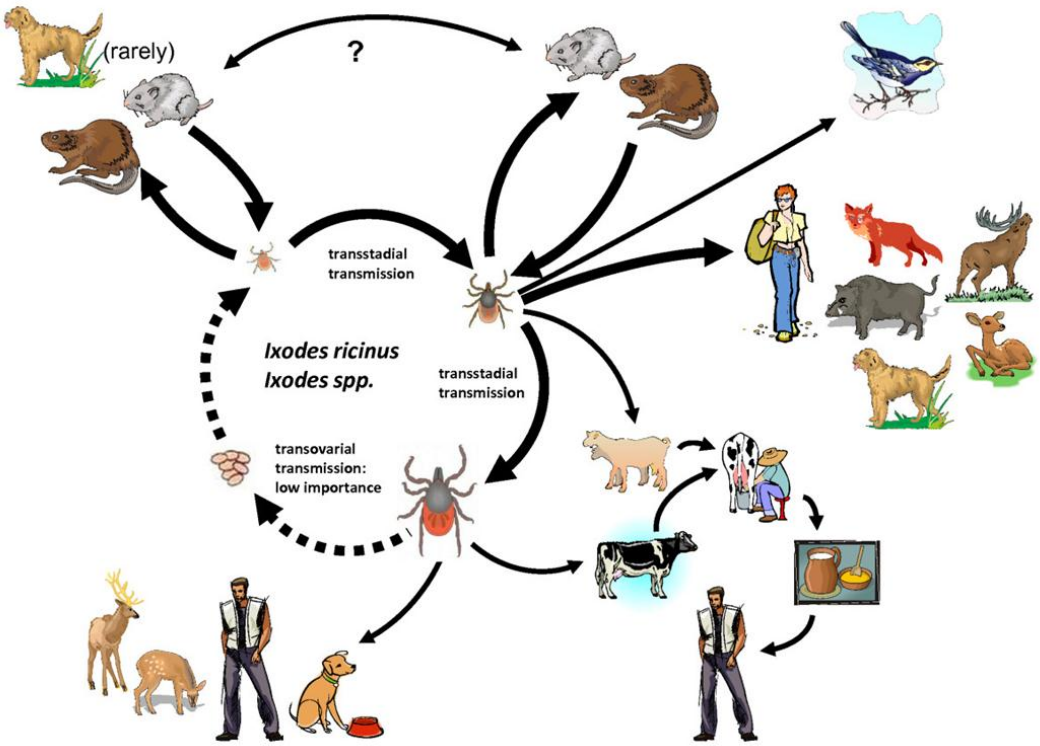

Figure 1.6 Transmission cycle of TBEV

TBEV is transmitted by *I. ricinus* or *I. persulcatus* ticks in nature. Ticks become infected either by feeding on viraemic hosts or through co-feeding of infected and non-infected ticks in close proximity on the same host. Within the tick population the virus is maintained transstadially from one developmental stage to the next, as well as to a small extent by transovarial transmission from infected adult females to eggs. Small mammals, mainly rodents, are considered reservoir hosts for the virus, whereas humans are considered dead-end hosts which either become infected by a tick bite or by the consumption of raw unpasteurised milk from infected ruminants. The figure was taken from Pfeffer & Dobler, 2011.

Ticks can acquire TBEV either by feeding on viraemic hosts (Labuda et al., 1993a, 1993b) or by co-feeding in close proximity on non-viraemic (Labuda et al., 1993c, 1996; Rosà et al., 2003) and even on TBEV-immune hosts with detectable levels of neutralising antibodies (Labuda et al., 1997). After infection the virus is maintained transstadially from one developmental stage to the next within the tick and even transovarial transmission from infected female ticks to eggs has been reported since virus was found in unfed larvae (Danielová et al., 2002). The infected ticks can then transmit TBEV to a vertebrate host within minutes following attachment (Alekseev & Chunikhin, 1990). Small mammals, upon which larvae and nymphs preferentially feed, act as maintenance, amplifying and reservoir hosts for the virus (Süss, 2003). In contrast, larger animal hosts upon which nymphs and adult ticks might feed are not

considered to play an important role for virus transmission between ticks (Gritsun, Lashkevich & Gould, 2003). Similarly humans are considered accidental hosts, which do not play any role in maintaining the virus in nature. Humans can be infected either by tick bite or by non-vectored transmission including the consumption of raw milk or raw milk products from viraemic animals, such as goats (Balogh et al., 2010; Holzmann et al., 2009; Hudopisk et al., 2013; Kerbo et al., 2005), sheep (Gresíková et al., 1975) or cattle (Vereta et al., 1991).

1.2.2 Tick cell lines

The first continuous tick cell line derived from *R. appendiculatus* was established forty years ago (Varma, Pudney & Leake, 1975); since then the number of available tick cell lines has grown to a total of 57, with 47 derived from 14 ixodid tick species and 10 from two argasid species (Bell-Sakyi et al., 2012). They were all derived from either moulting nymphs, after removal of the digestive and excretory system, moulting larval explants or embryos (Bell-Sakyi et al., 2007, 2012). Due to the preparation method all currently available tick cell lines are phenotypically and genetically heterogenous, which can be advantageous when, for example, viruses from field or clinical samples are isolated and the cell type which supports replication is unknown, but can also be disadvantageous, since the study of specific cell types is not possible. However, attempts to clone tick cells, with the aim of achieving a homogenous cell line, have so far failed (Bell-Sakyi et al., 2007, 2012; Munderloh et al., 1994). Furthermore some individual cells within a tick cell culture show a tendency to gain or lose chromosomes without affecting their survival (Chen, Munderloh & Kurtti, 1994; Kurtti, Munderloh & Ahlstrand, 1988; Varma, Pudney & Leake, 1975).

In the 1970s and 1980s continuous tick cell lines were mostly used for studying their potential to propagate different mosquito- and tick-borne viruses or to look at persistent infection (Bhat & Yunker, 1979; Leake, Pudney & Varma, 1980; Pudney, 1987; Rehacek, 1987; Varma, 1989; Varma, Pudney & Leake, 1975), since tick cell cultures are, like their parent ticks, quite long-lived. These studies revealed that tick cell lines are able to support infection with a variety of mosquito-borne viruses but mosquito cells do not support tick-borne virus infections. In contrast to mammalian

cell cultures which generally die upon virus infection, tick cell cultures show no obvious cytopathic effect and are able to replicate and produce infectious virus particles for relatively long time periods (Leake, 1987; Leake, Pudney & Varma, 1980); an individual tick cell culture was reported to produce infectious SFV for over a year (Bell-Sakyi et al., 2012). In the last decade however, with the advancement of technology and molecular techniques and the availability of several different tick cell lines derived from important vector species, the use of tick cell lines for research has broadened to include studies on tick biology, genomics, proteomics, genetic manipulation and the tick-pathogen interface (Bell-Sakyi et al., 2007, 2012).

As with mammalian cell lines which are invaluable for answering important research questions, tick cell lines are powerful tools and will be useful to elucidate the complex interactions of viruses and their vectors at the cellular and molecular level (Nuttall, 2009), especially since RNA interference (RNAi) can be successfully employed for knocking down tick genes *in vitro* (Barry et al., 2013; Blouin et al., 2008).

With respect to TBEV and LGTV, research in tick cells has been limited with most studies, especially in the early 1970s and 1980s but also more recently, focusing on propagating both viruses in either primary tick cell cultures (Rehacek, 1964, 1965, 1973, 1987) or continuous tick cell lines (Bell-Sakyi, Růzek & Gould, 2009; Bhat & Yunker, 1979; Lawrie et al., 2004; Leake, Pudney & Varma, 1980; Pudney, Varma & Leake, 1979; Růzek et al., 2008; Varma, Pudney & Leake, 1975; Yunker, Cory & Meibos, 1981). However, some of these studies in addition to showing susceptibility of tick cell lines for these viruses, revealed other important aspects, including that tick cell lines might be useful tools to study vector-virus and non-vector-virus relationships, since cell lines derived from natural vectors of TBEV produced higher viral titres than non-vector cell lines (Růzek et al., 2008). Furthermore, they demonstrated the occurrence of homologous interference upon superinfection with either wildtype or temperature sensitive strains of TBEV (Kopecký & Stanková, 1998) and heterologous interference between an orbivirus and TBEV in primary tick cell cultures (Rehacek, 1987). More recently, studies employed TBEV- or LGTV-infected tick cells for studying and comparing the distribution of viral proteins and the virus maturation cycle, including the induction of ultrastructural changes upon

virus infection, between tick and mammalian cells (Offerdahl et al., 2012; Senigl, Grubhoffer & Kopecký, 2006; Senigl, Kopecký & Grubhoffer, 2004). A comparative study in which the NS2B/3 cleavage site of the C protein of TBEV was replaced with a 2A cleavage site of foot-and-mouth disease virus (FMDV), showed that virus replication is abrogated by this mutation in tick cells but not in mammalian cells, suggesting that interactions between the viral C protein and cellular factors are different in mammalian and tick cells (Schrauf et al., 2009). Furthermore, a study comparing phenotypic changes in TBEV with or without the protein E *N*-linked glycan, in mammalian cells, mice and a tick cell line, showed that glycosylation is critical for virus activity in mammals but not in tick cells (Yoshii et al., 2013). These studies highlight the fact that tick cells are useful research tools for studying the interactions between a virus and its tick vector at the cellular and molecular level.

1.3 Innate immunity

1.3.1 Antiviral innate immunity in arthropods

Arthropod immunity was generally considered to rely solely on innate immune defences, in contrast to vertebrates which have both innate and adaptive immune responses protecting them from virus infections (Little & Kraaijeveld, 2004; Quintin et al., 2014). However, there is also evidence in arthropods for an immune response resembling the adaptive immunity of vertebrates. The hypervariable immunoglobulin (Ig)-superfamily receptor Down syndrome cell adhesion molecule (Dscam) exhibits pathogen specificity in insects and crustaceans (Chiang et al., 2013; Dong, Taylor & Dimopoulos, 2006; Watson et al., 2005). Most of the knowledge of antiviral immunity in arthropods has been obtained from studies in insects (Fragkoudis et al., 2009; Fullaondo & Lee, 2012; Kemp & Imler, 2009; Kingsolver, Huang & Hardy, 2013; Merkling & van Rij, 2012; Sabin, Hanna & Cherry, 2010) but there is also increasing evidence for antiviral defence responses in crustaceans (Li & Xiang, 2013a; Liu, Söderhäll & Jiravanichpaisal, 2009). When arboviruses are taken up in a blood meal by blood-feeding vectors they have to overcome several barriers within the arthropod vector, namely the midgut, haemolymph/haemocoel and salivary glands, and face the corresponding cellular and humoral immune responses before

they can be transmitted to another vertebrate host. In general, innate immune defence is characterised by recognition of pathogen-associated molecular patterns (PAMPs) by pattern recognition receptors (PRRs), which upon binding of PAMPs start a signalling cascade leading to the production of antimicrobial effector molecules. Interestingly, true insect pathogens can be cleared by innate immune responses (Kingsolver, Huang & Hardy, 2013), whereas the insect innate immune system only limits the spread of arboviruses it does not clear the infection allowing for transmission of the virus to a vertebrate host. Possibly the most important antiviral response in insects discovered to date is RNAi (Blair, 2011) but Toll, Immune deficiency (IMD) and Janus kinase-signal transducers and activators of transcription (JAK/STAT) signalling pathways, melanisation, autophagy and possibly heat-shock proteins (HSP) also play a role in limiting virus infection (Kingsolver, Huang & Hardy, 2013; Merkling & van Rij, 2012).

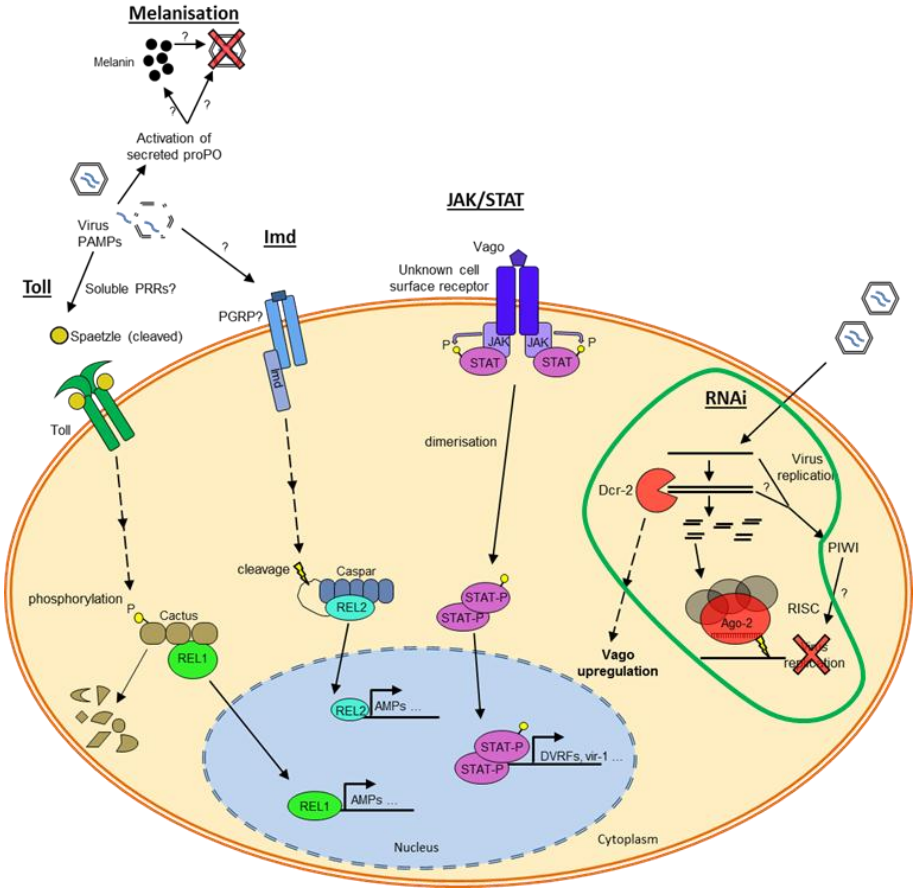

Figure 1.7 Major antiviral innate immunity pathways in mosquitoes and ticks

The only antiviral innate immunity pathways shown to be effective in ticks, RNAi, is delineated by a green circle. Toll pathway: Detection of PAMPs, possibly virus debris or virus PAMPS, by an extracellular PRR triggers a signalling cascade activating the cytokine Spaetzle. Active Spaetzle binds to the Toll receptor, inducing its dimerisation, and a downstream signalling cascade phosphorylates and thus targets the negative regulator Cactus for degradation. This releases Relish (REL) 1 which translocates to the nucleus to activate the transcription of effector genes. IMD pathway: Binding of peptidoglycan from Gram-negative bacteria, virus debris or virus PAMPs to a peptidoglycan recognition protein (PRGP)-like receptor activates IMD and subsequently activates a signalling cascade which results in cleavage of Caspar. The released REL2 translocates to the nucleus and activates transcription of effector genes. JAK/STAT pathway: Upon recognition of viral dsRNA by Dicer (Dcr)-2 a signalling cascade is activated leading to the secretion of the interferon-like molecule Vago which binds to an unknown surface receptor on neighbouring cells. Binding of Vago leads to activation of JAK, which phosphorylates STAT and phosphorylated STAT dimerises. The dimers of STAT act as transcription factors activating the transcription of effector genes. RNAi: Dcr-2 recognises viral dsRNA and cleaves it into 21 nt virus-derived small interfering RNAs (viRNAs) which become incorporated into the RNA-induced silencing complex (RISC). The passenger strand of the dsRNA is subsequently degraded and the guide strand used to target the viral genome. Argonaute (Ago)-2 in the RISC complex degrades viral RNA and inhibits the synthesis of viral proteins. Melanisation: Recognition of bacteria and some viruses leads to cleavage of prophenoloxidase (proPO) by the prophenoloxidase-activating (PAP) enzyme. The active phenoloxidase (PO) results in the production of melanin and also reduction of infectious virus production, however it is not clear if this is caused by melanin. Image was adapted from Rückert et al. (Rückert et al., accepted for publication in Virus disease 2014).

1.3.1.1 RNA interference pathways

RNAi as an antiviral response is conserved in many organisms including plants and invertebrates (Ding & Voinnet, 2007). Most of the information about the different components of the RNAi pathway and the biology of small RNAs in invertebrates has been obtained from the model organism *Drosophila* (Kemp & Imler, 2009) but among arbovirus vectors mosquitoes are the most thoroughly studied in respect to RNAi. There are currently three different RNAi-related pathways characterised, namely the exogenous or endogenous small interfering RNA (siRNA) pathway, the micro-RNA (miRNA) pathway and the p-element induced wimpy testis (PIWI)-interacting RNA (piRNA) pathway. The one currently believed to be most important in antiviral immunity is the exogenous siRNA pathway, although miRNA and piRNA pathways have also been implicated in the control of virus infection (Donald, Kohl & Schnettler, 2012; Rückert et al., accepted for publication in Virus disease 2014; Vijayendran et al., 2013).

The exogenous siRNA pathway is considered to be the most important antiviral pathway in arbovirus vectors such as mosquitoes (Blair, 2011) with a mechanism similar to the one described for *Drosophila* (Donald, Kohl & Schnettler, 2012; Fragkoudis et al., 2009). Upon virus infection siRNAs can be generated from dsRNA genomes, from dsRNAs formed as replication intermediates during ssRNA virus infection or from secondary structures of ssRNA genomes (Ding, 2010; Fragkoudis et al., 2009; Kingsolver, Huang & Hardy, 2013). The mechanism of siRNA gene silencing starts with the recognition of dsRNA as a PAMP by the RNAse III endoribonuclease Dcr-2 which, together with the dsRNA binding protein R2D2 (Liu et al., 2003), cleaves dsRNA into virus-derived siRNA (viRNA) (Bernstein et al., 2001; Lee et al., 2004) usually 21 nt in length, although slightly longer viRNAs, of 22 nt in length, have recently been observed in ticks (Schnettler et al., 2014). Upon cleavage, double-stranded viRNAs are incorporated into the RNA-induced silencing complex (RISC), where Ago-2, an integral part of the RISC also known as slicer, unwinds and incorporates the so-called guide strand of the RNA (Okamura et al., 2004). The unnecessary passenger strand is removed by the endonuclease C3PO (Liu et al., 2009). The guide strand is then used to recognise complementary RNA sequences such as viral ssRNA. Upon interaction with the target RNA, Ago-2

cleaves the target (Rand et al., 2004) resulting in silencing and, in the case of viral RNA, suppression of viral replication. Interestingly, the PRR Dcr-2 has also been implicated in signalling in *Culex* mosquitoes, by leading to secretion of a JAK/STAT-activating ligand with an interferon-like function (Paradkar et al., 2012), linking the RNAi pathway to the antiviral signalling response. The importance of the RNAi pathway in antiviral defence was demonstrated by studies done in *Drosophila* which showed that flies with null or loss-of-function-mutations in *Dcr-2* or *Ago-2* failed to control virus replication leading to higher disease prevalence in comparison to wild-type counterparts (Galiana-Arnoux et al., 2006; van Rij et al., 2006; Wang et al., 2006; Zambon, Vakharia & Wu, 2006). Similarly inhibition of the RNAi pathway in mosquitoes by the Flock house virus (FHV) B2 protein upon SINV infection resulted in increased pathogenesis accompanied by higher virus accumulation (Myles et al., 2008). An important feature of effective antiviral RNAi-based immunity is the systemic spread of RNAi. Systemic RNAi and amplification of small RNAs by RdRP have been observed in plants and *Caenorhabditis elegans* (Voinnet, 2005), but to date no RdRP has been identified in insects (Lipardi & Paterson, 2011) although ticks, according to Kurscheid et al (2009), seem to encode an RdRP but its role in amplification of small RNAs has not been proven. Studies in *Drosophila* cells have identified components of the dsRNA uptake machinery (Karlikow, Goic & Saleh, 2014) and, although they lack RdRP, a mechanism for amplification of the dsRNA signal through integration of a DNA copy into the genome of infected cells was proposed (Goic et al., 2013). In the suggested model, viral RNA is reverse-transcribed and integrated into retrotransposable elements in the cell genome serving as template for the generation of new viral RNA (Goic et al., 2013). Interestingly, a study done in *Haemaphysalis longicornis* implicated the class B scavenger receptor CD36 as playing an essential role in the systemic spread of RNAi in ticks (Aung et al., 2011), however the detailed mechanism remains unknown.

It has been shown that many insect and plant viruses are able to suppress or evade the RNAi response (Donald, Kohl & Schnettler, 2012; Kingsolver, Huang & Hardy, 2013). However arboviruses, although they appear to be able to evade the RNAi response and establish a persistent infection with little pathogenesis (Kingsolver, Huang & Hardy, 2013), they are generally not thought to encode efficient

suppressors of RNAi. The only arboviruses currently known to encode RNAi suppressors belong to the family *Flaviviridae*. Both WNV and DENV-1 were shown to encode a subgenomic flavivirus RNA (sfRNA) corresponding to the 3' untranslated region, that countered the RNAi response in both mammalian and insect cells (Schnettler et al., 2012). In the case of WNV, this disrupted the function of Dcr (Schnettler et al., 2012). Although Schnettler et al (2012) did not identify any role for viral proteins in the inhibition of RNAi, a subsequent study in mammalian and insect cells using DENV-2 has implicated NS4B as a suppressor of the miRNA and siRNA pathway (Kakumani et al., 2013).

The miRNA pathway is an important mechanism for regulation of gene expression at the post-transcriptional level and is shared by many organisms including plants, mammals and invertebrates (Berezikov, 2011). The biogenesis of RNA was recently reviewed (Lucas & Raikhel, 2013): in brief, miRNAs are encoded within the genome and transcribed by RNA polymerase II resulting in transcripts which form partial dsRNA stem-loop structure molecules called primary miRNA (pri-miRNA). In *Drosophila* this pri-miRNA is recognised and cleaved by the microprocessor complex, consisting of the RNase III enzyme Drosha and the dsRNA binding protein Pasha, into ~70 nt long precursor miRNA (pre-miRNA) with a 2 nt 3' overhang which is subsequently exported from the nucleus. Further processing of the pre-miRNA by Dcr-1 in coordination with its cofactor Loquacious, a dsRNA binding protein, in the cytoplasm results in 21-24 nt long mature miRNA/miRNA* duplex molecules which, unlike siRNAs, are not completely double-stranded. One strand of the duplex is incorporated into a miRNA-induced silencing complex (miRISC) with the key component Ago-1 and serves as guide strand for either degradation or translational inhibition of perfectly- or partly-complementary RNA sequences respectively. Although this process was described in more detail in *Drosophila* it is widely believed that the mechanism is conserved among insects including mosquitoes. A number of different miRNAs, conserved and species-specific, have been observed in different arthropods such as mosquitoes (Li et al., 2009b; Mendes et al., 2010; Skalsky et al., 2010) and ticks (Barrero et al., 2011). In *Drosophila melanogaster* some miRNAs have been implicated in regulation of the immune response (Asgari, 2013), such as miR-8 (Choi & Hyun, 2012) and let-7 (Garbuzov &

Tatar, 2010) miRNAs which are involved in the regulation of antimicrobial peptides (AMPs). Similarly a study in the shrimp *Marsupenaeus japonicus* identified a total of 24 miRNAs possibly involved in the regulation of the innate immune responses apoptosis, phagocytosis and melanisation (Yang et al., 2012). In the mosquito species *Anopheles gambiae* and *Ae. aegypti*, miRNAs controlling melanisation (Thirugnanasambantham et al., 2013) or immune-related genes, respectively, such as *Cactus* and *Rel1* (Hussain et al., 2013), have been identified and one miRNA was shown to enhance DENV-2 infection of mosquito cells (Hussain et al., 2013). Interestingly, WNV (Kunjin strain) encodes a miRNA-like molecule in the 3' untranslated region which seems to regulate a target transcript important for virus replication (Hussain et al., 2012).

The piRNA-pathway is different from the other small RNA pathways by being Dcr-independent (Vagin et al., 2006). Initially it was thought that the piRNA pathway is only present in germline cells, however PIWI proteins have also been detected in somatic cells (Brennecke et al., 2007). The exact mechanism of piRNA biogenesis is not yet entirely clear and appears to vary between *Drosophila* and mosquitoes (Donald, Kohl & Schnettler, 2012) and between germline and somatic cells (Handler et al., 2013). In *D. melanogaster* piRNAs are generated in two pathways, which are referred to as primary and secondary processing (Ishizu, Siomi & Siomi, 2012; Siomi et al., 2011). During primary processing piRNA clusters or transposons encoded within the genome are transcribed in antisense, are subsequently shortened forming the 5' end of the mature piRNA, and the 3' ends are trimmed by a PIWI protein generating mature piRNAs of 24-32 nt in length. The loaded piRNA-induced silencing complex (piRISC) will then target and cleave complementary RNA. Secondary processing in the so-called ping-pong amplification loop does not occur in all cell types (Siomi et al., 2011). Briefly, primary piRNAs interact with complementary RNA which is cleaved by piRISC resulting in secondary piRNAs in sense orientation. These secondary piRNAs are then incorporated into Ago-3 which targets complementary antisense RNA giving again rise to primary piRNAs, completing the loop. piRNAs are not only distinct from other small RNAs in that they are produced independent of Dcr, but also in that they do not generally form hairpin or other secondary structures, do exhibit a bias for Uracil at position 1 in the

primary antisense piRNAs and do exhibit a bias for Adenosine at position 10 in the secondary sense piRNAs. The role of piRNAi was thought to be only in protecting germline cells from transposable elements but, with the discovery of virus-specific piRNAs in *Drosophila* ovary somatic sheet cells, a possible role for piRNAs in antiviral defence was suggested (Wu et al., 2010). This was followed by several reports of virus-specific piRNAs produced in different mosquito species or mosquito-derived cell lines upon infection with CHIKV (Morazzani et al., 2012), DENV (Hess et al., 2011; Scott et al., 2010), SINV (Vodovar et al., 2012), La Crosse virus (LACV) (Vodovar et al., 2012), Rift Valley fever virus (RVFV) (Léger et al., 2013), Schmallenberg virus (Schnettler et al., 2012) and SFV (Schnettler et al., 2013a) hinting at a possible role during virus infection. A study done by Schnettler et al. (2013) showed that on knocking down PIWI 4 in mosquito cells, SFV replication increased demonstrating that the piRNA pathway is involved in the antiviral defence in mosquitoes. The antiviral role in other arthropods is currently unknown.

1.3.1.2 Toll, IMD and JAK/STAT pathways in antiviral defence

In addition to RNAi there is evidence for the involvement of several other signalling pathways in the control of virus infection in arthropod vectors. These pathways include the JAK/STAT, Toll and IMD pathways (Fragkoudis et al., 2009; Kingsolver, Huang & Hardy, 2013; Merkling & van Rij, 2012; Rückert et al., Rückert et al., accepted for publication in Virus disease 2014). All three pathways also play a role during development and in the defence response against other pathogens, with Toll acting against Gram-positive bacteria and fungi and IMD acting against Gram-negative bacteria (Ferrandon et al., 2007). As with RNAi, all three pathways are very well-studied in *Drosophila* and the core signalling pathways remain highly conserved between *Drosophila* and mosquitoes (Waterhouse et al., 2007). The signalling cascades of all three pathways are depicted in Figure 1.7.

The JAK/STAT pathway can be activated by both pathogenic insect viruses (e.g. *Drosophila* C virus (DCV) (Deddouche et al., 2008; Dostert et al., 2005) and FHV (Dostert et al., 2005) in *Drosophila* as well as by arboviruses (e.g. SINV, DENV and WNV) in *Drosophila* and mosquitoes. Upon DCV and SINV virus infection of *Drosophila*, Vago mRNA levels were up-regulated (Deddouche et al., 2008; Dostert

et al., 2005) and Vago, a small cytokine with a function similar to IFN, was subsequently characterised as a secreted protein activating the JAK/STAT pathway during WNV infection in *Culex quinquefasciatus* cells (Paradkar et al., 2012). However, interestingly Vago does not bind to the known JAK/STAT-activating transmembrane receptor Domeless (Dome) suggesting a novel receptor contributing to JAK/STAT activation in insects. The expression of Vago was shown to be dependent on Dcr-2 (Deddouche et al., 2008; Paradkar et al., 2012), which recognises viral dsRNA in a manner similar to mammalian retinoic acid-inducible gene 1 (RIG-I) and melanoma differentiation-associated protein 5 (MDA-5) and initiates a signalling cascade independent of other RNAi components (Deddouche et al., 2008; Paradkar et al., 2012), leading to the expression and secretion of Vago (Paradkar et al., 2012). Secreted Vago then activates the JAK/STAT pathway in neighbouring cells resulting in activation and translocation of STAT. In the nucleus STAT induces the expression of AMPs, such as two DENV restriction factors upon DENV infection (Souza-Neto, Sim & Dimopoulos, 2009) and vir-1 upon WNV infection (Paradkar et al., 2012). JAK/STAT pathway activation inhibited the replication of DENV and WNV in *Ae. aegypti* mosquitoes (Souza-Neto, Sim & Dimopoulos, 2009) and *C. quinquefasciatus* mosquito cells (Paradkar et al., 2012) respectively. However no up-regulation of Vago and activation of STAT was observed upon poly I:C (synthetic dsRNA analogue) or bluetongue virus (BTV) dsRNA transfection in *C. quinquefasciatus* cells (Paradkar et al., 2012) and no activation of STAT was observed in SFV-infected *Ae. albopictus* U4.4 cells (Fragkoudis et al., 2008) which suggests a tailoring of immune responses for specific viruses. However, prior activation of the JAK/STAT pathway using heat-inactivated *Escherichia coli* in U4.4 cells resulted in a reduction in SFV replication but it is unclear if this reduction was caused by JAK/STAT or the IMD pathway or both (Fragkoudis et al., 2008). Furthermore SINV infection of *D. melanogaster* resulted in increased expression of Vago and the AMP attacin-C which was shown to have an antiviral function against SINV (Huang et al., 2013).

In other arthropods such as shrimps, JAK/STAT is suspected to play a role during white spot syndrome virus (WSSV) infection, since transcription of STAT was modulated (Chen et al., 2008; Liu et al., 2007; Sun et al., 2011) and it was shown that

STAT was used to activate viral gene expression. However, further clarification of the function of JAK/STAT during virus infection is needed not only for shrimps but also for other arthropods. A recent study in ticks identified JAK/STAT as an antimicrobial defence against the intracellular bacterium *Anaplasma phagocytophilum* (Liu et al., 2012b), reviewed below in 1.3.2.3, but there is currently no information on whether this pathway is also involved in antiviral defence in ticks.

The Toll pathway of arthropods shows similarity with the mammalian toll-like receptor (TLR) pathway, at least in the downstream signalling cascade. The most pronounced difference however is that, unlike mammalian TLRs, arthropod Toll receptors are not PRRs; instead pattern recognition is mediated by extracellular PRRs (Kurata, Ariki & Kawabata, 2006; Li & Xiang, 2013b). Upon recognition of PAMP from Gram-positive bacteria, fungi and possibly also virus debris (Merkling & van Rij, 2012), the cytokine spaetzle is activated by removal of the prodomain, allowing direct binding to Toll (Arnot, Gay & Gangloff, 2010; Weber et al., 2003). This triggers a signalling cascade resulting in the degradation of the inhibitor κB (IκB) orthologue Cactus and activation of the transcription factor REL1, an orthologue of nuclear factor κB (NFκB) in mosquitoes (Shin et al., 2005), which subsequently translocates to the nucleus for transcription initiation of AMPs. Upon DENV-2 infection of *Ae. aegypti* mosquitoes, several Toll pathway-related transcripts were differentially expressed and subsequent knockdown of the negative regulator Cactus or the Toll pathway component myeloid differentiation primary response genes (MYD88) led to decrease or increase of virus titres respectively (Xi, Ramirez & Dimopoulos, 2008), demonstrating the important antiviral role of the Toll pathway. This was confirmed by another study using different DENV serotypes in *Ae. aegypti* mosquitoes (Ramirez & Dimopoulos, 2010). Although up-regulation of the Toll dependent transcription factor REL1 was observed upon SINV infection of *Ae. aegypti* mosquitoes (Sanders et al., 2005), the current evidence suggests that Toll might not be involved in the control of alphavirus infection in insects. An antiviral role for Toll could be established neither for SFV in U4.4 cells in which a constitutively active Toll did not reduce SFV replication (Fragkoudis et al., 2008) nor for SINV in *Drosophila* in which mutations in the transcription factors Dorsal and Dorsal- related immune factor (Dif) did not show any effect on virus replication

(Avadhanula et al., 2009). Furthermore, infection of *A. gambiae* with the alphavirus ONNV failed to induce the expression of Toll pathway components and knockdown of either Cactus nor REL1 showed no effect on virus titres, suggesting that Toll is not involved in the antiviral response to ONNV (Waldock, Olson & Christophides, 2012). The above-mentioned studies showed that Toll might be involved in the antiviral defence response to flaviviruses but not alphaviruses in insects.

In other arthropods the antiviral role of Toll has not yet been characterised apart from in shrimps, in which Toll and spaetzle orthologues were found to be up-regulated upon WSSV infection (Wang et al., 2012) but silencing of Toll did not increase mortality of the infected shrimps (Labreuche et al., 2009).

The IMD pathway in mosquitoes is known to be active against Gram-negative bacteria. Upon recognition of peptidoglycan by PRRs both intra- and extracellularly, a signalling cascade (Kingsolver, Huang & Hardy, 2013; Merkling & van Rij, 2012) is activated leading to the cleavage and activation of REL2 (Shin et al., 2002), another NF-κB orthologue with homology to *Drosophila* relish (Shin et al., 2002), leading to the transcriptional activation of AMPs such as Diptericin. In *Drosophila* the IMD pathway has been implicated in the antiviral defence against insect viruses including cricket paralysis virus (CrPV) (Costa et al., 2009), nora virus (Cordes, Licking-Murray & Carlson, 2013) and the rhabdovirus sigma virus (SIGMAV) (Tsai et al., 2008). Another study using SIGMAV in *Drosophila* however did not find any activation of the IMD pathway, which was suggested to result from a different experimental design including the genetic background of the *Drosophila* strains used (Carpenter et al., 2009). With respect to arboviruses in insects, so far only alphaviruses have been shown to be controlled by the IMD pathway (Kingsolver, Huang & Hardy, 2013; Merkling & van Rij, 2012; Rückert et al., Rückert et al., accepted for publication in Virus disease 2014). Transgenic *D. melanogaster* flies harbouring SINV replicons showed increased replicon RNA levels upon mutation of IMD pathway components (Avadhanula et al., 2009). SINV activation of the IMD pathway was accompanied by an increase in Diptericin B which was shown in a follow-up study to have an antiviral effect on SINV (Huang et al., 2013). Furthermore, heat-inactivated *E. coli* pre-activation of the IMD pathway in mosquito cells resulted in a decrease in SFV replication (Fragkoudis et al., 2008). A study in

the mosquito *A. gambiae* observed differential expression of IMD pathway components and effector molecules upon ONNV infection but subsequent knockdown of REL2 did not result in changes in virus titres (Waldock, Olson & Christophides, 2012). The authors suggested that this reflects a minor contribution of the IMD pathway in the antiviral response against ONNV, with RNAi having the most influence. In contrast to the Toll pathway which was shown to play a role in the antiviral defence against flaviviruses but not alphaviruses, current evidence indicates that IMD is involved in alphavirus but not flavivirus antiviral defence, suggesting that different signalling pathways have adapted to control different virus families.

In arthropods such as shrimps and ticks, not much is known about the biological role of the IMD pathway either during viral or microbial infection. In shrimps orthologues of IMD (Wang et al., 2009) and Relish (Huang et al., 2009; Li et al., 2009a) have been identified which were both differentially expressed upon virus infection (Li et al., 2010; Wang et al., 2009), suggesting a role for the IMD pathway during virus infection in these crustaceans. In ticks, orthologous of REL2 and Caspar but not IMD itself were identified in the *I. scapularis* genome (Kopácek et al., 2010). Interestingly NF-κB orthologues RelA and RelB, which act as transcription factors, showed increased binding activity in ISE6 cells upon *A. phagocytophilum* infection (Naranjo et al., 2013) suggesting a possible activation of the IMD pathway. The role during virus infection however is unclear. Further studies are needed to identify further components of the IMD pathway in shrimps and ticks and to clarify their role during viral and/or bacterial infection.

1.3.1.3 Melanisation

Melanisation is an important process involved in wound healing and in the defence response against pathogens in arthropods and some other invertebrates (Amparyup, Charoensapsri & Tassanakajon, 2013; Cerenius, Lee & Söderhäll, 2008; Christensen et al., 2005). The humoral immune response takes place in the haemolymph and is initiated by a serine protease cascade upon pathogen recognition, leading to the activation of a prophenoloxidase activating enzyme (PAP) which subsequently cleaves the prophenoloxidase (proPO) into catalytically active phenoloxidase (PO), resulting in the production of cytotoxic intermediates as well as melanin (Amparyup,

Charoensapsri & Tassanakajon, 2013; Cerenius, Lee & Söderhäll, 2008; Christensen et al., 2005). The first study implicating the PO cascade in the antiviral defence response in mosquitoes showed that knocking down proPO I in *Amigeres subalbatus* by dsRNA expressed from recombinant SINV resulted in not only reduced PO activity but also higher SINV titres (Tamang et al., 2004). The antiviral role of PO was recently confirmed in *Ae. aegypti* mosquitoes upon SFV infection (Rodriguez-Andres et al., 2012). The authors showed that SFV induces PO activity at a level similar to *E. coli*, which in conditioned medium is accompanied by reduced virus titres. Furthermore they showed that upon integration into the SFV genome of the PO cascade inhibitor Egf1.0, a viral protein from *Microplitis demolitor* bracovirus which inhibits the activation of proPAP to PAP, virus replication increased accompanied by higher mortality of the infected mosquitoes (Rodriguez-Andres et al., 2012). A study done by Waldock et al. (2012) showed that ONNV infection of *A. gambiae* led to up-regulation of melanisation inhibitors suggesting a suppression of the melanisation cascade which was confirmed by a reduction of *Plasmodium* ookinete melanisation upon co-infection (Waldock, Olson & Christophides, 2012).

The role of the PO cascade during viral infection in other arthropods however has not yet been elucidated although WSSV infection of *Litopenaeus vannamei* shrimps resulted in down-regulation of proPO transcripts (Ai et al., 2008, 2009) suggesting that, similar to ONNV in mosquitoes, WSSV might suppress melanisation.

1.3.1.4 Other antiviral defence responses

Besides RNAi, Toll, IMD and JAK/STAT signalling pathways and melanisation there are other responses in arthropods involved in controlling virus infection including cell stress responses such as autophagy and the regulation of HSPs (Kingsolver, Huang & Hardy, 2013; Merkling & van Rij, 2012).

Autophagy is an important process for growth and homoeostasis through degradation of cell components and recycling of organelles under nutrient-deprived conditions (Kuma et al., 2004; Mizushima et al., 2004). The signalling of autophagy is mediated through the phosphoinositide3-kinase (PI3K)-Akt pathway which activates the negative regulator target of rapamycin (TOR) thereby inhibiting autophagy. The loss

of signalling through this pathway, on the other hand, allows autophagy to occur. A direct antiviral role for autophagy was shown in a study using the rhabdovirus vesicular stomatitis virus (VSV) in *Drosophila* (Shelly et al., 2009). In this study, dsRNA silencing of autophagy pathway components resulted in increased VSV production in both *Drosopila* S2 cells and adult flies and the authors showed that the glycoprotein of VSV, rather than virus replication, serves as the PAMP to trigger autophagy (Shelly et al., 2009). The *Drosophila* TLR7 was subsequently implicated as a PRR upstream of the autophagy pathway, binding VSV at the cell surface and thereby activating autophagy (Nakamoto et al., 2012). Interestingly, rather than showing an antiviral role as was observed during VSV infection, PI3K-Akt pathway exhibited a proviral role in *Ae. albopictus* cells and *Drosophila* upon SINV infection (Patel & Hardy, 2012). Furthermore SINV infection activates the PI3K-Akt pathway, possibly by the formation of replication complexes, leading to higher virus titres and increased cap-dependent translation (Patel & Hardy, 2012). One of the difficulties in studying virus-autophagy interactions, as suggested by Cherry (2009), is that many pathogens have developed strategies to evade autophagy, thus the use of virus-host pairs that have not coevolved, such as VSV and *Drosophila*, might reveal antiviral activities which would be masked under natural conditions (Cherry, 2009). Other possible antiviral molecules include HSPs since for example knockdown of HSC70B, a member of the HSP70 family, increased ONNV replication in *A. gambiae* and resulted in a decreased survival rate (Sim et al., 2007), suggesting an important role during virus infection. Interestingly a study done in *Drosophila* S2 cells revealed that the HSP70/HSP90 machinery is required for loading siRNAs into the RISC, implying that HSP up-regulation indirectly exhibits an antiviral role by supporting efficient antiviral RNAi (Iwasaki et al., 2010).

1.3.2 Tick innate immunity

In comparison to other arthropods such as *Drosophila*, mosquitoes, horseshoe crab and shrimps, there is only fragmentary knowledge about the tick innate immune system (Hajdušek et al., 2013; Kopácek et al., 2010; Taylor, 2006) and very little knowledge about the antiviral defence response. However, RNAi has been

implicated as an antiviral defence response in ticks (Garcia et al., 2005, 2006; Schnettler et al., 2014).

What is known about the tick innate immune system however shows that ticks can protect themselves against microbial infection by cell-mediated and/or humoral immune responses. These processes are not independent of each other but contribute synergistically to the innate defence response in ticks.

1.3.2.1 Cellular defence response

The cellular defence response is mediated by haemocytes and includes the processes of phagocytosis, encapsulation and nodulation. Three major haemocyte classes, plasmatocytes and granulocytes I and II, were described in hard and soft ticks with a fourth, namely spherulocytes, only described in the soft tick *O. moubata* (Borovičková & Hypša, 2005). Of these haemocyte classes, plasmatocytes and granulocytes I are involved in phagocytosis. Several studies in different tick species have shown *in vitro* and *in vivo* that haemocytes are capable of phagocytosing inert foreign material (Inoue et al., 2001; Kuhn & Haug, 1994) and different microbes including yeast (Esteves et al., 2008; Loosová, Jindrák & Kopácek, 2001; Pereira et al., 2001) and bacteria (Bazlikova, Kazar & Schramek, 1984; Buresová, Franta & Kopácek, 2006; Johns et al., 2001; Johns, Sonenshine & Hynes, 2000; Kuhn & Haug, 1994; Rittig et al., 1996). Interestingly, several tick cell lines, such as the *Dermacentor andersoni*-derived cell line DAE15 and the *I. scapularis*-derived cell line IDE12 have also been shown to be capable of phagocytosis of the spirochaete *B. burgdorferi* (Mattila, Munderloh & Kurtti, 2007) using, at least in part, the process of "coiling" phagocytosis which was described for the uptake of *B. burgdorferi* in vertebrate and invertebrate species (Rittig et al., 1996). Although phagocytosis usually results in the elimination of microbes, two studies using a mould in tick cell lines (Kurtti & Keyhani, 2008) and *A. phagocytophilum* in *I. scapularis* haemocytes (Liu et al., 2011) implicated that some pathogens might take advantage of the process of phagocytosis to gain entry into cells or migrate to salivary glands respectively, thus possibly hiding from attack by humoral immune responses (Hajdušek et al., 2013). Apart from the ability to engulf and degrade pathogens, little is known about the regulation of the haemocyte-mediated cellular immune response in ticks, such as

recognition, signalling or degradation, in comparison to insects (Lavine & Strand, 2002; Marmaras & Lampropoulou, 2009). Studies in *I. ricinus* ticks however revealed that phagocytosis of *Chryseobacterium indologenes* and *E. coli* by haemocytes is mediated by complement-like molecules (Buresova et al., 2009, 2011) linking the cellular and humoral immune responses. Another study done in *Rhipicephalus microplus* experimentally infected with bacteria showed the production of reactive oxygen species (ROS) by haemocytes after stimulation with the gram-positive bacterium *Micrococcus luteus* and suggested a role for ROS in killing of microbes and/or signalling within the NF-kB pathway (Pereira et al., 2001). Several PRRs are known in vertebrates (Hansen, Vojtech & Laing, 2011) and arthropods (Kurata, Ariki & Kawabata, 2006; Li & Xiang, 2013a; Pal & Wu, 2009; Wang & Wang, 2013) and one of these, HlSRB, a homologue of the class B Scavenger receptor CD36, is up-regulated upon *E. coli* infection of *H. longicornis* haemocytes where it has been shown to play a vital role in granulocyte-mediated phagocytosis (Aung et al., 2012). The studies described above indicate the importance of phagocytosis in the antimicrobial defence response in ticks.

Other defence responses at the cellular level, which have also been shown to be important in insects (Lavine & Strand, 2002; Marmaras & Lampropoulou, 2009), include nodulation, which is a process leading to the entrapment of a large number of bacteria in multicellular haemocytic aggregates (Taylor, 2006), and the encapsulation reaction which refers to the binding of haemocytes to larger targets forming a multilayer capsule around the invader (Eggenberger, Lamoreaux & Coons, 1990). Haemocytic encapsulation of epon-araldite implants with the involvement of plasmatocytes and granulocytes I and II in the formation of a capsule with multiple cell layers around the implant (Eggenberger, Lamoreaux & Coons, 1990) and nodulation of *E. coli* in which bacterial clumps were surrounded by haemocytes forming a nodule (Ceraul, Sonenshine & Hynes, 2002) were described in the tick *Dermacentor variabilis*, suggesting a possible role of these processes in the tick innate immune response.

1.3.2.2 Humoral immune response

The humoral immune response of ticks includes lectins, complement-related molecules, a broad spectrum of common and specific AMPs and possibly immune molecules of the host (Hajdušek et al., 2013; Kopácek et al., 2010; Taylor, 2006). Several lectins with binding specificity for N-acetyl-S-hexosamine, sialic acid and different glycoconjugates have been isolated from different tick species and they are believed to play a key role in understanding self/nonself recognition in defence reactions against bacteria or fungi, in pathogen transmission and also in activation of the complement system based on evidence of binding specificity and sequence similiarity to vertebrate and invertebrate lectins (Grubhoffer & Jindrák, 1998; Grubhoffer, Kovář & Rudenko, 2004; Hajdušek et al., 2013; Kopácek et al., 2010; Kopacek, Hajdusek & Buresova, 2012). The broad spectrum of antimicrobial peptides in ticks includes lysozymes, defensins, defensin-like peptides, molecules which seem to be tick-specific and haemoglobin fragments. Lysozymes have been shown to be active against a number of different bacteria species in soft as well as hard ticks (Hajdušek et al., 2013; Kopácek et al., 2010; Taylor, 2006), and lyse bacteria by cleaving glycosidic bonds within the peptidoglycan cell wall. The most-studied antimicrobial peptides in both soft and hard ticks belong to the group of defensins, with a recent study showing that a huge number of defensins grouped into scapularisin and scasin multi-gene families are encoded in the *I. scapularis* genome (Wang & Zhu, 2011). The mode of antimicrobial action of tick defensins was elucidated in a study done by Nakajima et al. (2003), who reported that *O. moubata* defensins cause cytoplasmic membrane lysis in *Micrococcus luteus* (Nakajima et al., 2003a). Furthermore, tick defensins have been shown to be effective against Gram-positive bacteria, Gram-negative bacteria and fungi; however there are differences in the response between tick species as well as differences in the impact depending on the infectious pathogen (Hajdušek et al., 2013; Kopácek et al., 2010; Taylor, 2006), as described for *Anaplasma marginale* in *D. variabilis* ticks in which silencing of the defensin varisin resulted in a decrease in bacterial infection (Kocan et al., 2008). Tick-specific molecules with antimicrobial function include histidine- and/or cysteine-rich AMPs such as microplusin (Fogaça et al., 2004) and ixodidin (Fogaça et al., 2006) isolated from *R. microplus* and hebraein isolated from *Amblyomma*

hebraeum (Lai et al., 2004). The antibacterial function of microplusin is based on its capacity to sequester copper which bacteria require for their respiration (Silva et al., 2009). Other tick-specific AMPs include ixosin (Yu et al., 2006) and ixosin B (Liu et al., 2008) isolated from *Ixodes sinensis*, for which however direct interaction with pathogens has not yet been reported, and IsAMP isolated from *I. scapularis* exerting activity against Gram-negative and -positive bacteria (Pichu, Ribeiro & Mather, 2009). Furthermore, not only tick proteins but also host proteins taken up by ticks seem to play a role during the innate immune response. These host molecules include, for example, haemoglobin fragments which show antimicrobial activity in the midgut of both soft and hard ticks (Fogaça et al., 1999; Nakajima et al., 2003b; Sonenshine et al., 2005), by possibly permeabilising the microbial membrane as determined by structural analysis (Machado et al., 2007; Sforça et al., 2005). The generation of antimicrobial haemoglobin fragments, so called hemocidins, is suspected to occur in the digestive cells by the action of cathepsin D-type and cathepsin L-type aspartic and cysteine peptidases, respectively (Cruz et al., 2010; Horn et al., 2009).

Other molecules important for the tick innate immune response are so-called cystatins, which are reversible papain-like cysteine protease inhibitors, with antimicrobial activity known for L-cystatin against Gram-negative bacteria in the horseshoe crab (Agarwala et al., 1996). In ticks, cystatins were up-regulated upon *Babesia gibsoni* infection in *H. longicornis* ticks and the addition of recombinant cystatin resulted in a slight reduction of *Babesia bovis* growth in culture, suggesting a possible role for cystatins in tick innate immunity (Zhou et al., 2006); however their role during tick infestation has not yet been experimentally examined (Hajdušek et al., 2013).

Interestingly, ticks are unique among invertebrates examined to date in that they contain all major components of the complement system, which includes the protease inhibitor α_2-macroglobulin, C3 complement components, insect thioester-containing proteins (TEP) and macroglobulin-complement related molecules (Buresova et al., 2011). The role of the complement system in the antimicrobial defence response was highlighted by two studies done by Bureseova et al. (2009, 2011). Her first study showed that, upon silencing of an α_2-macroglobulin termed IrAM, decreased

phagocytosis by haemocytes of *C. indologenes* but not *B. burgdorferi* or the Gram–positive bacterium *Staphylococcus xylosus* was observed, suggesting that the observed specificity, which was also observed in *Drosophila* S2 cells (Stroschein-Stevenson et al., 2005), is mediated by an interaction between IrAM and the active metalloprotease secreted by *C. indologenes* (Buresova et al., 2009). The specificity of the complement system was further elucidated by her second study in which the knockdown of two α_2-macroglobulins (IsAM1 and 2) resulted in decreased phagocytosis of *C. indologenes*, while knockdown of TEP (IsAM3) resulted in decreased phagocytosis of *E. coli* but not *C. indologenes* (Buresova et al., 2011). Furthermore, knockdown of C3, which is a central component of the vertebrate complement system, established its absolute requirement in ticks for phagocytosis of both pathogens (Buresova et al., 2011). The authors therefore hypothesised that there are two independent pathways, one initated by α_2-macroglobulin upon infection with protease-secreting bacteria and the other initiated by TEP upon infection with other Gram-negative bacteria, which then ultimately converge in the activation of C3 components leading to phagocytosis (Buresova et al., 2011). These studies highlight the existence of a primitive complement system with importance in the antimicrobial defence response (Kopacek, Hajdusek & Buresova, 2012).

Haemolymph clotting is another important antmicrobial defence response, which is triggered upon recognition of lipopolysaccharide (LPS) (Iwanaga & Lee, 2005; Kawabata & Muta, 2010; Muta & Iwanaga, 1996). Due to the presence of tick molecules related to the horseshoe crab Factor C, which triggers the limulus clotting cascade and the presence of transglutaminase which are involved in crosslinking during the final stage of mesh formation, ticks might also have a system for haemolymph coagulation. However, apart from the study by Eggenberger et al. (1990) which showed the formation of a fibrous matrix around the Epon-Araldite implant in *D. variabilis*, no further evidence has yet been supplied. The presence of an antimicrobial and antiviral proPO system (as described in 1.3.1) in ticks is controversial, since no proPO activity was found in *Amblyomma americanum, D. variabilis* and *I. scapularis* (Zhioua, Yeh & LeBrun, 1997), whereas a study done in *O. moubata* observed proPO activity (Kadota et al., 2002). Furthermore, a factor D-like serine protease that was up-regulated upon *E. coli* infection in *D. variabilis*

showed similarity to insect proPO activating cofactor (Simser et al., 2004). Nevertheless, the absence of a proPO-related gene in the *I. scapularis* genome (Megy et al., 2012) or within the available expressed sequence tag (EST) dataset (Kopácek et al., 2010) might suggest that ticks do not have a functional proPO system.

1.3.2.3 Signalling cascades regulating antimicrobial response

Although the induction and effectiveness of immune molecules against microbes has been shown in several studies mentioned above, there is little knowledge about the regulation of the immune response in ticks. The major signalling pathways in innate immunity in other arthropods include the Toll, IMD and JAK/STAT pathways (Welchman 2009, Ferrandon 2007). Several components of these pathways have been identified in the *I. scapularis* genome (Li et al., 2012b, Megy et al., 2012; Severo et al., 2013a) but there is only one recent study reporting an important role for JAK/STAT in *I. scapularis* ticks during *A. phagocytophilum* infection (Liu et al., 2012b). These authors showed that upon knockdown of STAT or JAK the *A. phagocytophilum* burden increased in infected ticks and that the JAK/STAT pathway controls *A. phagocytophilum* infection by regulating the expression of AMPs of the 5.3 kD gene family. Silencing of members of the Toll and IMD pathways, such as Toll-1, transforming growth factor β activated kinase-1 (TAK1) and TAK1-binding protein (TAB1) however did not have any effect on the bacterial burden (Liu et al., 2012b) but further studies silencing different components of these pathways or testing different bacteria would be required to completely rule out their involvement in antimicrobial defence. Another regulatory protein is subolesin, an orthologue of vertebrate and insect akirins (Galindo et al., 2009; Mangold, Galindo & de la Fuente, 2009), which was found to be involved in the control of gene expression in ticks through interaction with regulatory proteins such as GI and GII (de la Fuente et al., 2008b). An RNAi study in *I. scapularis* suggested that NF-kB participates in the transcription of subolesin while subolesin regulates NF-kB expression in return (Galindo et al., 2009). This was further evaluated in a recent study in ISE6 cells, which found that subolesin is not only involved in the regulation of NF-kB (Relish) gene expression but also NF-kB-independent gene expression, suggesting a regulatory network of cross-regulation between subolesin and NF-kB and also

subolesin autoregulation (Naranjo et al., 2013). Interestingly, upon *A. phagocytophilum* infection of ISE6 cells, Naranjo et al. (2013) observed an increase in binding activity of the NF-kB orthologues RelA and RelB indicating possible activation of the IMD pathway; however no IMD homologue was identified. Additionally, several studies observed differential expression of subolesin and an involvement in tick innate immunity in response to pathogen infection (Kocan et al., 2009; de la Fuente et al., 2006, 2007a, 2008c, 2010; Zivkovic et al., 2010a, 2010b). Not only the immune response but also several other molecular pathways important for physiology and development in ticks could be regulated by the transcription factor activity of subolesin. With the observations that ubiquitin-related molecules are differentially expressed upon *A. marginale* infection of the *I. scapularis* cell line IDE8 (de la Fuente et al., 2007a) and that knockdown of the E3 ubiquitin ligase XIAP increases *A. phagocytophilum* levels in the *I. scapularis* cell line ISE6 and *I. scapularis* midguts and salivary glands (Severo et al., 2013b), more attention is drawn to the ubiquitination process which has been shown to be an important regulator of immune responses not only in mammals (Jiang & Chen, 2012) but also in *Drosophila* (Ferrandon et al., 2007) and other arthropods (Choy et al., 2013; Severo et al., 2013a).

1.3.2.4 RNAi – antiviral defence in ticks?

The only currently-known mechanism with a possible antiviral role in ticks is RNAi (Figure 1.7). RNAi is efficiently exploited for the silencing of genes in ticks and tick cell lines (Blouin et al., 2008; de la Fuente et al., 2007b) and the genome of *I. scapularis* has been shown to contain most of the important components of the endogenous and exogenous RNAi pathway such as Ago, Dcr, dsRNA binding proteins, exonucleases and interestingly also an RdRp (Kurscheid et al., 2009). Furthermore the production of viRNAs (Schnettler et al., 2014; Garcia et al., 2005) and the discovery that viral suppressors, identified in plants and insect cells, are able to interfere with RNAi-mediated silencing of virus (Garcia et al., 2006) supports the role of RNAi as an innate antiviral response in tick cells.

1.4 Hypothesis

TBEV infection of tick cell lines causes differential expression of genes and differential representation of proteins involved in antiviral defence responses.

1.5 Aims of this study

- To characterise viral infection in tick cell lines using the mosquito-borne virus SFV and the tick-borne viruses LGTV and TBEV (Chapter 3)
- To identify novel antiviral defence mechanisms in tick cell lines upon TBEV infection using transcriptomic and proteomic analysis (Chapter 4)
- To determine whether selected differentially-expressed genes and differentially-represented proteins affect virus replication and production (Chapter 5)

2 Chapter 2 Materials and Methods

2.1 Cell lines

2.1.1 Tick cell lines

I. scapularis and *I. ricinus*-derived cell lines ISE6 (Kurtti et al., 1996) and IRE/CTVM19 (Bell-Sakyi et al., 2007) were maintained in sealed flat-sided tubes (Nunc) in 2.2 ml L-15 (Leibovitz) medium supplemented with 10% tryptose phosphate broth (TPB, Sigma), 20% foetal calf serum (FCS, Biosera), 2 mM L-glutamine (Sigma) and antibiotics (100 U/ml penicillin and 100 µg/ml streptomycin [pen/strep], Sigma). The *I. scapularis* cell line IDE8 (Munderloh et al. 1994) was cultured in 2.2 ml L-15B medium (Munderloh & Kurtti, 1989, Appenix I) supplemented with 10% TPB, 5% FCS, 0.1% bovine lipoprotein (MP Biomedicals), 2 mM L-glutamine and pen/strep. IDE8 and ISE6 were incubated at 32°C and IRE/CTVM19 at 28ºC in ambient air in dry incubators. Medium was changed once a week by removal and replacement of 1.5 ml medium. Every 2- 3 weeks cells were subcultured by adding 2.2 ml fresh medium, detaching the cells by pipetting and transferring 2.2 ml cell suspension to a new tube. Tick cell lines were continuously passaged without freezing.

2.1.2 Mammalian cell lines

All mammalian cell lines were maintained in sterile plasticware (Nunc) at 37°C in a humidified incubator with an atmosphere of 5% CO_2 in air. Baby hamster kidney (BHK)-21 cells and BSR cells (a clone from BHK-21 cells) were grown in Glasgow's Minimal Essential Medium (GMEM, Gibco) supplemented with 5% newborn calf serum (NBCS, Biosera), 10% TPB, 2 mM L-glutamine and pen/strep (5% NBCS GMEM). Porcine kidney stable (PS) cells (Kozuch & Mayer, 1975) were maintained in L-15 supplemented with 3% NBCS, 10% TPB, 1% glutamine, 1% antibiotic antimycotic solution (containing 100 units/ml penicillin, 100 µg/ml streptomycin and 0.25 µg/ml amphotericin B, Sigma). African green monkey kidney cells (Vero) were maintained in Dulbecco's Modified Eagle's Medium (DMEM, Gibco) supplemented with 10% FCS and pen/strep. All mammalian cell lines were grown in 175 cm^2 flasks and passaged using the same procedure. When cells were

confluent, the medium was removed and the monolayer was washed with 5 ml of neutral phosphate buffered saline (PBS). The PBS was replaced with 5 ml of trypsin/EDTA (0.05% trypsin, 0.53 mM EDTA, Gibco) and incubated at 37°C until the cells detached. Trypsination was stopped by adding 5 ml of appropriate complete culture medium containing serum to neutralise the trypsin. The suspension was centrifuged for 5 min at 450 x g at room temperature, the supernatant discarded and the cell pellet resuspended in 10 ml complete culture medium. Between 1 and 2 ml of the resuspended cells were seeded in sterile 175 cm^2 tissue culture flasks, complete culture medium was added to a final volume of 20 ml and the flasks were incubated at 37°C. When cell growth slowed down, cells were replaced by fresh stocks from liquid nitrogen as described below in 2.1.4.

2.1.3 Counting cells

To seed cells at the correct density for experiments, cells were counted using a Neubauer haemocytometer. In brief, cells were harvested, in the case of tick cells by pipetting (2.1.1) and in the case of mammalian cells by trypsination (2.1.2), pelleted by centrifugation for 5 min at 450 x g at room temperature and the supernatant was discarded. The cells were resuspended in 10 ml complete culture medium and 100 µl of the cell suspension was diluted in 900 µl of growth medium. A 10 µl aliquot was applied to the haemocytometer and the cells in four quadrants, with each quadrant corresponding to a set of 16 squares, were counted. The cell density was calculated using the following formula:

$$mean\ number\ of\ cells\ in\ 1\ ml = \left(\frac{total\ number\ of\ cells}{4}\right) x\ dilution\ factor\ x\ 10^4$$

The cell suspension was diluted with complete culture medium to the required concentration before seeding into multiwell plates or flasks.

2.1.4 Freezing and thawing mammalian cells

To freeze mammalian cells, cells were harvested as described above for passaging (2.1.2), counted and diluted to approximately 5 x 10^6 cells per ml. The cell suspension was then mixed with an equal volume of the appropriate complete culture

medium containing 20% FCS or NBCS and 20% dimethylsulphoxide (DMSO, Sigma-Aldrich). Aliquots of 1 ml of cell suspension were transferred to cryovials (Nunc) and placed in a Mr Frosty Freezing Container (Thermo Scientific) at -80ºC overnight to allow cells to freeze gradually. The next day cells were transferred to the vapour phase of a liquid nitrogen container.

To thaw mammalian cells, the cryovials were removed from liquid nitrogen and immediately placed into a 37°C water bath to allow the cells to thaw quickly. When only a small amount of ice was left in the vial a few drops of prewarmed complete culture medium were added to the cells before pipetting them into a 25 cm^2 tissue culture flask containing 20 ml of prewarmed complete culture medium. Cells were left overnight to settle and medium was either changed the next day to further dilute the toxic DMSO or cells were passaged when confluent.

2.2 Microscopy

2.2.1 Light microscopy

To visualise tick cell cultures growing in tubes, a Zeiss Axiovert Observer inverted microscope was used with filters suitable for eGFP or ZsGreen (green). When cells were grown on coverslips, immunostained and mounted on slides, either a Zeiss Axioskop2 microscope or a Zeiss LSM710 confocal microscope was used with filters suitable for green fluorescence (488 nm) and DAPI (UV). For experiments done in the Czech Republic an Olympus Fluoview FV10 confocal microscope was used. All microscopes were equipped with a charge coupled device (CCD) camera for taking pictures.

2.2.2 Electron microscopy

2.2.2.1 Glutaraldehyde fixation

Uninfected and virus-infected tick cells were harvested into 1.5 ml microfuge tubes and centrifuged at 200 x g for 5 min. Cells were then washed with PBS and centrifuged again. After removing the PBS the cell pellet was resuspended in 1 ml of

3% glutaraldehyde in cacodylate buffer and sent for further processing to the Electron Microscope Unit in the School of Biological Sciences, University of Edinburgh. Steven Mitchell processed the samples as follows: after holding for 2-24 h on ice, cells were post-fixed in 1% osmium tetroxide in cacodylate buffer, dehydrated in acetone and embedded in Araldite resin. The resin blocks were cut into ultrathin sections using a Reichert OMU4 ultramicrotome (Leica) and sections were stained in uranyl acetate and lead citrate. Sections were viewed in a Philips CM120 transmission electron microscope (TEM) and images were taken using a Gatan Orius CCD camera.

2.2.2.2 Cryofixation

To investigate replication complexes in tick cells infected with TBEV, cells were cryofixed and prepared for TEM by Marie Vancová, Laboratory of Electron Microscopy, Institute of Parasitology, University of South Bohemia, Budweis, Czech Republic. In brief, tick cells were harvested into microfuge tubes and centrifuged at 400 x g for 5 min. The supernatant was removed and the cell pellet was overlayed with cryoprotectant consisting of 20% bovine serum albumin (BSA) in PBS and immediately put on ice until freezing. Just before transferring cell pellets onto gold-plated flat specimen carriers (Leica) the cryoprotectant was removed. The cell pellets on specimen carriers were then immediately cryofixed using a Leica EMPACT2 high pressure freezer. The specimens were then either stained for ultrastructural evaluation with 2% osmium tetroxide in 100% acetone or prepared for immuno-localisation in 0.1% glutaraldehyde in 100% acetone. The specimens were embedded in resin blocks; ultrathin sections were cut and transferred onto grids. Samples prepared for ultrastructural analysis were viewed in a JEM-1010 TEM (JEOL) using the MegaView III Soft Imaging system (Olympus). Samples prepared for immuno-localisation were immunolabelled as described below (2.2.2.3).

2.2.2.3 Immunolabelling of cryofixed specimens

For immunolabelling of grids a layer of parafilm was attached to the bottom of a 150 mm x 15 mm petri dish and pieces of wet filter paper were placed around the

edges to create a moist chamber. All solutions used for immunolabelling were filtered through a 0.45 µm syringe filter and centrifuged at 5,000 x g for 2 min. To prevent nonspecific background binding, grids were transferred into drops of 5% goat serum in PBS, pH 7.4 supplemented with 0.02 M glycine and incubated for 60 min at room temperature. After blocking, grids were transferred into drops of E or NS1 protein antibodies (Table 2.9) diluted 1:10, 1:50 and 1:100 in 0.5% goat serum in PBS and incubated for 60 min at room temperature. Grids were then washed 6 x 2 min in drops of PBS prior to staining in drops of gold-labelled anti-mouse secondary antibody (Aurion). Gold particles had a size of 6 nm. After staining, cells were washed 3 x 2 min in PBS before washing 4 x 1 min in de-ionised water. Specimens were then dried and viewed using the JEM-1010 TEM as above (2.2.2.2).

2.3 Bacterial techniques

2.3.1 Bacterial culture

The three *E. coli* strains DH5α (Genotype: F-, φ80dlacZΔM15, Δ(lacZYA-argF), U169, recA1, endA1, hsdR17 (rk-, mk+), phoA, supE44, λ-, thi-1, gyrA96, relA1; Invitrogen), SURE 2 supercompetent (e14-(McrA-), Δ(mcrCB-hsdSMR-mrr)171, endA1, gyrA96, thi-1, supE44, relA1, lacrecB, recJ, sbcC, umuC::Tn5, (Kan^r), uvrC, [F'proAB$lacI^qZ\Delta M15$, Tn10 (Tet^r), Amy Cam^r]; Stratagene) and HB101 (F–, thi-1, hsdS20 (r_B–, m_B–), supE44, recA13, ara-14, leuB6, proA2, lacY1, galK2, rpsL20 (str^r), xyl-5, mtl-1; Promega) were used. Bacteria were grown in either Luria-Bertani (LB) medium or on LB plates containing 1.5% agar. Both substrates were sterilised by autoclaving and supplemented with the appropriate antibiotic (ampicillin (100 µg/ml), kanamycin (50 µg/ml) or tetracycline (15 µg/ml)) to select for clones which were successfully transformed with the respective plasmid. To prepare agar plates, melted LB agar containing antibiotics was poured into 10 cm Petri dishes (Nunc) and left to cool. Transformed bacteria were spread on the agar surface with bacterial cell spreaders and left to dry, before incubating them inverted, to prevent condensation dropping onto the surface, overnight at 37ºC. The process of preparing plates and spreading bacteria was done under aseptic conditions either using a Bunsen burner or in a containment level (CL)-1 cabinet. To grow bacteria, single

colonies were picked from plates, inoculated into LB medium supplemented with the required antibiotic and incubated for approximately 16 h at 37ºC with constant shaking at 225 rpm.

2.3.2 Transformation of bacteria

SURE 2 supercompetent cells, DH5α and HB101 were transformed according to the manufacturer's instructions with plasmids listed in Table 2.1. Briefly, bacteria were thawed on ice and 100 µl aliquots were transferred into 1.5 ml pre-chilled sterile microfuge tubes. For transformation of SURE 2 supercompetent cells, bacteria were spiked with 2 µl of β-mercaptoethanol and incubated for 10 min on ice with gentle swirling every 2 min. Approximately 50 ng of the plasmid DNA in 1 µl was added to the bacteria and the tubes were incubated for 30 min on ice. Bacteria were then heat-shocked for 30 sec at 42ºC and kept on ice for 2 min before pre-warmed Super Optimal broth with Catabolite repression (SOC) medium (Invitrogen) was added to a final volume of 1 ml. For transformation of DH5α, 0.5 µl containing 50 ng of plasmid DNA was added and cells were incubated for 10 min on ice before being heat-shocked for 45 sec at 42ºC. Bacteria were transferred quickly onto ice, where they were left for 2 min prior to adding pre-warmed SOC medium as above. HB101 cells were transformed with between 50 and 100 ng plasmid DNA in 1 µl, gently mixed and incubated on ice for 10 min. Bacteria were then heat-shocked for 50 sec at 42ºC and immediately transferred onto ice for 2 min before adding cold SOC medium. All bacteria in SOC medium were then incubated at 37ºC for 1 h while shaking constantly at 225 rpm in an orbital shaker to allow bacteria to express the antibiotic resistance genes provided by the plasmid. After incubation, aliquots of 50 or 100 µl of the plasmid-transformed bacteria, and bacteria transformed with water alone as a negative control, were plated on pre-warmed LB agar plates supplemented with the respective antibiotic. When the plates were dry, they were inverted and incubated at 37ºC overnight. Only bacteria containing the plasmid and expressing the antibiotic resistance genes grew into colonies, as verified by negative control bacteria not growing on plates containing antibiotics. Single colonies were picked and used to prepare DNA minipreps, maxipreps and glycerol stocks as described below in 2.4.1.1, 2.4.1.2 and 2.3.3 respectively.

Table 2.1 List of plasmids used for cloning, quantitative PCR (qPCR), virus propagation and replicon generation

Plasmids were diluted to the appropriate concentration in nuclease-free water before use. Plasmid pSFV4(3F)-ZsGreen was kindly provided by Dr Rennos Fragkoudis and all plasmids grown in *E.coli* HB101 were kindly provided by Prof. Franz X. Heinz.

Plasmid	*E. coli* strain	Resistance	Source
pJET1.2-NS5	DH5α	Ampicillin	Self-generated (2.9.1), backbone Fermentas
pIRES2-eGFP	DH5α	Kanamycin	Clontech
pRL-SV40	DH5α	Ampicillin	Promega
pGL3-Basic Vector	DH5α	Zeocin	Promega
pSFV4(3F)-ZsGreen	SURE 2 supercompetent	Ampicillin	(Tamberg et al., 2007)
pE5repRluc2B/3	DH5α	Tetracycline	(Schnettler et al., 2014)
pTND/c-EGFP	HB101	Ampicillin	(Gehrke et al., 2005)
pTND/ΔME	HB101	Ampicillin	(Gehrke et al., 2003)
pTND/ΔME-EGFP	HB101	Ampicillin	(Gehrke et al., 2005)
pTND/c	HB101	Ampicillin	(Mandl et al., 1997)
pC17Rluc	HB101	Ampicillin	(Hoenninger et al., 2008)
pC27Rluc	HB101	Ampicillin	(Hoenninger et al., 2008)
pC37Rluc	HB101	Ampicillin	(Hoenninger et al., 2008)
pC17Fluc	HB101	Ampicillin	(Hoenninger et al., 2008)
p17Fluc-FMDV2A	HB101	Ampicillin	(Hoenninger et al., 2008)
pC17Fluc-TAV2A	HB101	Ampicillin	(Hoenninger et al., 2008)

2.3.3 Preparation of glycerol stocks

Frozen stocks of transformed bacteria were made in order to standardise the starting material for maxipreps and minipreps. A single colony of transformed bacteria was picked from an agar plate, inoculated into 5 ml LB medium supplemented with the respective antibiotic and incubated overnight at 37ºC in an orbital shaker at 225 rpm. The next day, 800 µl aliquots of overnight culture were added to 200 µl of sterile glycerol and immediately transferred to -80 ºC. When required a pipette tip was used to scratch the surface of the frozen bacterial suspension and transfer some bacteria to LB medium without allowing the glycerol stock to thaw.

2.4 Nucleic acid techniques

2.4.1 Plasmid DNA extraction from transformed bacteria

All centrifugation steps were carried out at room temperature unless otherwise indicated.

2.4.1.1 Plasmid DNA Miniprep

Plasmid DNA was extracted from transformed bacteria on a small scale using the Isolate II Plasmid Mini Kit (Bioline) according to the manufacturer's instructions, as follows. The volumes of reagents for isolation of low copy plasmids (pTND/c and pTND/c-eGPF) are shown in square brackets.

Single colonies of transformed bacteria were inoculated into 5 ml [10 ml] of antibiotic-containing LB medium which was incubated at 37ºC as described above (2.3.2). The bacteria were then pelleted by centrifugation at 1500 x g for 5 min and the liquid discarded. After resuspending the pellet in 250 µl [500 µl] of resuspension buffer P1, the cell suspension was transferred to a sterile 1.5 ml microfuge tube. Cells were then lysed by addition of 250 µl [500 µl] lysis buffer P2, which solubilises the bacterial membrane and dissociates DNA and proteins. When the lysate appeared clear or after a maximum of 5 min, lysis was stopped by adding 300 µl [600 µl] neutralisation buffer P3 and mixed by inverting the tube. The precipitated protein and membrane lipids were removed by centrifugation at 11,000 x g for 5 min and the supernatant was transferred to an isolate II plasmid mini spin column. After centrifugation at 11,000 x g for 1 min, the flow-through was discarded and the silica membrane washed twice with 500 µl wash buffer PW1 and centrifugation at 11,000 x g for 1 min. Impurities such as salts, metabolites and cellular components were removed by washing with 600 µl of the second washing buffer PW2 and centrifugation at 11,000 x g for 1 min. The flow-through was discarded and the silica membrane dried by centrifugation at 11,000 x g for 2 min. Plasmid DNA was eluted from the column by applying 40 µl RNase/DNase free water directly to the membrane and allowing it to stand for 1 min at room temperature before collecting the plasmid DNA in a 1.5 ml microfuge tube by

centrifugation at 11,000 x g for 1 min. The purified plasmid DNA was then stored at -20ºC.

2.4.1.2 Plasmid DNA Maxiprep

The EndoFree Plasmid Maxi Kit (Qiagen) was used to extract large amounts of plasmid DNA from large volumes of bacterial culture. A single colony was isolated from an LB agar plate and used to inoculate a starter culture of 5 ml LB medium containing antibiotics. After an incubation period of 8 h at 37ºC in an orbital shaker (225 rpm), 500 µl of the starter culture was inoculated into either 250 ml LB medium for high-copy plasmids or 500 ml LB medium for low-copy plasmids supplemented with the appropriate antibiotic and incubated for 16 h at 37ºC with constant shaking. Bacterial cells were harvested by centrifugation at 6,000 x g for 20 min at 4ºC. The cell pellet was then resuspended in 10 ml buffer P1 supplemented with RNase A solution and transferred to a 50 ml centrifuge tube. Bacteria were lysed, as described for the miniprep procedure, by addition of 10 ml lysis buffer P2 and gently mixed by inversion. The mixture was allowed to stand for no more than 5 min before 10 ml of chilled buffer P3 was added to neutralise the lysate which was then poured into the barrel of the QIAfilter Cartridge. After incubation for 10 min at room temperature, to allow the precipitate formed in the previous step to settle at the top of the cartridge, the lysate was pushed through the filter into a 50 ml centrifuge tube. Then 2.5 ml of buffer ER was added to the flow-through, mixed by inverting 10 times and incubated on ice for 30 min. During the incubation period a QIAGEN-tip 500 was equilibrated by applying 10 ml of buffer QBT and allowing it to flow through by gravity. After the 30 min incubation the filtered lysate was added to the QIAGEN-tip, to allow the plasmid DNA to bind to the membrane, and the tip was washed twice with 30 ml buffer QC which was allowed to move through the tip by gravity flow. The DNA was then eluted using 15 ml of buffer QN. In order to precipitate the DNA, 10.5 ml of isopropanol was added and the mixture was centrifuged at 15,000 x g for 30 min at 4ºC. The DNA pellet, formed by precipitation at the bottom of the tube, was washed with 5 ml of 70% ethanol and centrifuged at 15,000 x g for 10 min. After removing the supernatant, the pellet was air-dried for approximately 10 min and

redissolved in 500 µl of endotoxin free Tris-EDTA (TE) buffer (Qiagen). Samples were stored at -20ºC.

2.4.2 Restriction digest

The appropriate restriction enzymes were used to digest different plasmids according to published protocols and/or specified in experiments reported in Chapter 3, 4 and 5. In general, 1 µg of plasmid DNA was digested with 1 unit of enzyme. The enzyme unit indicates the amount of enzyme required to digest 1 µg of plasmid DNA in 1 hour at its optimum temperature in a total reaction volume of 50 µl. The restriction enzyme digests were therefore carried out in a final volume of 40 – 50 µl and the reaction mixture contained respectively: 4 µl or 5 µl of digestion buffer, 4 µl or 5 µl of 10X BSA (Sigma), 1 µl or 3 µl of restriction endonucleases, plasmid DNA (volume varied from 3 -37 µl depending on the concentration of plasmid DNA) and DNase-free water to the final volume. The reaction was then incubated for 2 – 4 h at the appropriate temperature and the linearised products were purified as described below (2.4.3). Some aliquots were tested for correct digestion by agarose gel electrophoresis (2.4.5).

2.4.3 Purification of restriction digest

After restriction digestion, DNA fragments were purified using a phenol/chloroform/isoamylalcohol (25:24:1, Sigma) purification protocol (Sambrook, Fritsch & Maniatis, 1989). The phenol phase was equilibrated to pH 8 using the Tris based equilibration buffer provided with the phenol/chloroform/isoamylalcohol, to ensure that the DNA remains in the aqueous phase. In brief, the linearised plasmid was diluted to a final volume of 100 µl with RNase/DNase free water before an equal amount of phenol/chloroform/ isoamylalcohol was added. The samples were vortexed for 30 s to mix the phases, centrifuged for 15 min at 11,000 x g and the upper aqueous phase containing the DNA was transferred to a microfuge tube. To precipitate the DNA, 10 µl of 3 M sodium acetate pH 7.5 (Sigma) and 250 µl of 100% ethanol was added to the aqueous phase and the mixture incubated for approximately 1h at -80°C. After

incubation the sample was centrifuged for 15 min at 17,000 x g, the supernatant discarded and the DNA pellet washed in 500 µl of 70% ethanol. After another 15 min centrifugation at 17,000 x g, the supernatant was decanted and the pellet air-dried for 5 to 10 min before dissolving in 20 µl of RNase/DNase free water. The purified, linearised plasmid DNA was stored at -20°C.

2.4.4 *In vitro* transcription

The MEGAscript SP6 or T7 kit (Ambion) was used to *in vitro* transcribe approximately 1 µg of linearised and purified plasmid DNA. The RNA was synthesised at 37ºC for 2 or 4h respectively, using the Cap Analog m7G(5')ppp(5')G (Ambion) to produce capped viral RNA transcripts. The composition of the reaction is shown in Table 2.2.

Table 2.2 Reaction mixture for *in vitro* transcription of linearised plasmid DNA encoding viral or replicon sequences

XX refers to the volume required for the appropriate amount of DNA in the case of linearised plasmid DNA and the respective volume of water for the total volume of the *in vitro* transcription mixture

Reagent	SP6 kit quantity	T7 kit quantity
Nuclease free water	xx µl	xx µl
ATP solution	2 µl (50 mM)	2 µl (75 mM)
CTP solution	2 µl (50 mM)	2 µl (75 mM)
UTP solution	2 µl (50 mM)	2 µl (75 mM)
1:5 dilution of GTP solution	2 µl (10 mM)	2 µl (15 mM)
M 7 G (5')ppp (5') G (cap)	2 µl (4 mM)	3 µl (6 mM)
10X reaction buffer	3 µl	3 µl
linearised plasmid DNA (1µg)	xx µl	xx µl
Enzyme mix	2 µl	2 µl
Total volume	**30 µl**	**30 µl**

In vitro transcripts were used immediately for infection or transfection of cells as described in 2.5.4 or 2.5.5 respectively.

2.4.5 Agarose gel electrophoresis

DNA fragments were separated by agarose gel electrophoresis. A 1 – 2 % agarose gel was prepared in 0.5 M Tris-borate (TBE) buffer (Severn Biotech) with 0.5 µg/ml ethidium bromide (Biosciences) to enable visualisation of DNA under UV-light. After mixing the samples with 6x loading buffer (New England Biolabs (NEB)) and loading them into wells of the agarose gel, an electric current of 100 V was applied for approximately 1 h to separate different nucleic acid fragments. As a size marker, a 100 bp or 1 Kb DNA ladder (Promega) was used. DNA was visualised using an UV transilluminator (UVP).

2.4.6 DNA purification from agarose gel

DNA fragments were extracted from agarose gels using either the Illustra GFX PCR DNA and Gel Band Purification kit (GE Healthcare) or the NucleoSpin Gel and PCR Clean-up kit (Machery-Nagel) according to the manufacturers' instructions. Volumes, buffers and temperatures will be given for the GE Healthcare kit, and those used with the Machery-Nagel kit will be shown in square brackets.

Briefly, DNA fragments were separated by electrophoresis and a long wavelength UV transilluminator was used to visualise the fragments. The band with the correct size was excised from the agarose gel using a sterile scalpel, placed into a microfuge tube and weighed. 100 µl of Capture buffer type 3 [200 µl of buffer NTI] per 100 mg of gel slice was added and the sample incubated at 60ºC [50ºC] with occasional vortexing until completely dissolved. The sample was then applied to a filter column and centrifuged at 12,000 x g for 30 s to bind the DNA onto the silica membrane. The flow-through was discarded and the column washed twice with 500 µl wash buffer type 1 [700 µl buffer NT3]. After drying the column by centrifugation for 1 min at 12,000 x g, DNA was eluted using 20 µl DNase-free water [20 µl buffer NE]. DNase-free water was directly applied to the silica membrane and incubated for 1 min at room temperature before collecting DNA into a microfuge tube by centrifugation at 12,000 x g for 1 min. Samples were stored at -20ºC until further use.

2.4.7 RNA extraction from tick cell lines

Total RNA was isolated from tick cells using either TRI Reagent (Sigma-Aldrich) or the RNeasy Mini Kit (Qiagen) according to the manufacturers' guidelines. Tick cells were harvested into RNase free microfuge tubes. The tubes were centrifuged at 500 x g for 5 min and the cell pellet lysed.

For total RNA isolation using TRI Reagent, cells were lysed by repeated pipetting in 1 ml TRI Reagent. After an incubation time of 15 min at room temperature with sporadic vortexing, the lysed samples were mixed with 200 µl of chloroform, vortexed for 30 s and incubated for 10 min at room temperature. Following centrifugation at 12,000 x g for 15 min at 4ºC, the upper aqueous phase containing the total RNA was transferred to an RNase-free microfuge tube and the interphase and lower organic phase containing proteins, precipitated membranes, fat, polysaccharides and high molecular weight DNA was discarded. 500 µl of isopropanol (Invitrogen) was added to the aqueous phase to precipitate the RNA. The mixture was incubated for 10 min at room temperature, and then the RNA was pelleted by centrifugation at 12,000 x g for 10 min at 4ºC. The supernatant was discarded without disturbing the RNA pellet. The pellet was washed with 1 ml of 75% ethanol and after a centrifugation step of 10,000 x g for 5 min at 4ºC, the supernatant was discarded and the RNA pellet air-dried for 15 min. RNA samples were dissolved in 40 µl RNase free water on ice for approximately 1 h and then stored at -80ºC.

For the Qiagen approach cells were lysed in 350 µl of buffer RLT containing 1% β-mercaptoethanol (Sigma-Aldrich). After vortexing, the lysate was thoroughly disrupted and homogenised by passing at least 10 times through a 20-gauge needle attached to a 2 ml syringe. After allowing the sample to stand for 5 min, 350 µl of 70% ethanol was added to the homogenised lysate and mixed by pipetting. 700 µl of the sample was then transferred to an RNeasy spin column and after centrifugation for 15 sec at 8,000 x g, the flow-through was applied again to the spin column and centrifuged for 15 sec at 8,000 x g to ensure that all RNA was bound to the column. The column was washed with 350 µl of RW1 buffer, centrifuged for 15 s at 8,000 x g and the flow-through was discarded. Then 40 µl of DNase incubation mix (5 µl DNase in 35 µl RDD buffer, Qiagen) was added directly to the spin column membrane and incubated for 15 min at room

temperature. This step removed DNA contamination by degrading the DNA attached to the column membrane. After another washing step with 350 µl buffer RW1 as above, the column was transferred to another collection tube. In order to precipitate the RNA, 500 µl of RPE buffer was added and the column centrifuged for 15 s at 8,000 x g. After discarding the flow-through, another 500 µl of RPE buffer was added and centrifuged for 2 min at 8,000 x g to ensure that all ethanol was removed. The RNA was eluted from the column by twice applying 40 µl of RNase free water to the membrane and centrifuging for 1min at 17,000 x g. Total RNA was stored at -80ºC.

2.4.8 Nucleic acid quantification

All RNA and DNA samples were quantified using a NanoDrop ND-1000 spectrophotometer (Thermo Fisher Scientific). Before measurements were undertaken the NanoDrop was initialised with water and blanked against the buffer used for diluting the nucleic acid sample. After blanking, 1 µl of nucleic acid was placed on the lens of the NanoDrop and the quantity and purity was measured.

2.4.9 Assessing RNA quality

All total RNA samples sent for RNA-Seq were prepared using the RNA 6000 Nano Kit (Agilent) according to the manufacturer's instructions and tested for RNA integrity using the 2100 Bioanalyzer (Agilent). Briefly, RNA 6000 Nano dye was thawed and left to equilibrate to room temperature for 30 min. Meanwhile 550 µl of RNA 6000 Nano gel matrix was transferred into a spin filter and centrifuged at 1500 x g for 10 min. The dye solution was vortexed, centrifuged for 10 s and 1 µl was added to a 65 µl aliquot of filtered gel. The gel-dye mix was vortexed and centrifuged for 10 min at 13,000 g prior to loading the mix on the RNA 6000 Nano chip. For loading, the chip was placed into the chip priming station and 9 µl of gel-dye mix were added to the well marked with a white G on a black background. The priming station was closed and the plunger was pressed down and held for 30 s, to allow the gel to distribute equally into all 16 wells, before releasing the plunger. The two other wells marked with a G were each loaded with 9 µl of gel-dye mix before 5 µl of the RNA 6000 Nano marker, which compensates for drift effects that may occur during the course of a chip run, was added to each of the 12 sample wells of

the Nano chip. In the meantime samples were heat-denatured for 2 min at 70ºC and immediately placed on ice. This process destabilises secondary structures and breaks up RNA which suffers cleavage but is still held together by extensive base-pairing allowing the detection of degraded RNA. 1 µl of each heat-denatured sample was added to separate wells and 1 µl of the RNA 6000 ladder was added to its appropriate well. The chip was briefly vortexed on an IKA vortexer (Agilent) and measured on the 2100 Bioanalyzer. After the run finished, RNA integrity was assessed using 2100 Expert software version 2.6 (Agilent).

2.4.10 Polymerase chain reaction (PCR)

Specific primers and reaction cycles were used depending on the PCR approach and length of the sequence. The PCR approaches used, standard PCR (2.4.10.1), colony PCR (2.4.10.2) and qPCR (2.4.10.4) are described in separate sections. Primer sequences are listed in Table 2.3 including the PCR approach they were used for and their appropriate annealing temperatures.

Table 2.3 List of PCR primers with their respective annealing temperatures (Temp)

F: Forward; R: Reverse
* Lower case and upper case denote sequences of T7 and primer, respectively.

Primer name	Sequence 5' to 3' *	PCR approach	Annealing Temp
TBEV NS5 F	GCCGTCACTGGGAACATAGT	qPCR	55°C
TBEV NS5 R	ACACACCTCGTTCCAACTCC	qPCR	55°C
LGTV NS5 F	ACCCAAGACTGCTACGTGTGGAAA	qPCR	60°C
LGTV NS5 R	TGAGGAAGTAAAGGGCCTTGCTGA	qPCR	60°C
beta actin F	AAGGACCTGTACGCCAACAC	qPCR	58°C
beta actin R	ACATCTGCTGGAAGGTGGAC	qPCR	58°C
Ribosomal protein L13A F	GTGGGCTGGAAGTACCAGAA	qPCR	58°C
Ribosomal protein L13A R	CTAGCTGAACCTTGGCTTCG	qPCR	58°C
Complement Factor H F	ACATCCTTTGGTGCTGGAAC	qPCR	58°C
Complement Factor H R	CACAACGCTGTCCTCAAAGA	qPCR	58°C
Coagulation Factor F	TTACGATGAAGACCCGAACC	qPCR	58°C
Coagulation Factor R	AGATGGACTTCGACCCTCCT	qPCR	58°C
HSP90 F	AGGACGAGCTCCACAACATC	qPCR	58°C
HSP90 R	CGGACGAACACCTCTTTCTC	qPCR	58°C
gp96 F	GCACAAGTTGCTGAAGGTGA	qPCR	58°C
gp96 R	CGGTTGGTAGTGTCCTCGAT	qPCR	58°C

Peroxinectin F	TCTGCGACAACTCAAACCTG	qPCR	58°C
Peroxinectin R	GTAGTGGCCCTACGTCCAGA	qPCR	58°C
4SCN-Tudor IRE/CTVM19 F	CTGTCTGGGGACACGGTAGT	qPCR	58°C
4SCN-Tudor IRE/CTVM19 R	TGGTCTCACTGATGGTCTCG	qPCR	58°C
4SCN-Tudor IDE8 F	GGCCAAGTACTTCACGGAGA	qPCR	58°C
4SCN-Tudor IDE8 R	GAACCTCCAGTGACCGTTGT	qPCR	58°C
Calreticulin IRE/CTVM19 F	CCCAAGGTGTACCTCAAGGA	qPCR	58°C
Calreticulin IRE/CTVM19 R	GTAAAAGCGGGCATCTTCAG	qPCR	58°C
Calreticulin IDE8 F	TGAAGCACGAGCAGAACATC	qPCR	58°C
Calreticulin IDE8 R	GCAGGTTCTTGCCCTTGTAG	qPCR	58°C
Trypsin IRE/CTVM19 F	GACACCTACGCCAACAACCT	qPCR	58°C
Trypsin IRE/CTVM19 R	GTGTCGTAGCGGTTGACCTT	qPCR	58°C
Trypsin IDE8 F	CCTGAGATCCTCCTGGTTCA	qPCR	58°C
Trypsin IDE8 R	AGGTTGTTGGCGTAGGTGTC	qPCR	58°C
HSP70 IRE/CTVM19 F	GCCAAGATGAAGGAAACTGC	qPCR	58°C
HSP70 IRE/CTVM19 R	ACATTGAGACCGGCGATAAC	qPCR	58°C
HSP70 IDE8 F	GCTCAGTCCACTTCCTCGAC	qPCR	58°C
HSP70 IDE8 R	ACTTTGTCCTGGATGGATGC	qPCR	58°C
Cniwi F	AGAAGGTGGTGCATGGAAAC	qPCR	58°C
Cniwi R	CACATGACCGTCCATGAGTC	qPCR	58°C
CD36 F	CACGGAGGAGTTCGAGTTCT	qPCR	58°C
CD36 R	CAGCCGAACTTAGTCGAAGG	qPCR	58°C
α-crystallin B F	GCTTCTACATCCAGCCCAAA	qPCR	58°C
α-crystallin B R	TCCGACTTCTCTTCGTGCTT	qPCR	58°C
IRES F	GCGCCCGCGGGCCCCTCTCCCTCCCCCCCCCTAACGTTACTGG	PCR	55°C
IRES R	CCGGGCGGCCGCTGTGGCCATATTATCATC	PCR	55°C
Fluc F	GCGCGCGGCCGCACCATGGGATCAGGCAGCG	PCR	55°C
Fluc R	CCGGGCGGCCGCTTACACGGCGATCTTGC	PCR	55°C
Rluc F	GCGCGCGGCCGCACCATGACTTCGAAAGTTTATGATC	PCR	55°C
Rluc R	CCGGGCGGCCGCTTATTGTTCATTTTTGAGAACTCG	PCR	55°C
dsT7-eGFP F	taatacgactcactatagggATGGTGAGCAAGGGCGAGGAGCTGTTC	PCR	60°C
dsT7-eGFP R	taatacgactcactatagggCTGGGTGCTCAGGTAGTGGTTGTCGGGC	PCR	60°C
pJET1.2 (Fermentas) F	CGACTCACTATAGGGAGAGCGGC	colony PCR	60°C
pJET1.2 (Fermentas) R	AAGAACATCGATTTTCCATGGCAG	colony PCR	60°C
dsT7-Rluc F	taatacgactcactatagggATGACTTCGAAAGTTTATGATCCAG	PCR	60°C
dsT7-Rluc R	taatacgactcactatagggCTGCAAATTCTTCTGGT TCTAACTTTC	PCR	60°C

dsT7-Ago-16 F	taatacgactcactatagggAAGATCACGAGGGTATCGGTAGT	PCR	60°C
dsT7-Ago-16 R	taatacgactcactatagggACTTTTCTGCACCACGTCTTG	PCR	60°C
dsT7-Ago-16-2 F	taatacgactcactatagggCGTTATGAAGGGGTGATCAGAAG	PCR	60°C
dsT7-Ago-16-2 R	taatacgactcactatagggGACTGGTACTGATTCTCCCA	PCR	60°C
dsT7-Dicer-90 F	taatacgactcactatagggATCCTCAAGGAGTACAAGCC	PCR	60°C
dsT7-Dicer-90 R	taata cgactcactatagggACAGAGCATTAGGGTCGTC	PCR	60°C
dsT7-Ago-30 F	taatacgactcactatagggACATACGAGCACTGACGG	PCR	60°C
dsT7-Ago-30 R	taatacgactcactatagggTGGTGCAACATTTTATCGA	PCR	60°C
dsT7-Calreticulin F	taatacgactcactatagggACAAGGGCAAGAACCTGCT	PCR	60°C
dsT7-Calreticulin R	taatacgactcactatagggAAGATTGTGCCGGACTTGAC	PCR	60°C
dsT7-gp96-1 F	taatacgactcactatagggCGGACTATGTGACACGGATG	PCR	60°C
dsT7-gp96-1 R	taatacgactcactatagggCTCATGGTGTCCTGGGACTT	PCR	60°C
dsT7-gp96-2 F	taatacgactcactatagggGAGGATTACCAGCGCTTCTG	PCR	60°C
dsT7-gp96-2 R	taatacgactcactatagggCTCATGGTGTCCTGGGACTT	PCR	60°C
dsT7-trypsin F	taatacgactcactatagggGACACCTACGCCAACAACCT	PCR	60°C
dsT7-trypsin R	taatacgactcactatagggATGGTCACGTCCTCCTTGAG	PCR	60°C
dsT7-HSP90-1 F	taatacgactcactatagggCTGCCCACAAAGTTGCTGTA	PCR	60°C
dsT7-HSP90-1 R	taatacgactcactatagggCTCCGAGAAAGAGGTGTTCG	PCR	60°C
dsT7-HSP90-2 F	taatacgactcactatagggCGAGAAGGAGGAGATTGCAC	PCR	60°C
dsT7-HSP90-2 R	taatacgactcactatagggGGATGACTCTGGAGCCTCTG	PCR	60°C
dsT7-Peroxinectin F	taatacgactcactatagggCATCGTGCAGTCTCTTGGAA	PCR	60°C
dsT7-Peroxinectin R	taatacgactcactatagggAGAAGTGATCGTTGGCATCC	PCR	60°C
dsT7-Coagulation Factor F	taatacgactcactatagggCGGACAGGCTGACTACAACA	PCR	60°C
dsT7-Coagulation Factor R	taatacgactcactatagggGCAGCTTGGAGTAGGACTCG	PCR	60°C
dsT7-Complement Factor H IRE/CTVM19 F	taatacgactcactatagggTCCCCTTCATCTGTCAGGTC	PCR	60°C
dsT7-Complement Factor H IRE/CTVM19 R	taatacgactcactatagggCGAAGCTGGAACGGAAGTAG	PCR	60°C
dsT7-Complement Factor H IDE8 F	taatacgactcactatagggACAAATCGGCCGACACTTAC	PCR	60°C

dsT7-Complement Factor H IDE8 R	taatacgactcactatagggGATGGTGTGC ACGGTATGAG	PCR	60°C
dsT7-HSP70 IDE8 F	taatacgactcactatagggTCTCGAACGAA CAGGAGAGC	PCR	60°C
dsT7-HSP70 IDE8 R	taatacgactcactatagggACATTGAGACC GGCGATAAC	PCR	60°C
dsT7-HSP70 IRE/CTVM19 F	taatacgactcactatagggGCTCAGTCCA CTTCCTCGAC	PCR	60°C
dsT7-HSP70 IRE/CTVM19 R	taatacgactcactatagggTGGGAACCTTC AACTTGACC	PCR	60°C

2.4.10.1 Standard PCR

Three different polymerases, KOD Hot Start DNA polymerase (KOD, Novagen), Vent DNA polymerase (Vent, NEB) and GoTaq DNA polymerase (GoTaq, Promega), were used according to the manufacturers' instructions. The PCR reaction mix for all polymerases had a final volume of 50 µl. For KOD the mix contained 5 µl 10x PCR buffer, 3 µl MgSO4 (25 mM) (Novagen), 5 µl dNTPs (2 mM each) (Novagen), 1.5 µl of each forward and reverse primer (10 µM) (Sigma-Aldrich), 1 µl KOD (1 U/µl), DNA template and RNase/DNase free water to a final volume of 50 µl. For the PCR with Vent, the mix was composed of 5 µl 10x ThermoPol reaction buffer (NEB), 1 µl dNTPs (10 mM) (Bioline), 5 µl each forward and reverse primer (10 µM) (Sigma-Aldrich), 2 µl Vent (2 U/µl), DNA template and RNase/DNase free water to a final volume of 50 µl. For the GoTaq PCR reaction mix 10 µl 5x Green GoTaq buffer (Promega), 1 µl dNTPs (10 mM) (Bioline), 4 µl $MgCl_2$ (25 mM) (NEB), 5 µl each forward and reverse primer (10 µM) (Sigma-Aldrich), 0.5 µl GoTaq (5 U/µl), DNA template and RNase/DNase free water to a final volume of 50 µl. The reactions were incubated in a thermocycler (Veriti®, Applied Biosystems) using the conditions shown in Table 2.4. After the initial denaturation stage, the amplification stage, which consists of denaturation, annealing and extension, was run for 30- 35 cycles, before a final extension stage. The annealing temperature (X in Table 2.4) for each primer is listed in Table 2.3. The duration of the extension was dependent on the length of the amplified region.

Table 2.4 PCR cycling conditions

Stages	Vent	KOD	GoTaq
initial denaturation	95°C for 2 min	95°C for 2 min	95°C for 2 min
denaturation	95°C for 30 s	95°C for 20 s	95°C for 30 s
annealing	X°C for 30 s	X °C for 20 s	X°C for 30 s
extension	72°C for 2 min	70°C for 20 s	72°C for 30 or 50 s
final extension	72°C for 7 min	70°C for 7 min	72°C for 7 min
holding	4°C for 0-24 h	4°C for 0-24 h	4°C for 0-24 h

A negative control, without DNA template but containing all other components of the reaction mix, was used to test for possible contamination. The PCR products were visualised by agarose gel electrophoresis and stored at -20°C.

2.4.10.2 Reverse transcription PCR (RT-PCR)

RT-PCR was used to generate cDNA from RNA templates using random primers (Promega) with either the SuperScript III kit (Invitrogen) or the High-Capacity cDNA Reverse Transcription kit (Applied Biosystems) according to the manufacturers' instructions. The incubation at different temperatures was done in a thermocycler (Veriti®, Applied Biosystems). For the SuperScript III kit each reaction contained 1 µl dNTP solution (10 mM) (Bioline), 1 µl random primers (500 µg/ml) (Promega), 1 µg of RNA and RNase/DNase-free water made up to a total volume of 12.5 µl. This mixture was incubated at 65°C for 5 min and then cooled at 4°C for 5 min. Meanwhile 4 µl 5x first strand buffer, 2 µl dithiothreitol (DTT, 0.1 M), 0.5 µl RNase Inhibitor (Ambion) and 1 µl SuperScript III were mixed and added to the previous mixture. This reaction was then incubated at 50°C for 1 h before inactivation by heating to 72°C for 10 min.

For cDNA synthesis using the High-Capacity cDNA Reverse Transcription kit a mixture of 2 µl 10x Reverse transcription (RT) buffer, 0.8 µl 25x dNTP mix (100 mM), 2 µl 10x RT random primers, 1 µl RT enzyme, 1 µl RNase Inhibitor (Ambion), 1 µg of RNA and RNase/DNase-free water to a final volume of 20 µl was incubated in a thermocycler using the following conditions: 25°C for 10 min, 37°C for 2 h and 85°C for 5 min.

All resultant cDNA samples were stored at -20°C.

2.4.10.3 Colony PCR

A colony PCR using the sequencing primers (Table 2.3) supplied with the CloneJET PCR Cloning Kit (Fermentas) was performed to screen bacterial colonies for the successful integration of PCR products into the pJET1.2 vector (2.9.1). The instructions supplied with the kit were followed. In brief, single colonies were isolated from a LB agar plate and used to inoculate individual overnight cultures of 5 ml LB medium containing ampicillin (100 µg/ml). After an incubation period of 16 h at 37ºC in an orbital shaker (225 rpm), 10 µl of the overnight culture was mixed with 2 µl 10x Green GoTaq buffer (Promega), 2 µl dNTPs (2 mM each) (Novagen), 1.2 µl $MgCl_2$ (25 mM), 0.4 µl of each pJET1.2 sequencing forward and reverse primers, 3.9 µl nuclease-free water and 0.1 µl GoTaq polymerase (5 U/ µl). The mixture was incubated in a thermocycler using the following conditions: initial denaturation stage at 95ºC for 3 min, 25 cycles of the amplification stage with denaturation at 94°C for 30 s, annealing at 60ºC for 30 s and elongation at 72ºC for 30 s. The PCR products were visualised on a 1% agarose gel.

2.4.10.4 qPCR

Two qPCR machines were used to calculate the relative expression of genes, the Rotor-GENE Q (Qiagen) or the ViiA7 Real-Time PCR system (Applied Biosystems), using the appropriate master mixes, FastStart SYBR Green Master (Roche) or FastStart Universal SYBR Green Master (Rox) (Roche), respectively. Although the ViiA7 Real-Time PCR machine does not depend on the presence or absence of the reference dye ROX, which reduces the noise within the PCR run, the presence of ROX gave more consistent results. In brief, 10 µl of either master mix was mixed with 0.6 µl of each forward and reverse primer (Table 2.3) and 2 µl of cDNA and made up to 20 µl with nuclease-free water. The mixture was then applied to either 4-strip PCR tubes (VWR) for the Rotor Gene machine or 96-well plates (MicroAmp) for the ViiA7 machine. The run parameters including acquisition of SYBR Green are listed in Table 2.5. The amplification stage, consisting of

denaturation, annealing and extension was repeated 40x in the Rotor-GENE Q and 45x in the ViiA7 Real-time PCR system.

Table 2.5 qPCR cycling conditions for use with primers for TBEV or tick gene transcripts

Stages	Rotor-GENE Q	ViiA7
initial denaturation	95°C for 5 min	95°C for 10 min
denaturation	94°C for 20 s	95°C for 15 or 20 s
annealing	X°C for 20 s	X°C for 20 or 30 s
extension (acquire SYBR Green)	72°C for 15 s	72°C for 15 or 30 s
final denaturation	95°C for 20 s	95°C for 15 s
Meltcurve (acquire SYBR Green)	64-94°C, 1 min hold on first step, then 5 s each step	60-95°C, 1 min hold on first step, then 0.05°C per second

Data was analysed using either the Rotor-GENE software version 6.1.93 or the ViiA7 software version 1.0. To determine the absolute or relative quantity of gene transcripts/virus genomes, a standard curve method or a variation of the ΔΔCT method (Livak & Schmittgen, 2001; Schmittgen & Livak, 2008) were used respectively.

For the standard curve method, the linearised plasmid was 9 x 10-fold serially diluted starting with 2 ng and the corresponding copy numbers were entered into the Rotor-GENE software which generated the standard curve and calculated the copy numbers for each unknown sample automatically. The copy number of the linearised plasmid containing the gene of interest was calculated using the following formula:

$$\text{Number of copies} = \frac{amount\ of\ plasmid\ (ng) \times 6.022\ x\ 10^{23}\ \left(\frac{molecules}{mol}\right)}{length\ (bp) \times 1\ x\ 10^{9}\ \left(\frac{ng}{g}\right) \times 660\ \left(\frac{g}{mol\ of\ bp}\right)}$$

For the ΔΔCT method, primer efficiencies were established for each primer and calculated using the following formula:

$$\text{Efficiency (\%)} = (10^{\left(-\frac{1}{slope}\right)} - 1) \times 100$$

Since primers showed efficiencies between 90 and 110% a variation of the ΔΔCT method was used to calculate relative quantity of gene transcripts as follows:

1) Relative gene expression in control $= 2^{((average(reference\ genes) - target\ gene))}$
2) Relative gene expression in infected $= 2^{((average(reference\ genes) - target\ gene))}$

3) Fold change $= \frac{Relative\ gene\ expression\ of\ infected}{Relative\ gene\ expression\ of\ control}$

2.4.11 Generation of dsRNA

Long dsRNA transcripts were produced using the MegaScript RNAi kit (Ambion) according to the manufacturer's instructions. Since the kit uses a T7 DNA-dependent RNA polymerase all primers were designed to contain a T7 sequence as indicated in Table 2.3. In brief, cDNA generated by reverse transcription (2.4.10.2) from total RNA of tick cells or plasmids was used as template to generate specific PCR products using T7 primers by PCR (2.4.10.1). The generated products were visualised by agarose gel electrophoresis (2.4.5), bands of the correct length were extracted and purified using either the Machery-Nagel kit (long dsRNA) or the GE Healthcare kit (fluorescently labelled dsRNA) (2.4.6) and subjected to an additional amplification by PCR. The amplified DNA templates were then transcribed using the MegaScript kit. To generate fluorescently labelled dsRNA the Fluorescein RNA Labelling Mix (Roche) was used, which contains fluorescein-labelled UTP nucleotides. For transcription, 1 µg DNA template was mixed with 2 µl 10x T7 reaction buffer (Ambion), 2 µl of each dNTP (ATP, CTP, GTP and UTP) or fluorescein RNA Labelling Mix, 2 µl T7 Enzyme mix (Ambion) and nuclease-free water to a final volume of 20 µl. The mixture was then incubated at 37°C for 4h. To remove the DNA template and any single-stranded RNA the 20 µl mixture was incubated with 2 µl DNase I, 2 µl RNase, 5 µl digestion buffer and 21 µl nuclease-free water at 37°C for 1h. After digestion the dsRNA was purified with the solid-phase adsorption system provided with the appropriate purification kit to remove protein as well as mono- and oligonucleotides. To bind dsRNA to the membrane of the filter cartridge a mixture of 50 µl dsRNA solution, 50 µl 10x binding buffer, 150 µl nuclease-free water and 250 µl 100% ethanol was prepared and applied to the filter. After centrifugation at 13,000 x g for 2 min the flow-through was discarded. Then the bound dsRNA was washed twice with 500 µl wash solution and centrifugation at 13,000 x g for 2 min. After drying the filter by another centrifugation at 13,000 x g for 30 s, the dsRNA was eluted into a fresh collection tube by applying 2x 50 µl of preheated elution solution to the filter and

centrifugation at 13,000 x g for 2 min. Purified dsRNA (407-615 bp) was stored at -80°C.

2.5 Viruses, replicons and related techniques

2.5.1 Alphavirus propagation

The following SFV4 reporter viruses were used in this project (Table 2.6, Figure 2.1). All recombinant viruses were constructed in the Estonian Biocentre, University of Tartu, Tartu, Estonia by Professor Andres Merits and co-workers.

Table 2.6 List of SFV strains and their modifications

Virus strain/name	Modification	Reference
SFV4-steGFP	Insertion of enhanced green fluorescence protein gene between capsid and p62 in the structural region	(Fragkoudis et al., 2007)
SFV4(3F)-ZsGreen	Insertion of ZsGreen gene fused to nsP3 in the non-structural region	as described in (Tamberg et al., 2007)
SFV4(3H)-Rluc	Insertion of *Renilla* luciferase gene between nsP3 and nsP4 in the non-structural region	(Kiiver et al., 2008)
SFV4-StRluc	Insertion of *Renilla* luciferase gene between capsid and p62 in the structural region	(Kiiver et al., 2008)

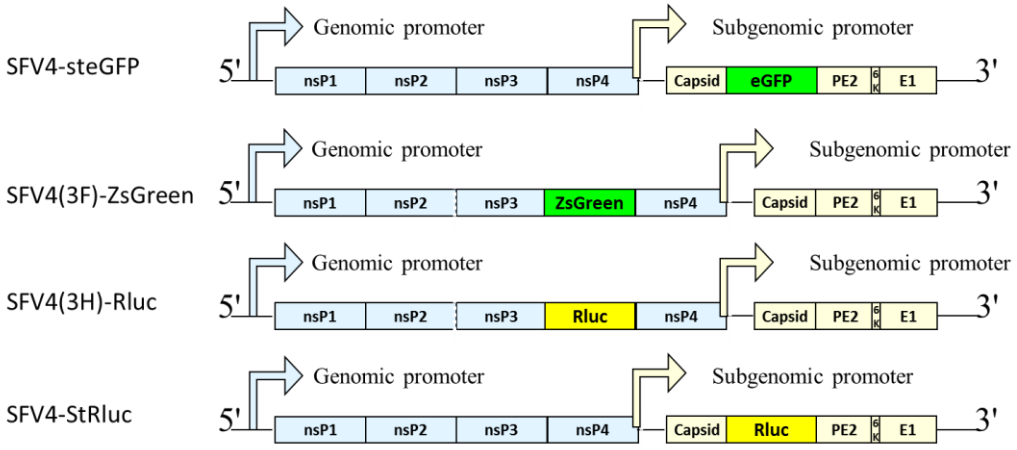

Figure 2.1 Structure of SFV reporter constructs

Genome organisation of the SFV4-steGFP, SFV4(3F)-ZsGreen, SFV4(3H)-Rluc and SFV4-StRluc constructs.

The viruses SFV4-steGFP, SFV4-StRluc and SFV4(3H)-Rluc were propagated and kindly donated by Dr. Gerald Barry and Ms Claire Donald, University of Edinburgh. For the propagation of SFV4(3F)-ZsGreen, plasmids were extracted (2.4.1) and quantified following growth of transformed Sure2 supercompetent cells (2.3.2). 10 µg of the plasmid DNA was then linearised using *Spe*I restriction endonuclease (2.4.2), purified (2.4.3) and transcribed *in vitro* using the SP6 kit to produce capped transcripts (2.4.4).

BHK-21 cells were electroporated with the *in vitro* transcript to produce infectious virus using a BioRad Gene Pulser Xcell electroporator. Cells from an 80% confluent 175 cm^2 tissue culture flask were harvested, centrifuged at 300 x g for 5 min and the cell pellet was resuspended in 800 µl cold PBS. One half of the cell suspension was transferred to a 0.4 cm electroporation cuvette (BioRad) and 10 µl of the RNA transcript was added. The cells were pulsed twice using a square wave of 850 volts for 0.4 milliseconds with a 5 s pulse interval. The electroporated cells were transferred to a 175 cm^2 tissue culture flask containing 20 ml of prewarmed GMEM containing 10% NBCS and the procedure was repeated with the other half of the BHK-21 cell suspension. The cell suspensions were split and electroporated in two halves to improve electroporation efficiency. Flasks were incubated overnight. At 24 h and 48 h after transfection, supernatant was collected from the flasks, clarified by centrifugation at 5,500 x g for 30 min to remove any cell debris and stored at -80°C.

Thawed supernatant was transferred to sterile, 500 ml screw-cap glass bottles and 23 g/L NaCl (Sigma) and 70 g/L polyethylene glycol (PEG) 8000 (Sigma) were added. The mixture was stirred for 16 h at 4°C during which time proteinaceous material precipitated. After centrifugation at 3,000 x g for 45 min the supernatant was discarded and the pellet, containing the virus, was resuspended in 12 ml of sterile TNE buffer (50 mM Tris HCl, 100 mM NaCl and 0.1 mM EDTA, pH 7.4). Approximately 18 ml of 20% (w/v) sucrose in TNE buffer was added to the ultracentrifugation tube (25x89 mm, Beckman) and 12 ml of TNE buffer containing the virus was carefully layered on top of the sucrose cushion using a 20 ml pipette. The ultracentrifugation tube filled to the top was balanced using a fine balance against a tube filled with approximately 18 ml 20% sucrose and 12 ml of water.

Tubes were ultracentrifuged in the L8-70M Ultracentrifuge (Beckman) at 125,000 x g for 90 min at 4°C. The supernatant was decanted and the virus pellet was resuspended in 400 µl TNE buffer and incubated overnight at 4°C. Each 400 µl aliquot of virus suspension was transferred to an eppendorf tube and the centrifuge tube was rinsed with an additional 600 µl TNE buffer which was mixed with the initial 400 µl aliquot. 100 µl aliquots of the resultant virus suspension were frozen at -80°C.

2.5.2 Flavivirus propagation

The LGTV and TBEV strains used are described in Table 2.7 and depicted in Figure 2.2.

Table 2.7 List of flavivirus strains used in this project

Virus strain/name	Description	Publication
LGTV TP-21	Wild type, isolated from *I. granulatus* ticks in Malaysia in 1956	(Smith, 1956)
TBEV Neudoerfl	Wild type, isolated from *I. ricinus* tick in Austria 1971; complete genome sequence published in 1989	(Mandl et al., 1989)
TBEV Neudoerfl	Wild type derived from plasmid pTND/c	(Mandl et al., 1997)

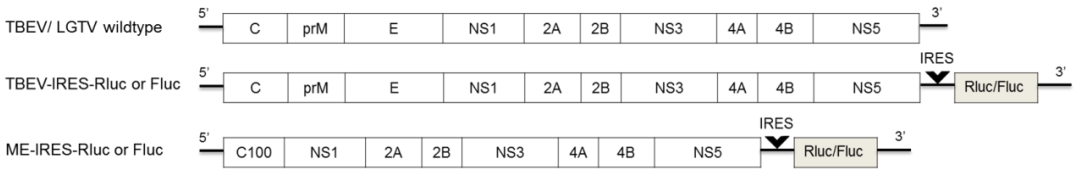

Figure 2.2 Structure of TBEV and TBEV replicon reporter constructs

Genome organisation of wildtype TBEV/ LGTV (top) and of full length TBEV (middle) and TBEV replicon (no prM and E protein, bottom) constructs. TBEV constructs were cloned using as backbone the plasmids pTND/c-eGFP (Gehrke et al., 2005) and pTND/ME-eGFP (Gehrke et al., 2005) respectively. The IRES-eGFP cassette in the 3' non-structural region of the backbones was replaced with an IRES-Rluc or IRES-Fluc cassette.

The wildtype LGTV strain TP-21 was kindly provided by Dr Sonja Best of the Laboratory of Virology, Rocky Mountain Laboratories, NIAID, NIH, Hamilton, Montana via Dr Esther Schnettler, Centre for Virus Research at the University of Glasgow, Institute of Infection, Immunity and Inflammation, Glasgow, UK. LGTV-TP21 kindly provided by Ms Claudia Rückert, University of Edinburgh having been

propagated as follows. Vero cells were seeded at a density of 1x 10^7 in 175 cm^2 flasks and infected with LGTV suspension (in DMEM supplemented with 10% FCS) at a multiplicity of infection (MOI) of 0.01. Supernatant was harvested on day 5 p.i. and centrifuged for 30 min at 3100 x g to remove any cell debris. Aliquots of the virus-containing supernatant were frozen at -80ºC.

The TBEV wildtype virus was provided by Ms Hana Tykalová and Dr Daniel Růžek of the University of South Bohemia, Department of Parasitology, Budweis, Czech Republic and was originally obtained by them from Professor Franz X. Heinz, Clinical Institute of Virology, Medical University of Vienna, Austria. TBEV propagation was carried out by Ms Hana Tykalovà and Dr Daniel Růžek at the Institute of Parasitology, University of South Bohemia, Czech Republic. A general approval of experiments was given by the Czech Central Commission for Animal Welfare (State Organ). In brief, TBEV was propagated by passaging 5 times through suckling mouse brain. For the present study 5 day old suckling CD1 mice were intracranially infected with 1 µl of TBEV-infected mouse brain suspension, corresponding to 100 PFU per mouse, or mock-infected with the same volume of uninfected mouse brain suspension. The mice were observed daily for symptoms of TBEV infection (leaving the nest, uncoordinated movements, paresis and "bristled" tail). After the onset of symptoms, which was usually within 4 to 5 days p.i., the TBEV-infected mice were euthanised and the brains removed. For the mock-infected mice, brains were removed 2 days later to prevent cross contamination while handling the samples. The brains were homogenised in PS cell complete culture medium (2.1.2) to obtain a 20% mouse brain suspension (w/v) using a Tissue Lyzer II (Retsch) at 30 Hz (30/s) for 2 min. The homogenate was then centrifuged for 10 min at 16,000 x g at 4ºC and supernatant stored at -80ºC.

The plasmid pTND/c containing the infectious clone of TBEV strain Neudoerfl was kindly provided by Professor Franz X. Heinz. For propagation of the plasmid-derived TBEV, the plasmid pTND/c was grown in HB101 (2.3.2), purified (2.4.1.2) and quantified. After quantification, 10 µg of the plasmid were linearised using the restriction enzyme Nhe1, purified using phenol/chloroform/isoamylalcohol (2.4.3) and *in vitro*-transcribed using the T7 kit (2.4.4). BHK-21 cells, seeded at a density of 1x10^5 cells per well in a 24-well plate, were transfected (2.5.5) with the capped *in*

vitro transcript using Lipofectamine 2000 (Invitrogen) transfection reagent. After transfection, cells were incubated for 4 days before the supernatant of 4 wells was pooled and passaged onto BHK-21 cells grown to 80% confluence in a 25 cm^2 flask. To increase virus yield, supernatant was passaged a second time on BHK-21 cells grown in 80 cm^2 flasks before collecting and freezing the supernatant at -80ºC.

2.5.3 Flavivirus replicons

The LGTV replicon E5repRluc2B/3 (Table 2.8, Figure 2.3) was constructed and provided by Dr Mayuri Sharma and Prof. Richard Kuhn of Purdue University, Department of Biological Sciences, West Lafayette, Indiana and Dr Sonja Best. The TBEV replicons (Table 2.8, Figure 2.3) were constructed from wildtype strain Neudoerfl by Dr Verena M. Hoenninger and provided by Professor Franz X. Heinz.

Table 2.8 List of flavivirus replicons and their modifications

Virus/ Replicon name	Modification	Reference
LGTV E5repRluc2B/3	Insertion of *Renilla* luciferase behind truncated capsid (first 17 amino acids retained) replacing entire prM and most of E; LGTV NS2B/3 protease cleavage site between marker gene and E	(Schnettler et al., 2014)
TBEV C17Fluc	Insertion of firefly luciferase behind truncated capsid (first 17 amino acids retained) replacing entire prM and most of E; TBEV NS2B/3 protease cleavage site between marker gene and E	(Hoenninger et al., 2008)
TBEV C17Fluc-FMDV2A	Insertion of firefly luciferase behind truncated capsid (first 17 amino acids retained) replacing entire prM and most of E; FMDV 2A cleavage site between marker gene and E	(Hoenninger et al., 2008)
TBEV C17Fluc-TaV2A	Insertion of firefly luciferase behind truncated capsid (first 17 amino acids retained) replacing entire prM and most of E; *Thosea asigna virus* 2A (TAV2A) cleavage site between marker gene and E	(Hoenninger et al., 2008)
TBEV C27Rluc	Insertion of *Renilla* luciferase behind truncated capsid (first 27 amino acids retained) replacing entire prM and most of E; TBEV NS2B/3 protease cleavage site between marker gene and E	(Hoenninger et al., 2008)
TBEV C37Rluc	Insertion of *Renilla* luciferase behind truncated capsid (first 37 amino acids retained) replacing entire prM and most of E; TBEV NS2B/3 protease cleavage site between marker gene and E	(Hoenninger et al., 2008)

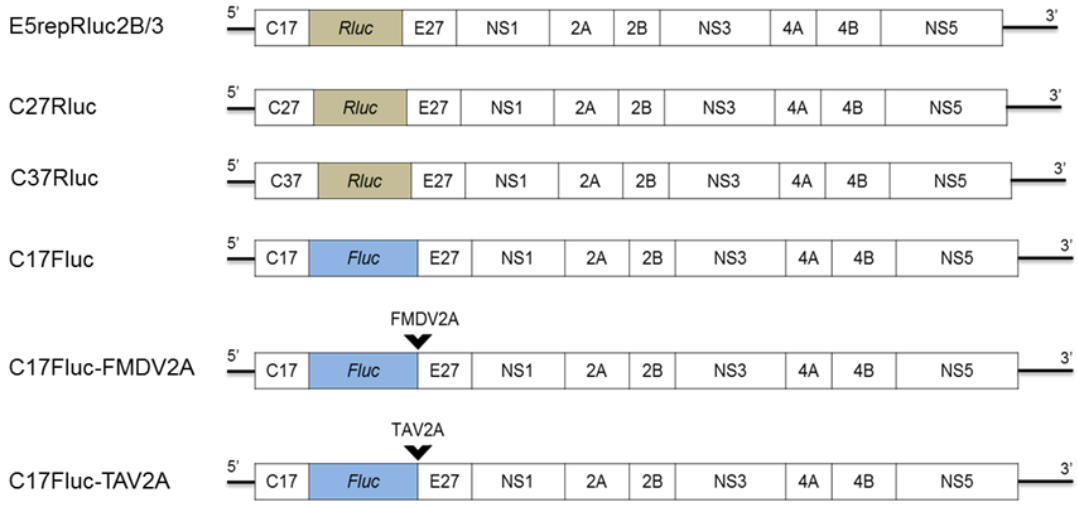

Figure 2.3 Schematic representation of LGTV and TBEV replicons containing luciferase reporter genes

The LGTV replicon (E5repRluc2B/3, (Schnettler et al., 2014) and TBEV replicons (C27Rluc, C37Rluc, C17Fluc, C17Fluc-FMDV2A and C17Fluc-TAV2A (Hoenninger et al., 2008)) contain the first 17, 27 or 37 residues (indicated by C17, C27 or C37) and the last 27 residues of the envelope protein, as well as all non-structural proteins. Sequences coding for Rluc or Fluc were inserted behind the truncated capsid followed, in the case of E5repRluc2B/3, by a LGTV NS2B/3 cleavage site or, in the case of C27Rluc, C37Rluc and C17Fluc, by a TBEV NS2B/3 cleavage site. In the case of C17Fluc-FMDV2A, Fluc is followed by a FMDV2A cleavage site, whereas in C17Fluc-TAV2A Fluc is followed by a TAV2A cleavage site.

Flavivirus replicons were derived from plasmids (Table 2.1). Plasmids were linearised by restriction digest (2.4.2), purified (2.4.3) and *in vitro* transcribed (2.4.4) with a Cap Analog using a SP6 kit or T7 kit for LGTV and TBEV, respectively. Capped transcripts were immediately transfected into cells (2.5.5).

2.5.4 Infection of tick cell lines

Tick cells were harvested and seeded at a density of $5x10^5$ cells per ml in 24-well plates (1 ml) or flat-sided tubes (2 ml) and incubated for 24 h. Virus diluted in either PBS and BSA (PBSA, 0.75 g BSA per 100 ml PBS (0.75 %) (SFV) or complete culture medium (TBEV, LGTV) was added to the cells at the required MOI. After incubation for the required time, supernatant medium containing virus was collected if required and cells harvested for analysis.

2.5.5 Transfection of BHK-21 cells and tick cell lines

BHK-21 cells were either electroporated with viral RNA to grow virus (2.5.1) or transfected with replicon RNA using Lipofectamine 2000 transfection reagent (Invitrogen). Tick cell lines were transfected with replicon, siRNA or dsRNA using either Lipofectamine 2000 or X-tremeGENE siRNA transfection reagent (Roche). BHK-21 cells were seeded at a density of $1x10^5$ cells/well in 24-well plates, and tick cells were seeded at a density of $5x10^5$ cells/well in 24-well plates. All cell lines were incubated for 24 h at the appropriate temperature prior to transfection. For each well, 50 µl OptiMEM (PAA Laboratories) was mixed with 2 µl transfection reagent by gentle shaking and incubated for 5 min at room temperature. In a separate RNase-free tube, RNA was diluted with OptiMEM to a final volume of 50 µl and kept for 5 min at room temperature. The transfection reagent mixture was added to the diluted RNA and incubated for 30 min at room temperature (transfection mix). After incubation, 100 µl of the transfection mix was added to each well and incubated at the appropriate temperature. To prevent BHK-21 cells from dying due to the toxicity of the transfection reagent, medium was replaced with fresh growth medium 5 h after transfection. Tick cells are not negatively affected by transfection reagent and were kept without medium change until sampling.

2.5.6 Plaque assay

2.5.6.1 Titration of SFV

Titres of SFV present in the supernatant were determined by plaque assay in BHK-21 cells. A 4% solution of agar was prepared by mixing 4 g of Bacto-agar per 100 ml of PBS and sterilised by autoclaving. BHK-21 cells were seeded in six-well plates at a density of $3x10^5$ cells/well with 2 ml of GMEM/5%NBCS and were kept at 37ºC overnight. Virus stocks or samples to be titrated were serially diluted ten-fold to a final dilution of 10^{-11} in PBSA. When the cells were 80% confluent, growth medium was removed and 400 µl of each dilution was added to duplicate wells starting with the highest dilution. The plates were incubated for 1 h at room temperature on a shaker to spread the inoculum evenly over the BHK-21 monolayers. In the

meantime, the agar was melted in a water bath at 90°C and then cooled to 55°C. Pre-warmed GMEM containing 2% NBCS (v/v) was mixed with 4% agar, in a 3:1v/v ratio (medium:agar), and 3 ml of the mixture was carefully added to each well. The plates were then incubated for 2-3 days. After incubation, cells were fixed with 3 ml of 10% neutral buffered formaldehyde (Leica) for 1 h at room temperature. The formaldehyde was poured off and the agar plugs removed using a metal spatula. Cell monolayers were then stained with 0.1% toluidine blue for 30 min. After incubation, the dye was removed, the plates washed once or twice with tap water and the plaques counted. To calculate the number of plaque-forming units (PFU) per ml contained in each sample the following formula was used:

$$PFU/ml = \left(\frac{average\ number\ of\ plaques}{amount\ of\ inoculum\ (ml)}\right) \times dilutionfactor$$

2.5.6.2 Titration of LGTV

Plaque assays for the titration of LGTV were performed on BHK-21 cells in 12-well plates using microcrystalline cellulose Avicel overlay. Cells were seeded at a density of $1.5x10^5$ cells per well in 1 ml of GMEM/5%NBCS and incubated at 37ºC overnight. When the cells were 80% confluent, medium was removed and replaced with 400 µl of virus-containing supernatant (2.5.2, 2.5.4) 10-fold serially diluted in GMEM/2% NBCS. Virus dilutions were applied to 2 wells each, starting with the highest serial dilution and incubated for 1 h at room temperature on a shaker. During the incubation the sterilised Avicel suspension (1.2 g Avicel RC-581 (FMC Biopolymer) in 100 ml PBS) was mixed in a 1:1 ratio with 2x Minimum Essential Medium (Gibco) supplemented with 5% FCS. Infected cells were overlayed with 1.5 ml of the Avicel-medium mix and incubated for 4 days. Cells were then fixed, stained and plaques counted as described above in 2.5.6.1 .

2.5.6.3 Titration of TBEV

The titration of TBEV was done using a plaque assay on PS cells (De Madrid & Porterfield, 1969) in a 24-well plate. In each well, 20 µl of virus-containing supernatant (2.5.2, 2.5.4) was ten-fold serially diluted in 180 µl of L-15 /3% NBCS

in duplicate and then 300 µl of $1.2x10^5$ PS cells suspended in L-15/3% NBCS were added to each well. The plates were incubated for 4 h to allow the PS cells to attach to the bottom of each well. To prepare the overlay, 2x concentrated L-15 containing 6% NBCS was mixed in a 1:1 ratio with a 1.5% carboxymethyl cellulose (CMC) solution (w/v). When cells were attached, 400 µl of the overlay mixture was added to each well and the plates were incubated for 5-6 days. After incubation, cells were washed in physiological saline (0.9% NaCl) to remove the overlay and finally stained for 45 min with naphthalene black staining solution (De Madrid & Porterfield, 1969). Naphthalene black staining solution comprised 1 g Naphthol blue black (Sigma), 60 ml glacial acetic acid (Sigma), 13.6 g sodium acetate and 1 l water. To calculate the number of PFUs the formula described in 2.5.6.1 was used.

2.6 Luciferase assay

A Dual-Glo Luciferase assay system (Promega) was used to measure both Rluc and firefly luciferase (Fluc). Infected or transfected mammalian or tick cells were lysed by removing the culture medium and adding 100 µl of 1 x passive lysis buffer (Promega) diluted in water. Cells were then incubated for 1 h on a shaker to ensure complete cell lysis. After cell lysis, 40 µl aliquots of the samples were analysed in a 96-well plate using the appropriate substrate of the Dual Luciferase Reporter assay according to the manufacturer's instructions. Luminescence was measured with a GloMax-Multi+Detection system (Promega). In brief, injectors were set to dispense 70 µl of LARII reagent, which is the Fluc substrate and/or 70 µl of Stop&Glo reagent, which quenches the signal of the Fluc and activates Rluc. For the measurement of luciferase a delay of 2 s and integration time of 10 s were used. Luminescence results, expressed in light units, were analysed using the Instinct software (Promega) supplied with the GloMax detection system.

2.7 Immunostaining and antibodies

Primary and secondary antibodies used for immunostaining are listed in Table 2.9. TBEV-infected tick cells were immunostained with the mouse Anti-Flavivirus Group Antigen Antibody (Millipore) that reacts with the TBEV E protein (Haridas et al.,

2013; Henchal et al., 1982) or the NS1 antibody (Iacono-Connors et al., 1996) provided by Prof. Franz Heinz. LGTV-infected tick cells were immunostained using the chicken monoclonal NS5 antibody (Offerdahl et al., 2012), provided by Dr Sonja Best via Dr Esther Schnettler. The immunostaining for LGTV was done by Claudia Rückert.

Table 2.9 List of antibodies used during this project

Target	Name/Clone	Source	Host	Isotype	Dilution
TBEV E protein	Anti-Flavivirus Group Antigen Antibody/ Clone D1-4G2-4-15	Millipore	Mouse	monoclonal IgG2a	1:100
TBEV NS1 protein	Clone 5D9	Franz X. Heinz	Mouse	monoclonal	1:100
LGTV NS5 protein	-	Sonja Best and Esther Schnettler	Chicken	polyclonal	1:800
Alexa Fluor 488 anti-chicken	Alexa Fluor® 488 Goat Anti-Chicken IgG (H+L)	Life Technologies	Goat	monoclonal IgG	1:1000
DyLight 488 anti-mouse	Goat anti-Mouse IgG (H+L) DyLight 488 conjugate	Pierce Thermo Scientific	Goat	polyclonal IgG	1:1000

Tick cells were grown on 12 mm diameter glass coverslips in 24-well plates and were infected with either TBEV strain Neudoerfl or LGTV (TP-21) for the time-period specified in each experiment. At the time of sampling medium was removed, cells were washed once with PBS and fixed in 10% neutral buffered formaldehyde (Leica) for at least 45 min. After fixation, coverslips were washed with PBS for 5 min before permeabilising the cells using 300 µl of 0.3% TritonX-100 (Sigma-Aldrich) in PBS per well. After 30 min incubation the TritonX-100 was removed and the cells were further permeabilised using 0.1% SDS in PBS for 10 min. Cells were washed for 5 min with PBS and treated, in the case of TBEV-infected cells, with 300 µl of 1% BSA in PBS, or in the case of LGTV-infected cells, with 300 µl of CAS-block (Invitrogen) for 60 min. Both solutions are blocking agents that reduce nonspecific background staining. After 60 min the blocking solution was removed and the primary antibodies diluted in 1% BSA in PBS (TBEV) or CAS-block (LGTV), as shown in Table 2.9, were added to the cells and incubated for 2 h at room temperature or overnight at 4ºC. After washing 3 x for 5 - 10 min in PBS the appropriate secondary antibody diluted 1:1000 in 1% BSA in PBS for TBEV or

CAS-block for LGTV was added and incubated for 1 h. The coverslips were washed 3 times with PBS for 5 min each and mounted with Vectashield HardSet mounting medium containing DAPI (4'-6-Diamidino-2-phenylindole; Vector Laboratories) on slides. After the mounting medium hardened, immunostaining was visualised using fluorescence microscopy (2.2.1).

2.8 Protein techniques

2.8.1 Protein extraction from tick cells

Proteins from tick cells were extracted using the mild non-ionic detergent Triton X-100 (Sigma-Aldrich). In brief, tick cells were harvested into microfuge tubes and centrifuged at 500 x g for 5 min. The supernatant was discarded and the cell pellet was washed twice with ice-cold PBS to remove traces of medium and extracellular virus. To isolate soluble proteins, the cell pellet was resuspended in 350 µl ice-cold PBS supplemented with 1% Triton X-100, 50 µl cOmplete, Mini, EDTA-free Protease Inhibitor Cocktail (Roche) and 3.5 µl Halt Phosphatase Inhibitor Cocktail (Thermo Scientific Pierce). The mixture was incubated for approximately 1 h on ice to allow disruption of the cell membrane and release of intracellular material in soluble form. After incubation the cell suspension was homogenised using a micro pestle (Sigma) on ice and centrifuged at 200 x g for 5 min to remove any cell debris. The supernatant containing the soluble proteins was transferred to a new microfuge tube. Protein concentration was measured by bicinchoninic acid (BCA) protein assay as described below (2.8.2). Protein samples were stored at -80°C.

2.8.2 BCA protein assay

The concentration of soluble proteins within protein extracts was measured using the BCA protein assay kit (Thermo Scientific Pierce) according to the manufacturer's instructions. The kit was chosen for compatibility with Triton X-100. BSA was used to generate a standard curve: a stock solution of 2 mg BSA per ml of milli-Q water was diluted in the solvent used for protein extraction (PBS supplemented with 1% Triton X-100, 142.9 µl protease-inhibitor and 10 µl phosphatase-inhibitor; 2.8.1) to

achieve a working range of 125 to 2000 µg BSA per ml diluent. To measure the concentration of protein, 200 µl of the BCA working reagent, which is a mixture of 50 parts Reagent A containing BCA and 1 part Reagent B containing cupric sulphate, was added to 10 µl of each of the BSA standard dilutions and 10 µl of each sample in a 96-well plate. The plate was covered and incubated in the dark at 37°C for 30 min. The proteins within the samples reduce Cu^{2+} to cuprous ion which in turn forms a complex with BCA leading to a purple-coloured reaction, the intensity of which corresponds linearly to the amount of protein within the sample. After 30 min incubation absorbance was measured at 540 nm wavelength using an Infinite m200 microplate reader (Tecan) and the protein concentration was calculated using an equation obtained from the BSA standard curve.

Equation: $$concentration = \frac{absorbance}{slope}$$

2.8.3 Sodium dodecyl sulphate – polyacrylamide gel electrophoresis (SDS-PAGE)

To evaluate the protein quality, soluble proteins were separated by SDS-PAGE and subsequently stained with Coomassie Blue (2.8.4). A 12% acrylamide resolving gel was prepared with 6 ml 40% acrylamide (Sigma), 8.7 ml deionised water, 5 ml 1.5 M Tris-base pH 8.8 (Sigma) and 200 µl 10% SDS (Sigma). To polymerise the solution 40 µl tetramethylethylenediamine (TEMED) (Sigma) and 200 µl 10% ammonium persulphate (APS) (Sigma) were added. The solution was immediately poured between the glass plates (1.5 mm thick, Mini PROTEAN 3 system, BioRad) used to make a gel leaving approximately 2 - 3 cm of space at the top to accommodate the stacking gel. The empty space was filled with water to straighten the gel and to prevent air bubbles from forming. Once the resolving gel had set, the water was removed and a 4% stacking gel prepared with 0.4 ml 40% bisacrylamide, 2.56 ml deionised water, 1 ml 0.5 M Tris-base pH 6.8 (Sigma), 40 µl 10% SDS, 16 µl TEMED and 80 µl 10% APS was poured on top. A comb forming ten wells was inserted and once the stacking gel had set, the gel was placed into an electrophoresis tank and the comb removed. The tank was filled with running buffer, made up of 25 mM Tris-base (Sigma), 250 mM glycine (Sigma) and 0.1% SDS. Protein samples

were mixed 1:1 (v/v) with 2x Laemmli buffer (Biorad) supplemented with 5% β-mercaptoethanol (Sigma) and heated at 96°C for 10 min to reduce disulphide bonds and denature the proteins to allow separation by size. The samples were then loaded into the wells and the gel run for 30 min at 40 V to allow the proteins to enter and pass through the stacking gel slowly. After 30 min a higher voltage of 120 was applied until the bromophenol blue band, a component of the Laemmli buffer, reached the bottom of the gel indicating that the proteins had separated through the gel.

2.8.4 Staining of SDS-PAGE gels with Coomassie

For staining gels a solution consisting of 0.25 g Coomassie Brilliant Blue R-250 (Coomassie; Thermo Scientific Pierce) dissolved in 45 ml water, 45 ml methanol (Sigma-Aldrich) and 10 ml glacial acetic acid (Fisher Scientific) was prepared. The protein gels were immersed in the staining solution and placed on a slow rocker for a minimum of 3 h. To remove the excess stain, gels were placed into a de-staining solution which consisted of 45 ml methanol, 45 ml water and 10 ml glacial acetic acid and heated for 30 s in the microwave. The de-staining solution was changed several times until the protein bands were clearly visible.

2.8.5 In-gel digestion of proteomes

To prepare protein extracts for proteomic analysis by mass spectrometry (MS) proteins extracted from tick cells (2.8.1) were in-gel digested following the method described by Shevchenko (2006) (Shevchenko et al., 2006). In brief, protein extracts equivalent to 100 µg, obtained by pooling equal aliquots from the replicates in each experimental group, were suspended in a volume of 100 µl of Laemmli buffer supplemented with 5% β-mercaptoethanol. The suspension was applied onto an SDS-PAGE gel prepared as described in 2.8.3, except that a comb generating 1.2 cm-wide wells was used. As soon as the samples entered approximately 3 mm into the resolving gel the electrophoretic run was stopped, so that the whole proteome became concentrated in the stacking/resolving gel interface. The proteome was visualised by staining as described above (2.8.4) except that Bio-Safe Coomassie

Stain G-250 (BioRad) was used, the proteome band was excised and cut into cubes of 2 x 2 mm.

The cubes were placed in 0.5 ml microfuge tubes and the gel pieces were destained in a 1:1 (v:v) mixture of acetonitrile (AcN) (Carlo Erba) and water. Further washing and destaining were performed by dehydrating the cubes using 100% AcN and incubating for 5 min. The AcN was removed and the cubes rehydrated in 50 mM ammonium bicarbonate (Sigma-Aldrich) pH 8.5 for 5 min before addition of an equal amount of AcN and incubation for 15 min. The liquid was removed and the gel pieces washed with 250 µl AcN for 5 min before addition of 55 mM Iodoacetamide (GE Healthcare) and incubation for 30 min in the dark. The liquid was removed and the gel pieces washed twice with 50% aqueous AcN solution for 5 min and then dehydrated using sufficient AcN to cover the gel cube. The AcN was removed and the gel pieces were dried in a Concentrator Plus vacuum concentrator centrifuge (Eppendorf) for approximately 30 min.

After these washing steps the proteome was digested *in situ* with sequencing grade trypsin (Promega). For digestion the dried gel pieces were re-swollen in 332 µl of 50 mM ammonium bicarbonate pH 8.8 containing 60 ng/µl trypsin (ratio of 5 parts protein: one part trypsin w/w). The tubes were kept on ice for 2 h and were then incubated at 37°C for 12 h. Digestion was stopped by the addition of 1% trifluoroacetic acid (TFA) (Carlo Erba). The supernatant containing the proteins was then desalted using OMIX Pipette tips C18 (Agilent) according to the manufacturer's instructions. Briefly, pipette tips were humidified with 60 µl 50% AcN twice, followed by 60 µl 100% AcN twice. Once humidified, tips were equilibrated three times with 60 µl 0.1% TFA, and the protein bound to the filter by taking up and releasing the sample approximately 10 times. The bound proteins were then washed twice with 100 µl 0.1% TFA to remove excess salt and eluted into a clean microfuge tube using 50 µl 0.1% TFA in 50% AcN. Once desalted the supernatant was dried down in the vacuum concentrator centrifuge and the protein was stored at -20ºC until analysed by MS.

2.8.6 2D- Difference in gel electrophoresis (DIGE)

2.8.6.1 Sample preparation

Differential protein expression in response to TBEV infection was determined by 2D-DIGE of infected and mock-infected IRE/CTVM19 cells. Protein extracts of each condition and each day were separately pooled using 100 µg of each replicate. To concentrate tick cell samples, proteins were precipitated using 500 µl ice-cold acetone (Carlo Erba) overnight at -20°C. The precipitate was centrifuged at 12,000 x g for 10 min, the acetone was removed and samples were allowed to dry on ice. The resultant air-dried protein pellets were resuspended in 30 µl CLS buffer, consisting of 7 M UREA (Merck), 2 M thiourea (Merck) and 4% (w/v) CHAPS electrophoresis reagent (Sigma) made up to a final volume of 25 ml with deionised water.

2.8.6.2 Labelling with fluorescent dyes

Protein concentration was measured using BCA protein assay (2.8.2) and samples were labelled using the CyDye DIGE Fluor Kit (GE Healthcare, Amersham). Dyes were prepared by adding 1.5 parts of N,N-Dimethylformamide (Sigma) to 1 part of dye. The solution was vortexed and centrifuged at 12,000 x g for 30 sec. Aliquots containing 50 µg protein from each infected and mock-infected sample were labelled with either 1 µl of Cy5 or Cy3 in a randomised set-up. Equal amounts of proteins in CLS buffer from each infected and mock-infected sample were pooled to generate an internal pool which was labelled with Cy2 dye. This labelled pool was included in all gel runs as standard to aid cross-gel statistical analysis. Staining was done for 30 min on ice in the dark and the reaction was stopped by addition of 1 µl 10 nM lysine. The mixture was incubated for 10 min on ice and frozen until use.

2.8.6.3 Isoelectric focusing and second dimension SDS-PAGE

To separate proteins effectively they were first separated according to their isoelectric point using a pH gradient on Immobilised pH gradient (IPG) strips (Immobiline DryStrip (pH 3-11 NL, 24 cm); GE Healthcare) and then in the second dimension according to their size by SDS-PAGE. IPG strips used for isoelectric

focusing were rehydrated in DeStreak Rehydration solution (GE Healthcare) in wells of an Immobiline DryStrip Reswelling Cassette (GE Healthcare). Each well was overlayed with Immobiline drystrip cover fluid (GE Healthcare) preventing evaporation during overnight incubation. The next day, excess oil was removed from the IPG strips by blotting on absorbent paper, the strips were transferred to a ceramic IPGphor chamber (GE Healthcare) with gel side up, electrode pads soaked in 100 µl deionised water were put on top of both ends of the strips and electrodes were attached. Loading cups (GE Healthcare) were fixed to the cathode side of the gels and the plate was covered with 100 ml of Immobiline drystrip cover fluid. Meanwhile, frozen Cy3, Cy5 and Cy2 labelled samples were thawed and 20 µl of each were mixed together and added to 60 µl 2x lysis buffer (7 M urea, 2 M thiourea, 4% CHAPS, 30 mM Tris-HCl pH 8.8) supplemented with 2% (v/v) IPG buffer (GE Healthcare) and 130 mM DTT (Merck). The mixture was incubated on ice for 10 min, then 120 µl aliquots were added into the loading cups and overlayed with 20 µl drystrip cover fluid. Isoelectric focusing was carried out with the Ettan IPGphor 3 IEF System (GE Healthcare) using the following parameters: rehydration time 0h, temperature 20°C, pH gradient 3-11 NL, current per strip 50 µA, strip length 24 cm. The run profile (voltage settings and times) is shown in Table 2.10.

Table 2.10 Run profile for isoelectric focusing.

Steps	Voltage	Time
1	300V	3h
2 Gradient	1000V	6h
3 Gradient	10000V	3h
4 Gradient	10000V	3h
5	500 V	3h
Total		**18h**

After 18h the progress of the focusing was checked and strips were refocused at 10,000 V for 15 min. After refocusing IPG strips were removed from the chamber and each IPG strip was transferred into a 10 ml pipette tip containing 8.5 ml equilibration buffer 1 and incubated for 15 min with both ends of the pipette sealed with parafilm. The equilibration buffer 1 consisted of 6M urea, 2% SDS, 50 mM Tris pH 8.8, 0.02% bromophenol blue (GE Healthcare) 30% glycerol and 200 ml

deionised water supplemented with 0.6 g DTT. After incubation the liquid was removed and the strips were transferred to a pipette containing equilibration buffer 2, which was prepared as above but supplemented with 0.25 g iodoacetamide instead of DTT. Strips were again incubated for 15 min before loading onto second-dimension SDS-PAGE gels prepared as follows.

500 ml of resolving gel was prepared as described in 2.8.3 and poured into an Ettan DALTsix Gel Caster (GE Healthcare), overlayed with isopropanol (Sigma) and left to polymerise overnight. The next day the isopropanol was removed, any traces washed away with water and the strip transferred to the gel caster taking care that the strip was in contact with the gel and formation of bubbles was avoided. After overlaying the gel with 0.5% agarose overlay, consisting of 100 ml electrophoresis running buffer (450 ml 10x Tris/glycine/SDS made up to 4.5l with deionised water), 0.5 g low melting agarose (Fermentas) and 1% bromophenol blue, the reswelling cassette was transferred to the electrophoresis chamber which was then filled up to the marked point with electrophoresis running buffer. The upper buffer chamber was filled with 2x electrophoresis running buffer and the gel was run at 0.5 W per gel for 1 h, before increasing to 15 W/gel applied for 4 h. After second-dimension SDS-PAGE, the gel was scanned using the Ettan DIGE Imager (GE Healthcare) with Ettan DIGE Imager software. Pictures were taken at a 100 µm pixel size. Images were analysed by Margarita Villar Rayo, SaBio, Instituto de Investigación en Recursos Cinegéticos, University of Castilla-La Mancha, Ciudad Real, Spain.

2.9 Cloning

2.9.1 Vector for qPCR standard curve (pJET-NS5)

A plasmid suitable for creating a standard curve to facilitate caluculation of TBEV infection levels by qPCR (2.4.10.4) was cloned using the CloneJET PCR Cloning Kit (Fermentas). The plasmid pTND/ΔME (Table 2.1) was linearised by restriction digest (2.4.2), purified (2.4.3) and used as DNA template for amplification of TBEV NS5 (Table 2.3) using KOD polymerase (2.4.10.1). KOD polymerase leaves blunt ends on PCR products which are suitable for cloning into the blunt-end vector pJET1.2. An aliquot of the 187 bp PCR product was visualised by gel electrophoresis

and since only one band with the correct size was visible the non-purified product was directly used for ligation. For ligation, 10 µl 2x reaction buffer, 2 µl non-purified PCR product, 1 µl pJET1.2 blunt cloning vector, 6 µl of nuclease-free water and 1 µl of T4 DNA ligase were mixed by vortexing. The ligation mixture was incubated for 5 min at room temperature before using directly for transformation of DH5α (2.3.2). To check if the correct insert was cloned into the vector, the plasmid was tested by colony PCR as described in 2.4.10.3 and the plasmid was linearised and checked by conventional Taq polymerase PCR (2.4.10.1) using NS5 primers and pJET sequencing primers. The linearised plasmid was sent for sequencing to GATC Biotech (London, UK) and the sequences obtained were verified by alignment using BioEdit Version 7.0.5.3.

2.9.2 Vector encoding TBEV with luciferase marker genes

To generate TBEV with Rluc and Fluc insertions the plasmids pTND/c-eGFP and pTND/ΔME-eGFP (Table 2.1) were used as backbone. PCR products for internal ribosomal entry site (IRES), Rluc and Fluc were generated by PCR using Vent polymerase (2.4.10.1) from the plasmids IRES2-eGFP, pRL-SV40 and pGL3-Basic Vector (Table 2.1) respectively. To generate PCR products with restriction sites for insertion into the backbone, specific primers (Table 2.3, Table 2.11) were designed encoding restriction sites *SacII* and *NotI* for IRES and two *NotI* restriction sites including a Kozak sequence which is required for recognition by ribosomes and is a translation start site.

Table 2.11 Design of primers including restriction sites

Complete sequences of these primers are shown in Table 2.3

Primer Name	Primer design	Expected product size (bp)
IRES F	GCGC *SacII* IRES	585
IRES R	GGCC *NotI* IRES	585
Rluc F	GCGC NotI Kozac ATG Rluc	936
Rluc R	GGCC NotI STOP Rluc	936
Fluc F	GCGC NotI Kozac ATG Fluc	1668
Fluc R	GGCC NotI STOP Fluc	1668

PCR products were visualised by agarose gel electrophoresis (2.4.5) and the bands of the expected size were excised and purified using the GE Healthcare kit (2.4.6). Before ligation, plasmids and the purified IRES sequence were cut with *SacII* and *NotI* (2.4.2) and gel-purified (2.4.6). To prevent the plasmids from reconnecting without insert during ligation, plasmids were dephosphorylated by adding 1 µl shrimp alkaline phosphatase (Roche), 2 µl 10X buffer and nuclease-free water to a final volume of 20 µl. The mixture was incubated for 20 min before the enzyme was inactivated by heating at 67°C for 15 min. Ligation was achieved by addition of 3 µl 10x T4 DNA ligase buffer (NEB), 2 µl T4 DNA ligase (NEB) and the IRES PCR product in a vector:insert ratio of 1:3, and incubation at 16°C for 4h. To stop the reaction, samples were heated at 65°C and the enzyme removed by purification using the GE Healthcare kit. Insertion of IRES was verified by restriction digest (2.4.2) and subsequent visualisation of restriction fragments by gel electrophoresis. Additionally the linearised plasmids were sent for sequencing to GATC Biotech. After insertion was verified, plasmids containing IRES and the Rluc and Fluc PCR products were digested with *NotI* restriction enzymes, visualised by gel electrophoresis and gel purified (2.4.6). Then plasmids were dephosphorylated and ligated with Fluc or Rluc as described above. Insertion was verified by restriction digest and sequencing at GATC Biotech using IRES F primers. Constructs are depicted in Figure 2.2.

2.10 Flow cytometry

To determine the number of tick cells positive for SFV infection, cells were analysed by flow cytometry. In brief, tick cells were harvested into microfuge tubes and centrifuged at 400 x g for 5 min. The supernatant was discarded and the cell pellet resuspended in 200 µl 10 % neutral-buffered formaldehyde. Cells were fixed for 30 min at room temperature before pelleting by centrifugation at 400 x g for 5 min. Fixative was removed, the cells resuspended in 150 µl PBS and transferred into a 5 ml round-bottom tube. Depending on the amount of cells, they were further diluted up to a maximal volume of 500 µl. Cells were then analysed by flow cytometry on a Beckman FACSCalibur for green fluorescence.

3 Chapter 3 Characterisation of viral infection in tick cells

3.1 Introduction

The first continuous tick cell lines were established nearly 40 years ago (Varma, Pudney & Leake, 1975); since then the focus has expanded from propagating bacteria, different arboviruses and non-arboviruses and looking at persistent virus infection to research on tick biology, functional genomics and proteomics, antibiotic resistance, acaricide resistance, vaccine development and genetic manipulation (Bell-Sakyi et al., 2007, 2012). The earliest studies showed that although many mosquito-borne viruses and most tick-borne viruses could infect a number of tick cell lines, the pattern of infection, including virus replication and production, varied with the virus and the cell line used (Bhat & Yunker, 1979; Leake, Pudney & Varma, 1980; Pudney, 1987; Rehacek, 1987; Varma, 1989; Varma, Pudney & Leake, 1975). Therefore it is important to establish basic infection parameters using the virus and cell line of interest before further experiments are undertaken. For the present study the cell lines ISE6 and IDE8, derived from *I. scapularis* eggs, and IRE/CTVM19, derived from *I. ricinus* eggs, were used to characterise viral infection using a mosquito-borne alphavirus (SFV) and two tick-borne flaviviruses (LGTV, TBEV). Previously IDE8 and ISE6 had been mostly used for the propagation of bacteria (Bell-Sakyi et al., 2007); ISE6 had also been used to propagate WNV, POWV, LIV, Dugbe virus, Hazara virus, LGTV, TBEV and SFV (Barry et al., 2013; Garcia et al., 2005; Lawrie et al., 2004). The cell line IRE/CTVM19 was used for the propagation of *A. phagocytophilum* (Pedra et al., 2010) but TBEV was the only virus reported to have been grown in this cell line (Růzek et al., 2008) at the start of this study, though subsequently Barry et al. (2013) reported growth of SFV in IRE/CTVM19 cells.

3.2 Objectives

1. To determine what proportion of cells can be infected with SFV, LGTV and TBEV in a tick cell line
2. To determine the kinetics of SFV, LGTV and TBEV infection in tick cells
3. To determine whether replication complexes or similar structures are formed in virus-infected tick cells

4. To determine uptake and transfection efficiency of dsRNA and siRNA in tick cells

3.3 Experimental set-up

Different techniques, viruses and cell lines were used in the present study. Tick cells were cultured in flat-sided tubes (2.1.1) and seeded at a cell density of either 5 $x10^5$ cells per well in 24-well plates or 1 x 10^6 cells per tube in flat-sided tubes (2.5.4). Cells were then infected (2.5.4) at different MOIs by adding either SFV reporter viruses (2.5.1), LGTV (2.5.2) or TBEV (2.5.2) to the culture.

To determine what proportion of cells can be infected with virus, LGTV- and TBEV-infected cells were stained with virus-specific antibodies as described in 2.7 and the virus-positive and negative cells were visually counted using light microscopy with concurrent brightfield and UV illumination (2.2.1). For infection with SFV, SFV reporter viruses containing fluorescent markers were used and the proportion of virus-positive cells determined either by visual counting using light microscopy or by Fluorescence-activated cell sorting (FACS; 2.10).

For determining the kinetics of SFV, LGTV or TBEV infection, cells were either infected with wildtype virus or transfected (2.5.5) with replicons derived from plasmids (2.3.2, 2.4.1 – 2.4.4). Tick cells were infected with SFV reporter viruses encoding Rluc in their structural or non-structural reading frame. At different time-points p.i. supernatant was collected to establish virus production curves using plaque assay in BHK-21 cells (2.1.2, 2.5.6.1) and cells were lysed to measure Rluc expression by luciferase assay (2.6). One experiment, which generated relevant data highly important for this PhD, was done by my colleague Claudia Rückert and is therefore included here (*in italics*). *To determine the kinetics of LGTV infection, tick cells were infected with wildtype LGTV, the supernatant was collected for titrating the virus in BHK-21 cells and RNA was isolated using the RNeasy mini kit for measuring virus RNA levels by qRT-PCR.* The methods that Claudia Rückert used can be found in sections 2.5.2, 2.1.2, 2.5.6.1, 2.4.7, 2.4.10.2 and 2.4.10.4. To assess the kinetics of virus replication further a LGTV replicon encoding Rluc was transfected into tick cells (2.5.3, 2.5.5) and Rluc expression measured by luciferase

assay. The kinetics of TBEV production in tick cells were determined by establishing virus growth curves from supernatant of infected cells. Virus present in supernatant was titrated by plaque assay on PS cells (2.5.6.3). Additionally, the kinetics of virus replication were determined by using different TBEV replicons encoding Rluc or Fluc, cloned either behind an IRES in the 3' non-structural region (2.9.2) or behind the capsid protein (2.5.3). The backbone for the IRES-containing replicon and the replicons with Rluc or Fluc inserted behind the capsid were provided by Prof Franz X. Heinz (2.5.3). Replication was assessed by measuring luciferase expression in a luciferase assay and, in the case of the IRES-containing replicon (2.9.2), also by qRT-PCR (2.4.10.2, 2.4.10.4).

Whether or not virus infection caused ultrastructural changes such as the formation of replication complexes in virus-infected tick cells was assessed in the case of SFV infection by TEM (2.2.2.1). In the case of TBEV-infected tick cells, samples were either cryofixed (2.2.2.2) and directly assessed by TEM or cryofixed, immunolabelled (2.2.2.3) and then assessed by TEM.

To determine the uptake and transfection efficiency of dsRNA and siRNA in tick cells, tick cells were transfected in the presence or absence of different transfection reagents with fluorescently labelled dsRNA (2.4.11) or siRNA. The uptake was confirmed by confocal microscopy (2.2.1) and the transfection efficiency was calculated from photographs taken under a light microscope by counting the proportion of fluorescing cells.

Experimental details not described in Chapter 2 Materials and Methods will be presented in each Results section.

3.4 Results

3.4.1 Infection of tick cells with SFV, LGTV and TBEV

It was necessary to establish basic infection parameters in order to perform subsequent studies on the responses of tick cells to virus infection. The proportion of cells that could be infected with virus at various MOIs was first determined. This was especially important for heterogeneous tick cell lines (Bell-Sakyi et al., 2007, 2012; Yunker, 1987) since some cell types within these cultures might not support virus infection. To address this issue tick cells were infected with SFV-derived reporter viruses, LGTV or TBEV.

Triplicate cultures of ISE6 and IRE/CTVM19 cells were infected with SFV4-steGFP at MOI 0.1, 5 and 10, while control cells were mock-infected with PBSA (Figure 3.1, Figure 3.2). Inverted microscope images were taken of three randomly-selected fields every 12 h for the first 3 days and then every 24 h up to day 7 (Figure 3.1). The numbers of eGFP-positive and negative ISE6 cells were counted using three images of each triplicate sample and the percentage of eGFP-positive cells was calculated (Figure 3.2). Counting of eGFP-positive and negative IRE/CTVM19 cells was not attempted since the auto-fluorescence of these cells could not be distinguished from eGFP fluorescence caused by SFV4-steGFP infection (Figure 3.1).

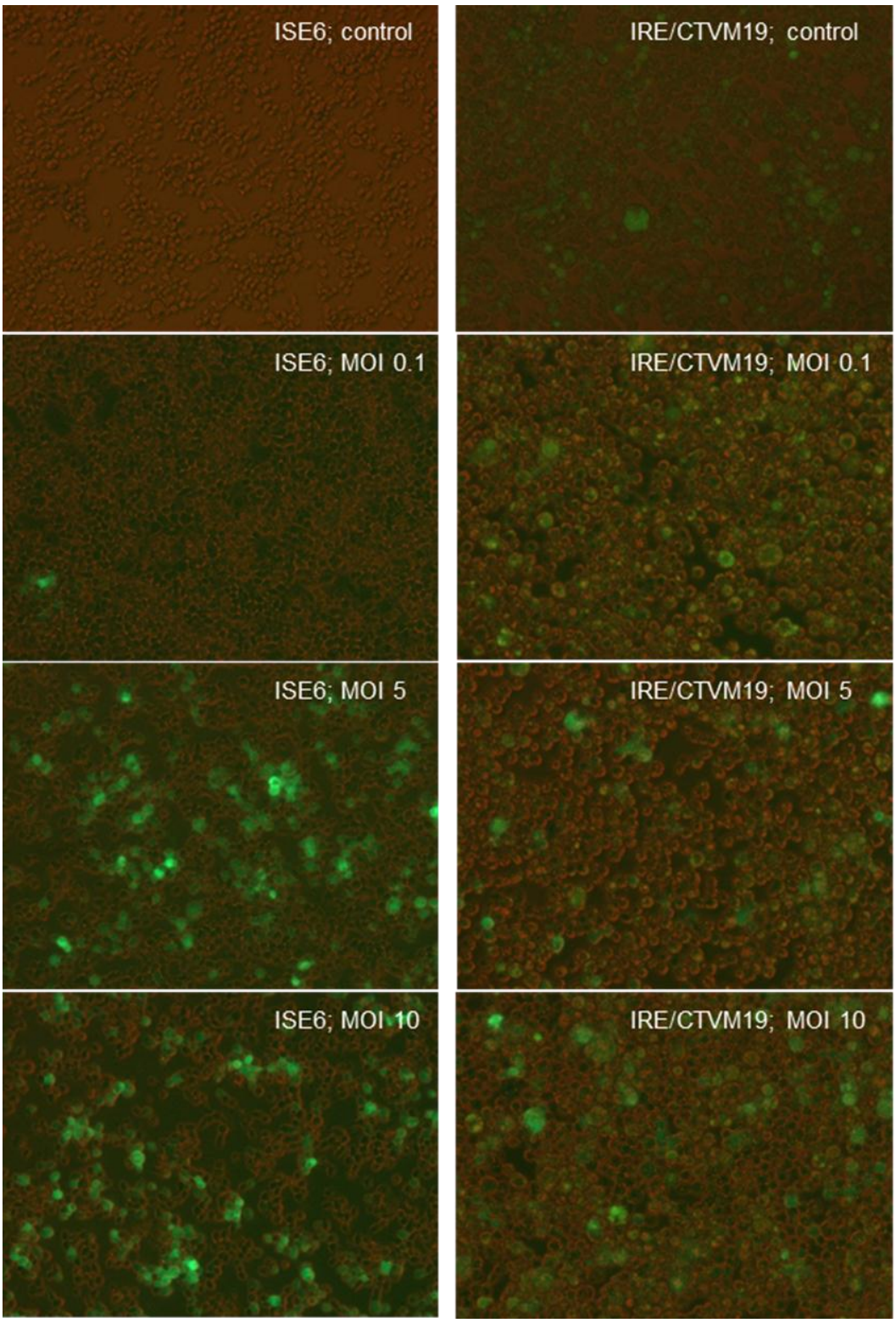

Figure 3.1 Images of control and eGFP-positive tick cells following infection with SFV4-steGFP

ISE6 and IRE/CTVM19 cells were infected with SFV4-steGFP at MOI 0.1, 5 and 10. Images show ISE6 (left panel) and IRE/CTVM19 (right panel) at day 1 p.i.. Pictures were taken using the Zeiss Axiovert Observer D1 inverted microscope at 100x magnification with concurrent bright field and UV illumination.

In ISE6 the percentage of eGFP-positive cells increased more rapidly at MOI 5 and 10 than at MOI 0.1 (Figure 3.2). There was no difference in the percentage of eGFP-positive cells between MOI 5 and 10. At 24 – 36 h p.i. approximately 53% of cells were eGFP-positive and this value did not increase any further with time. For ISE6 infected at MOI 0.1, the percentage of eGFP-positive cells increased and reached a plateau, at approximately 49% eGFP-positive cells, at 2.5 days p.i.. The overall percentage of ISE6 cells containing replicating virus, as determined by detectable eGFP expression from the virus subgenomic promoter, was 49% (± 2.78) (data derived from days 4, 5 and 6 in all three studies combined).

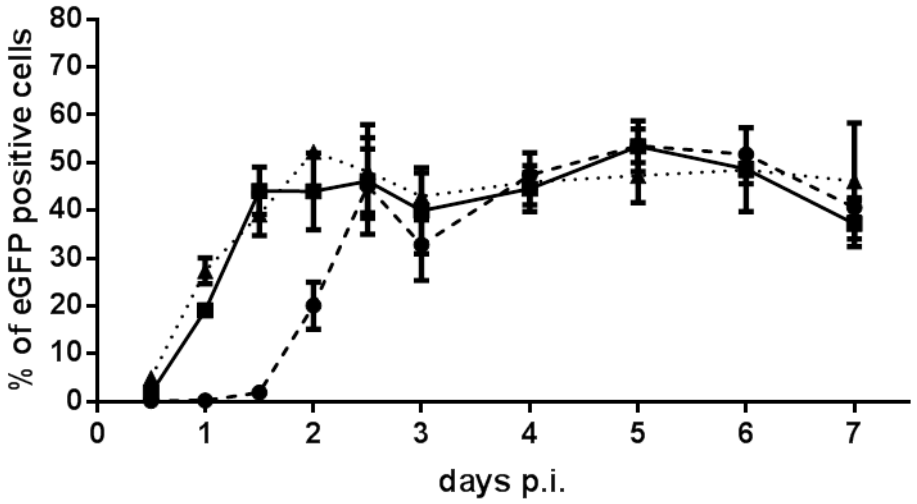

Figure 3.2 Percentage of eGFP-positive ISE6 cells upon infection with SFV4-steGFP

ISE6 cells were infected with SFV4-steGFP at MOI 0.1 (- - -), 5 (——) and 10 (····). Percentage of eGFP-positive ISE6 cells was determined by visual counting over a 7 day time-period. Experiment was done once in triplicate. Error bars are standard deviations.

A solution for the difficulty in distinguishing auto-fluorescence from fluorescence caused by infection was found by using a different SFV-derived reporter virus, SFV4(3F)-ZsGreen. This reporter virus has the marker gene ZsGreen fused to SFV nsp3 and shows a very distinctive, punctate fluorescence (indicating the location of replication complexes) making it easier to distinguish between ZsGreen-positive and negative cells. IRE/CTVM19 and IDE8 cells were infected with SFV4(3F)-ZsGreen at MOI 1, 5 and 10 and controls were mock-infected with PBSA. Images were taken at 12 h, 18 h and every 24 h thereafter up to day 7 as described above (Figure 3.3).

ZsGreen-positive and negative cells were counted using three images of each triplicate sample and the percentage of ZsGreen-positive cells was calculated (Figure 3.4 A and B).

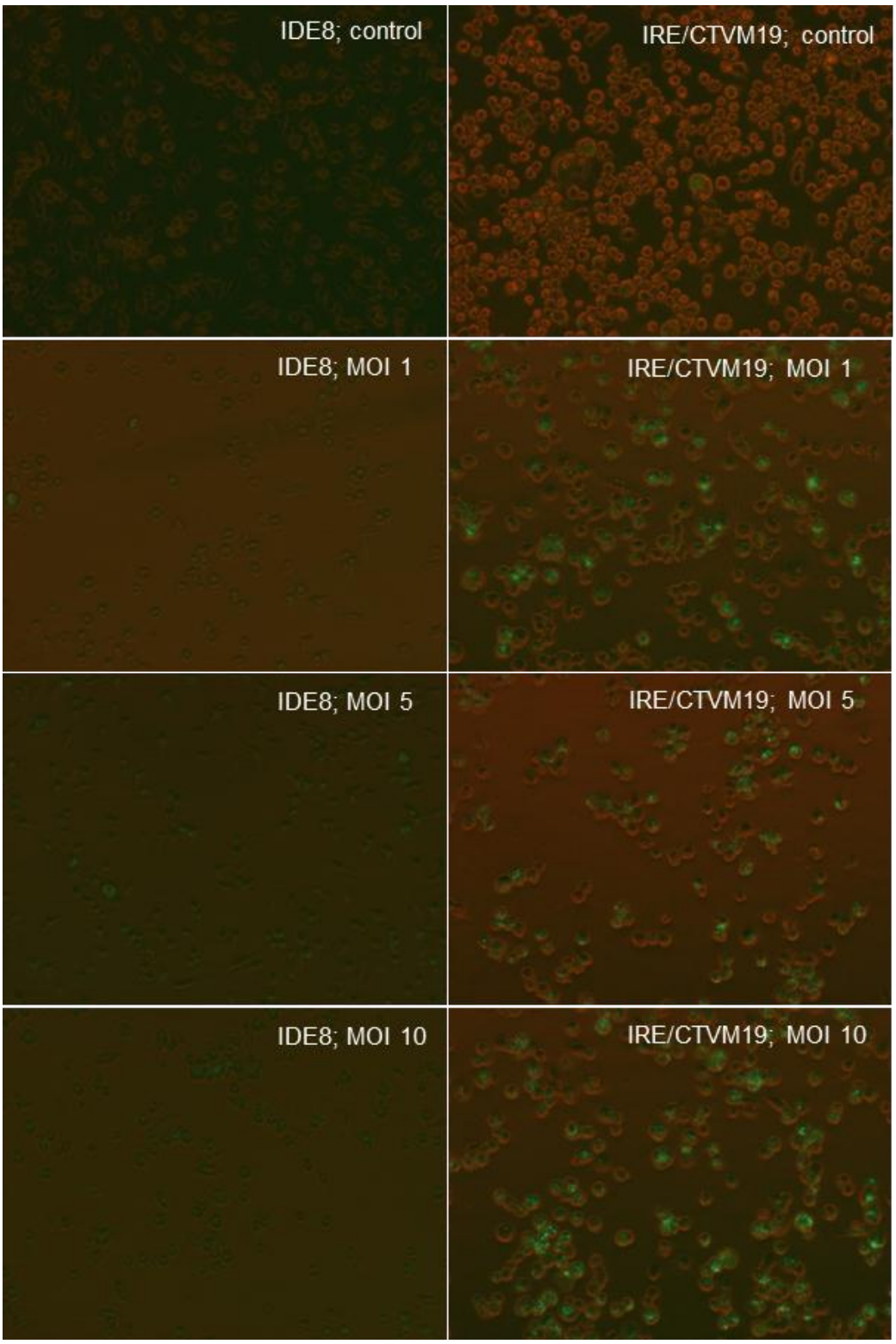

Figure 3.3 Images of control and ZsGreen-positive tick cells following infection with SFV4(3F)-ZsGreen

IDE8 and IRE/CTVM19 cells were infected with SFV4(3F)-ZsGreen at MOI 1, 5 and 10. Images show IDE8 (left panel) and IRE/CTVM19 (right panel) at day 1 p.i.. Pictures were taken using the Zeiss Axiovert Observer D1 inverted microscope at 100x magnification with concurrent bright field and UV illumination.

In IDE8 cells, similar numbers of cells were ZsGreen-positive at MOI 5 and 10 over the 7 day time-period (Figure 3.4 A). The maximum number of cells productively infected was between 40 and 50% at day 1. Cells infected at MOI 1 had a lower level of productive infection reaching a maximum of 40% of ZsGreen-positive cells at day 5. Between 65 and 70% of IRE/CTVM19 cells were positive for ZsGreen between days 1 and 2 when infected with MOI of 5 or 10. When infected at MOI 1, numbers of ZsGreen-positive cells reached a maximum of 60- 70% at day 2 (Figure 3.4 B). Thereafter in both cell lines the percentage of ZsGreen-positive cells decreased with time. Compared to IRE/CTVM19, about 20-30% fewer IDE8 cells were infected, suggesting that IDE8 cells are either less permissive to infection with SFV or, although they are infected, fewer cells express ZsGreen. When comparing how many cells can be productively infected, resulting in expression of ZsGreen, in the *I. scapularis*-derived cell lines ISE6 (Figure 3.2) and IDE8 (Figure 3.4 A), approximately 10% more ISE6 cells were infected than IDE8. However as different SFV constructs were used in the two experiments, it is not clear whether the difference in infection levels resulting in fluorescent marker gene expression was due to differences between the cell lines or the virus constructs.

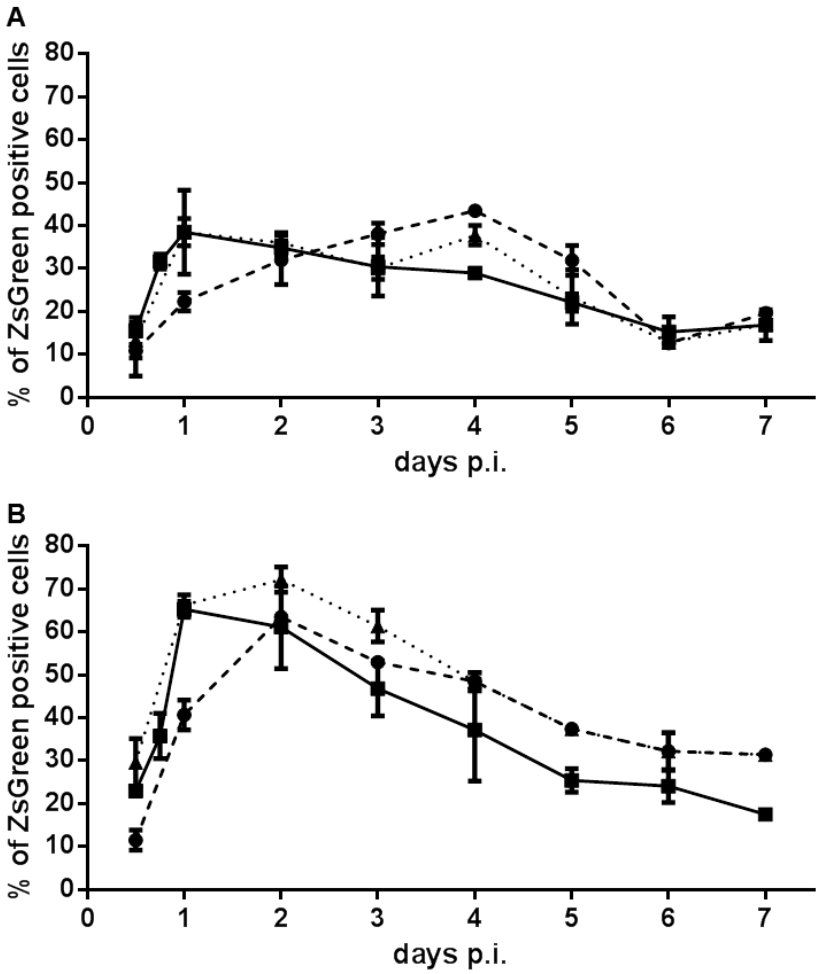

Figure 3.4 Percentage of ZsGreen-positive tick cells following infection with SFV4(3F)-ZsGreen

IDE8 (A) and IRE/CTVM19 (B) cells were infected with SFV4(3F)-ZsGreen at MOI 1 (- - ·), 5 (——) and 10 (····). Percentages of ZsGreen-positive cells were determined by visual counting over a 7 day time-period. Experiment was done once in triplicate. Error bars are standard deviations.

Visual counting to determine the time-course of an infection is a very time-consuming approach. To determine whether FACS analysis could be applied to infected tick cells, thereby saving time, IDE8 and IRE/CTVM19 cells were infected with SFV4(3F)-ZsGreen at MOI of 5 and images were taken as described previously. The cells were then fixed and counted using the BD FACSCalibur Flow Cytometer (2.10).

When comparing visual counting to FACS analysis, a dramatic difference in the percentage of ZsGreen-positive cells was observed in both cell lines. In IDE8 the maximum proportion of ZsGreen-positive cells detected by FACS analysis was 6%

as opposed to 40% by visual counting (Figure 3.5 A); by both methods the maxima were reached on day 1. In IRE/CTVM19 maximum proportions of ZsGreen-positive cells detected by visual counting were around 65% on day 1, and by FACS were around 30% on day 3 (Figure 3.5 B). Further investigation is required to determine if this underestimation by FACS analysis is due to sample preparation methods, such as length of time for fixing cells, missing a proportion of the infected population in the very heterogeneous cell lines during gating or inability to distinguish between auto-fluorescence and ZsGreen staining. Optimisation would be required for each cell line and fluorescent marker. This would be time-consuming but potentially worth the effort if many experiments using marker genes were planned. This possibility was not pursued further in the present study.

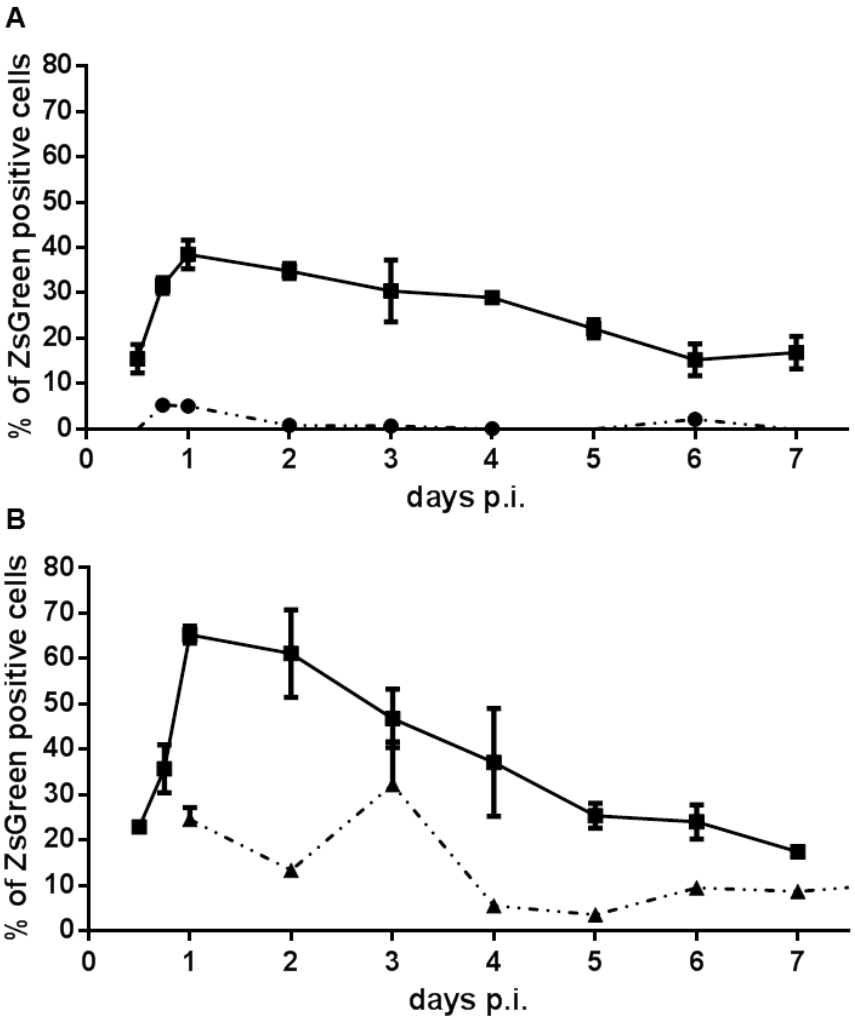

Figure 3.5 Comparison of the percentage of ZsGreen-positive tick cells determined by visual counting and by FACS

IDE8 (A) and IRE/CTVM19 (B) cells were infected with SFV4(3F)-ZsGreen at MOI 5. Percentage of ZsGreen-positive cells was determined either by visual counting of ZsGreen-positive and negative cells (——) or by FACS analysis (- · ·). Experiment was done once in triplicate. Error bars are standard deviations.

Since the infectability of tick cells varies depending on the virus used for infection, experiments similar to those described above were carried out with TBEV. Since none of the available TBEV reporter viruses containing fluorescent markers functioned in tick cells, infected cells were fixed with 4% paraformaldehyde and immunostained with E protein antibody as primary antibody and DyLight 488 nm-conjugated secondary antibody. IRE/CTVM19 cells were grown on coverslips in 24-well plates and infected with TBEV at an MOI of 5 (Figure 3.6). On days 1-6 p.i. cells were fixed and immunostained. Images were taken of randomly-selected fields

using the Olympus Fluoview FV10 confocal microscope and the percentage of green cells calculated by counting the number of green and non-green cells in three photographs for each time-point. At days 2 and 3 p.i., approximately 70% of the cells were E protein-positive (Figure 3.6). The number of E protein-positive cells decreased thereafter.

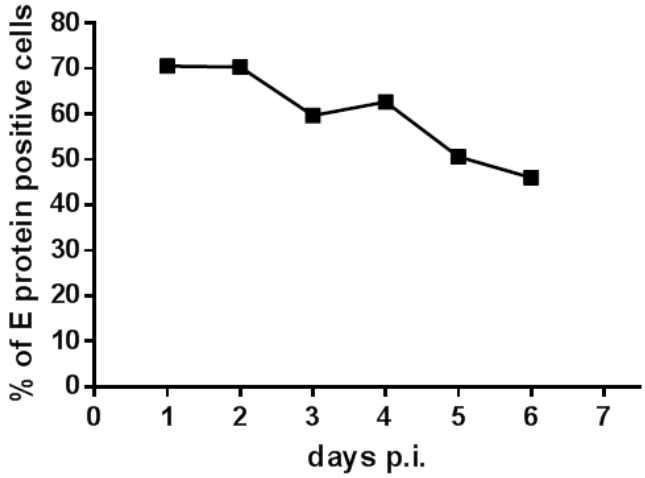

Figure 3.6 Percentage of E protein-positive IRE/CTVM19 cells following TBEV infection

IRE/CTVM19 cells were infected with TBEV at MOI 5. Cells were fixed, immunostained and the percentage of E protein-positive cells was counted over a 6 day time-period. Experiment was done once. Data points are the means of duplicates.

Although an MOI of 5 resulted in 70% of the IRE/CTVM19 cells being positive for E protein as early as 1 or 2 days p.i. (Figure 3.6), a lower MOI might be advantageous depending on the experiment planned. Therefore IDE8 and IRE/CTM19 cells were grown on coverslips, infected with TBEV at MOIs of 0.1, 1 and 5, fixed at day 2 p.i. and immunostained. Images were taken (Figure 3.7) and the percentage of green cells was calculated as described above (Figure 3.8).

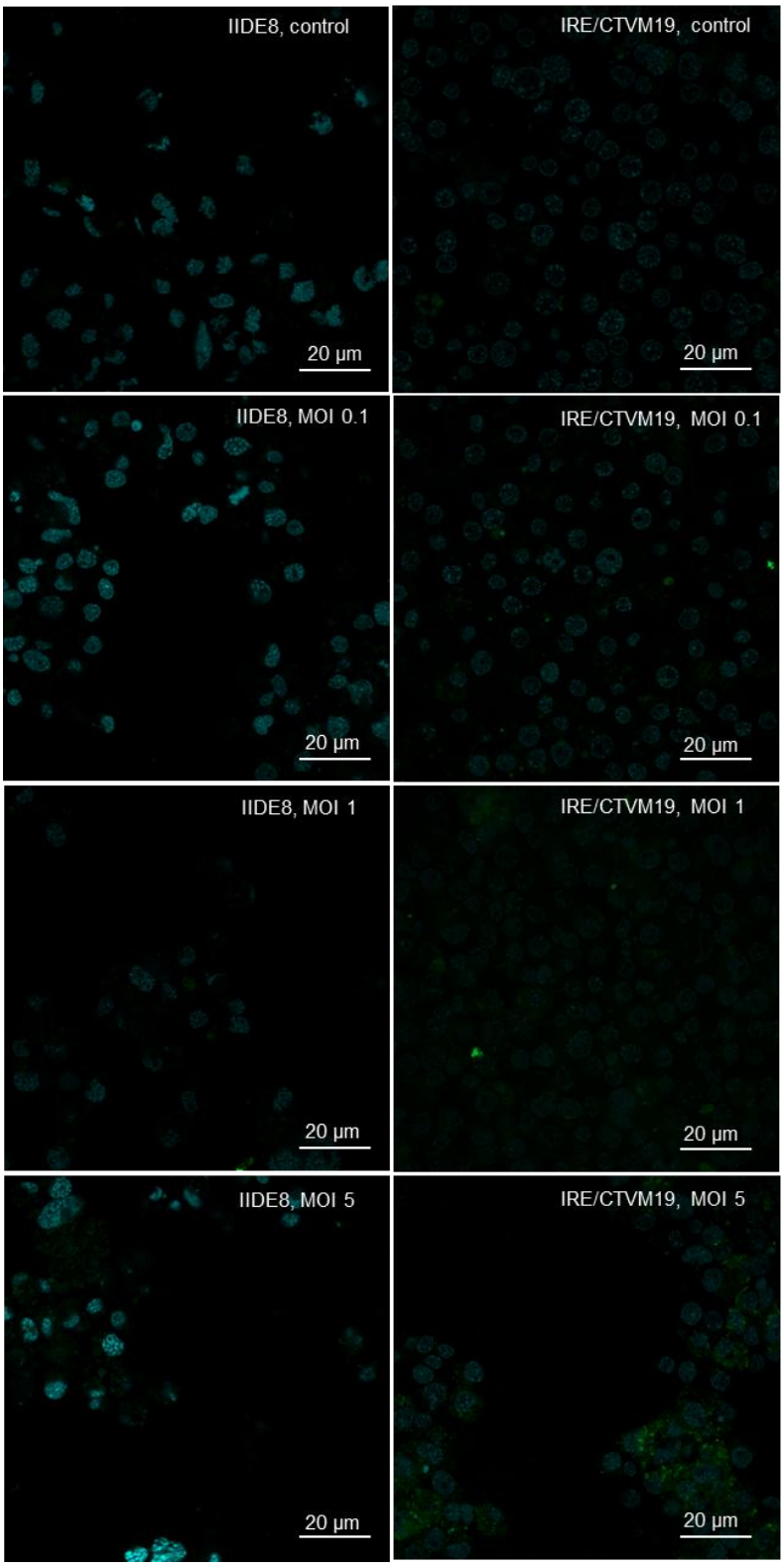

Figure 3.7 Images of E protein-positive tick cells following TBEV infection

TBEV-infected and uninfected control IDE8 and IRE/CTVM19 cells were immunostained for TBEV E protein on day 2 p.i.. Images were taken with the Olympus Fluoview FV10 confocal microscope at 600x magnification of IDE8 (left panel) and IRE/CTVM19 (right panel) cells uninfected or infected with TBEV at MOI 0.1, 1 and 5. DAPI : blue, E protein: green

MOIs 0.1 and 1 resulted in approximately 40% of E protein-positive IRE/CTVM19 cells in comparison to 70% at MOI 5 (Figure 3.8). It is possible that the level of E protein-positive cells would have reached the maximum of 70% later during infection in those cells infected with lower MOIs, as seen with SFV (Figure 3.2, Figure 3.4). In IDE8, however, less than 10% of cells were E protein-positive at day 2 when infected with MOI 0.1, approximately 25% with MOI 1 and 55% with MOI 5. It is likely that the latter is the maximum number of cells of this cell line that can be productively infected with TBEV. As observed with SFV (Figure 3.4), IDE8 cells were less permissive to infection with TBEV than IRE/CTVM19 cells.

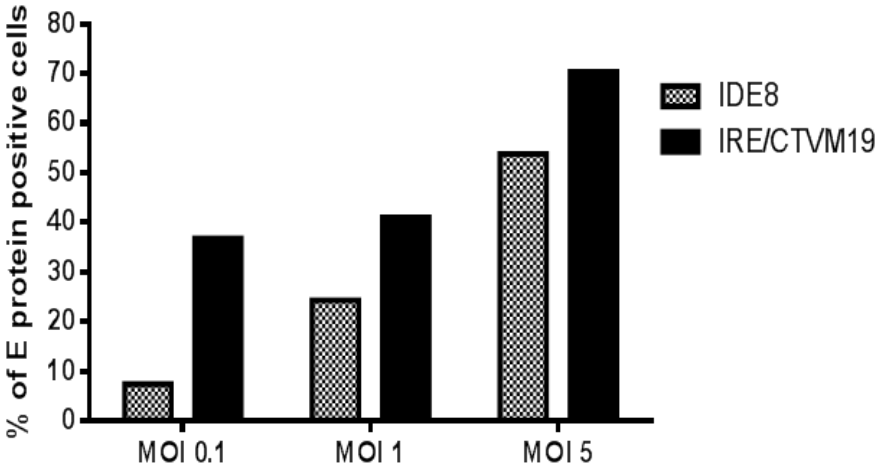

Figure 3.8 Percentage of E protein-positive tick cells following TBEV infection

IDE8 and IRE/CTVM19 cells were infected with TBEV at MOI 0.1, 1 and 5. Cells were fixed and immunostained 2 days p.i. and the percentage of E protein-positive cells was calculated. Experiment was done once. Values are means of duplicates.

Similar experiments determining the infection levels of LGTV in IDE8 cells were undertaken by my colleague, Claudia Rückert, who seeded cells on coverslips in 24-well plates and infected triplicate cultures with MOI 1. At day 2 p.i, the cells were fixed and immunostained with LGTV NS5 antibody and anti-chicken FITC as secondary antibody. Photographs of three randomly-selected fields were taken using the Leica SP2 confocal microscope. NS5 protein-positive and negative cells were counted and the percentage of positive cells calculated. Approximately 97% (± 0.84) of IDE8 cells were permissive for LGTV infection.

Overall an MOI of 5 was considered to be suitable for all subsequent experiments since this MOI infected most of the permissive cells within the first 1 to 2 days. Having confirmed that tick cells can be infected with the mosquito-borne virus SFV and the tick-borne viruses LGTV and TBEV, the course of virus replication and production was determined in more detail.

3.4.2 Kinetics of SFV replication and production and their effect on tick cell growth

To measure production of SFV in the tick cell lines ISE6 and IRE/CTVM19, cells were seeded in 24-well plates at a density of $5x10^5$ cells per well, incubated overnight and then infected with SFV4-StRluc, which contains the gene coding for *Rluc* in the structural region, at a MOI of 5 and three replicate wells were sampled every 12 h for 3 days and every 24 h up to day 7 thereafter. For the first 3 days medium was changed 12 h prior to sampling, whereas for the following time-points medium was changed 24 h prior to sampling. Separate wells were sampled for each time-point and uninfected control wells were treated in the same way as infected wells. The supernatant collected for plaque assay therefore contained virus produced between the time of sampling and the previous sampling time-point (Figure 3.9 A middle). To determine the effect of virus infection on the culture, cells were also harvested at each time-point and counted using a haemocytometer (Figure 3.9 A bottom). After counting, cells were lysed in 1x passive lysis buffer and luciferase values determined as a measure of viral replication (Figure 3.9 A top). The experiment was done once.

Expression of Rluc from SFV4-StRluc allows the quantitative assessment of late virus gene expression as shown previously (Fragkoudis et al., 2008; Kiiver et al., 2008). In ISE6 cells luciferase expression increased up to day 1.5 until it reached a plateau and dropped after day 3 (Figure 3.9 A top, green). In IRE/CTVM19 cells luciferase activity peaked at day 1 p.i. and decreased after day 2.5. Rluc activity was lower overall in IRE/CTVM19 compared to ISE6.

The kinetics of infectious virus particle production were determined by plaque assay in BHK-21 cells. In ISE6 high levels of infectious virus production were observed

during the whole time period (Figure 3.9 A middle green). Virus production steadily increased until 60 h p.i., was stable between 60 h and day 4 p.i. and dropped steadily thereafter. IRE/CTVM19, however, showed a different pattern of infectious virus particle production with a steady increase from day 3 peaking at day 6 p.i. (Figure 3.9 A middle, black). This pattern of virus production is similar to the results obtained by Ruzek et al. (2008) with TBEV in this cell line.

To determine if the infection with SFV has a negative effect on tick cell growth, cells in infected and uninfected cultures were counted at each time-point. Cell numbers in infected and uninfected ISE6 cultures, grown in 24-well plates, increased at a similar rate over the first 5 days. (Figure 3.9 A bottom, infected: green; control: blue). Late in infection uninfected cultures grew faster than infected cultures. In IRE/CTVM19 cultures no cell growth could be detected (Figure 3.9 A bottom, infected: black; control: grey); cell numbers stayed the same and even started to decrease slightly after day 5 p.i.. In both tick cell lines, no cytopathic effect due to SFV infection was detectable by microscopic examination. A longer time-course would be required to test if the reduction in the number of cells in SFV-infected ISE6 at day 7 p.i. was due to cells dying, slower cell division or an artefact.

ISE6 cells grew steadily in 24-well plates and the change in Rluc expression, which is indicative for replication and translation of the genes coding for the structural proteins, was followed by a similar change in virus production 12 – 24 hours later. Although there was no detectable cytopathic effect of SFV infection on IRE/CTVM19, there was also no cell growth detectable in either infected or uninfected cultures, which suggests a very slow metabolism probably due to the effect of being in an unsealed 24-well plate where the pH of the medium cannot be maintained. This slowed metabolism or absence of cell growth might explain the lower Rluc expression and the delayed onset of increase in virus production.

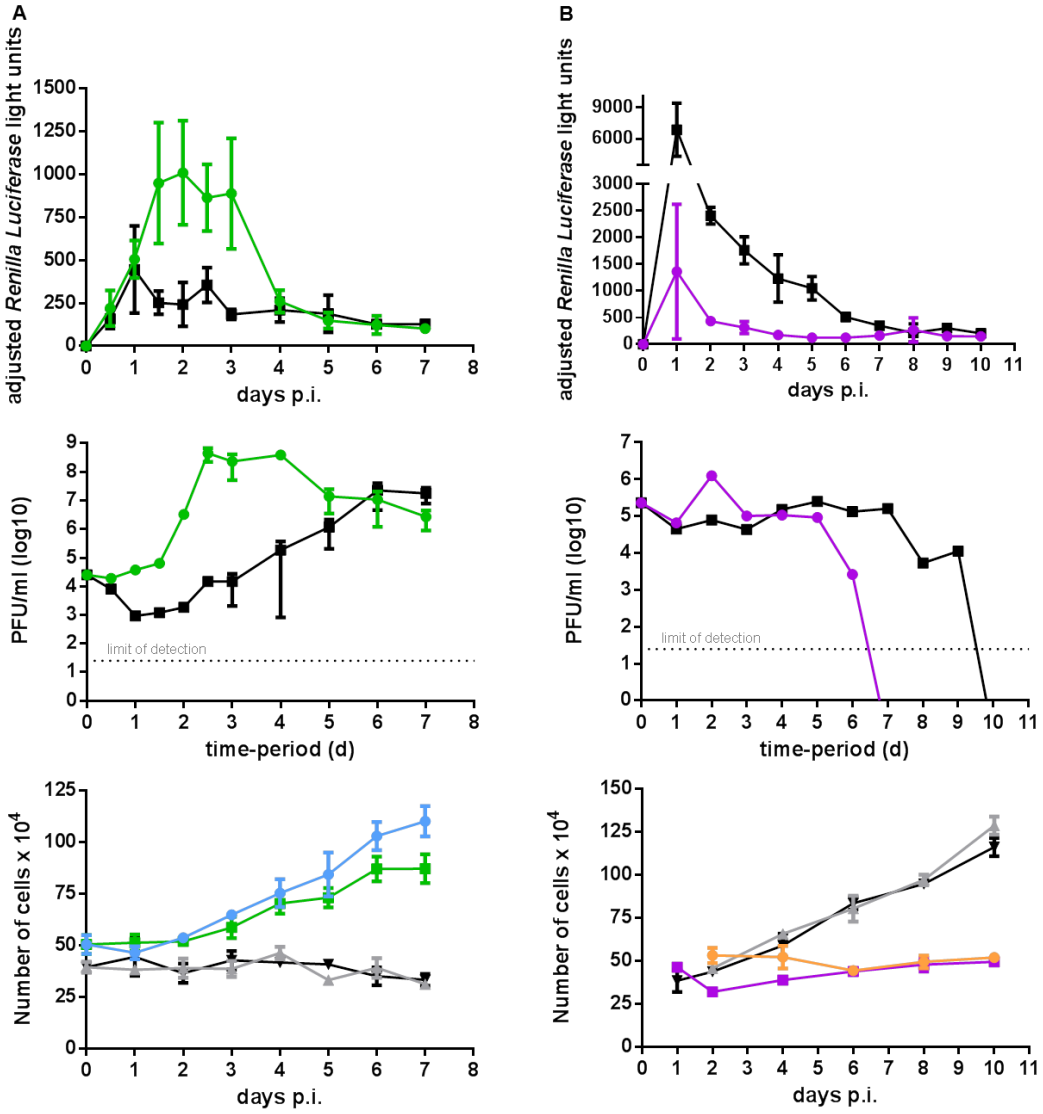

Figure 3.9 Kinetics of SFV4-StRluc and SFV4(3H)-Rluc virus growth in different *Ixodes* spp cell lines and its effect on tick cell growth

(A) ISE6 (green) and IRE/CTVM19 (black) cells were grown in 24-well plates and infected with SFV4-StRluc (MOI 5). Experiment was done once in triplicate; error bars indicate standard deviation. (B) IDE8 (pink) and IRE/CTVM19 (black) were grown and infected with SFV4(3H)-Rluc (MOI 5) in flat-sided tubes. Experiment was done once in duplicate; error bars indicate standard deviation. The dotted line represents the detection limit.
In both experiments medium was changed at the time-point previous to sampling. The top graph shows replication of SFV4-StRluc (A) or SFV4(3H)-Rluc (B). Cells were lysed at the indicated time-points and Rluc activity was measured. Adjusted light units represent light units minus background luminescence calculated from uninfected control cultures at each time point. The middle graph shows newly-produced infectious virus present in the supernatant. Virus was titrated using plaque assays on BHK-21 cells. The dotted line represents the detection limit of 25 PFU/ml in a 10^{-1} dilution. The bottom graph represents the numbers of infected (green) and uninfected (blue) ISE6 cells (A), infected (black) and uninfected (grey) IRE/CTVM19 (A+B) and infected (pink) and uninfected (orange) IDE8 (B).

The experiment was repeated using SFV4(3H)-Rluc which contains the gene coding for Rluc in the non-structural region, allowing assessment of replication and translation of early viral genes (Fragkoudis et al., 2008; Kiiver et al., 2008). On this occasion IRE/CTVM19 and IDE8 cells were grown and infected in sealed flat-sided tubes thus facilitating maintenance of an acid pH (Bell-Sakyi et al., 2007). When looking at virus replication, Rluc activity peaked in both cell lines at day 1 p.i. and dropped to almost background level in IDE8 at day 4 p.i. and in IRE/CTVM19 at day 7 p.i. (Figure 3.9 B top, IDE8 green, IRE/CTVM19 black). Almost 4 times higher Rluc activity was measured in IRE/CTVM19 than in IDE8 at day 1 p.i.; however in this experiment this difference did not result in a higher amount of virus produced by the cells.

In IDE8 cells virus production peaked at day 2 p.i., plateaued from day 3 to day 5 and then dropped below the detection limit of 25 PFU/ml in a 10^{-1} dilution (Figure 3.9 B middle, purple). From day 7 to the end of the experiment on day 10, infectious virus particle production was below the detection limit. A similar amount of virus was produced by IRE/CTVM19 cells but production plateaued for a longer time, up to day 7, before dropping less rapidly up to day 9 (Figure 3.9 B middle, black). At the end of the experiment, day 10, virus production was below the detection limit.

There was no detectable effect of SFV infection on IDE8 or IRE/CTVM19 tick cell growth in flat-sided tubes (Figure 3.9 B bottom). Both infected and mock-infected IRE/CTVM19 cells were growing steadily (Figure 3.9 B bottom infected: black, control: grey) which if compared to the experiment done in 24-well plates suggests that experiments should be done, at least with IRE/CTVM19, in tubes rather than 24-well plates (Figure 3.9 A bottom infected: black, control: grey). Although IDE8 cell numbers differed in infected and control cells up to day 6, and even decreased from day 1 to day 2, this difference could be explained by difficulty in removing all the adherent cells from the surface of the tubes, since IDE8 are much more adherent than IRE/CTVM19 (Figure 3.9 B bottom infected: purple, control: orange).

Overall, SFV replication and production patterns were similar in IDE8 and IRE/CTVM19 when the experiment was done in tubes, with peaks at day 1 p.i..

Short-term experiments, for up to 5 days, can be done in 24-well plates with IRE/CTVM19, but experiments in tubes are recommended.

3.4.3 Kinetics of Flavivirus replication and production

After establishing the growth parameters for a mosquito-borne arbovirus in tick cells, replication and production of the tick-borne flaviviruses TBEV and LGTV were examined in IDE8 and IRE/CTVM19 cells.

Virus production and accumulated virus growth curves were established for TBEV. Cells were seeded in a series of tubes and 24 h later infected at MOI 5. To establish a virus production curve, for time-points 12, 18 and 24 h cells were washed and medium was changed 2 h after infection, and for the remaining time-points cells were washed and medium was changed 24 h prior to sampling. For the accumulated growth curve, samples were collected from the same replicate tubes prior to medium change on days 1 to 9.

TBEV showed similar patterns in both growth curves and in both cell lines (Figure 3.10). In the virus production curve the maximum amount of virus was produced between days 1 and 4 in IDE8 and between days 2 and 3 in IRE/CTVM19, and virus production in both cell lines slowly decreased from day 4 to the end of the experiment (Figure 3.10 A). The virus titres were approximately 2 logs higher in the vector cell line IRE/CTVM19 than in the non-vector cell line IDE8. The same was seen in the accumulated virus growth curve (Figure 3.10 B). The accumulated virus growth curve resembled the virus production curve but with higher titres. The titration of TBEV was done on PS cells in which the virus formed big, easily-countable plaques (Figure 3.10 C).

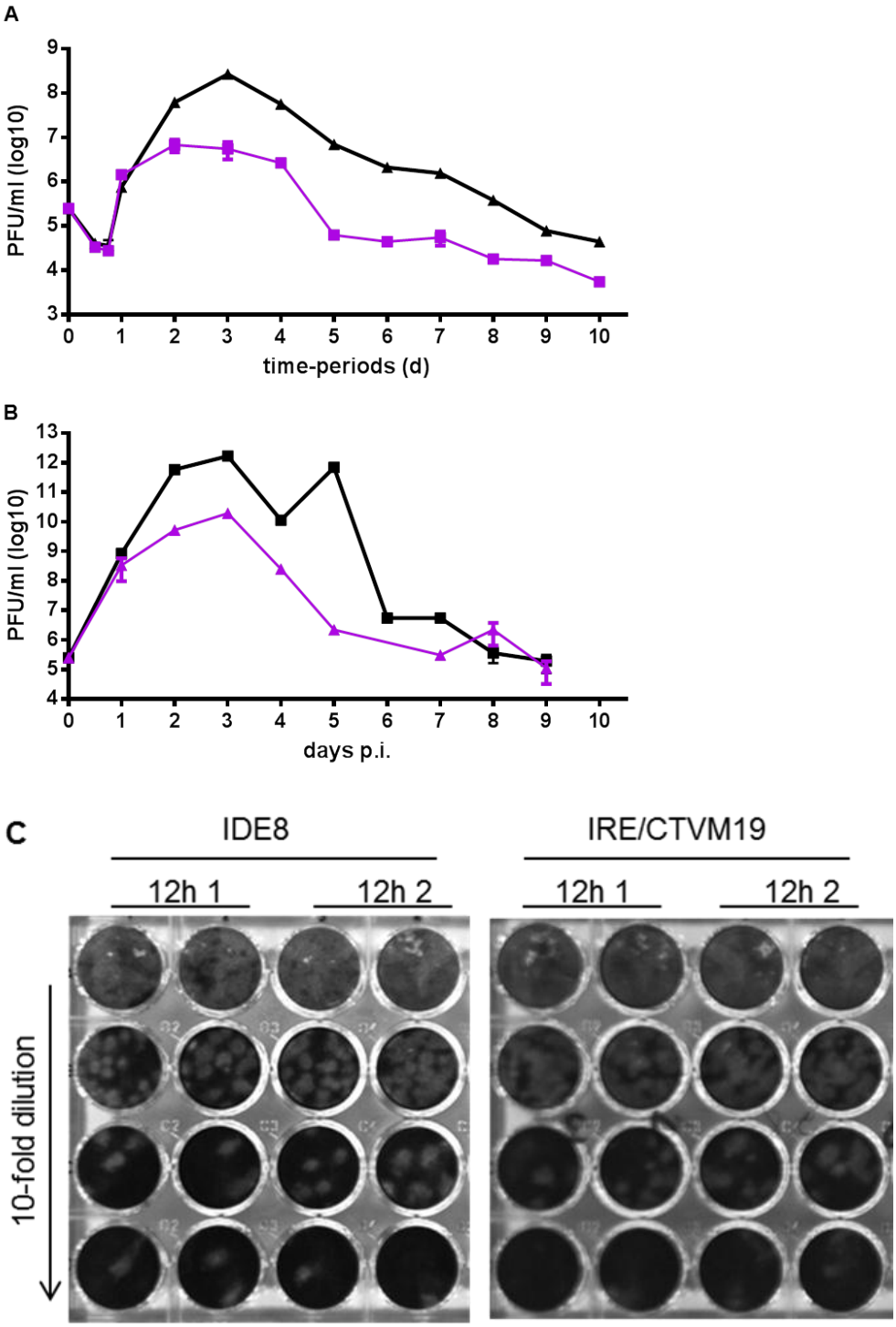

Figure 3.10 Growth curves of TBEV in tick cell lines and plaque assay in PS cells

IDE8 (pink) and IRE/CTVM19 (black) cells were infected with TBEV at MOI 5 and virus was titrated by plaque assay in PS cells. Experiment was done once in duplicate, error bars are standard deviations. (A) Newly-produced infectious virus present in the supernatant. (B) Accumulated virus in supernatant. (C) Photographs of plaque assays in PS cells of supernatant from infected IDE8 and IRE/CTVM19 cells at 12 h time-point. Virus supernatant was 10-fold serially diluted, starting with a 1 in 10 dilution.

The following experiment using LGTV was done by my colleague Claudia Rückert. IDE8 cells were seeded in tubes and infected with LGTV at MOI 0.05 and 1. To measure newly-produced virus, medium was changed 24 h prior to sampling and titrated on BHK-21 cells. Cells were harvested, RNA was isolated using the RNeasy mini kit (Qiagen) and cDNA generated using the high-yield cDNA reverse transcription kit (Applied Biosystems). To quantify virus RNA levels, the cDNA was used in a qPCR assay to determine LGTV NS5 expression.

LGTV RNA levels within the cells increased up to day 2 indicating that virus replication was occurring in the cells infected at both MOIs (Figure 3.11 A). This pattern matched the increase in infectious LGTV particles released (Figure 3.11 B). In cells infected with MOI 1, virus RNA levels dropped between days 2 and 3 and then stayed constant up to day 7. With MOI of 0.05 however NS5 expression stayed more or less constant from day 2 to the end of the experiment which was again similar to what was observed for virus production in these cells.

As shown for TBEV (Figure 3.10 A, purple) the production of LGTV peaked at day 2 p.i. (Figure 3.11 B). If the increase by 1 log from day 6 to day 7 in LGTV-infected cells represented a continuing increase or only an irregularity is impossible to say without looking at a longer time-course. Overall, the LGTV titres were 2 logs lower than those seen with TBEV but a similar production pattern was observed.

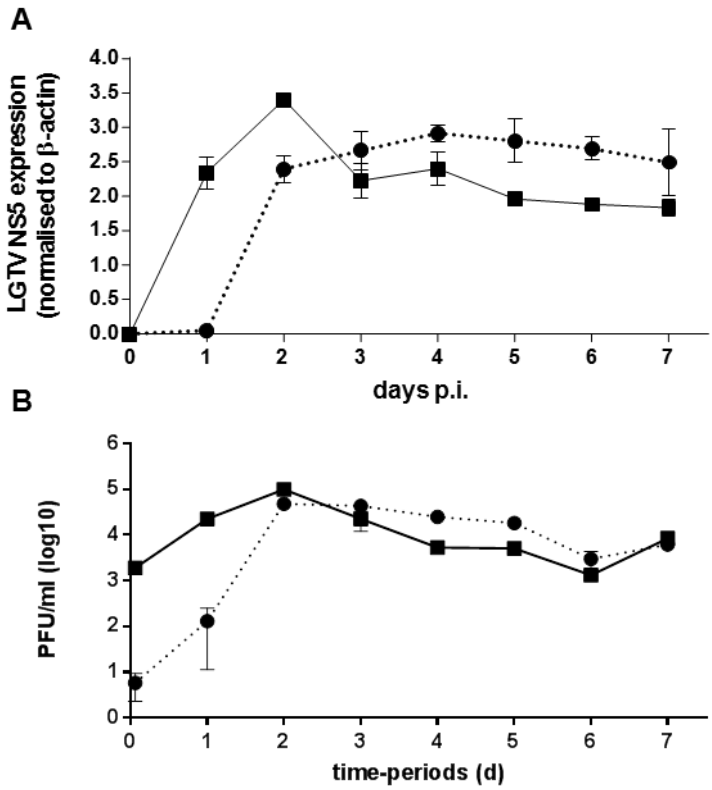

Figure 3.11 LGTV RNA levels and production curve in IDE8 (Claudia Rückert)

Tick cells were infected with LGTV at MOI 0.05 (●) or 1 (■). Experiment was done once in duplicate, error bars are standard deviations. (A) LGTV NS5 expression normalised to β-actin measured by qPCR. (B) Newly-produced infectious virus present in the supernatant within 24 h time-periods. Virus was titrated on BHK-21 cells.

Although different MOIs were used for infection with TBEV (MOI 5) and LGTV (MOI 0.05 and 1), virus production curves in IDE8 cells were similar for both viruses.

3.4.4 Kinetics of replication of flavivirus replicons

SFV reporter viruses containing Rluc allowed a quick readout of virus replication. Unfortunately, no equivalent luciferase reporter viruses were available for TBEV or LGTV at the time this study was commenced.

To facilitate the present and future studies TBEV luciferase reporter constructs were designed. The TBEV plasmids pTND/c-eGFP encoding the complete genome of TBEV, and pTND/ME-eGFP encoding a TBEV replicon without the structural membrane and envelope protein sequences, were used as backbones. Both plasmids

contained the sequence for eGFP in their 3' non-structural region behind an IRES. This IRES-eGFP cassette was replaced with either an IRES-Rluc or an IRES-Fluc cassette generating pTND/c-IRES-Rluc, pTND/c-IRES-Fluc, pTND/ME-IRES-Rluc and pTND/ME-IRES-Fluc (Figure 2.2). These constructs were tested in mammalian and tick cells. Since infectious TBEV experiments have to be done at CL3, a trial experiment was done first using the replicons derived from the plasmids pTND/ME-IRES-Rluc and pTND/ME-IRES-Fluc (Figure 3.12), which can be used at CL2, since it lacks the structural proteins prM and E.

For this experiment the TBEV plasmids pTND/ME-IRES-Rluc and pTND/ME-IRES-fluc were linearised, *in vitro*-transcribed in the presence of Cap Analog, and the same volume of transcribed replicon was transfected into 4 wells of either mammalian or tick cells. The LGTV replicon E5repRluc2B/3 which contains a *Rluc* reporter gene replacing parts of the structural protein coding sequence (Figure 2.3) was used as a transfection control. Cells from three wells were lysed for luciferase assay and RNA was isolated from the fourth culture using Trizol for qPCR analysis

Infection with the LGTV replicon resulted in luciferase expression in both mammalian and tick cells whereas the TBEV replicons only produced luciferase in mammalian cells (Figure 3.12 A). To test if the difference in luciferase expression by the TBEV replicons in mammalian and tick cells was due to uptake and replicon levels within the cells, TBEV NS5 copy numbers were measured by qRT-PCR. In all cell lines used, TBEV RNA was present and levels were even 0.5 to 1 log higher in tick cells than in the mammalian cells (Figure 3.12 B). This suggests that the transfection was not the problem.

As the replicon derived from the plasmid pTND/ME-IRES-Rluc failed to express luciferase in tick cells it was not considered necessary to further test the plasmids pTND/c-IRES-Rluc or Fluc, coding for the whole virus, at CL3.

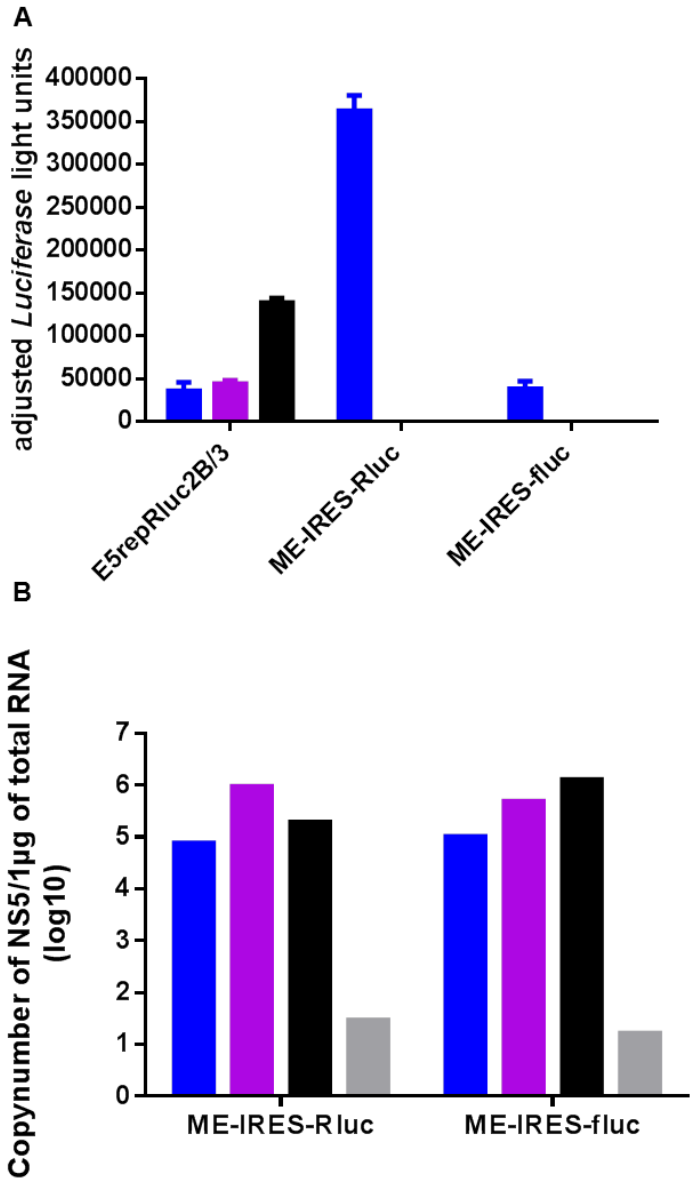

Figure 3.12 Uptake of TBEV replicons and expression of luciferase

LGTV replicon (E5repRluc2B/3) and TBEV replicons (ME-IRES-Rluc,ME-IRES-fluc) were transfected into BHK-21 (blue), IDE8 (pink) and IRE/CTVM19 (black) cells. At 24 h post-transfection (p.t.) cells were lysed for luciferase assay from 3 wells and RNA was isolated from one well. (A) Luciferase activity of replicons in mammalian and tick cells. Adjusted light units represent light units minus background luminescence calculated from uninfected control cultures at each time point. Two experiments done in triplicate showed the same trend. (B) TBEV NS5 copy numbers per µg of total RNA measured by qRT-PCR using pJET-vector with TBEV NS5 insert to generate standard curve and calculate copy numbers. Non-infected control cells (IRE/CTVM19) are in grey. Experiment was done once.

Since the replicons containing an IRES did not function in tick cells but the LGTV replicon successfully expressed Rluc, several different TBEV replicons, which were

originally used as templates for designing the LGTV replicon (Dr. Esther Schnettler, personal communication), were kindly provided by Prof Franz X. Heinz, Clinical Institute of Virology, Medical University of Vienna, Austria (Hoenninger et al., 2008) and tested in IDE8 and IRE/CTVM19 cells. Cells were seeded in 24-well plates and transfected in triplicate with TBEV replicons containing *Fluc* (C17Fluc, C17Fluc-TAV2A, C17Fluc-FMDV2A) or *Rluc* (C27Rluc and C37Rluc) or with LGTV replicon E5repRluc2B/3 (Figure 2.3). All transfected wells received the same volume of an *in vitro* transcription of 1 µg linearised plasmid DNA. Cells were harvested on days 1 to 5 p.t., lysed and Rluc or Fluc activity was measured as an indicator of replication.

Fluc or Rluc activity was observed for all replicons with a peak at day 1 p.t.. Activity progressively decreased afterwards in IDE8 (Figure 3.13 A) and IRE/CTVM19 (Figure 3.13 B) cells. The replicons C17Fluc-TAV2A and C17Fluc-FMDV2A showed higher firefly luciferase activity than C17Fluc in both IDE8 (Figure 3.13 top A) and IRE/CTVM19 (Figure 3.13 top B). Activity of the replicon C17Fluc-TAV2A was still measureable at 5 days p.t. suggesting that it was still replicating within the cell. The highest luciferase activity however was observed for the LGTV replicon (Figure 3.13 bottom), which was higher in IRE/CTVM19 than in IDE8. Levels remained high at 5 days p.t. in IRE/CTVM19 but not in IDE8. Replicons C27Rluc and C37Rluc showed no luciferase expression after their peak at 24 h in IDE8 and low levels in IRE/CTVM19 suggesting that the replicons might not be replicating and the initial peak at 24 h was due to the presence of the original transfected replicon within the cell.

As it gave the highest readings in both IDE8 and IRE/CTVM19 (Figure 3.13), and based on results obtained by Dr. Esther Schnettler (Institute of Infection, Immunity and Inflammation, Centre for Virus Research, University of Glasgow, UK) with the LGTV replicon (Dr. Esther Schnettler personal communication), the TBEV replicon C17Fluc-TAV2A were selected for further study as being most likely to replicate in tick cells and express luciferase.

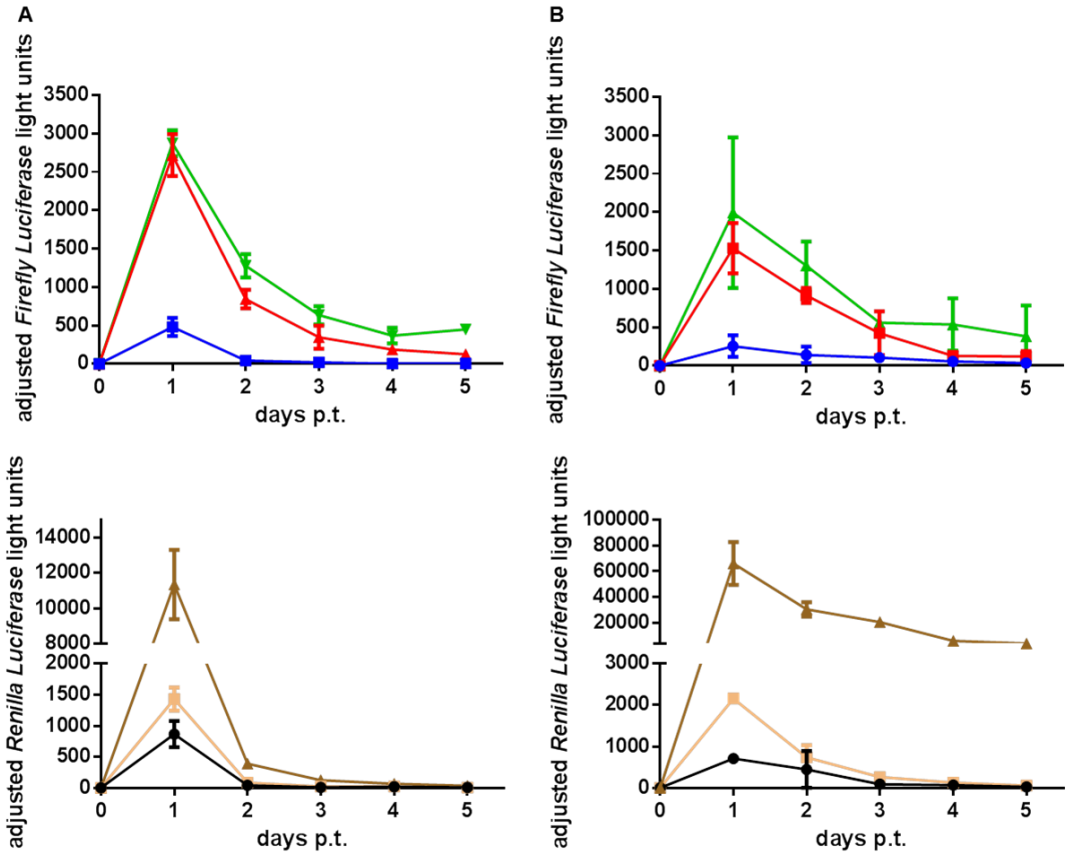

Figure 3.13 Replication kinetics of LGTV and TBEV replicons in IDE8 and IRE/CTVM19 cells

IDE8 (A) and IRE/CTVM19 (B) cells were transfected with either a LGTV replicon or one of 5 TBEV replicons. The LGTV replicon E5repRluc2B/3 (brown) contained a *Renilla* luciferase marker gene, whereas the TBEV replicons contained either a firefly luciferase reporter gene (C17Fluc 2B/3 [blue], C17Fluc FMDV2A [red], C17Fluc TAV2A [green]) or a *Renilla* luciferase marker (C27 Rluc [beige] and C37 Rluc [black]). Cells were harvested at time-points indicated and luciferase activity was determined. The experiment was done once in triplicate; error bars are standard deviations. Adjusted light units represent light units minus background luminescence. Similar results were obtained with LGTV replicon in 3 independent experiments.

3.4.5 Visualisation of virus replication complexes in tick cells

The mosquito-borne alphavirus SFV (Figure 3.9) and the two tick-borne flaviviruses (Figure 3.10, Figure 3.11) replicated and produced infectious virus particles in ISE6, IDE8 and IRE/CTVM19 cells but whether they lead to ultrastructural changes in tick cells, including the formation of replication complexes, has only been investigated for LGTV in ISE6 (Offerdahl et al., 2012) and for TBEV in the *I. scapularis* cell line IDE2 and the *R. appendiculatus* cell line RA-257 (Senigl, Grubhoffer & Kopecký, 2006).

In an attempt to visualise virus replication complexes in ISE6 and IRE/CTVM19 cells, cells were infected with SFV4(3F)-ZsGreen at MOI 50. This virus construct contains ZsGreen fused to the replicase protein nsP3. Replication complexes can therefore be seen by light microscopy as foci of green fluorescence within infected cells (Figure 3.14). At 24 h p.i. photographs were taken of control and infected cells before harvesting and processing them for TEM. Images of BDE/CTVM16 infected with SFV4(3F)-ZsGreen (Figure 3.15c; Figure 3.16 c) generated in a separate study outside the scope of this project were included as examples of the appearance of SFV particles within tick cells.

Infected ISE6 and IRE/CTVM19 cells both showed punctate fluorescence at 24 h p.i. with approximately 50% of ISE6 and 70% of IRE/CTVM19 cells ZsGreen-positive, whereas control cells showed no staining (Figure 3.14). TEM was used to investigate whether replication complexes were present.

Interestingly, uninfected ISE6 and IRE/CTVM19 cells both already contained endogenous reovirus-like particles (Figure 3.15 a; Figure 3.16 a), which were also present in the infected samples (Figure 3.15 b; Figure 3.16 b). Although visual inspection of samples by light microscopy showed that cells were infected with SFV, no virus particles resembling SFV were observed in any of the infected ISE6 and IRE/CTVM19 cells by TEM. The viruses observed within these cells do not resemble SFV particles, which were observed in SFV4(3F)-ZsGreen infected BDE/CTVM16 cells (Figure 3.15 c; Figure 3.16 c) highlighting the difference in appearance between SFV and the endogenous viruses observed in ISE6 and IRE/CTVM19 cells. The endogenous viruses in the latter two cell lines resemble reovirus-like particles, similar to SCRV observed in IDE8, but were found not to be SCRV by PCR and are still unidentified (Alberdi et al., 2012). Furthermore, no structures similar to SFV replication complexes, as described in mammalian cells (Grimley et al., 1972; Grimley, Berezesky & Friedman, 1968; Kujala et al., 2001; Spuul et al., 2007, 2011; Virtanen & Wartiovaara, 1974), could be identified in the *Ixodes* spp. tick cell lines.

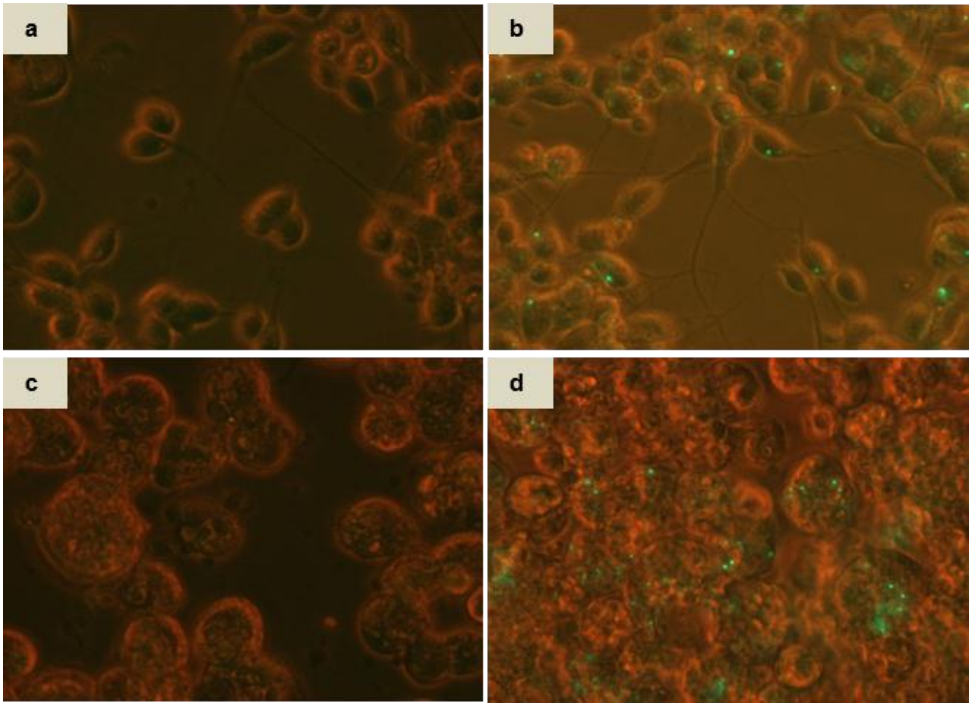

Figure 3.14 Fluorescence microscopy images of uninfected and SFV-infected ISE6 and IRE/CTVM19 cells

ISE6 and IRE/CTVM19 cells were infected with SFV4(3F)-ZsGreen at an MOI of 50, fixed 24 h p.i. and viewed by light microscopy using the Zeiss Axiovert Observer D1 inverted microscope at 400x magnification. (a) Uninfected ISE6 cells; (b) SFV-infected ISE6 cells; (c) uninfected IRE/CTVM19 cells; (d) SFV-infected IRE/CTVM19 cells.

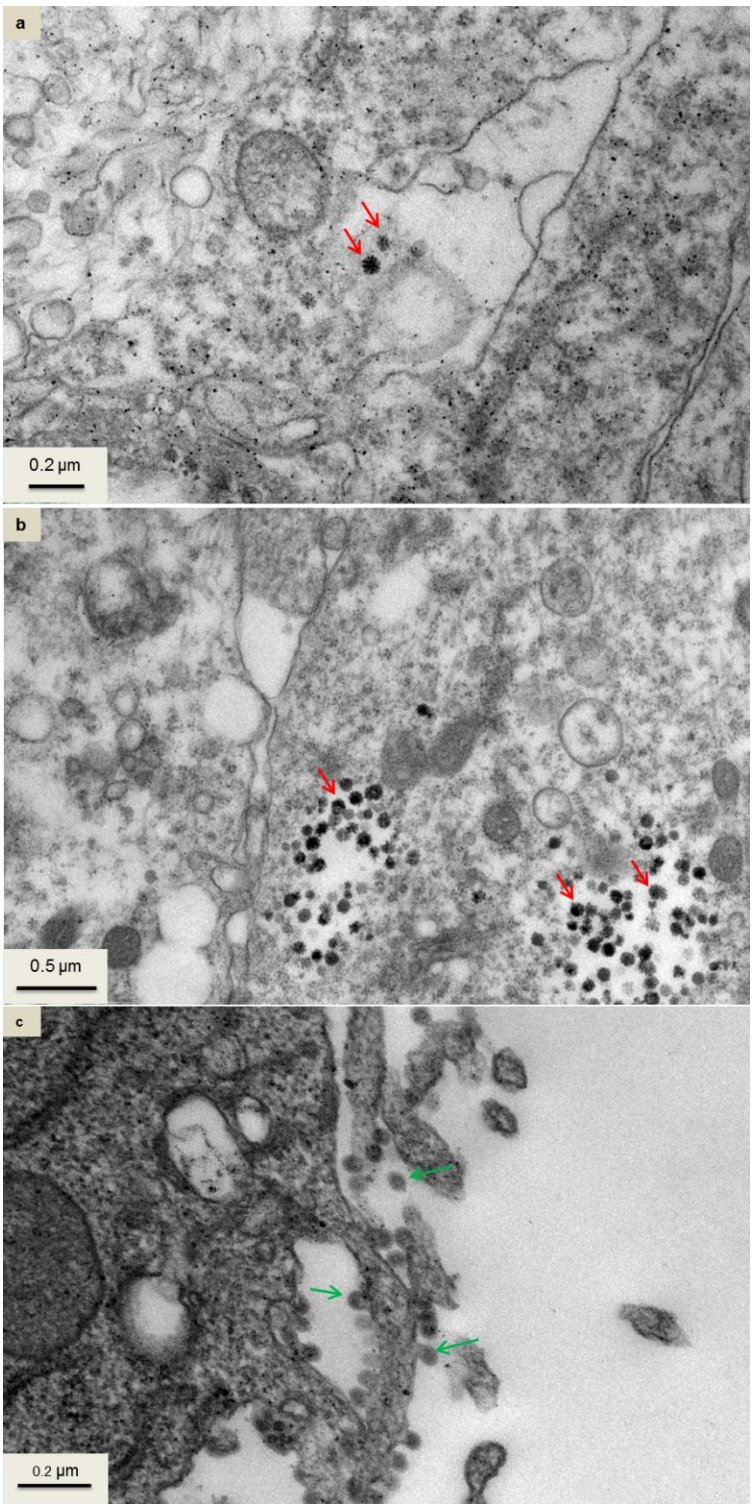

Figure 3.15 TEM images of uninfected and SFV-infected ISE6 cells and SFV-infected BDE/CTVM16 cells

ISE6 and BDE/CTVM16 cells were infected with SFV4(3F)-ZsGreen at an MOI of 50, fixed 24 h p.i. and processed for TEM. (a) part of an uninfected ISE6 cell; (b) part of a cell in an SFV-infected ISE6 culture; (c) part of an SFV-infected BDE/CTVM16 cell. Red arrows indicate endogenous reovirus-like particles. Green arrows indicate SFV particles.

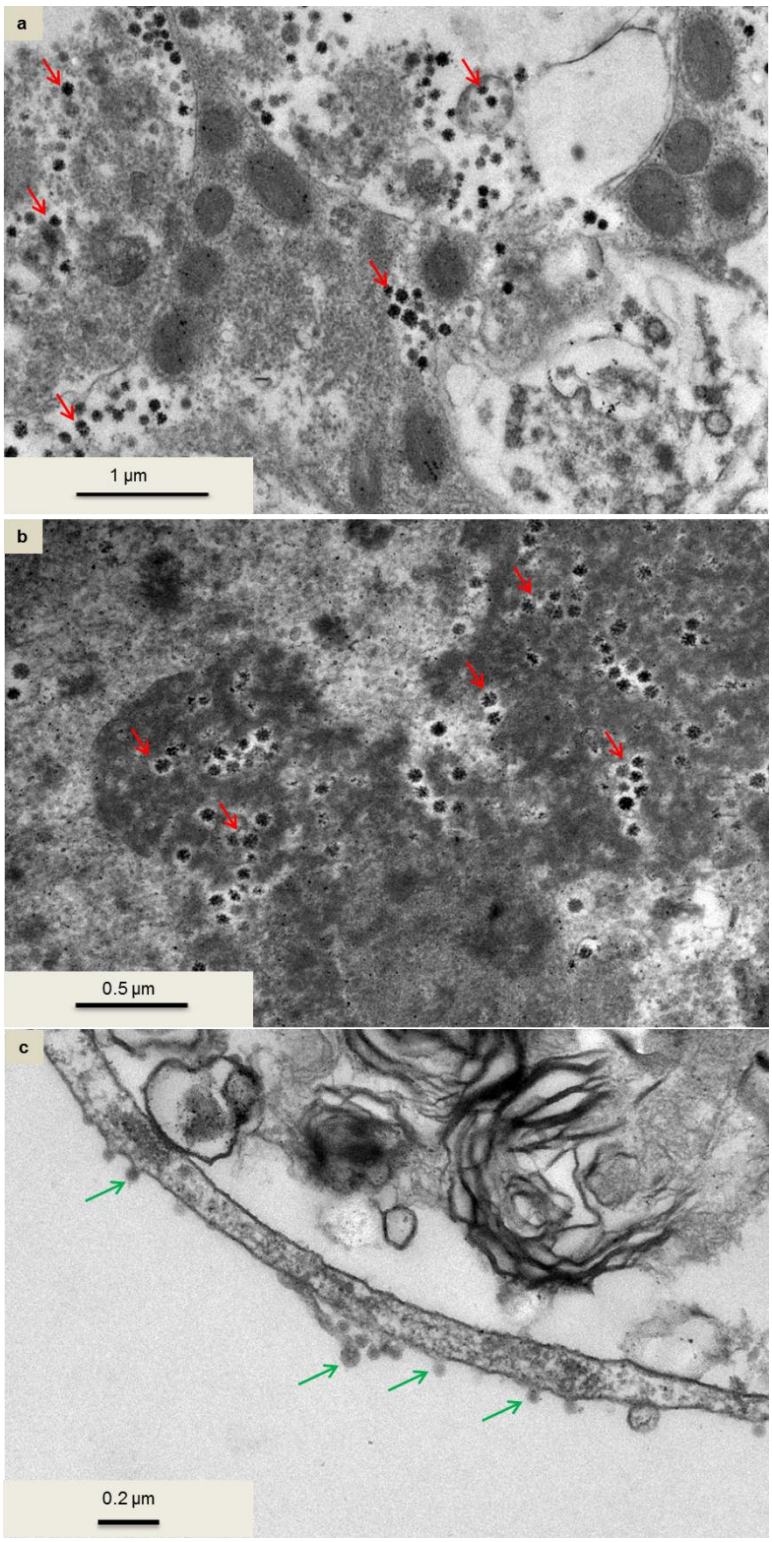

Figure 3.16 TEM images of uninfected and SFV-infected IRE/CTVM19 cells and SFV-infected BDE/CTVM16 cells

IRE/CTVM19 and BDE/CTVM16 cells were infected with SFV4(3F)-ZsGreen at an MOI of 50, fixed 24 h p.i. and processed for TEM. (a) Uninfected IRE/CTVM19 cell; (b) part of a cell in an SFV-infected IRE/CTVM19 culture; (c) part of an SFV-infected BDE/CTVM16 cell. Red arrows indicate endogenous reovirus-like particles. Green arrows indicate SFV particles.

To elucidate whether TBEV infection leads to changes in the ultrastructure of tick cells, IDE8 and IRE/CTVM19 cells, grown in tubes, were infected with TBEV at MOI 5, harvested at day 2 p.i., transferred onto grids and cryofixed immediately (2.2.2.2). After cryofixation grids were prepared by Maria Vancová, Laboratory of Electron Microscopy, Institute of Parasitology, University of South Bohemia, Budweis, Czech Republic for electron microscopy and images were taken using the Jeol JEM 1010 TEM.

In uninfected control IDE8 and IRE/CTVM19 cells reovirus-like particles were observed (Figure 3.17; Figure 3.18), which in the case of IDE8 was probably the endogenous orbivirus SCRV (Alberdi et al., 2012; Attoui et al., 2001). Additionally infected cells of both cell lines showed TBEV virus particles within vesicles either in the cytoplasm or in the ER (Figure 3.17 b, g, h, i, j; Figure 3.18); these structures were not seen in uninfected control cells. In comparison to uninfected cells, membrane proliferation and ER expansion was more pronounced in infected cells suggesting an influence of TBEV on the ultrastructure of the tick cells.

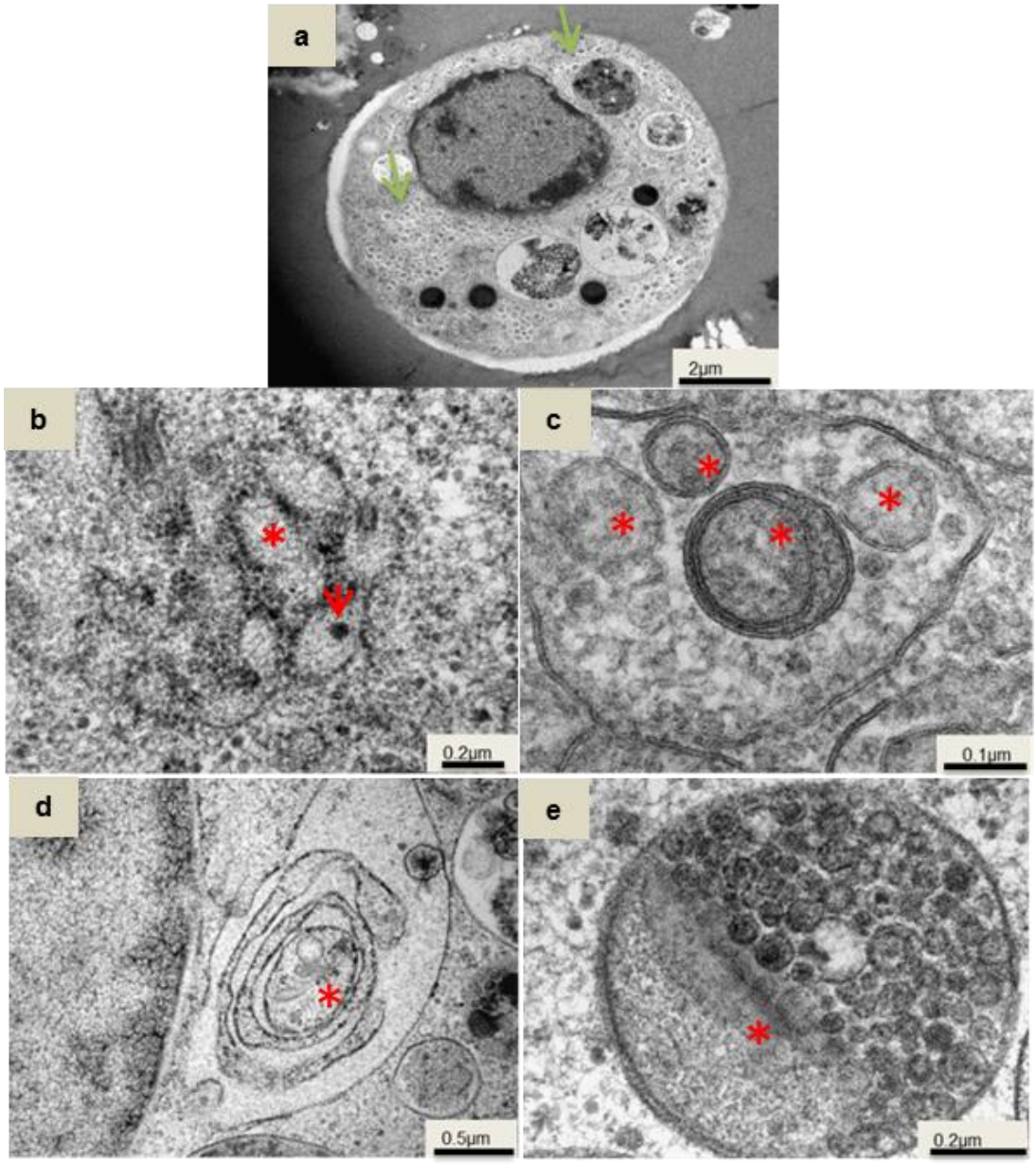

Figure 3.17 TEM of uninfected and TBEV-infected IDE8 cells

IDE8 cells were infected with TBEV at MOI 5, cryofixed at day 2 p.i. and prepared for TEM. Green arrows indicate endogenous virus particles, red arrows indicate TBEV particles and red stars indicate ultrastructural changes. Uninfected control cell (a), parts of TBEV-infected cells (b – e). Experiment was done once.

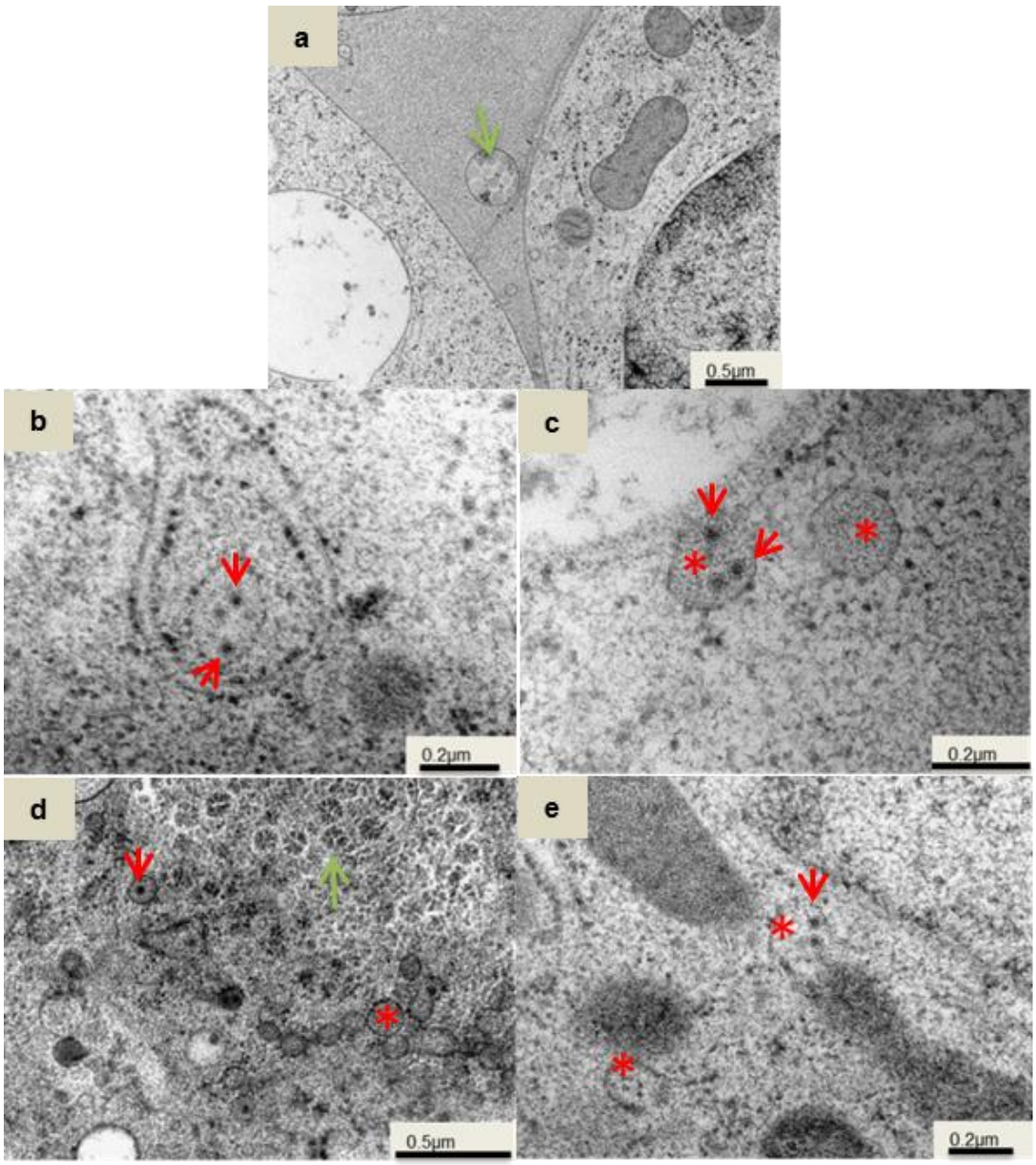

Figure 3.18 TEM of uninfected and TBEV-infected IRE/CTVM19 cells

IRE/CTVM19 cells were infected with TBEV at MOI 5, cryofixed at day 2 p.i. and prepared for TEM. Green arrows indicate endogenous virus particles, red arrows indicate TBEV particles and red stars indicate ultrastructural changes. Parts of uninfected control cell (a), TBEV-infected cells (b – e). Experiment was done once.

Although some of the observed structures had striking similarity to replication complexes observed for other flaviviruses (Gillespie et al., 2010; Mackenzie et al., 1999; Mackenzie, Khromykh & Parton, 2007; Offerdahl et al., 2012; Senigl, Grubhoffer & Kopecky, 2006; Welsch et al., 2009), to test if these ER expansions and vesicles observed upon TBEV infection in tick cells actually are replication complexes, immunolabelling of TBEV NS1 protein in TEM sections on grids was

attempted (2.2.2.3). Since the cryopreservation in this experiment resulted in poor ultrastructural preservation and in addition the immunolabelling led to high background labelling, no usable pictures were obtained. Further experiments were not carried out in the present study.

3.4.6 Uptake and transfection efficiency of dsRNA and siRNA in tick cells

siRNA and dsRNA are regularly used in mammalian and arthropod cells to silence genes by exploiting the innate defence and gene regulation mechanism RNAi. This mechanism allows for knocking down genes of interest to elucidate their role in the organism. To test if ISE6, IDE8 and IRE/CTVM19 cells take up dsRNA and siRNA and which approach, either with or without transfection reagent, is the most efficient to achieve uptake, cells were seeded either in tubes to determine transfection efficiency or on coverslips in 24-well plates for confocal imaging. For experiments to determine transfection efficiency 400 ng of fluorescently-labelled dsRNA (~ 600 bp) and 50 nM of BLOCK-iT green fluorescent siRNA (Invitrogen) were used per culture tube, while 200 ng of dsRNA and 50 nM of siRNA were used per well for confocal imaging. dsRNA or siRNA in OptiMEM were either added directly to the medium or mixed with the transfection reagents Lipofectamine2000 or X-tremeGENE and then added to the medium. Culture tubes were viewed with an inverted microscope. Images were taken and a minimum of 400 cells were examined. Transfection efficiency was calculated as percentage of cells positive for siRNA or dsRNA (Table 3.1). For confocal microscopy, cells were fixed and images taken on the Zeiss LSM710 microscope (Figure 3.19).

All tick cell lines took up siRNA and dsRNA when transfection reagents were used, as shown by confocal microscopy for IDE8 and IRE/CTVM19 (Figure 3.19). When siRNA alone, without transfection reagent, was added to the medium none of the tick cell lines took it up (Figure 3.19 A,Table 3.1). When dsRNA alone was added to the medium, low numbers of cells took it up (Figure 3.19 B, Table 3.1).

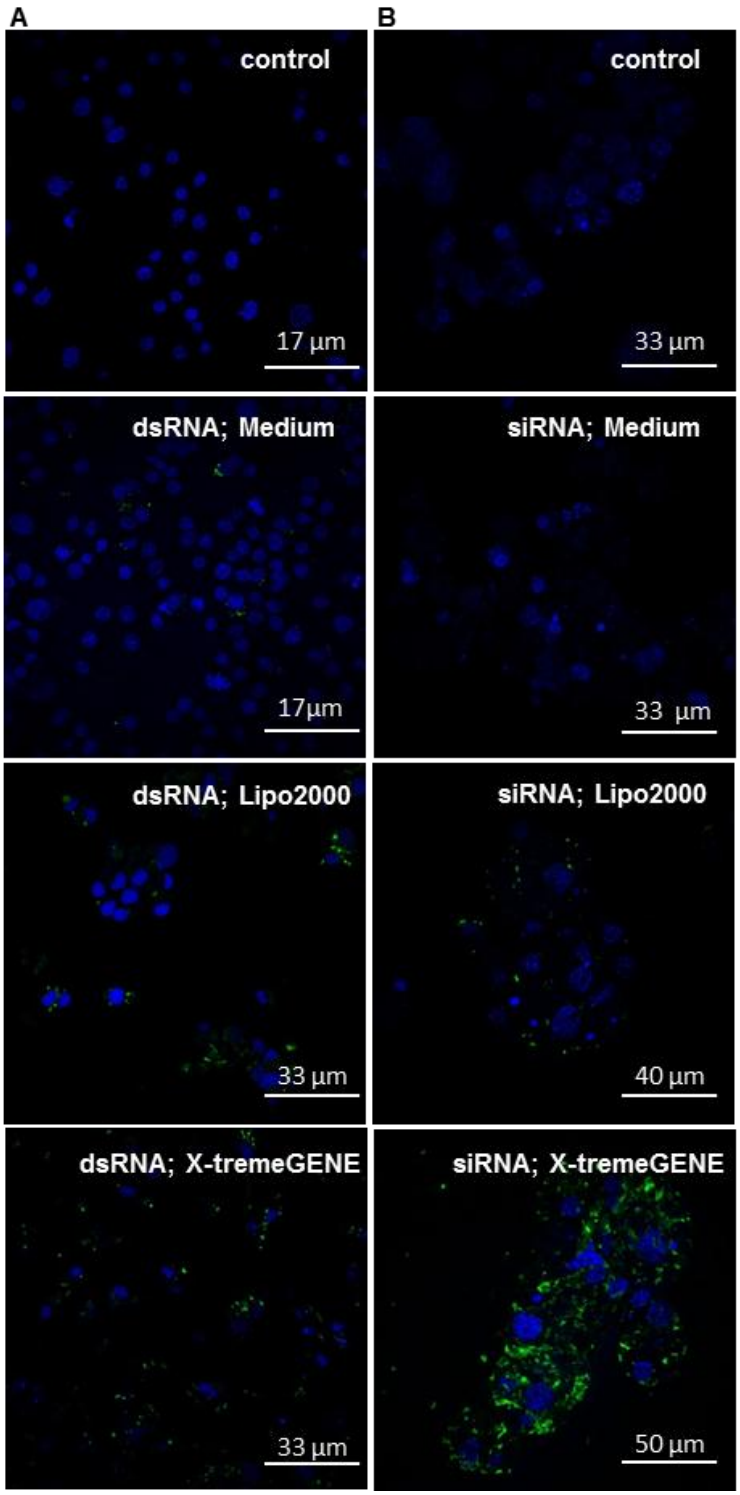

Figure 3.19 Uptake of siRNA or dsRNA by tick cells in the presence or absence of transfection reagent

Fluorescently labelled siRNA or dsRNA was added to tick cells in the presence or absence of either Lipofectamine 2000 (Lipo2000) or X-tremeGENE and incubated for 24 h. Confocal images were taken on the LSM710 microscope at x630 magnification. Confocal images of dsRNA in IDE8 (A) or siRNA in IRE/CTVM19 (B) cells.

Table 3.1 Transfection efficiencies of ISE6, IDE8 and IRE/CTVM19 cells.

	ISE6		IDE8		IRE/CTVM19	
	dsRNA	siRNA	dsRNA	siRNA	dsRNA	siRNA
Lipofectamine 2000	53%	23%	45%	20%	29%	19%
X-tremeGENE	77%	33%	51%	31%	62%	67%
Medium	<2%	0%	4%	0%	<2%	0%

The best transfection efficiency was observed with the transfection reagent Xtreme-Gene followed by Lipofectamine2000 in all cell lines (Table 3.1); in both cases transfection efficiency was more than 10 times higher than that achieved by adding siRNA or dsRNA alone to the medium (Table 3.1).

3.5 Summary of findings

- All tick cell lines used (ISE6, IDE8 and IRE/CTVM19) were able to be infected with the alphavirus SFV and either or both of the flaviviruses LGTV and TBEV and supported virus replication and production.
- The virus production curves for TBEV-infected IDE8 and IRE/CTVM19 cells enabled the selection of time-points for subsequent transcriptomic and proteomic experiments.
- Visual counting of infected cells was compared to FACS analysis, with the former detecting a much higher proportion of infected cells than the latter. Therefore if FACS analysis is to be used for determining the percentage of infected tick cells, it requires further optimisation.
- Virus infection of tick cells did not result in any cytopathic effect as determined by microscopic examination. Furthermore, experiments longer than 5 days with IRE/CTVM19 should be carried out in flat-sided culture tubes rather than in 24-well plates.
- Failure of TBEV reporter constructs with an Encephalomyocarditis virus (EMCV) IRES in the 3' non-structural region to express luciferase in tick cells revealed that EMCV IRES-driven gene expression is not supported in tick cells in contrast to mammalian cells.

- All tick cell lines used in the present study (ISE6, IDE8 and IRE/CTVM19) were confirmed to harbour endogenous reovirus-like particles. The identities of those in ISE6 and IRE/CTVM19 cells are unknown.
- Ultrastructural features resembling replication complexes were not observed upon SFV infection of ISE6 and IRE/CTVM19 cells, while ultrastructural features possibly resembling replication complexes were observed in TBEV-infected IDE8 and IRE/CTVM19 cells.
- All the tick cell lines took up siRNA or dsRNA in the presence of a transfection reagent. Use of a transfection reagent was essential for uptake of siRNA, but not of dsRNA.

3.6 Discussion

Tick cell lines have proved to be vital tools in the study of human and animal pathogens (Bell-Sakyi et al., 2007), and since the establishment of the first continuous tick cell lines derived from *R. appendiculatus* in 1975 (Varma, Pudney & Leake, 1975) the number of available tick cell lines has increased to over 50 and even soft tick cell lines are now readily available (Bell-Sakyi et al., 2012). Many studies since 1975 have focussed on propagating different arboviruses and non-arboviruses and looked at persistent infection with some of these viruses. The results showed that although many of the known tick-borne as well as mosquito-borne viruses can be grown in one tick cell line or another, the kinetics of virus infection differ depending on the virus and cell line used (Bhat & Yunker, 1979; Leake, Pudney & Varma, 1980; Pudney, 1987; Rehacek, 1987; Varma, 1989; Varma, Pudney & Leake, 1975). This was confirmed in the present study, since all the tick cell lines used were readily infected with the mosquito-borne virus SFV and the tick-borne viruses TBEV and LGTV but the percentage of infected cells and the kinetics of virus replication and production varied. Approximately 97% of IDE8 cells were permissive for LGTV, between 50 and 70% of IDE8 and IRE/CTVM19 cells were permissive for TBEV and about 40- 50% of ISE6, IDE8 and IRE/CTVM19 cells were permissive for SFV. Although the kinetics of virus production were similar in cell lines infected with LGTV and TBEV, the amount of virus produced was

considerably lower in non-vector cell lines, which is consistent with published studies (Bhat & Yunker, 1979; Lawrie et al., 2004; Růzek et al., 2008), and suggests that higher virus titres might be an indicator of vector capacity. Růzek et al. (2008) used the IRE/CTVM19 cell line for infection with TBEV strain Neudoerfl at MOI 1 and although the peak of virus production in their study was at day 5 and in the present study was between days 3 and 4, a similar temporal pattern of virus production was observed. The peak titre obtained in the present study was, however, approximately 100 times higher than in Růzek et al.'s study. The differences in timing of peak virus production and titre could be explained by different experimental set-ups. For example, Růzek et al. infected cells with MOI 1 whereas MOI 5 was used in the present study. More importantly they infected cells in suspension before seeding them at a density of 2.5×10^4 cells per well in a 96-well plate, which is a cell density approximately one quarter of that used in the present study, in which cells were seeded at a density of 1×10^6 cells per tube. As IRE/CTVM19 cells do not grow efficiently in multiwell plates opposed to flat-sided tubes, lower starting cell density and growth rate could explain the large difference in the amount of virus produced.

Although SFV has been isolated from field ticks removed from livestock in Kenya (Lwande et al., 2013), there is no data on whether ticks can transmit this virus. However several studies in the 1970s showed that SFV was able to infect tick cells and that tick cells produce infectious virus particles (Leake, Pudney & Varma, 1980; Pudney, 1987), which was confirmed in the present study. In the cell lines used, SFV production peaked between days 3 and 5 in ISE6 and at day 2 in IDE8 and IRE/CTVM19 before plateauing. This pattern in virus production is different to what was seen in previous studies using *Rhiphicephalus* and *Boophilus* spp. cell lines infected with SFV (Leake, 1987; Leake, Pudney & Varma, 1980; Pudney, 1987). In those studies virus production peaked at day 1 and rapidly decreased thereafter. The pattern of virus growth in TBEV- and LGTV-infected tick cells differed greatly from that of SFV, which highlights the point that each tick cell line should be characterised with the virus of interest to be able to determine basic growth parameters.

Due to the availability of reporter viruses, which were not available in the 1970s and 1980s, new information such as infection rate and virus replication could be elucidated in the present study. SFV reporter viruses containing fluorescent markers, such as ZsGreen and eGFP, were used to determine that approximately 30-70% of tick cells were both susceptible to SFV infection as well as supportive of virus replication and/or translation which resulted in fluorescent marker expression. This result was obtained by visual counting of fluorescing and non-fluorescing cells, since the direct comparison of visual counting and FACS analysis resulted in an underestimation by the latter. Possible explanations for this underestimation of infected tick cells by FACS analysis might be that during the gating process a large proportion of the infected cells were excluded due to their heterogeneity in size and granularity, or that the auto-fluorescence of tick cells interfered with the detection of green fluorescence emitted by marker genes. Further optimisation of sample preparation and gating processes is required to establish FACS analysis for the detection of virus infection in tick cells.

SFV reporter viruses encoding Rluc in either the structural or non-structural reading frames were used to elucidate the pattern of virus replication in different tick cell lines. Similar to what was observed by others in mammalian and mosquito cells (Fragkoudis et al., 2008; Kiiver et al., 2008), infection of tick cells with SFV4(3H)-Rluc, encoding Rluc in the non-structural reading frame, led to Rluc expression early in infection, up to day 1, whereas Rluc expression from SFV4-StRluc, encoding Rluc in the subgenomic RNA, resulted in Rluc expression late in infection, from day 1 – 4. This suggests that replication and translation of the early non-structural genes occurred early in infection and was slowly down-regulated to allow replication and translation of the subgenomic RNA encoding the structural genes, which confirms the observations previously reported for SFV by others (Fragkoudis et al., 2008; Kiiver et al., 2008).

The use of reporter viruses is a useful tool for quick readout of infection rate and to elucidate virus replication in tick cells as has been shown for SFV in the present study. Although there are several different infectious reporter viruses available for SFV, only one is available for TBEV (Gehrke et al., 2005) and there are none for LGTV. In the present study an infectious TBEV reporter virus and replicon reporter

were cloned by inserting an EMCV IRES linked to Rluc or Fluc into the 3' non-structural reading frame using the previously described plasmids pTND/c-eGFP, encoding the infectious virus, and the plasmid pTND/ΔME-eGFP, encoding a virus replicon, as templates (Gehrke et al., 2005). For safety reasons, only replicons encoding Rluc and Fluc were transfected into mammalian and tick cells. Both mammalian and tick cells were positive for replicon RNA by qRT-PCR but only the mammalian cells expressed luciferase. This result suggested that tick cells are unable to express proteins under the control of an EMCV IRES. This finding confirmed similar studies comparing different viral-derived IRES in mammalian and arthropod cells (Finkelstein et al., 1999; Guerbois et al., 2013; Volkova et al., 2008; Woolaway et al., 2001; Wu et al., 2008). They showed that expression driven by the IRES from EMCV is functional in mammalian cells but not in mosquito cells (Finkelstein et al., 1999; Guerbois et al., 2013; Volkova et al., 2008), but they also showed that arthropod cells can express genes driven by an IRES if the correct IRES is chosen (Woolaway et al., 2001; Wu et al., 2008). Since so far no study has looked at IRES-driven expression in tick cells, the present study is the first to show that, as in insect cells, EMCV IRES elements do not function in tick cells. Instead of testing the infectious virus containing the same insert as the replicon, which did not function in tick cells, different TBEV replicons as described by Hoenninger et al. (2008) were used. These replicons all expressed luciferase with a peak at 24h p.i, which is in contrast to the biphasic profile Hoenninger et al. (2008) observed in mammalian cells, suggesting that these replicons might not replicate efficiently in tick cells. However, the LGTV replicon which was designed in exactly the same way as the TBEV replicons and showed a similar pattern of Rluc expression as the TBEV replicons had been shown to replicate in tick cells by Dr. Esther Schnettler (Schnettler et al., 2014). Her results suggest that the replicons are replicating efficiently but that the virus may be targeted by the innate immune defence mechanism RNAi thus degrading viral RNA and subsequently inhibiting Rluc expression.

In attempts to identify ultrastructural changes resembling replication complexes, caused by SFV and TBEV infection, tick cells infected with SFV and TBEV were studied by TEM. However, while ultrastructural changes caused by SFV infection

were not detected, the presence of endogenous viruses in the tick cells was observed. The viruses found in ISE6 and IRE/CTVM19 cells appeared similar in size and structure to the orbivirus SCRV found in IDE8 (Attoui et al., 2001; Bell-Sakyi et al., 2007), which is considered to be a "tick-only" virus (Nuttall, 2009). A subsequent study screening for SCRV however revealed a negative result for both cell lines (Alberdi et al., 2012), leaving unanswered the question of which viruses are persistently infecting ISE6 and IRE/CTVM19 cells. Screening of all three cell lines for flaviviruses and nairoviruses within the same study gave negative results (Alberdi et al., 2012). In addition to carrying an endogenous virus, IRE/CTVM19 might also be infected with the intramitochondrial bacterial symbiont *Candidatus* Midichloria mitochondrii as shown by Najm (Najm et al., 2012), who detected a small fragment of bacterial DNA but failed to amplify larger sections of the same gene in the same sample. In nature, ticks transmit an enormous variety of pathogens including bacteria, protozoa and viruses and are often carrying more than one pathogen at the same time (Franke et al., 2010; Levin & Fish, 2000; Lwande et al., 2013). Continuous cell lines have been derived from some of these ticks and most lines have been screened for endosymbiotic bacteria and endogenous viruses (Alberdi et al., 2012; Attoui et al., 2001; Mattila et al., 2007; Munz, Reimann & Mahnel, 1987; Simser et al., 2001).

Despite the presence of these endogenous viruses in tick cells, virus infection, replication and production of TBEV, LGTV and SFV was still possible, which is in agreement with previous studies where it has been shown that superinfection with SFV of tick cells persistently infected with LGTV did not reduce production of SFV (Leake, Pudney & Varma, 1980). It is still unknown whether these endogenous viruses moderate or even suppress the innate immune response to infection with other arboviruses, and if this is perhaps an explanation for most arboviruses causing a low-level persistence without any cytopathic effect in tick cells. Although the *in vitro* situation resembles the situation in nature where ticks can be infected with several different pathogens at once, results from experiments on the innate immune response in tick cells towards a particular arbovirus need to be interpreted carefully.

Infections with most RNA viruses, whether in plants, insects or mammalian cells, induce changes in host membranes that accommodate different stages of the viral life

cycle (Gillespie et al., 2010; Mackenzie, 2005). Many studies on infection of mammalian cells have focused on elucidating the role of membrane changes in virus replication. For some RNA viruses, including viruses of the families *Flaviviridae* and *Togaviridae*, cellular membranes enclose the viral RNA and associated viral replicase proteins to create a microenvironment which probably not only provides a stable, confined surface for replication but also protects the viral mRNA from recognition and degradation by host response proteins (Froshauer, Kartenbeck & Helenius, 1988; Hoenen et al., 2007; Kopek et al., 2007; Mackenzie, Khromykh & Parton, 2007; Welsch et al., 2009). During SFV infection of mammalian cells late endosomes and lysosomes form cytopathic vesicles, termed CPV-I and CPV-II, which are important sites for, respectively, virus RNA synthesis and virus particle formation (Grimley, Berezesky & Friedman, 1968; Kujala et al., 2001; Virtanen & Wartiovaara, 1974). Although *Ixodes* spp. tick cells were infected with SFV4(3F)-ZsGreen in the present study, as proved by immunofluorescence, no SFV particles were observed by EM. Furthermore, no CPVs resembling those observed in SFV-infected mammalian cells (Froshauer, Kartenbeck & Helenius, 1988; Grimley et al., 1972; Grimley, Berezesky & Friedman, 1968; Kujala et al., 2001) could be seen. Possible explanations could be that although cells were infected and approximately 100 cells were screened, the proportion of infected cells (between 50 and 70%) never reached 100%, thus replication complexes might simply have been missed by examining cells or areas of infected cells in which the virus was not present. Another possibility would be that replication complexes in tick cells, which are not the natural vector of SFV, look different from those described in mammalian cells and might have been missed because of this. Finally, it may be that CPV-I- and CPV-II-like virus replication structures do not form in tick cells. Studies comparing mammalian and mosquito cells infected with the flavivirus DENV did not find differences between these cells in the structure of replication complexes (Barth, 1999; Rahman et al., 1998). The morphology of tick and mammalian cells is quite different, in that tick cells contain a large number of vacuoles and vesicles which might have made it more difficult to distinguish replication complexes in SFV-infected tick cells.

In addition an attempt was made to detect replication complexes of the tick-borne flavivirus TBEV in IDE8 and IRE/CTVM19 cells. TBEV particles are approximately

45 to 50 nm in diameter and appear with an electron-dense centre and a less dense envelope and thus should be distinguishable from the larger reovirus-like endogenous viruses. Ultrastructural changes induced by flaviviruses are marked by convoluted membranes, paracrystalline arrays and vesicle packets (VP). The membranes forming VP, which have been shown to contain dsRNA intermediates and are suspected to be the site of virus replication of WNV, are derived from the ER (Gillespie et al., 2010). Immunostaining showed that dsRNA, viral helicase and viral polymerase were localised to areas of ER expansion both in LGTV-infected Vero cells and in ISE6 cells acutely and persistently infected with the same virus, suggesting that replication complexes are associated with and derived from the ER in mammalian and tick cells (Offerdahl et al., 2012). In the present study ER expansion due to virus infection and round vesicle packets in close association with the ER were found which might possibly be replication complexes. TBEV particles of approximately 45 to 50 nm were found within vesicles in the cytoplasm and also within ER. The finding of TBEV particles within the ER is in contrast to the study of Senigl et al. (2006) in the *R. appendiculatus* cell line RA-257. These authors did not find virus particles associated with ER, but in the lumen of vacuoles, and also found viral proteins in the cytosol; they hypothesised that this suggested a *cis*-type maturation process for TBEV in tick cells whereas a *trans*-type maturation process occurred in mammalian cells. It was not possible to confirm if the structural changes identified in the present study were truly replication complexes by immunolabelling of cryosections due to their poor quality, but nevertheless the ultrastructural changes looked similar to those described in other studies of tick cells (Offerdahl et al., 2012; Senigl, Grubhoffer & Kopecký, 2006).

Gene silencing by RNAi is one of the most important research tools in many areas of biology and has been efficiently exploited in determining the role of genes and proteins in ticks and some tick cell lines (Barnard et al., 2012a; Blouin et al., 2008; Kocan, Manzano-Roman & de la Fuente, 2007; Kurscheid et al., 2009; Kurtti et al., 2008; de la Fuente et al., 2007a, 2007b; Nijhof et al., 2007; Zivkovic et al., 2010b). However, before the study of Barry et al. (2013), parameters to obtain an efficient knockdown across a range of different tick cell lines had not been established. As a contribution to that study the ISE6, IDE8 and IRE/CTVM19 tick cell lines were

treated with fluorescently labelled siRNA or dsRNA in the presence or absence of transfection reagents to examine their uptake and transfection efficiency by fluorescence microscopy. It was found that all three tick cell lines took up dsRNA from the medium although less efficiently than in the presence of transfection reagents, and that transfection reagent was required for the uptake of siRNA. Efficiencies of uptake or transfection varied depending on the cell line used and might be slightly higher than calculated since cells which only take up small amounts of dsRNA might have been missed due to the detection limit of fluorescence microscopy, but these small amounts might nevertheless be effective in gene silencing and knockdown of protein expression.

Further experiments done by Barry et al. (2013) proved the above assumption that, although the uptake of dsRNA straight from the culture medium appeared by fluorescence microscopy to be not very efficient, silencing of Rluc expressed from SFV4-StRluc and of tick genes achieved similar levels in the presence and absence of transfection reagents, at least in ISE6 and IDE8 cells (Barry et al., 2013). In IRE/CTVM19 cells silencing of Rluc expressed from SFV4-StRluc did not result in reduced Rluc activity whether or not transfection reagents were used (Barry et al., 2013). Taking all the results into account, for ISE6 and IDE8 cells dsRNA added directly to the medium without a transfection reagent is, especially if subsequently transfecting virus replicons into the cells, advantageous over having to transfect cells twice. In contrast, for IRE/CTVM19 siRNA would be advised but no experiments have been published to determine the efficiency of tick gene knockdown achieved by adding dsRNA alone to the medium.

Overall, ISE6, IDE8 and IRE/CTVM19 cells can all be infected with SFV, TBEV and LGTV and growth curves were established for each virus allowing selection of time-points for harvesting cells to isolate RNA and protein in subsequent transcriptomic, proteomic and knockdown experiments. Taking into account that knockdowns in IDE8 were more efficient than in ISE6 (Barry et al., 2013) and that although both cell lines contain endogenous viruses, the virus in IDE8 is identified and characterised, IDE8 was taken forward as the *I. scapularis* cell line of choice for future experiments. Although IDE8 is derived from a tick species which is not the natural vector of TBEV it is the only tick species with a sequenced genome. As the

IRE/CTVM19 cell line is derived from the natural vector *I. ricinus*, it was also used in the subsequent experiments.

4 Chapter 4: Transcriptomic and proteomic analysis of tick cell lines infected with TBEV

4.1 Introduction

Next generation sequencing and quantitative proteomics have become popular tools for identifying differentially expressed transcripts and proteins, but only very few papers have reported the use of either technology for the study of the tick transcriptome (Bissinger et al., 2011; Donohue et al., 2010; Karim, Singh & Ribeiro, 2011; Schwarz et al., 2013; Sonenshine et al., 2011; Villar et al., 2014) or proteome (de la Fuente et al., 2007a; Popara et al., 2013; Villar et al., 2010a, 2010b, 2013, 2014). Only three studies have applied quantitative proteomic approaches to characterising the tick proteome in response to bacterial infection (de la Fuente et al., 2007a; Villar et al., 2010a, 2010b). A single transcriptome study has examined viral infection of ticks, using microarrays for the comparison of salivary gland gene expression between uninfected and LGTV-infected *I. scapularis* ticks (McNally et al., 2012). There is a lack of genomic information on tick vectors. The only tick species whose genome has been sequenced so far is *I. scapularis* (Table 4.1). In contrast, several important mosquito vector genomes have been sequenced (Table 4.1). The assembly of contigs and alignments is considerably easier when a reference genome is available.

Table 4.1 Sequence data available to date for vector species

The genomes of major mosquito vector species and one tick species *I. scapularis* have been sequenced, assembled and partially annotated. Annotation and identification of gene function are still in progress (VectorBase, http://www.vectorbase.org).

Organism	Strain	Assembly version	Transcripts	Protein coding	Gene build
I. scapularis	WIKEL	IscaW1	24,925	20,486	IscaW1.2 May 2012
Ae. aegypti	Liverpool	AaegL2	18,520	17,143	AaegL2.1 December 2013
A. gambiae	PEST	AgamP3	15,322	14,667	AgamP3.7 October 2012
C. quinquefasciatus	Johannes -burg	CpipJ1	23,049	19,019	CpipJ1.3 April 2012
Anopheles stephensi	Indian	AsteI2	11,789	11,789	AsteI2.1 October 2013
Anopheles darling	Coari	AdarC2	10,827	10,457	AdarC2.1 December 2013

The next-generation sequencing technologies most commonly applied to transcriptomic studies are the Roche 454 platform and Illumina Solexa sequencing (Illumina). In the field of tick transcriptomics four studies have used the Roche 454 technology (Bissinger et al., 2011; Donohue et al., 2010; Karim, Singh & Ribeiro, 2011; Sonenshine et al., 2011), one has used a combination of Roche 454 and Illumina (Schwarz et al., 2013) and one used Illumina only (Villar et al., 2014). Quantitative proteomic studies apply techniques which are either gel-based or gel-free. The gel-free approaches either use isotope labelling or label-free approaches to quantify proteins (e.g. (Abdallah et al., 2012; Bantscheff et al., 2007)). The three studies quantifying differential protein expression in infected and uninfected ticks or tick cells used either gel-based approaches (de la Fuente et al., 2007a; Villar et al., 2010b) or a combination of gel-based and gel-free with isotope labelling (Villar et al., 2010a). In the present study the Illumina HiSeq2000 platform was used to sequence and assemble parts of the transcriptome, and a combination of gel-based and gel-free, label-free approaches were used for sequencing and quantifying the proteomes of IDE8 and IRE/CTVM19 cells infected or mock-infected with TBEV at two different time-points. All the technologies mentioned have different advantages and limitations which will be briefly described below (4.1.1, 4.1.2).

4.1.1 Roche 454 versus Illumina sequencing platform

RNA sequencing technologies are rapidly evolving and both the Roche 454 and Illumina Hiseq2000 platform were available at the beginning of this study. Comparing the two, Roche 454 sequencing produces longer reads of up to 700 bp, runs quicker but also has a lower throughput, leads to higher error rates and is more expensive (Liu et al., 2012c; Metzker, 2010; Tucker, Marra & Friedman, 2009). The Roche 454 platform is based on pyroseqeuncing which uses enzymes to produce light from phosphate released during dNTP integration. In brief, a cDNA library is ligated to 454 specific adaptors and mixed with agarose beads coated with complementary adapter sequences. Each bead containing a single cDNA fragment is isolated into a single water droplet in oil solution and cDNA fragments are subsequently amplified during an emulsion PCR. After amplification each bead

contains approximately 1 million copies of the same cDNA fragment and each bead is sequenced individually in picotiter plates. By addition of enzyme-coated beads and step-wise addition of dNTPs, light generated during dNTP incorporation is measured and the sequence obtained. The Illumina Solexa sequencing which includes the HiSeq2000 platform is based on a sequencing-by-synthesis approach and the workflow is depicted in Figure 4.1. To create a library, DNA is fragmented and adapters, which are complementary to adapters coated onto a flow cell, are ligated to both ends. Once the library is added to the flow cell, DNA hybridises and forms a bridge from which amplification is primed from the 3'end and finishes when it reaches the 5' end. Strands are denatured and the whole process begins again, so that after several steps of amplification clusters of fragments with the same sequence are created. These clusters are denatured prior to addition of primers, polymerase and all four fluorescently-labelled dNTPs. The 3'-OH group of the dNTPs is chemically inactivated ensuring the insertion of only one base at a time. After incorporation of the correct nucleotide, images are taken of each cluster, then the fluorescent marker is chemically removed and the 3'-OH group unblocked allowing the incorporation of the next nucleotide. This process can generate 2 x 100 bp long reads in a paired end sequencing approach on the Hiseq2000 platform.

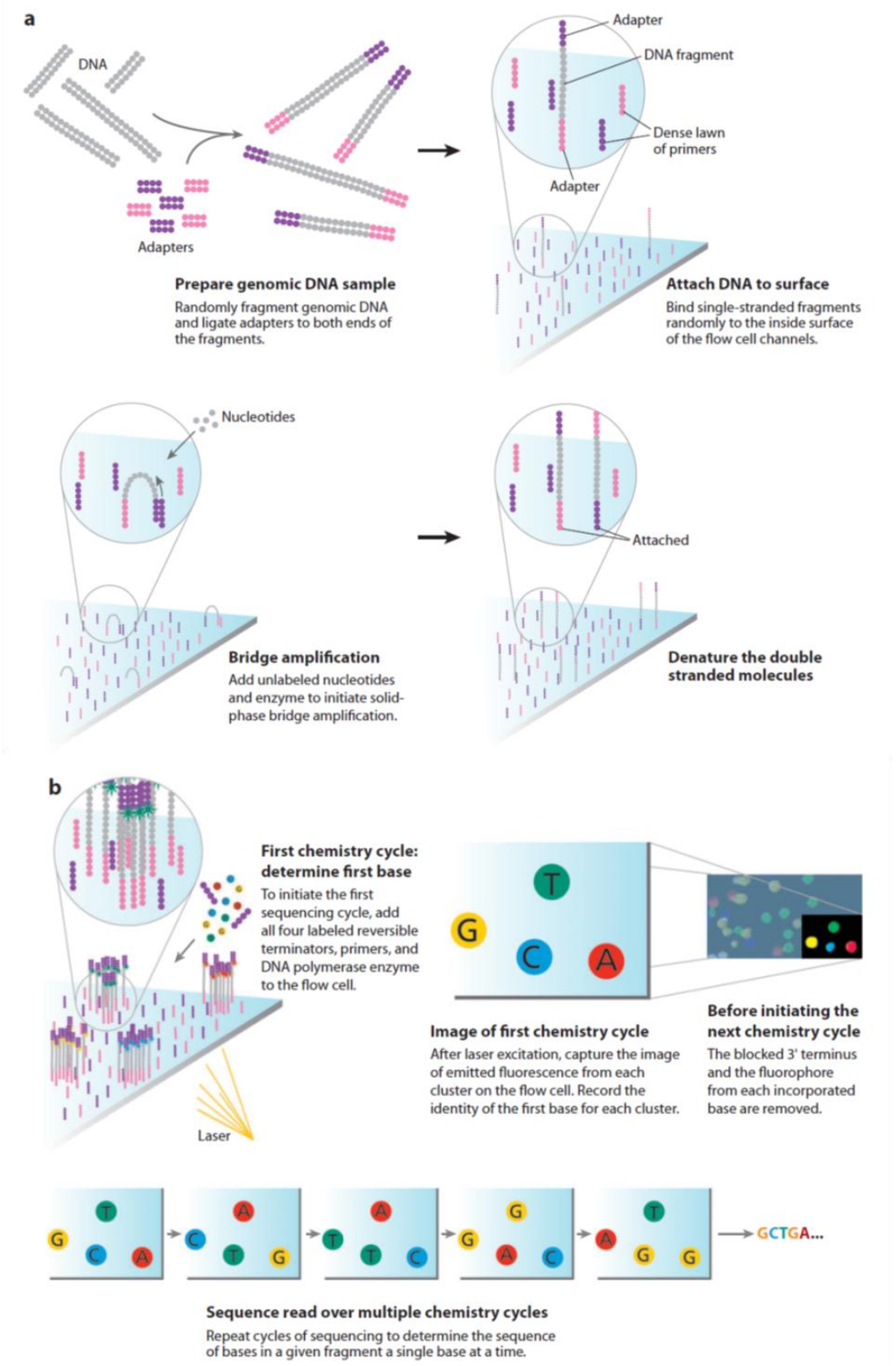
a
DNA
Adapters
Prepare genomic DNA sample
Randomly fragment genomic DNA and ligate adapters to both ends of the fragments.
Adapter
DNA fragment
Dense lawn of primers
Adapter
Attach DNA to surface
Bind single-stranded fragments randomly to the inside surface of the flow cell channels.
Nucleotides
Bridge amplification
Add unlabeled nucleotides and enzyme to initiate solid-phase bridge amplification.
Attached
Denature the double stranded molecules
b
First chemistry cycle: determine first base
To initiate the first sequencing cycle, add all four labeled reversible terminators, primers, and DNA polymerase enzyme to the flow cell.
Laser
Image of first chemistry cycle
After laser excitation, capture the image of emitted fluorescence from each cluster on the flow cell. Record the identity of the first base for each cluster.
Before initiating the next chemistry cycle
The blocked 3' terminus and the fluorophore from each incorporated base are removed.
GCTGA...
Sequence read over multiple chemistry cycles
Repeat cycles of sequencing to determine the sequence of bases in a given fragment a single base at a time.

Figure 4.1 Illumina solexa sequencing workflow.

a) During the preparation of genomic DNA, DNA fragments are ligated to adapters complementary to adapters coated onto a flow cell. After attachment, DNA sequences are amplified by bridge amplification and the double-stranded DNA molecules are denatured prior to sequencing. b) Sequencing reaction is initiated by addition of primers, fluorescently-labelled 3'-OH blocked nucleotides and polymerase. After incorporation of exactly one nucleotide in each cluster, images are taken and the 3'-OH terminator chemically removed to allow the incorporation of the next nucleotide. The cycle is repeated several times until 50-150 bp long reads are generated. From Mardis, 2008.

4.1.2 Gel-based versus gel-free quantitative proteomic approaches

Quantitative proteomics is used to compare and quantify differences between cellular states and has been classically divided into gel-based and gel-free approaches.

Gel-based approaches such as DIGE were the method of choice for separating intricate patterns of proteins on 2D polyacrylamide gels at high resolution. With the aid of fluorescent multiplexing, spots indicating differentially expressed proteins could be visualised but the identity of the underlying protein was not revealed unless it was subjected to MS. Poor reproducibility and difficulties in automation and detecting proteins with low abundance led to the development of gel-free approaches (Bantscheff et al., 2007; Patterson & Aebersold, 2003; Villar et al., 2012). Gel-free approaches usually introduce isotopes either at the cellular level, by metabolic labelling, or at the protein or peptide level by chemical or enzymatic labelling. These labelling approaches introduce a difference in mass between labelled and unlabelled forms which can be recognised by a mass spectrometer and quantified by comparing signal intensities. Although more accurate than label-free approaches, the necessity for large protein amounts, complex sample preparation, high costs of reagents and incomplete labelling are drawbacks (Bantscheff et al., 2007; Villar et al., 2012). To minimise these difficulties, label-free approaches were developed either to compare the signal intensities for any given peptide (Chelius & Bondarenko, 2002) or using the number of acquired spectra for a peptide or protein as an indicator for their concentration within a sample (Washburn, Wolters & Yates, 2001). Although peak intensities correlate linearly with concentration of protein, slight variations in sample preparation, sample injection or retention times make it difficult to align peaks for comparison and result in large variability and inaccuracy in quantification. To enable

accurate comparison, experiments have to be highly reproducible and peak alignment is essential in this approach (Zhu, Smith & Huang, 2010). In the spectral counting approach this is not necessary. This approach compares the number of spectra from the same protein across different liquid chromatography-tandem MS (LC-MS/MS) runs: the more spectra there are, the higher the protein abundance. This counting approach is possible since an increase in protein abundance results in an increase in proteolytic peptides which in turn results in a higher spectral count (Washburn, Wolters & Yates, 2001). The application of the spectrum counting approach is still controversial, since it is based on the assumption that the physical properties of a peptide are the same for every protein. In reality, the response is different for every peptide and may vary in aspects of chromatographic behaviour such as retention time and peak width. Furthermore, for the detection of small changes the number of required spectra increases exponentially, with at least 15 spectra required to detect a two-fold change in protein abundance (Bantscheff et al., 2007). Nevertheless, spectral counts have been shown to have a strong linear correlation with relative protein abundance (Liu, Sadygov & Yates, 2004) and are therefore a simple and reliable indication for protein quantification (Zhu, Smith & Huang, 2010).

4.2 Objectives

- To identify differential expression of mRNA transcripts and differential representation of proteins in IDE8 and IRE/CTVM19 cells after TBEV infection.
- To identify mRNA transcripts or proteins potentially involved in the antiviral response of tick cells to TBEV.

4.3 Experimental design

The time-points for isolating RNA and protein for transcriptomic and proteomic analysis were chosen from the TBEV virus production curve generated in Chapter 3 (Figure 3.10 A). Virus production increased in both cell lines up to day 3 and decreased thereafter. Therefore, to examine how the innate immune system reacts to

virus infection, two time-points, one early in infection (day 2) and one late in infection (day 6), were chosen for study. The hypothesis behind choosing these time-points was that early in infection, when virus production is still increasing, the virus is expected to be manipulating the activated host defence response to support virus replication and/or production whereas late in infection, when virus production is decreasing, the innate immune system is expected to be controlling or repressing virus replication and/or production.

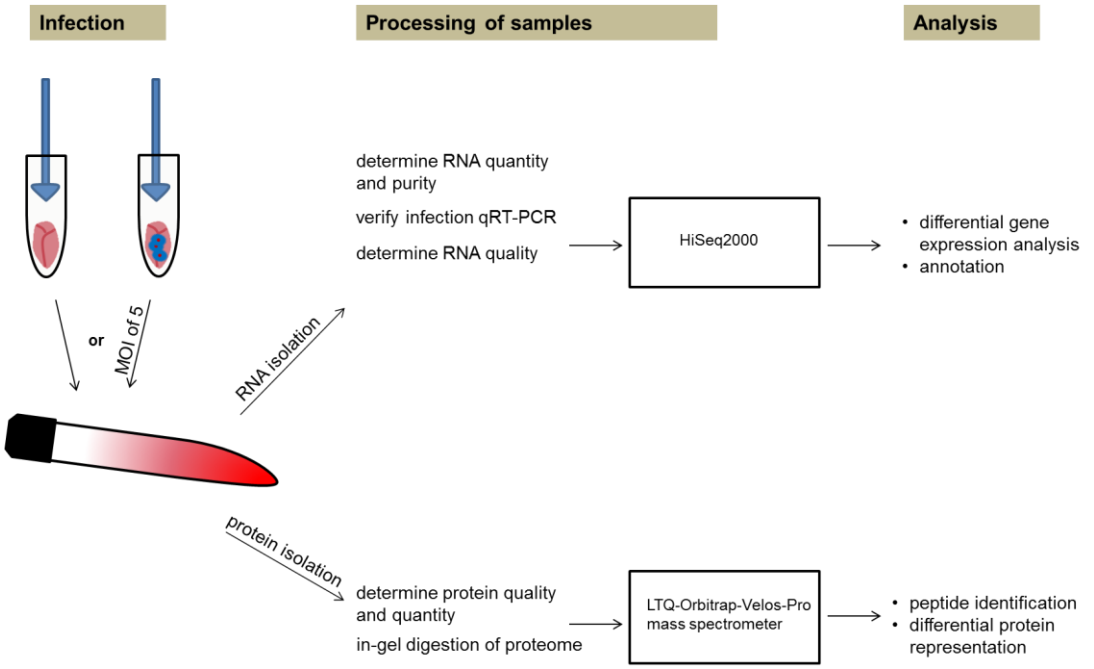

Figure 4.2 Experimental workflow for transcriptomic and proteomic analysis.

Tubes of IDE8 or IRE/CTVM19 cells were either mock-infected with uninfected mouse brain suspension or infected with TBEV-infected mouse brain suspension at MOI 5. At days 2 and 6 p.i. one half of the cells in each replicate culture were used for isolating RNA. RNA quantity, purity and quality were determined and infection with TBEV was verified by qRT-PCR. Samples were sequenced on the Illumina HiSeq2000 platform and assembled contigs and raw read counts were used for data analysis. Differential expression contigs/transcripts were identified using DESeq in R and the $\log_2$ 2-fold and statistically significantly differentially-expressed contigs/transcripts were annotated.
The other half of the cells in each replicate culture was used for protein isolation at days 2 and 6 p.i.. Protein quantity and quality was determined and samples were in-gel digested prior to sequencing on the LTQ-Orbitrap-Velos-Pro mass spectrometer. Peptides were identified using SEQUEST algorithm and annotated by an integrated decoy approach against the UniProt-Arthropoda and *Flaviviridae* databases, and statistically significantly differentially-represented proteins were determined by X^2 test.

Cells were seeded 24 h prior to infection in 12 flat-sided tubes per cell line per time-point at a density of $2x10^6$ cells per tube for IRE/CTVM19 and $3x10^6$ cells per tube for IDE8. The next day, 6 replicate tubes per time-point per cell line were infected with TBEV-infected mouse brain suspension (2.5.2, 2.5.4) diluted to MOI 5, and 6 tubes were mock-infected with the same volume of similarly-diluted uninfected mouse brain suspension. At days 2 and 6 p.i. cells were harvested and the cell suspension from each replicate tube was split into two aliquots of 1 ml, both aliquots of cell suspension were pelleted by centrifugation at 400 x g for 5 min and washed with ice-cold PBS prior to isolation of either RNA (1^{st} aliquot) (2.4.7) or protein (2^{nd} aliquot) (2.8.1). By splitting the cell suspension, RNA and protein isolates could be matched and it was guaranteed that samples derived from the same tubes were used for both transcriptomic and proteomic experiments. Before samples were sent for sequencing they had to pass several quality checks.

The first quality check for RNA was done by measuring the amount and purity of RNA on a Nanodrop (2.4.8). However, since the 260/230 ratio, indicating phenol or ethanol contamination, was low (<1.4), samples were further purified using the RNeasy Mini kit (2.4.7) to remove these contaminations. After the second purification, RNA samples were used for verification of infection by qRT-PCR (2.4.10.2, 2.4.10.4) and for determining degradation using the Agilent Bioanalyzer (2.4.9). The amount of protein in samples was measured using the BCA protein assay (2.8.2), using BSA as standard, and the quality was tested by Coomassie staining of samples separated on SDS-PAGE (2.8.3, 2.8.4). Samples which failed any of the above quality checks were excluded from further analysis and only samples which passed both the RNA and protein check were used, so that RNA and proteins were derived from the same individual replicates. Equal amounts of RNA or protein from the same time-point and the same condition were pooled. RNA was sent for sequencing on the Illumina HiSeq2000 platform to ARK-Genomics, which is a sequencing facility at the Roslin Institute in Edinburgh, and the protein was first in-gel digested using trypsin (2.8.5) before being subjected to quantitative MS on the LTQ-Orbitrap-Velos-Pro mass spectrometer (Thermo Scientific). MS and analysis

was done by Dr. Margarita Villar Rayo at SaBio, the Instituto de Investigación en Recursos Cinegéticos, University of Castilla-La Mancha in Ciudad Real, Spain.

The remainders of each of the RNA and protein samples used for the above analyses were stored separately for, respectively, verifying sequencing data and 2D-DIGE (2.8.6).

4.3.1.1 Illumina sequencing protocol, transcriptome assembly and differential gene expression

The pooled RNA samples were prepared by ARK-Genomics according to the Truseq RNA sample guide 1500813 (Illumina Inc). A flowchart showing the steps of library preparation from pooled RNA samples to generation of assembled contigs and count data is depicted in Figure 4.3. In brief, poly(A) tail-containing mRNA molecules were purified from total RNA using poly-T oligo-attached magnetic beads. The resulting mRNA was fragmented, first and second strand were synthesised, ends repaired and adapters ligated. After PCR amplification of the prepared cDNA, the library was quantified, multiplexed and sequenced on the HiSeq2000 platform generating paired end reads of approximately 2 x 100 bp in length. The reads were sorted into samples according to cell line, time-point and treatment using the software CASAVA 1.8 (Illumina, https://support.illumina.com/sequencing/sequencing_software/casava.ilmn). Reads obtained from the *I. scapularis*-derived cell line IDE8 were mapped with TopHat 2.0.3 (Kim et al., 2013) against the reference genome (iscapularis.SUPERCONTIGS-Wikel.IscaW1.fa). Counts of reads mapping to the genome were generated with HTSeq count 0.5.3p9 (http://www-huber.embl.de/users/anders/HTSeq/doc/count.html). The unmapped reads were *de novo* assembled with CLC genomic workbench 5.1 (http://www.clcbio.com/products/clc-genomics-workbench/) and mapped with BWA 0.6.1 (Li & Durbin, 2009) against the mapped, filtered (5x 400b) reads for generating counts using a Perl script. The data was split into mapped and unmapped as the original mapping rates for half of the samples were very low and would not have yielded enough data for differential expression analysis. By combining the

sequencing reads which mapped to the reference genome with the sequencing reads which did not map it would have been possible to increase the assembly rate. However, augmentation of assembly is complex and was not done by ARK-Genomics since it was not part of the project specification. Since there is no reference genome available for *I. ricinus* and mapping of reads resulted in less than 30% mapping to the *I. scapularis* genome, it was decided, in consultation with ARK-Genomics, to *de novo* assemble the reads obtained for IRE/CTVM19 in the same way as for the unmapped reads in IDE8.

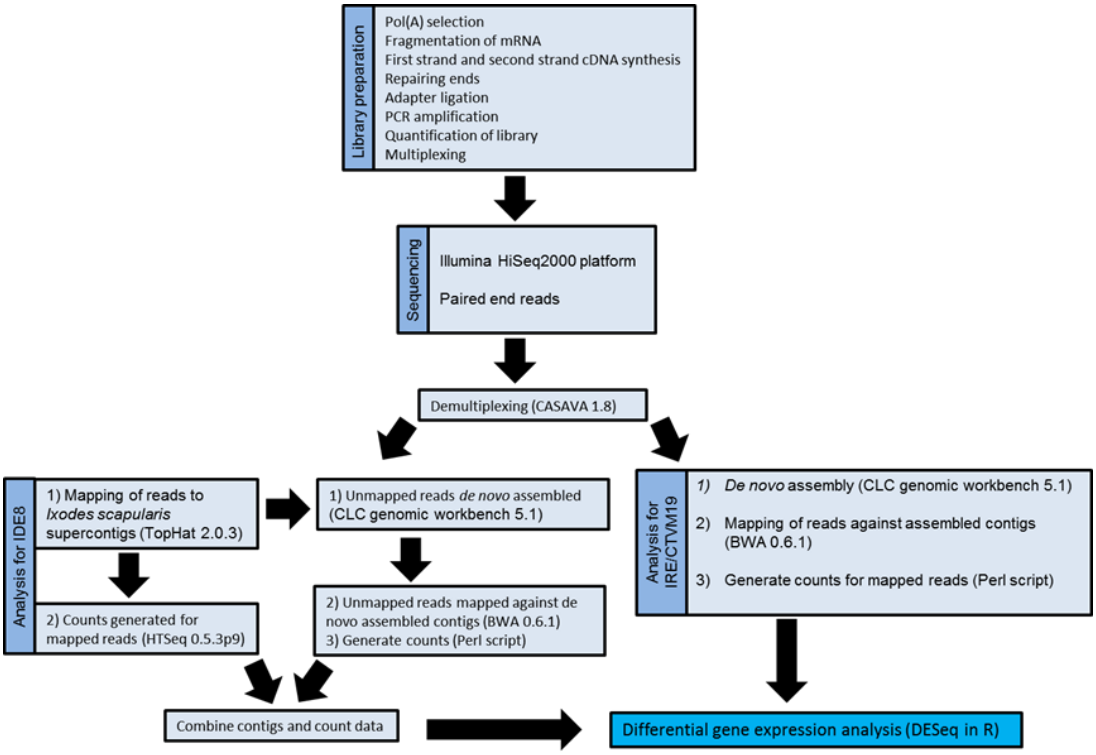

Figure 4.3 Flowchart of the library preparation, sequencing and bioinformatic analysis of RNA samples from infected and mock-infected IDE8 and IRE/CTVM19 cells

Pooled total RNA samples from infected and mock-infected IDE8 and IRE/CTVM19 cells were processed by ARK-Genomics. A library was prepared and samples were sequenced on the Illumina HiSeq2000 platform using a paired end RNA-Seq approach. After demultiplexing, IDE8 samples were mapped against the reference genome and read counts were generated. For those reads which did not map to the *I. scapularis* genome, contigs were *de novo* assembled and counts generated using a perl script by mapping to the *de novo* assembled contigs. In the case of IRE/CTVM19, reads were *de novo* assembled and mapped against the assembled contigs to generate counts using a perl script.The count and contig information for both mapped and *de novo* assembled IDE8 were combined and used for differential gene expression analysis using DESeq in R. Contig, and count data from IRE/CTVM19 were also analysed using DESeq in R.

Count data and a fasta file containing the assembled contigs/transcripts were provided by ARK-Genomics and used by me to determine differential gene expression analysis using DESeq in R (Anders & Huber, 2010). Since no biological replicates were used in this study, the DESeq script working without replicates was applied. The greater than $\log_2$ 2-fold, and statistically differentially expressed contigs/transcripts were annotated using Blast2GO (Conesa et al., 2005) and manually curated.

4.3.1.2 Quantitative MS, protein identification and differential representation

The pooled in-gel digested and desalted protein samples (2.8.5) were resuspended in 11 µl of 0.1% formic acid and analysed by reversed phase LC-MS/MS in an Easy-nLC II system coupled to an ion trap LTQ-Orbitrap-Velos-Pro mass spectrometer (Thermo Scientific, San Jose, CA, USA). The peptides were concentrated, on-line, by reverse phase chromatography using a 0.1 mm × 20 mm C18 RP precolumn (Thermo Scientific), and then separated using a 0.075 mm x 100 mm C18 RP column (Thermo Scientific) operating at 0.3 µl/min. Then peptides were eluted using a 180-min gradient from 5 to 40% solvent B (Solvent A: 0.1% formic acid in water, solvent B: 0.1% formic acid, 80% acetonitrile in water). ESI ionisation was done using a Nano-bore emitters Stainless Steel ID 30 µm (Thermo Scientific) interface. Peptides were detected in survey scans from 400 to 1600 atomic mass unit (amu, 1 µscan), followed by fifteen data-dependent MS/MS scans (Top 15), using an isolation width of 2 u (in mass-to-charge ratio units), normalised collision energy of 35%, and dynamic exclusion applied during 30 s periods. The peptides were identified from raw data using the SEQUEST algorithm (Proteome Discoverer 1.3, Thermo Scientific). Database search was performed against UniProt-Arthropoda.fasta and UniProt-*Flaviviridae*.fasta. The following constraints were used for the searches: tryptic cleavage after Arg and Lys, up to two missed cleavage sites, and tolerances of 10 ppm for precursor ions and 0.8 Da for MS/MS fragment ions and the searches were performed allowing optional methionine oxidation and cysteine

carbamidomethylation. Search was performed against a decoy database in an integrated decoy approach using false discovery rate (FDR) < 0.01.

Differential protein representation for individual proteins between different samples was determined using X^2 test statistics with Bonferroni correction in the IDEG6 software (http://telethon.bio.unipd.it/bioinfo/IDEG6 form/) ($p < 0.05$) (Popara et al., 2013). Samples with a p-value equal or lower than 0.05 were called as statistically significant.

4.4 Results

4.4.1 Quality checks prior to RNA and protein identification

4.4.1.1 RNA and protein quality

Before RNA and protein samples could be sent for sequencing the integrity of both was assessed on the Agilent Bioanalyzer for RNA and by SDS-PAGE and Coomassie staining for protein.

Total RNA was extracted from mock-infected and TBEV-infected IDE8 and IRE/CTVM19 cells at days 2 and 6 p.i. using TRI Reagent (2.4.7) and further purified using the RNeasy Mini kit (2.4.7). RNA samples were heat-denatured and 1 µl of each was then tested for the degree of degradation on the Bioanalyzer (2.4.9), which separates RNA fragments according to their size similarly to conventional gel electrophoresis. The Bioanalyzer software then calculates an RNA integrity number (RIN) taking the ratio of 28S to 18S ribosomal RNA (rRNA) and the entire electrophoretic trace into account (Schroeder et al., 2006). The results are then presented as a gel-like image (Figure 4.4 A) and an electropherogram (Figure 4.4 B).

An RIN could not be calculated by the Agilent software since all tick cell line samples showed only one peak at 42 seconds corresponding to the 18S rRNA peak of other eukaryotic species; there was no peak corresponding to 28S rRNA. Therefore RNA quality was assessed by looking for possible signs of degradation in the gel-like image and electropherogram (Figure 4.4). Several points in the electropherogram

(Figure 1.3) were used as indicators of degradation, such as a continuous shift towards shorter fragments, the height of the marker peak in comparison to the 18S rRNA peak and an uneven baseline (Schroeder et al., 2006). The samples which showed degradation were excluded from further analysis. In this example (Figure 4.4), samples 7 and 9 showed strong signs of degradation with partially or completely degraded 18S peaks at 42 s and a larger number of small degradation fragments between 25 and 40 s (Figure 4.4 B). All other samples presented in Figure 4.4, including sample 4 (Figure 4.4 B), showed strong and clear signals for 18S with almost no fragmentation.

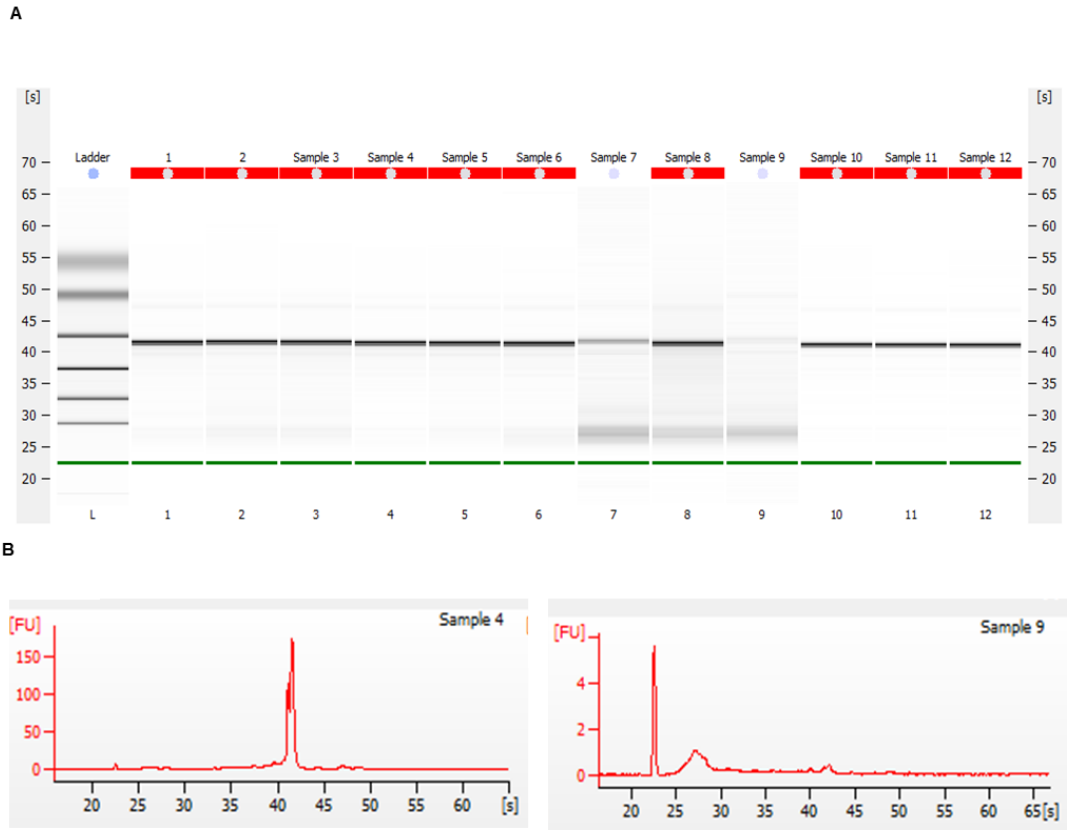

Figure 4.4 Examples of the gel-like image and electropherograms of total RNA generated by the Agilent Bioanalyzer.

Total RNA samples were run on the Agilent Bioanalyzer 2100 to assess the RNA integrity. (A) Gel-like image of RNA ladder and 12 RNA samples. Samples 7 and 9 showed degradation, all others showed no degradation. (B) Electropherograms of two RNA samples. The sample on the left is an example of intact tick cell RNA and the sample on the right is an example of degraded RNA.

All total RNA samples showing strong degradation like those seen for samples 7 and 9 were removed from further analysis. The corresponding protein samples were also excluded.

The soluble proteins, extracted with TritonX-100 in PBS, from mock-infected and TBEV-infected IDE8 and IRE/CTVM19 cells at days 2 and 6 p.i. were separated on a 12% polyacrylamide gel and stained with Coomassie (2.8.3, 2.8.4). Only those protein samples whose RNA passed the quality test are shown in Figure 4.5. Images were taken on the GelDoc XR system (BioRad).

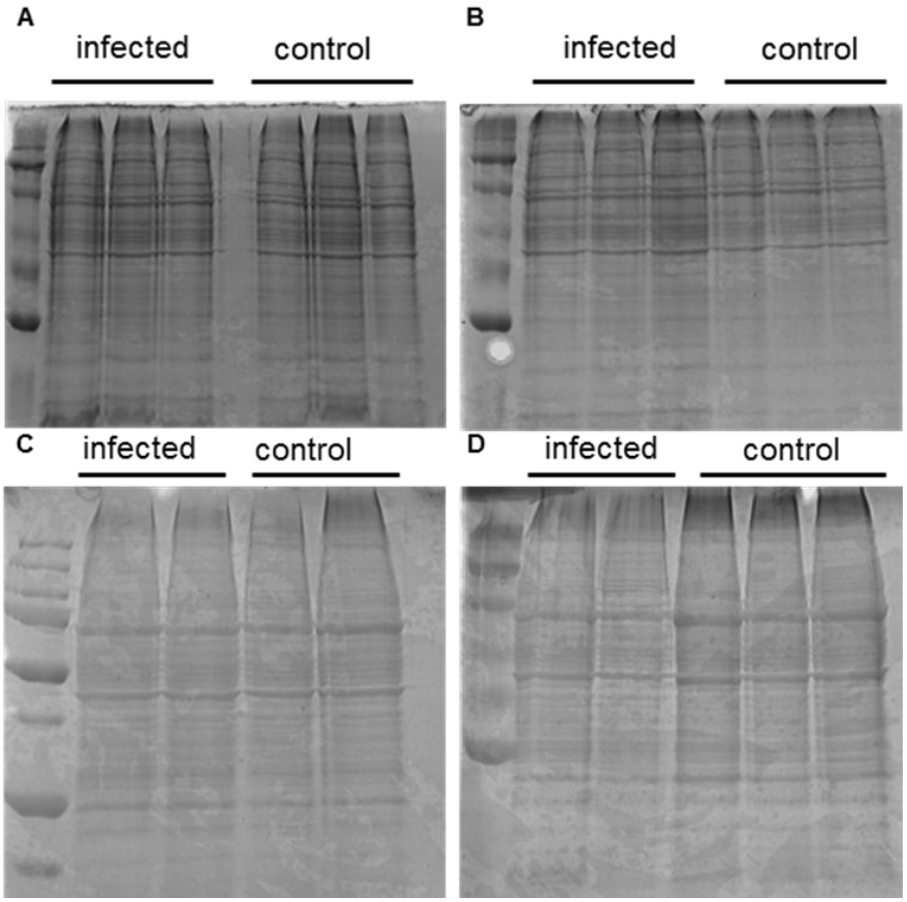

Figure 4.5 Gel images of total soluble proteins from tick cells.

Proteins, whose RNA passed the quality test, from TBEV-infected and mock-infected tick cells were separated on 12% SDS-PAGE and stained with Coomassie. Images were taken using a GelDoc XR system (BioRad). (A) IDE8 day 2 p.i. (B) IDE8 day 6 p.i. (C) IRE/CTVM19 day 2 p.i. (D) IRE/CTVM19 day 6 p.i. The term controls is used instead of mock-infected.

All tested protein samples from both tick cell lines showed good protein quality with clear, distinct bands and widely-distributed molecular masses (Figure 4.5).

4.4.1.2 Verification of infection

To test whether mock-infected and TBEV-infected IDE8 and IRE/CTVM19 cells were negative or positive for TBEV, 1 µg RNA of each sample was reverse-transcribed (2.4.10.2) and cDNA used for qPCR analysis (2.4.10.4) with primers detecting the NS5 sequence. Numbers of copies of NS5 were calculated using a standard curve generated with a linearised pJET-NS5 plasmid with NS5 insert and were normalised to 1 µg of total RNA. The limit of detection of the assay was determined by using the number of NS5 copies detectable in the highest dilution of the standard curve with a variance less than one threshold cycle (Ct; according to the qPCR application guide, 3rd edition, Integrated DNA Technologies) and normalising this to 1 µg of total RNA.

Some amplification occurred in all samples, whether TBEV-infected or mock-infected (Figure 4.6). Amplification in mock-infected tick cells, generally below the limit of detection, might be the result of primer dimers caused by nonspecific binding to tick genes, or the integration of viral sequences into the tick genome, as observed for flaviviruses in mosquito cells (Crochu et al., 2004). However, those mock-infected samples with readings corresponding to more than 360 copies, the limit of detection, were excluded from further analysis. All infected tick cell samples contained more than 10,000 copies of NS5. As expected, NS5 levels were generally higher at day 2 p.i. than at day 6 p.i. in infected IDE8, with the exception of sample 6 in which the opposite was the case (Figure 4.6 A). In IRE/CTVM19 however, two samples showed slightly higher NS5 copy numbers at 6 days compared to 2 days, two showed similar levels at both days and two showed slightly higher levels at 2 days compared to 6 days (Figure 4.6 B). However all samples in both cell lines were collected from separate tubes. Since all infected samples showed high NS5 copy numbers none of the infected samples were excluded.

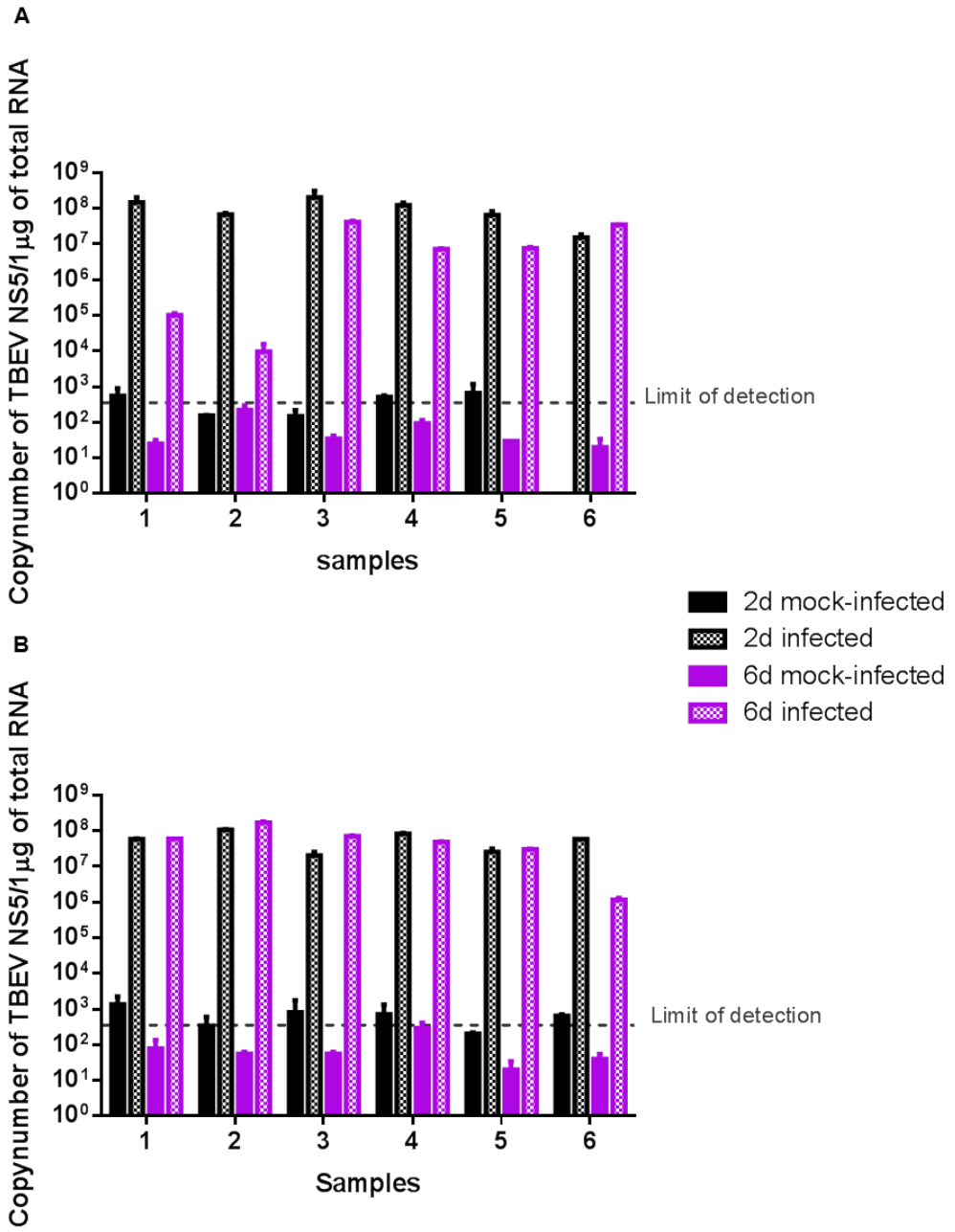

Figure 4.6 TBEV infection levels in mock-infected and infected tick cells.

Copynumbers of TBEV NS5 were determined by qRT-PCR using NS5 primers and the linearised plasmid pJET-NS5 to create a standard curve. Copy numbers were normalised to 1 µg of total RNA used for cDNA synthesis. The limit of detection was derived from the standard curve dilution series. The number of NS5 copies in the highest dilution still detectable with a variance of less than one Ct was normalised to 1 µg of total RNA used for cDNA synthesis. (A) IDE8 infected and mock-infected at day 2 and 6 p.i. (B) IRE/CTVM19 infected and mock-infected at day 2 and 6 p.i.. Error bars are standard deviations.

Overall, three samples each of days 2 and 6 infected IDE8, 6d mock-infected IDE8 and 6d infected and mock-infected IRE/CTVM19, and two samples each of 2d mock-infected IDE8 and infected and 2d mock-infected IRE/CTVM19 passed all quality checks (Table 4.2).

Table 4.2 Samples of infected and mock-infected IDE8 and IRE/CTVM19 cells which passed or failed quality checks

Colour code: pink indicates failure of quality check; blue indicates passing of quality check.

Sample 2d	Sample number	RNA purity	RNA quality	Level of infection
IDE8 infected	1			
IDE8 infected	2			
IDE8 infected	3			
IDE8 infected	4			
IDE8 infected	5			
IDE8 infected	6			
IDE8 mock-infected	1			
IDE8 mock-infected	2			
IDE8 mock-infected	3			
IDE8 mock-infected	4			
IDE8 mock-infected	5			
IRE/CTVM19 infected	1			
IRE/CTVM19 infected	2			
IRE/CTVM19 infected	3			
IRE/CTVM19 infected	4			
IRE/CTVM19 infected	5			
IRE/CTVM19 infected	6			
IRE/CTVM19 mock-infected	1			
IRE/CTVM19 mock-infected	2			
IRE/CTVM19 mock-infected	3			
IRE/CTVM19 mock-infected	4			
IRE/CTVM19 mock-infected	5			
IRE/CTVM19 mock-infected	6			

Samples 6d	Sample number	RNA purity	RNA quality	Level of infection
IDE8 infected	1			
IDE8 infected	2			
IDE8 infected	3			
IDE8 infected	4			
IDE8 infected	5			
IDE8 infected	6			
IDE8 mock-infected	1			
IDE8 mock-infected	2			
IDE8 mock-infected	3			
IDE8 mock-infected	4			
IDE8 mock-infected	5			
IDE8 mock-infected	6			
IRE/CTVM19 infected	1			
IRE/CTVM19 infected	2			
IRE/CTVM19 infected	3			
IRE/CTVM19 infected	4			
IRE/CTVM19 infected	5			
IRE/CTVM19 infected	6			
IRE/CTVM19 mock-infected	1			
IRE/CTVM19 mock-infected	2			
IRE/CTVM19 mock-infected	3			
IRE/CTVM19 mock-infected	4			
IRE/CTVM19 mock-infected	5			
IRE/CTVM19 mock-infected	6			

Aliquots of RNA samples and matching protein samples were pooled according to cell line and time-point and were sent for sequencing.

4.4.2 Sequencing of RNA transcripts

4.4.2.1 Data analysis

Pooled RNA samples were sent to ARK-Genomics for sequencing on the HiSeq2000 platform. A total of 2.6 - 4 $x10^7$ reads of approximately 100 bp in length were sequenced from both TBEV-infected and mock-infected IDE8 and IRE/CVTM19 cells (Table 4.3). For IDE8, between 44,474 and 44,907 contigs/transcripts (terms contigs and transcripts will be used interchangeably) were assembled with an average read length of 937 - 939 bp and an average of 607 - 760 copies. For IRE/CTVM19 cells, higher numbers of contigs/transcripts, 70,067 - 70,842, with a longer average read length of 1,086 - 1,092 bp were assembled in comparison to IDE8 cells. The average number of copies, 294 - 481, however was lower than for IDE8.

Table 4.3 Sequencing depth and assembly of RNA-Seq data from TBEV-infected and mock-infected IDE8 and IRE/CTVM19 cells

The term controls is used instead of mock-infected

Sample	Mean yield (bp) per lane	Mean reads per lane	Total number of contigs assembled	Mean copies per contig	Mean contig length
IDE8 control 2d	3.74E+09	3.71E+07	44562	679.24	938
IDE8 infected 2d	3.28E+09	3.25E+07	44907	760.73	937
IDE8 control 6d	3.21E+09	3.18E+07	44684	607.00	938
IDE8 infected 6d	2.99E+09	2.96E+07	44474	657.66	939
IRE/CTVM19 control 2d	3.06E+09	3.03E+07	70701	329.03	1087
IRE/CTVM19 infected 2d	2.72E+09	2.70E+07	70067	294.39	1092
IRE/CTVM19 control 6d	4.48E+09	4.44E+07	70842	481.29	1086
IRE/CTVM19 infected 6d	2.64E+09	2.61E+07	70273	294.07	1091

Using linear regression analysis to compare the transcript copy number to transcript length between infected and mock-infected cells, there was overall no difference between the length and transcript number distribution between infected and uninfected samples, with the exception of IRE/CTVM19 at day 2 p.i. However, all samples showed the same tendency towards a high abundance of longer transcripts

(linear regression: IDE8: infected 2d R^2=0.01361, mock-infected 2d R^2=0.00858, infected 6d R^2=0.01069, mock-infected 6d R^2=0.006611; IRE/CTVM19: infected 2d R^2=0.01801, mock-infected 2d R^2=0.04604, infected 6d R^2=0.008934, mock-infected 6d R^2=0.04428) and overall fewer transcripts in infected samples compared to controls.

4.4.2.2 Percentage of reads mapping to TBEV

The complete TBEV genome was *de novo* assembled by ARK-Genomics from reads derived from both infected cell lines at both time-points. Of the total number of reads generated for infected IDE8, 3.02% corresponded to the TBEV genome at day 2 p.i. and 2.84% aligned to TBEV at day 6 p.i.. In IRE/CTVM19 however, a higher percentage of reads, 7.70%, aligned to TBEV at day 6 p.i compared to 4.04% at day 2 p.i.. Overall, the proportion of reads mapping to the TBEV genome was higher in IRE/CTVM19 than in IDE8.

4.4.2.3 Differential gene expression analysis

The raw count data provided by ARK-Genomics for each transcript was used to determine differential gene expression between each of infected IDE8 and IRE/CTVM19 cells and their respective mock-infected controls at days 2 and 6 p.i. using DESeq (Anders & Huber, 2010) in R. DESeq normalises the count data by adjusting for different sequencing depth between samples and for the fact that a small number of highly expressed genes could claim a significant amount of the total sequence (Anders & Huber, 2010). Due to the lack of replicates, the script for working without replicates was used. In this approach dispersion was estimated across conditions and differential expression was determined using a negative binomial approach. Since the same transcripts were compared across different conditions, no adjustment for nucleotide composition and gene length was deemed necessary.

The histograms of the p-values generated with DESeq (Figure 4.7 A-D left panels) showed that only a small number of transcripts were statistically significantly

differentially expressed with a p-value lower than 0.05. The enrichment of p-values at the right hand side of the histogram corresponds to transcripts with very low counts which were given discrete values by DESeq. The scatter plots (Figure 4.7 A-D right panels) showed that although many of the transcripts were differentially expressed, only a few were statistically significant, marked in red, after multiple testing with Benjamin Hochberg procedure at a FDR of 10%. In IDE8 at both days 2 and 6 p.i. similar numbers of transcripts were statistically significantly differentially expressed with a FDR <5% but slightly more transcripts were more than $\log_2$ 2-fold differentially expressed at day 6 p.i. (Table 4.4). For IRE/CTVM19 approximately twice as many transcripts were statistically significantly differentially expressed and more than twice as many greater than $\log_2$ 2-fold differentially expressed compared to IDE8 (Table 4.4).

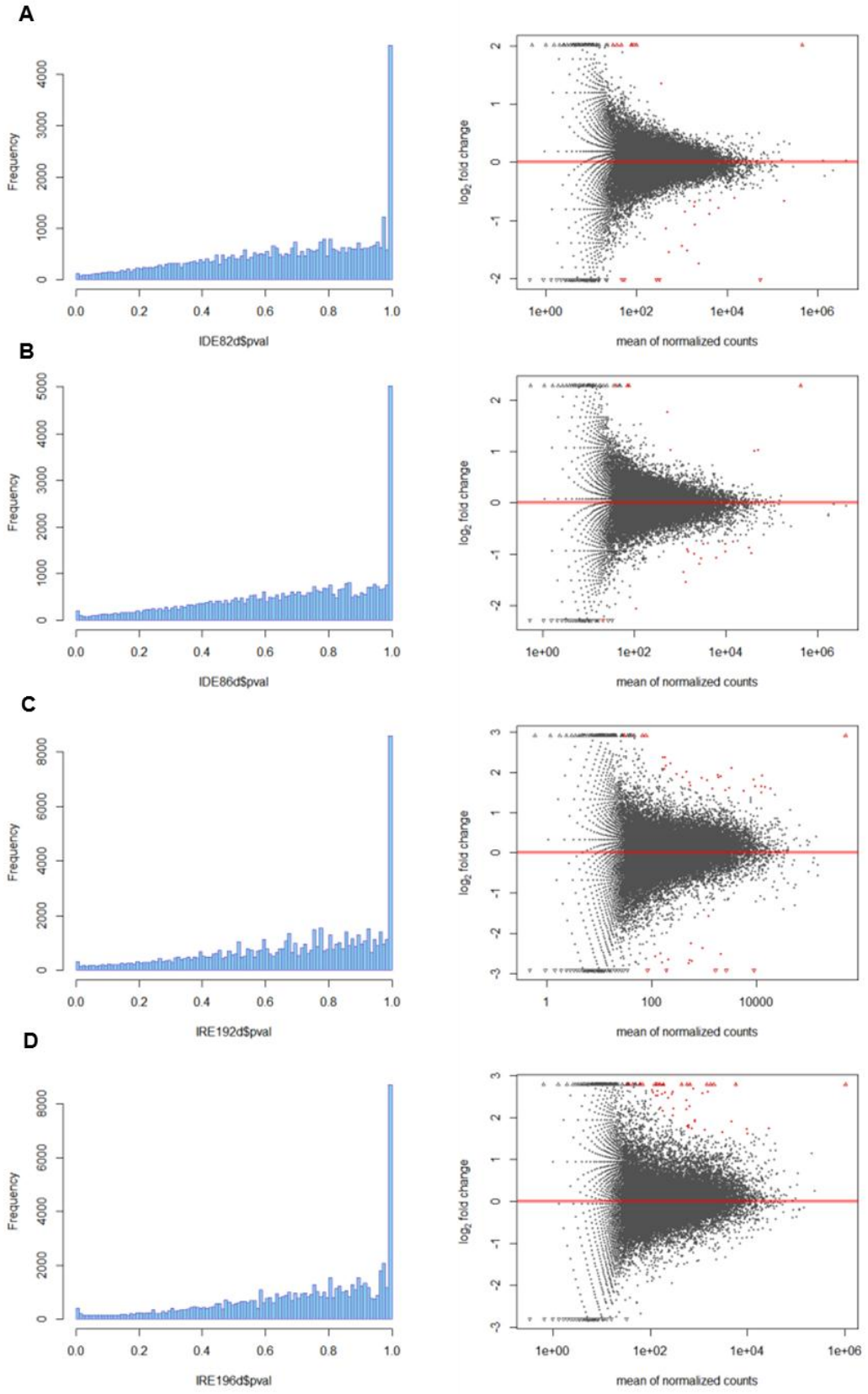
A
Frequency
IDE82d$pval
log2 fold change
mean of normalized counts
B
Frequency
IDE86d$pval
log2 fold change
mean of normalized counts
C
Frequency
IRE192d$pval
log2 fold change
mean of normalized counts
D
Frequency
IRE196d$pval
log2 fold change
mean of normalized counts

Figure 4.7 Testing for differential expression of mock-infected versus TBEV-infected tick cells.

Differential expression was determined for IDE8 at 2d p.i. (A) and 6d p.i. (B) and for IRE/CTVM19 at 2d p.i. (C) and 6d p.i. (D), compared to their respective mock-infected controls with DESeq. (A-D, left panel) Histogram of p-values plotted against their frequency in tick cells. (A-D, right panel) Scatter plot of $\log_2$ fold change versus normalised mean counts for the comparison of mock-infected versus infected cells. Transcripts on the red line are not differentially expressed. Transcripts which were statistically significantly differentially expressed at 10% FDR when Benjamin-Hochberg multiple testing adjustment was performed are marked in red.

Table 4.4 Number of transcripts differentially expressed upon TBEV infection of tick cell lines IDE8 and IRE/CTVM19

Cell line and time-point	>$\log_2$ 2-fold differentially expressed transcripts	Statistically significantly differentially expressed transcripts
IDE8 2d	385	22
IDE8 6d	449	21
IRE/CTVM19 2d	1973	40
IRE/CTVM19 6d	1771	43

Of those transcripts which were statistically significantly differentially expressed with FDR <5%, more transcripts were down-regulated than up-regulated in IDE8 at both time-points whereas the opposite was the case for IRE/CTVM19 (Table 4.5). In IRE/CTVM19 at day 6 p.i. only up-regulated transcripts were statistically significantly differentially expressed (Table 4.5, Figure 4.7).

Table 4.5 Number of statistically significantly expressed transcripts which were up- or down-regulated upon TBEV infection of tick cell lines IDE8 and IRE/CTVM19

Transcripts	IDE8		IRE/CTVM19	
	2d	6d	2d	6d
Up-regulated	7	7	24	43
Down-regulated	15	14	16	0
TOTAL	**22**	**21**	**40**	**43**

4.4.3 Protein identification

4.4.3.1 Data analysis

Pooled protein samples were analysed by MS and identified by searching against the arthropod and *flaviviridae* databases. The search against the arthropod database resulted in identification of 835 proteins in mock-infected and 762 in TBEV-infected IDE8 at day 2 p.i. For IRE/CTVM19 at day 2, 907 proteins were identified in mock-infected and 770 in TBEV-infected cells (Figure 4.8 A). A higher number of proteins were identified in IDE8 at day 6 p.i. compared to day 2, with 1133 for mock-infected and 1032 for TBEV-infected cells. Fewer proteins were found for IRE/CTVM19 at day 6 p.i. compared to day 2, with 824 in mock-infected and 725 in TBEV-infected cells. In both cell lines however, more proteins were identified in control cells compared to infected cells (Figure 4.8 A) hinting at a possible inhibitory effect of TBEV on protein expression. The number of peptides used for identification of each tick protein was similar in both cell lines for both time-points (Figure 4.8 B) indicating that the higher number of *I. scapularis* protein sequences compared to *I. ricinus* sequences in the arthropod database did not influence peptide/protein identification.

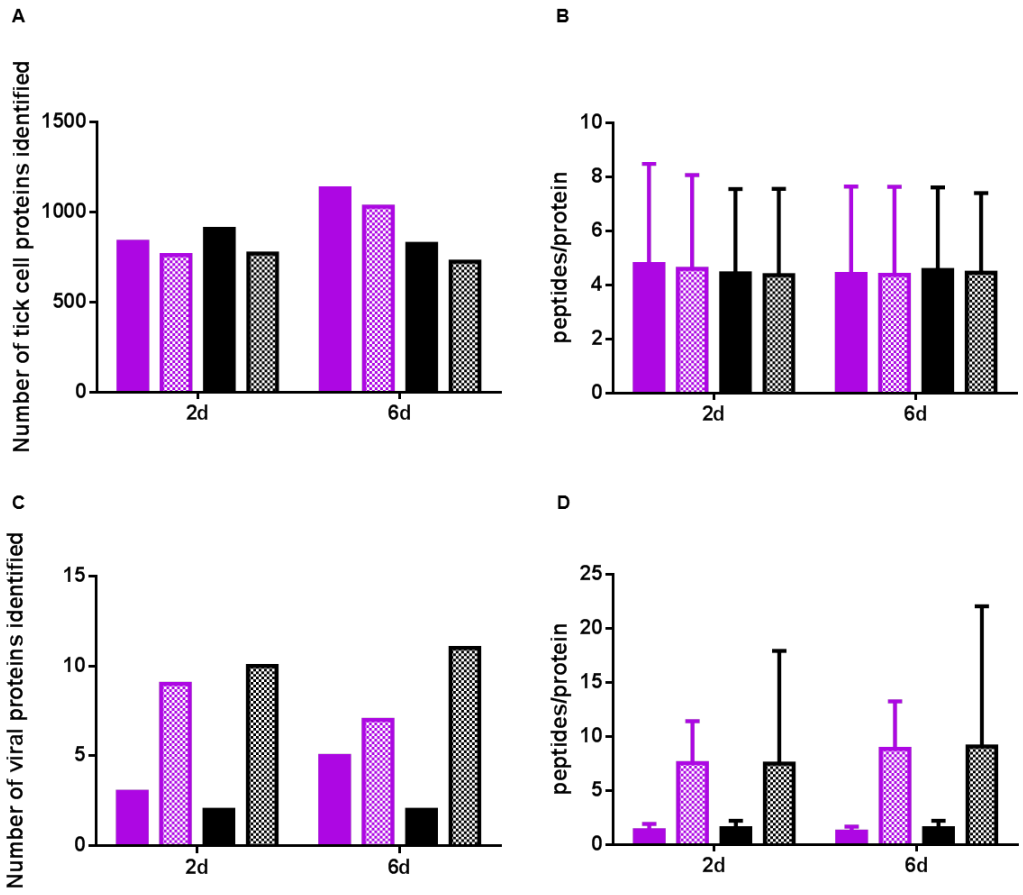

Figure 4.8 Total numbers of proteins identified and the number of peptides used for identification in tick cells.

Global proteomic analysis of mock-infected (pink) and TBEV-infected (pink hatched) IDE8 cells and mock-infected (black) and infected (black hatched) IRE/CTVM19 cells.
Left panel: number of tick cell proteins (A) and viral proteins (C) identified in tick cell lines at days 2 and 6 p.i.. Right panel: number of peptides used to identify each protein for tick cell (B) and viral (D) proteins. Data is presented as average of total peptides per protein and error bars indicate standard deviation.

In both mock-infected and TBEV-infected cells the search against the *flaviviridae* database resulted in hits for other flaviviral proteins (Figure 4.8 C,), but only infected cells were positive for TBEV. In mock-infected IDE8 cells at day 2 p.i. a single peptide was a homologue of TBEV polyprotein, whereas at day 6 p.i. one peptide each were homologues of Spondweni virus NS5 protein, DENV E protein and the polyprotein of Meaban virus. In IRE/CTVM19 at day 2 p.i. one peptide was a homologue of RdRp of Hepatitis C virus, whereas at day 6 p.i. one peptide was a homologue of the polyprotein of Hepatitis C virus. Only those proteins with more than one peptide hit were considered as correct whereas those with only one peptide

hit were considered false-positives, which might have resulted from the absence of the true peptide from the database or random matches in large datasets (Nesvizhskii & Aebersold, 2004). By setting the cut-off at a minimum of two peptides there is a significantly higher potential for these to be correct protein assignments (Carr et al., 2004).

Considering only those proteins with more than 1 peptide hit, only one viral protein apart from TBEV could be identified in both mock-infected and TBEV-infected cell lines, corresponding to the pestivirus bovine viral diarrhoea virus which is not known to be transmitted by ticks in nature but might have originated from the FCS used in the culture medium (Liu et al., 2012a). The number of peptides used for identification reflects the difference observed in the number of viral proteins identified in mock-infected and infected cells. Only an average of 2 peptides were positive for virus sequences in control cells, indicating the low number of viral proteins identified opposed to approximately 8 at day 2 and 10 to 13 at day 6 p.i. in infected cells (Figure 4.8 D).

From the total number of peptides, 1.64% and 1.7% corresponded to TBEV proteins in infected IDE8 at day 2 and 6 p.i. respectively. In infected IRE/CTVM19 compared to IDE8 slightly higher percentages of 1.94% at day 2 and 2.03% at day 6 corresponded to TBEV proteins.

4.4.3.2 Differential protein representation determined by MS

Protein levels in TBEV-infected cells determined by MS were compared to mock-infected cells considering only proteins with more than one peptide in at least one of the samples. A X^2 test with Bonferroni correction in IDEG6 software was then used to calculate which proteins were statistically significantly differentially represented.

The numbers of statistically significantly differentially represented proteins are shown in Table 4.6. In IDE8 cells a total of 52 proteins at day 2 and 24 at day 6 were differentially represented with the majority of proteins underrepresented at day 2 and slightly more overrepresented than underrepresented at day 6. The opposite was seen for IRE/CTVM19 cells: at day 2 fewer proteins were statistically significantly

differentially represented with equal numbers over- and underrepresented whereas a higher number of proteins were statistically significantly differentially represented at day 6 with more proteins underrepresented. Overall, more proteins were differentially represented in IRE/CTVM19 than in IDE8.

Table 4.6 Number of proteins differentially represented in tick cells upon TBEV infection

Total number of proteins	IDE8		IRE/CTVM19	
	2d	6d	2d	6d
overrepresented	20	14	10	24
underrepresented	32	10	10	85
TOTAL	**52**	**24**	**20**	**109**

4.4.3.3 Differential protein representation determined by DIGE

Replicate protein isolates from each of TBEV-infected and mock-infected IRE/CTVM19 cells on days 2 and 6 p.i. were pooled and split into three aliquots each, to generate technical replicates. Mock-infected and TBEV-infected cells were then labelled with either Cy5 (red) or Cy3 (green) dye in a randomised order and the pooled internal standard was labelled with Cy2 (blue). Labelled TBEV-infected, mock-infected and internal standards were run within the same gel. Thus in the present study six 2-D gels representing the three technical replicates for each of days 2 and 6, respectively, were run and evaluated for protein patterns by DeCyder software. Since the overlay of images taken from labelled mock-infected and TBEV-infected cells was practically the same at both time-points (Figure 4.9), no differentially represented proteins were identified by the DeCyder analysis. Three spots (marked by arrows in (Figure 4.9)) were visually different and only present in TBEV-infected cells, but normalisation against the internal standard, labelled with Cy2, masked the difference so that none of the proteins were identified as differentially represented by the DeCyder software. The lack of differentially expressed proteins was in contrast to the results obtained by quantitative MS analysis, where 20 and 109 proteins at days 2 and 6 respectively were statistically differentially represented.

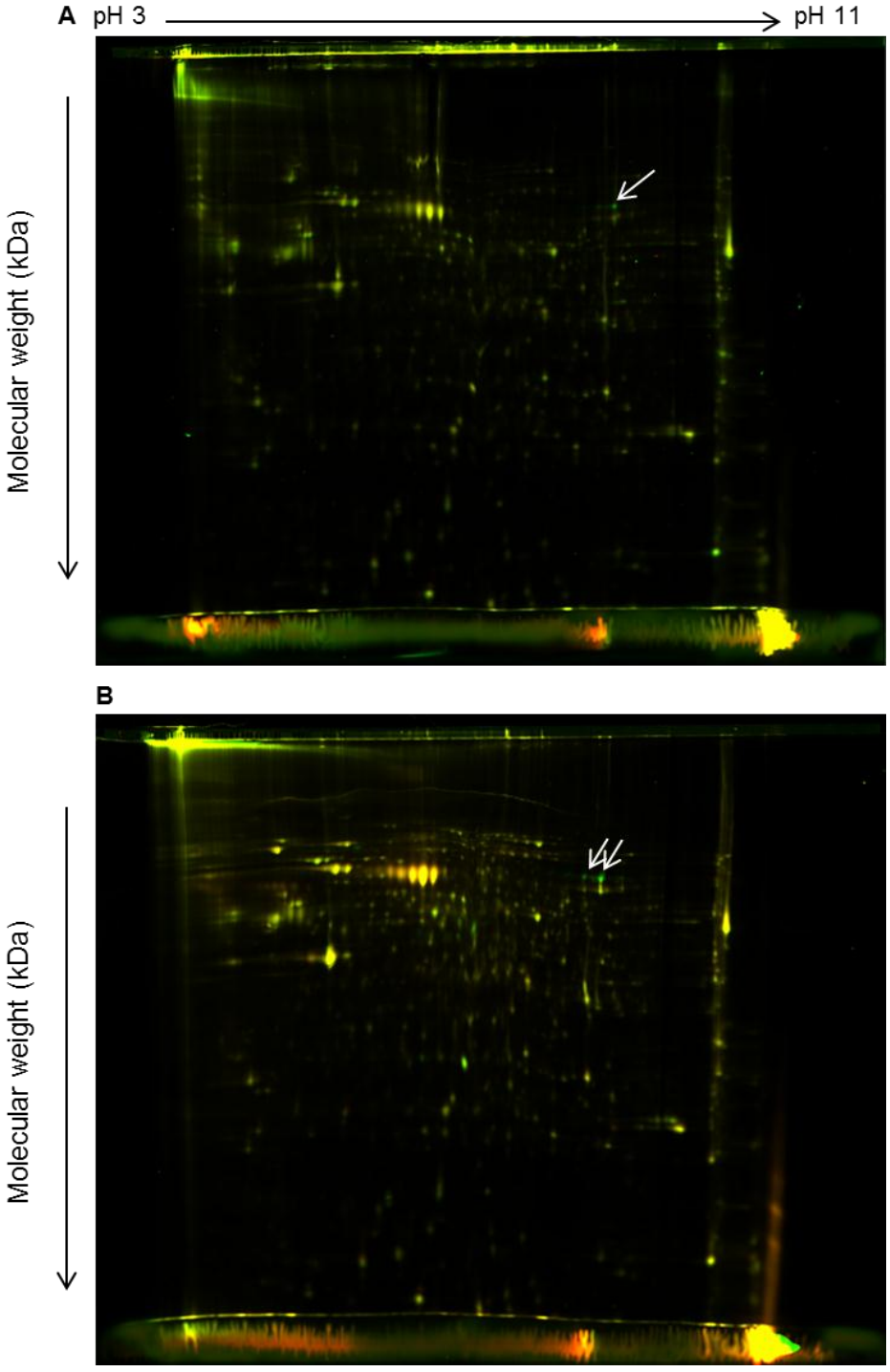

Figure 4.9 DIGE overlay images of proteins from infected and mock-infected IRE/CTVM19

Specific proteins for infected cells are represented in green (Cy3) whereas those of mock-infected cells are red (Cy5). The proteins present in both samples appear yellow. (A) IRE/CTVM19 at day 2 p.i. (B) IRE/CTVM19 at day 6 p.i. White arrows indicate proteins only present in infected cells.

4.4.4 Analysis and discussion of statistically significantly differentially expressed transcripts and represented proteins

4.4.4.1 Annotation and ontology of transcripts

Both contigs/transcripts which were more than $\log_2$ 2-fold differentially expressed, and those which were statistically significantly differentially expressed, were annotated. For a first rough annotation of sequences, the automatic annotation tool Blast2GO (Conesa et al., 2005) was used with a blastx algorithm against the NCBI (http://www.ncbi.nlm.nih.gov/) nr database at threshold of E-value < 10^{-6}. Results obtained for all sequences were then manually curated individually. Sequences which did not give any hits with Blast2GO were blasted again using the blastx and blastn algorithm against the NCBI protein and nucleotide databases and were included when they showed more than 50% coverage and more than 25% sequence similarity. All sequences obtained by Blast2GO and those obtained by manual blasting were additionally blasted against the UniProt/Swiss-Prot database and the *I. scapularis* database in VectorBase to retrieve ontology information, including those for conserved domains provided by NCBI or UniProt. For some transcripts, additional literature search was used to assign biological process groups. Since in total over 385 and 449 of the transcripts were more than $\log_2$ 2-fold differentially expressed in IDE8 cells at days 2 and 6 respectively, and even more in IRE/CTVM19 cells (1,973 at day 2 and 1,771 at day 6), further analysis focused only on those transcripts which were statistically significantly differentially expressed.

The majority of blast hits obtained for both IDE8 and IRE/CTVM19 corresponded to *I. scapularis* (Figure 4.10). For IRE/CTVM19 (Figure 4.10 B) however, a total of 83 contigs/transcripts were statistically significantly differentially expressed but only 54 corresponded to *I. scapularis*, two to TBEV and one each to *Rattus norvegicus* and the ant *Harpegnathos saltator*. The remaining contigs/transcripts did not return any blast hits. In IDE8 (Figure 4.10 A) all 43 transcripts had blast hits, with 32 corresponding to *I. scapularis* and two to TBEV, and 9 of the *de novo* assembled contigs/transcripts had highest similarity to rodent species.

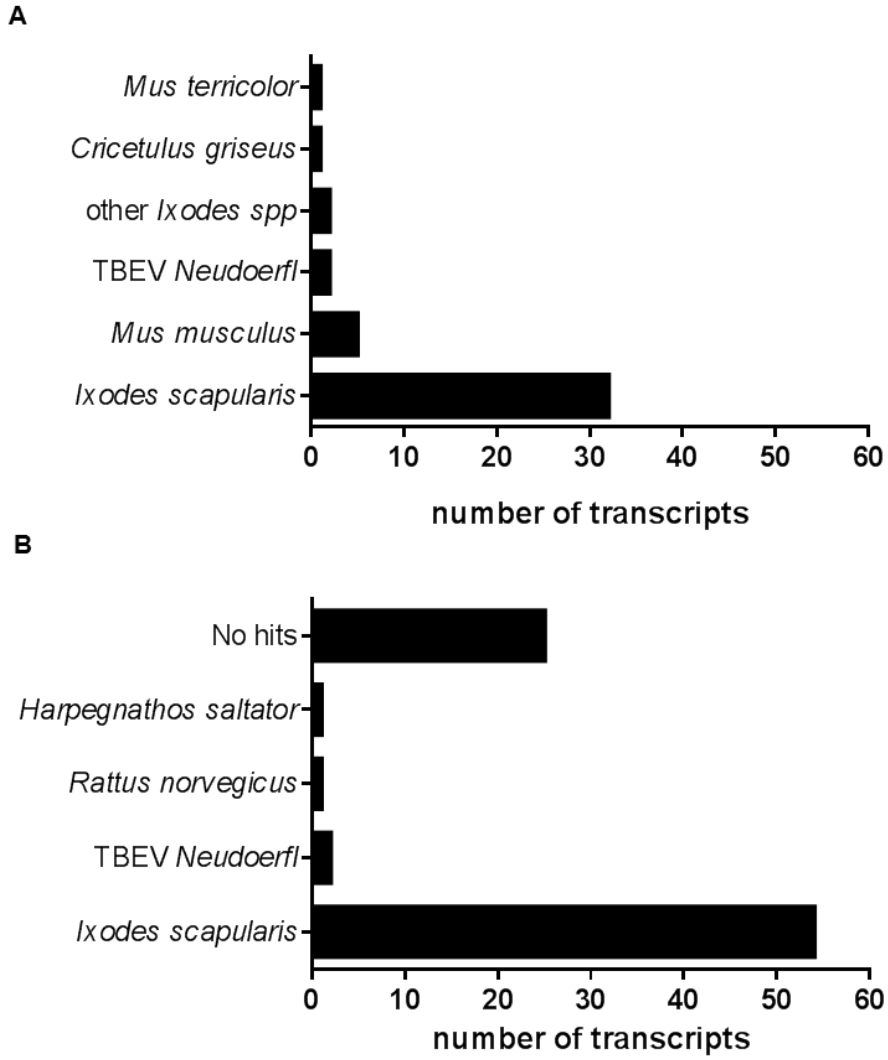

Figure 4.10 Blast hit species distribution for statistically significantly differentially expressed transcripts in TBEV-infected IDE8 and IRE/CTVM19 cells

The number of transcripts with blast hits for each species is shown on the x-axes for IDE8 (A) and IRE/CTVM19 (B). Transcript numbers include both time-points. Species to which the transcripts showed the highest homology are shown on the y-axes.

All transcripts which were statistically significantly differentially expressed are listed for IDE8 at days 2 (Table 4.7) and 6 (Table 4.8) p.i. and for IRE/CTVM19 at days 2 (Table 4.9) and 6 (Table 4.10) p.i.. The lists include information about gene ontology and were ranked according to their $\log_2$ fold change. Identified transcripts were allocated to functional classes; those belonging to nucleic acid processing, cell stress and immunity will be briefly discussed below.

The tick transcriptome is not fully annotated and annotation of transcripts, including inferrence of their possible function, relies in the majority of cases on sequence similiarity to other species rather than on experimental evidence for their true functional role in ticks. Ticks are quite evolutionarily distant from other well-annotated species, such as mammals and insect vectors (Figure 1.5); thus although homology is observed for a specific transcript, it might have evolved different functions within the organism. The lack of experimental evidence, the incomplete data annotation, and naming transcripts/proteins according to their closest homologue might be misleading and makes it difficult to infer the true biological role of a transcript/ protein based on literature search and conserved domains. Currently, to identify possible target genes within large datasets of ticks and other non-model organisms, the only mehod is to infer biological function from other better annotated organisms or from sequence similiarity to other model or non-model organisms.

In both cell lines at both time-points the most abundant transcript coded for the TBEV polyprotein.

For IDE8 only seven transcripts were up-regulated on each of days 2 (Table 4.7) and 6 (Table 4.8) p.i., whereas the majority were down-regulated. At both days, transcripts with unknown function included hypothetical proteins or those with the highest similarity to EST but no other blast hit, and thus could not be ontologically classified. At day 2, five of the up-regulated transcripts were involved in energy metabolism, more specifically in the oxidative phosphorylation system of the respiratory chain which is responsible for generating the cell's energy in the form of ATP. Only two transcripts involved in this mechanism were differentially expressed at day 6, with one up-regulated (cytochrome c oxidase) and the other down-regulated (NADH-ubiquinone oxidoreductase). Interestingly genes involved in transportation such as an ABC transporter and the phosphofurin acidic cluster sorting protein (PACS) were up-regulated. ABC transporters belong to a large superfamily of mostly integral membrane proteins involved in transportation of a broad spectrum of substrates, but they are of special interest in insects and ticks due to their role in pesticide resistance (Broehan et al., 2013; Pohl et al., 2012). PACS has an indirect transport function and directs proteins towards the TGN, including the endoprotease

furin (Wan et al., 1998) which plays a role in the maturation process of TBEV (Stadler et al., 1997). PACS might thus be indirectly involved in TBEV maturation. Another interesting observation was that the majority of down-regulated transcripts at day 2 p.i. were involved in cell stress or nucleic acid processing whereas none of the transcripts at day 6 p.i. were involved in cell stress. At day 6 p.i. down-regulated genes included those involved in nucleic acid processing, lipid metabolism (fatty acid synthase, Ipla2-eta, Mid1 interacting protein, insulin induced protein (INSIG)) or signal transduction.

Table 4.7 Statistically significantly differentially expressed transcripts in TBEV-infected IDE8 cells at day 2 p.i.

Annotated genes, including their log_2 fold change, their p-values after multiple testing and their ontology: CA (cell adhesion), CS (cell stress), IM (immunity), M (metabolism), NAP (nuclecic acid processing), PF (protein folding), UK (unknown), V (virus). All transcripts annotated as *I. scapularis* are indicated by vectorbase accession number ISCW, all others are marked by Uniprot or NCBI accession numbers. Padj refers to adjusted p-value.

IDE8 2d transcript/ protein	Annotation	log_2 fold up/down regulation	Padj	Ontology
P14336	TBEV polyprotein	11.01	0.00E+00	V
Q4JFN6	nadh dehydrogenase subunit 1	3.28	1.84E-02	M
Q7JCZ1	cytochrome c oxidase subunit II	3.17	2.22E-06	M
Q7JCX7	cytochrome c oxidase subunit III (mitochondrion)	2.68	1.73E-04	M
B2L0P2	atp synthase f0 subunit 6	2.53	1.22E-04	M
Q9MD68	cytochrome c oxidase subunit I	2.39	8.78E-05	M
ISCW023721-RA	cd36 antigen	1.36	1.73E-04	IM,CA
ISCW024057-RA	HSP70	-5.87	6.68E-219	CS, PF
ISCW015267-RA	heat shock protein (HSP70)	-2.87	5.45E-18	CS, PF
ISCW014572-RA	alternative splicing factor SRp20/9G8	-2.55	2.55E-02	NAP
ISCW001763-RA	heat shock HSP20 protein	-2.25	6.43E-13	CS, PF
ISCW024910-RA	heat shock protein (HSP70)	-1.75	2.74E-20	CS, PF
ISCW015266-RA	heat shock HSP20 protein	-1.55	2.98E-08	CS, PF
ISCW021730-RA	histone H2B	-1.52	1.17E-12	NAP
ISCW019498-RA	histone H4	-1.44	3.33E-10	NAP
ISCW002513-RA	alpha-crystallin B chain	-1.14	2.67E-03	CS, PF
ISCW012234-RA	histone	-1.07	2.39E-06	NAP
ISCW024295-RA	secreted protein	-0.89	8.78E-05	UK
ISCW024054-RA	heat shock protein 20	-0.85	1.07E-02	CS,PF
ISCW015615-RA	60S ribosomal protein L9	-0.78	1.29E-03	NAP
ISCW016597	hypothetical protein	-0.75	2.10E-02	UK
JN018404.1	28S ribosomal RNA	-0.67	1.51E-02	NAP

Lipid metabolism is essential for enveloped viruses replicating in the cytoplasm, not only for virus entry and budding but also for virus replication; extensive ultrastructural changes are induced in host membranes to provide a platform for virus replication and possibly assist in evading host immune responses. DENV leads to

strong alterations in the fatty acid metabolism of mosquito cells (Perera et al., 2012) and inhibition of fatty acid synthase strongly inhibits virus replication. Down-regulation of transcripts of fatty acid metabolism could be a cellular immune response attempting to down-regulate TBEV replication. However INSIG, which is indirectly involved in cholesterol synthesis as feedback control in mammalian cells, is also down-regulated which would lead to higher cholesterol synthesis supporting viral replication which is the case for WNV (Mackenzie, Khromykh & Parton, 2007). A recent study in *R. microplus* has shown that fungal infection resulted in alterations in the lipid metabolism including triacylglycerol and cholesterol (Angelo et al., 2013); however there is no knowledge about the influence of virus infection on lipid metabolism in ticks.

Table 4.8 Statistically significantly differentially expressed transcripts in TBEV-infected IDE8 cells at day 6 p.i.

Annotated transcripts, including their log_2 fold change, their p-values after multiple testing and their ontology: CA (cell adhesion), D (Development), IM (immunity), M (metabolism), NAP (nucleic acid processing), PR (proteolysis), SI (signal transduction), T (transport), UK (unknown), V (virus). All transcripts with VectorBase accession number starting with ISCW annotated as *I. scapularis*, all others are marked by UniProt or NCBI accession numbers. Padj refers to adjusted p-value.; EST= expressed sequence tag

IDE8 6d transcript/ protein	Annotation	log_2 fold up/down regulation	Padj	Ontology
P14336	TBEV polyprotein	13.53	0.00E+00	V
Q9MD68	cytochrome c oxidase subunit I	2.80	3.13E-03	M
ISCW016537-RA	transcription factor hes-1, putative	2.35	2.40E-02	NAP, D
ISCW023721-RA	cd36 antigen	1.78	1.01E-07	IM, CA
ISCW000475-RA	phosphofurin acidic cluster sorting protein 1	1.03	1.42E-04	T
EW897892.1	EST	1.03	4.91E-02	UK
ISCW006658-RA	ABC transporter	1.02	1.43E-04	M, T
ISCW020114-RA	cyclic nucleotide phosphodiesterase	-2.06	1.35E-02	SI
ISCW021730	histone H2B	-1.54	1.91E-08	NAP
G5BSF6	histone H4	-1.35	7.52E-06	NAP
ISCW001223-RA	mid1-interacting protein	-1.19	2.30E-05	M
EW890810.1	EST	-1.08	2.16E-04	UK
ISCW023537-RA	insulin induced protein	-1.06	1.42E-04	M
EW831219.1	EST	-0.99	4.00E-03	UK
ISCW009053-RA	fatty acid synthase	-0.98	4.41E-04	M
ISCW015615-RA	60S ribosomal protein L9	-0.95	1.54E-03	NAP
ISCW017608-RA	Ipla2-eta	-0.94	1.90E-02	M
ISCW012234-RA	histone, putative	-0.90	4.75E-02	NAP
ISCW004002-RA	longipain	-0.87	6.27E-03	IM, PR
Q8HQI4	NADH-ubiquinone oxidoreductase chain 5	-0.79	4.91E-02	M

In contrast to IDE8, the majority of transcripts in IRE/CTVM19 cells were up-regulated at day 2 p.i. (Table 1.8), and all 43 differentially expressed transcripts were up-regulated at day 6 p.i. (Table 1.9). Of the 40 and 43 transcripts differentially expressed at days 2 and 6 respectively, 10 and 15 contigs respectively could not be annotated, since blast searches returned no hits of suitable homology and they are

thus not included in the lists. At both days several transcripts, 13 at day 2 and 9 at day 6, could not be classified ontologically and are listed with function unknown. Of those down-regulated transcripts at day 2 p.i. to which a biological process could be allocated, the majority were involved in cell stress and protein folding as observed for IDE8 at the same time-point; only one transcript possibly involved in cell stress was up-regulated at day 6 p.i.. Two transcripts involved in cell structure were differentially expressed at day 2 p.i. (Table 4.9) but none at day 6. These were the down-regulated Nesprin-1, which is a giant actin binding protein localised at the outer nuclear envelope (Zhang et al., 2002), and the highly up-regulated glial fibrillary acidic protein (GFAP) which is the main intermediate filament protein in vertebrate astrocytes. GFAP-like proteins have been identified in other arthropods such as the silk moth (Kumar, Maida & Keil, 1996) and crab (Florim da Silva et al., 2004). Interestingly, overexpression of GFAP protected a rat neuronal cell line from apoptosis induced by heat stress (Sugaya-Fukasawa et al., 2011), suggesting that upregulation of GFAP in tick cells upon virus infection could be a protective response.

Transcripts up-regulated at day 2 p.i. (Table 4.9) were involved in immunity, cell stress, protein folding, energy metabolism (ATP synthase), carbohydrate metabolism (arylsufatase B), sulphate metabolism (sulfotransferase), transport (GABA transporter) and cell adhesion (fasciclin). Fasciclin is a cell adhesion protein with varied structures in different species and thus probably different functions. Fasciclin was up-regulated upon *Plasmodium* infection of mosquitoes (Vlachou et al., 2005) and bacterial infection in molluscs; in the latter study the authors hypothesised that the cell adhesion protein might have a role in innate immunity (Premachandra et al., 2013). Only one transcript involved in nucleic acid processing was up-regulated at day 2, whereas 6 were up-regulated at day 6 p.i. (Table 4.10) and will be further explained below in 4.4.4.2. The biological process groups of the other up-regulated transcripts at day 6 included immunity, cell stress, proteolysis, signalling (calcitonin receptor, LIN-12), transport (sulphate/bicarbonate/oxalate exchanger SAT-1), metabolism (maltase-glucoamylase, hypothetical protein (chitin metabolism),

secreted mucin (mucin (MUC) 17) and cell adhesion (Ig-like C2 type domain containing protein, hypothetical protein).

Interestingly several transcripts involved in the notch signalling patway, which is a highly conserved pathway important for intercellular signalling during cell fate decisions (Bray, 2006; Kimble & Simpson, 1997; Kurth et al., 2011), were up-regulated in the present study (Table 4.12). These were the notch receptor ortholog, LIN-12 isolated from *C. elegans*, the recombinant binding protein suppressor of hairless which either acts as activator or suppressor of LIN-12 in the presence of different coactivators or repressors, and the downstream target, hairy enhancer of split (hes) -1, a transcriptional repressor during cell fate decision (Bray, 2006; Fortini & Artavanis-Tsakonas, 1994; Kimble & Simpson, 1997; Kurth et al., 2011; Maier et al., 2011). In vertebrates the notch pathway has been implicated in regulating immune cell development and function, including those of cells of the adaptive and innate immune system (Osborne & Miele, 1999; Radtke, MacDonald & Tacchini-Cottier, 2013). Notch signalling in *Drosophila* is involved in haematopoeisis (Duvic et al., 2002; Lebestky, Jung & Banerjee, 2003), and fungal infection results in down-regulation which might allow progenitor cells to differentiate into immune effector molecules, implying crosstalk between the innate immune system and haematopoeisis mediated by notch signalling (Jin et al., 2009). The role of notch signalling in ticks in the development of haemocytes, which are involved in the cellular defence response, has not yet been examined.

Table 4.9 Statistically significantly differentially expressed transcripts in TBEV-infected IRE/CTVM19 cells at day 2 p.i.

Annotated transcripts, including their log_2 fold change, their p-values after multiple testing and their ontology: CA (cell adhesion), CS (cell stress), D (development), IM (immunity), M (metabolism), NAP (nucleic acid processing), PF (protein folding), PR (proteolysis), SI (signal transduction), ST (structural), T (transport), UK (unknown), V (virus). All transcripts with VectorBase accession number starting with ISCW annotated as *I. scapularis*, all others are marked by UniProt or NCBI accession numbers. Padj refers to adjusted p-value. EST=expressed sequence tag

IRE/CTVM19 2d Transcript/ protein	Annotation	log_2 fold up/down regulation	Padj	Ontology
P14336	TBEV polyprotein	12.49	2.85E-100	V
P03995	glial fibrillary acidic protein	6.30	3.46E-03	ST
Q66HI5	Fth1 protein	5.48	3.39E-03	IM, T, M
ISCW020299-RA	translation elongation factor EF-1 alpha/Tu	4.12	3.92E-04	NAP
Q7JCY9	ATPase subunit 6	3.30	2.86E-02	M, T
ISCW019955-RA	arylsulfatase B, putative	2.38	2.04E-02	M
ISCW020517 -RA	hypothetical protein	2.37	1.61E-02	UK
ISCW013094-RA	GABA transporter, putative	2.22	1.78E-02	T
ISCW000525-RA	secreted salivary gland peptide, putative	2.17	4.56E-02	UK
ISCW000297-RA	hypothetical protein	2.12	1.98E-04	UK
ISCW000868-RA	sulfotransferase	1.96	3.94E-02	M
ISCW008209-RA	hebreain	1.92	1.28E-03	IM
ISCW008185-RA	hypothetical protein	1.65	1.88E-02	UK
ISCW022766-RA	tumor rejection antigen (gp96)	1.65	1.88E-02	CS, IM,PF
ISCW008184-RA	calreticulin	1.63	2.04E-02	IM, CS,PF
ISCW001537 -RA	hypothetical protein	1.62	3.26E-02	UK
ISCW001538-RA	fasciclin	1.59	3.08E-02	CA
ISCW017179-RA	hypothetical protein	-2.24	9.18E-04	UK
EW936362.1	EST	-2.35	7.28E-05	UK
EFN84144.1	Nesprin-1	-2.50	2.04E-02	ST
ISCW024062-RA	heat shock HSP20 protein, putative	-2.51	2.43E-06	CS,PF
EW851229.1	EST	-2.65	1.46E-05	UK
EW962970.1	EST	-2.68	7.61E-06	UK
EW962971.1	EST	-2.68	7.61E-06	UK
ISCW010354 -RA	hyopthetical protein	-2.72	3.46E-03	UK
ISCW009537-RA	hypothetical protein	-2.74	7.61E-06	UK
ISCW015266-RA	heat shock HSP20 protein, putative	-3.17	4.67E-11	CS,PF

ISCW024474-RA	hypothetical protein	-3.19	1.61E-02	UK
ISCW024910-RA	HSP70	-3.21	6.75E-12	CS,PF
ISCW001763-RA	heat shock HSP20 protein, putative	-3.63	1.61E-13	CS,PF

The two immunoglobulin (Ig) domain-containing proteins, Ig-like C2-type domain-containing protein and the hypothetical protein ISCW013496, are both involved in cell adhesion according to the UniProt database. However, proteins with Ig-like domains can serve in many biological processes such as signalling, molecular recognition, immunity and cell adhesion as reviewed in several articles (Cannon et al., 2010; Johansson, 1999; Watson et al., 2005). A role of these proteins in immunity or other processes such as signalling in addition to cell adhesion can therefore not be excluded.

Table 4.10 Statistically significantly differentially expressed transcripts in TBEV-infected IRE/CTVM19 cells at day 6 p.i.

Annotated transcripts, including their log_2 fold change, their p-values after multiple testing and their ontology: CA (cell adhesion), CS (cell stress), D (development), IM (immunity), M (metabolism), NAP (nucleic acid processing), PR (proteolysis), SI (signal transduction), T (transport), UK (unknown), V (virus). All transcripts with VectorBase accession number starting with ISCW annotated as *I. scapularis*, all others are marked by UniProt or NCBI accession numbers. Padj refers to adjusted p-value. EST= expressed sequence tag

IRE/CTVM19 6d transcript/ protein	Annotation	log_2 fold up/down regulation	Padj	Ontology
P14336	TBEV polyprotein	13.81	1.59E-99	V
ISCW016537-RA	transcription factor hes-1	5.62	2.14E-25	NAP, D
ISCW020299-RA	translation elongation factor EF-1 alpha/Tu	4.74	1.33E-02	NAP
ISCW022022-RA	hypothetical protein	4.66	3.81E-03	UK
ISCW022021-RA	complement Factor H	4.53	3.45E-09	IM
ISCW022024-RA	hypothetical protein	4.18	1.33E-07	UK
ISCW011174-RA	coagulation factor precursor	4.00	1.13E-06	IM, PR
ISCW007552-RA	peroxinectin, putative	3.88	2.60E-13	CS, IM,CA
ISCW012970-RA	calcitonin receptor	3.31	1.45E-02	SI, M
ISCW006166-RA	trypsin, putative	3.29	8.58E-10	IM, PR
ISCW010197-RA	recombining binding protein suppressor of hairless	3.03	1.04E-08	NAP, D
ISCW003918-RA	conserved hypothetical protein	2.97	2.94E-04	UK
ISCW019766-RA	sulfate/bicarbonate/oxalate exchanger SAT-1	2.69	1.25E-05	T
EW832916.1	EST	2.67	2.98E-02	UK
ISCW016540-RA	transcription factor hes-1	2.62	8.83E-06	NAP, D
ISCW024120-RA	hypothetical protein	2.61	2.65E-03	M
ISCW000348-RA	secreted mucin MUC17	2.59	1.54E-05	M
ISCW011409-RA	IG-like C2-type domain-containing protein	2.57	1.02E-03	CA
ISCW012081-RA	maltase-glucoamylase	2.53	2.91E-02	M
ISCW007469-RA	hypothetical protein	2.48	3.74E-03	UK
ISCW013496-RA	hypothetical protein	2.42	5.25E-04	CA
ISCW010756-RA	hypothetical protein	2.29	1.23E-03	UK
ISCW019498-RA	histone H4, putative	2.22	1.36E-02	NAP
ISCW016870-RA	hypothetical protein	2.21	3.56E-03	UK
ISCW023076-RA	ribosomal protein L3	2.06	4.28E-02	NAP
ISCW013895-RA	hypothetical protein	1.91	2.46E-02	UK
EW789829.1	EST	1.91	9.18E-03	UK
ISCW007213-RA	LIN-12 protein	1.75	3.02E-02	SI, D

4.4.4.2 Nucleic acid processing

Transcripts in this category are involved in nucleic acid replication, transcription, processing and translation. Although this group of transcripts was found to be differentially regulated in several transcriptome studies in mosquitoes (Bartholomay et al., 2004; Colpitts et al., 2011a; Sim, Ramirez & Dimopoulos, 2012) and ticks (Heekin et al., 2013) it is not known if they have any immunological function. For histones, however, it is known that several viral proteins target histone proteins and host chromatin to interfere with host gene expression by various mechanisms and for different purposes (Wei & Zhou, 2010). The C protein of DENV targets core histones during infection disrupting the host cell genetic machinery in favour of viral replication (Colpitts et al., 2011b). The suppressor of hairless and the hes-1 are, as mentioned above, involved in the LIN-12/Notch signalling pathway. Interestingly all of the components were highly up-regulated at day 6 p.i. in IRE/CTVM19 (Table 4.12) cells but their role in virus infected arthropod cells has not been documented. Another interesting transcript is the elongation factor (EF) -1 alpha/Tu which was highly up-regulated at both days in IRE/CTVM19. EF-1 alpha has been previously shown to be up-regulated and to be an important host cell factor for virus replication during DENV or WNV infection in mammalian and mosquito cells (Blackwell & Brinton, 1997; Davis et al., 2007; Pattanakitsakul et al., 2007). In this context, EF-1 alpha might also be involved in TBEV replication in tick cells.

4.4.4.3 Cell stress and immunity

Only two transcripts possibly involved in immunity were differentially expressed in IDE8 (Table 4.11); these include the cysteine protease longipain and the class B scavenger receptor CD36. Longipain, which was found to be localised in and on the surface of lysosomes in the midgut of the tick *H. longicornis* was shown to not only be involved in blood digestion but also dose-dependently kill *Babesia* parasites (Tsuji et al., 2008). Although longipain showed high homology to cathepsin B, the pH and temperature preference against cathepsin B substrates was different and the authors suggested longipain to be midgut-specific. It is not clear if longipain may,

like cathepsin B, be indirectly involved in the immune response against viruses by triggering apoptosis as observed during DENV infection in mosquitoes (Sim, Ramirez & Dimopoulos, 2012), and/or through activation of TLRs 7 and 9 (Ewald et al., 2008; Matsumoto et al., 2008; Park et al., 2008). CD36 belongs to the class B scavenger receptors which are cell surface receptors expressed on a variety of cell types and is up-regulated upon bacterial infection of tick haemocytes (Aung et al., 2012). These authors showed that the CD36 homologue in *H. longicornis* contributed to granulocyte-mediated phagocytosis against *E. coli*. Interestingly, in an earlier study the same authors suggested that CD36 is important in the RNAi pathway, where it is not only involved in the uptake of dsRNA but possibly also in systemic RNAi (Aung et al., 2011), the main antiviral pathway known to be effective in ticks.

Another interesting result was that in IDE8 (Table 4.11) and IRE/CTVM19 at day 2 p.i. (Table 4.12), with the exception of the tumor rejection antigen (gp96) and calreticulin, all identified HSPs, including the small HSP alpha-crystallin B chain, were down-regulated. HSPs are the most abundant and ubiquitous soluble proteins in all forms of life which perform a multitude of housekeeping functions essential for cell survival (Srivastava, 2002). In contrast to the results obtained in the present study, vertebrate and invertebrate HSPs are usually up-regulated upon virus infection, since the generation of large amounts of viral proteins lead to cellular stress, and some viruses exploit the presence of HSPs to support virus infection (Nagy et al., 2011; Zhao & Jones, 2012). However, HSPs might also have an antiviral effect; strikingly, the HSP70/90 machinery has been implicated as having a critical role in loading siRNAs into the RISC complex in *Drosophila* (Iwasaki et al., 2010). Studies on tick cell responses to bacterial infection found that upon *A. marginale* infection of ISE6 cells both HSP20 and HSP70 were up-regulated (Villar et al., 2010), whereas during *A. phagocytophilum* infection mRNA levels did not change in ISE6 cells (Villar et al., 2010) but *in vivo* HSP20 was up-regulated and HSP70 was down-regulated (Busby et al., 2012), suggesting pathogen- and species-specific differences in the expression of HSPs.

Table 4.11 List of transcripts involved in immunity and cell stress differentially expressed in IDE8 cells infected with TBEV at days 2 (2d) and 6 (6d) p.i.

Colour code for differential expression: green = up-regulated, red = down-regulated, black = not statistically significant

Immunity

transcript/protein	annotation	2d	6d
ISCW023721-RA	cd36		
ISCW004002-RA	longipain		

Cell stress

transcript/protein	annotation	2d	6d
ISCW024057-RA	HSP70		
ISCW015267-RA	heat shock protein (HSP70)		
ISCW001763-RA	heat shock HSP20 protein		
ISCW024910-RA	heat shock protein (HSP70)		
ISCW015266-RA	heat shock HSP20 protein		
ISCW002513-RA	alpha-crystallin B chain		
ISCW024054-RA	heat shock protein 20		

In IRE/CTVM19 (Table 4.12) the two chaperones calreticulin and gp96, which are present in the ER, were up-regulated upon TBEV infection at day 2 p.i.. As a lectin-like ER chaperone, calreticulin is involved in Ca^{2+} homeostasis but also interacts with glycosylated proteins including viral glycoproteins and is important for their processing and maturation in mammalian cells (Michalak et al., 1999; Pieren et al., 2005). In the case of DENV infection of Vero cells, knockdown of calreticulin led to reduced yield of infectious DENV particles suggesting a proviral role for calreticulin (Limjindaporn et al., 2009). However, calreticulin is a multifunctional protein and might be involved at other levels in the immune response in ticks. A functional genomics study revealed the up-regulation of calreticulin in *Babesia bigemina*-infected *R. microplus* and *R. annulatus* ticks but knockdown only resulted in lower pathogen levels in *R. microplus* (Antunes et al., 2012). Gp96 is an ER paralogue of the cytosolic chaperone HSP90, which is essential for the chaperoning of TLR and integrins in mammalian cells. In *Drosophila* the orthologue gp93 exerts similar functions (Morales et al., 2009). However, up-regulation of ER chaperones such as

gp96 and calreticulin could also be a sign of ER stress and the unfolded protein response (UPR), as was previously reported upon JEV infection of mammalian cells (Su, Liao & Lin, 2002). The increase in gp96 and calreticulin could thus be a sign of ER stress upon TBEV infection, possibly triggering the UPR and, as a consequence, inhibiting translation, but no information on inhibition of translation or the regulation of UPR is available for ticks.

Another interesting transcript is complement Factor H which functions as a regulator of the alternative pathway of the complement system and, in certain circumstances, can work as a surface-bound inhibitor in vertebrates. Although ticks have been shown to contain a primitive complement system with all major TEP (Hajdušek et al., 2013; Kopacek, Hajdusek & Buresova, 2012), nothing is known about the antiviral effect of the complement system in ticks. However, the complement system of vertebrates is an integral part of the innate immune response against different families of viruses and has been reviewed extensively (Blue, Spiller & Blackbourn, 2004; Favoreel, 2003; Lachmann & Davies, 1997). For example WNV evades the complement system by recruiting and interacting with complement Factor H, accelerating the decay of other complement components and attenuating the opsonisation of infected cells (Chung et al., 2006).

Peroxinectins are cell adhesive peroxidases stored in the haemocyte granules of crustaceans. Upon infection they are released by degranulation and activated by serine-proteases to stimulate cell adhesion (Johansson & Söderhäll, 1988), phagocytosis (Thörnqvist, Johansson & Söderhäll, 1994), peroxidase activity (Johansson et al., 1995) and encapsulation (Kobayashi, Johansson & Söderhäll, 1990). In crustaceans peroxinectin is associated with the proPO system through sharing the PAP enzyme, a trypsin-like serine protease, in its activation (Lin et al., 2007; Sritunyalucksana et al., 2001). Furthermore, peroxinectin was suggested to be involved in the early defence response against WSSV infection in the mud crab by inhibiting virus replication (Du et al., 2013). The authors showed that the increased expression of peroxinectin in the first 48 h was concomitant with a latent period of WSSV proliferation. However, in contrast to other arthropods, ticks most likely lack the proPO activation system since no proPO-related gene has been identified so far

(Hajdušek et al., 2013; Kopácek et al., 2010). It is thus tempting to speculate that an alternative serine protease, possibly trypsin which was up-regulated at day 6 p.i. in IRE/CTVM19 cells (Table 4.12), might be responsible for the activation of peroxinectin cell adhesion activity in ticks.

The coagulation factor precursor identified in the present study has a 46% identity to the coagulation Factor B of the horseshoe crab which is involved in the haemolymph coagulation cascade. Although a homologue of Factor C, which triggers the limulus clotting cascade upon bacterial infection, has been identified in ticks (Hajdušek et al., 2013), homologues of horseshoe crab coagulogen or crustacean clotting protein have not been found (Kopácek et al., 2010). There is no convincing evidence of haemolymph coagulation in ticks so far (Hajdušek et al., 2013).

Table 4.12 List of transcripts involved in immunity and cell stress differentially expressed in IRE/CTVM19 cells infected with TBEV at days 2 (2d) and 6 (6d) p.i

Colour code for differential expression: green = up-regulated, red = down-regulated, black = not statistically significant

Immunity

transcript/protein	annotation	2d	6d
Q66HI5	Fth1 protein		
ISCW008209-RA	hebraein		
ISCW022766-RA	tumor rejection antigen (gp96)		
ISCW008184-RA	calreticulin		
ISCW022021-RA	complement Factor H		
ISCW011174-RA	coagulation factor precursor		
ISCW007552-RA	peroxinectin		
ISCW006166-RA	trypsin		

Cell stress

transcript/protein	annotation	2d	6d
ISCW022766-RA	tumor rejection antigen (gp96)		
ISCW008184-RA	calreticulin		
ISCW024062-RA	heat shock HSP20 protein		
ISCW024910-RA	HSP70		
ISCW001763-RA	heat shock HSP20 protein		
ISCW015266-RA	heat shock HSP20 protein		
ISCW007552-RA	peroxinectin		

Interestingly, two transcripts involved in the antimicrobial defence response were up-regulated at day 2 p.i.. Hebraein, which was first identified in *Amblyomma hebraeum*, is a histidine- and cysteine-rich antimicrobial peptide similar to microplusin of *R. microplus* (Lai et al., 2004). Its bacteriostatic effect is based on sequestering copper which is required for bacterial respiration (Silva et al., 2009). The second transcript is a ferritin with the highest homology to the rat Ferritin heavy chain (Fth)1. Ferritins are iron-binding proteins which by sequestering iron prevent bacteria from acquiring iron thereby inhibiting their multiplication (Ong et al., 2006). A tick heavy chain ferritin was shown to be up-regulated upon mechanical injury and bacterial infection in *D. variabilis* ticks, suggesting a possible antimicrobial role of

ferritin in ticks (Mulenga et al., 2003, 2004). The role of these two transcripts during virus infection in ticks has not been investigated to date.

4.4.5 Protein annotation and ontology

The peptides generated by trypsin digestion of protein extracts (2.8.5), derived from mock-infected and infected tick cells, were identified and annotated by database search against the UniProt-Arthropoda.fasta and UniProt-*Flaviviridae*.fasta using an integrated decoy approach with an FDR < 0.01 as described above in 4.3.1.2. The statistically significantly ($p<0.05$) differentially represented proteins, as determined by X^2 test, were then allocated to biological process groups. Ontology information for each protein was obtained by using information available on the UniProt/Swiss-Prot and Panther databases, including information for conserved domains. Information was curated manually by literature search.

The majority of blast hits obtained for both IDE8 (Figure 4.11 A) and IRE/CTVM19 (Figure 4.11 B) corresponded to *I. scapularis*, followed by other tick species which included *Amblyomma* spp., *Hyalomma marginatum rufipes* and *Haemaphysalis qinghaiensis* (Figure 4.11). Other proteins showed the highest homology to insects – mosquitoes, *Drosophila*, ants (*Acromyrmex ecchinatior*, *Camponotus floridanus*, *Atta cephalotes*), moths (*Heliothis virescens*, *Manducta sexta*, *Xestia cnigrum*, *Bombyx mori*), red flour beetle (*Tribolium castaneum*), body louse (*Pediculus humanus corporis*) and planthopper (*Nilaparvata lugens*); to the crustaceans water flea (*Daphnia pulex*), crab (*Eriocheir sinensis*) and salmon louse (*Lepeophtheirus salmonis*); or to the arachnid *Aphonopelma chalcodes*.

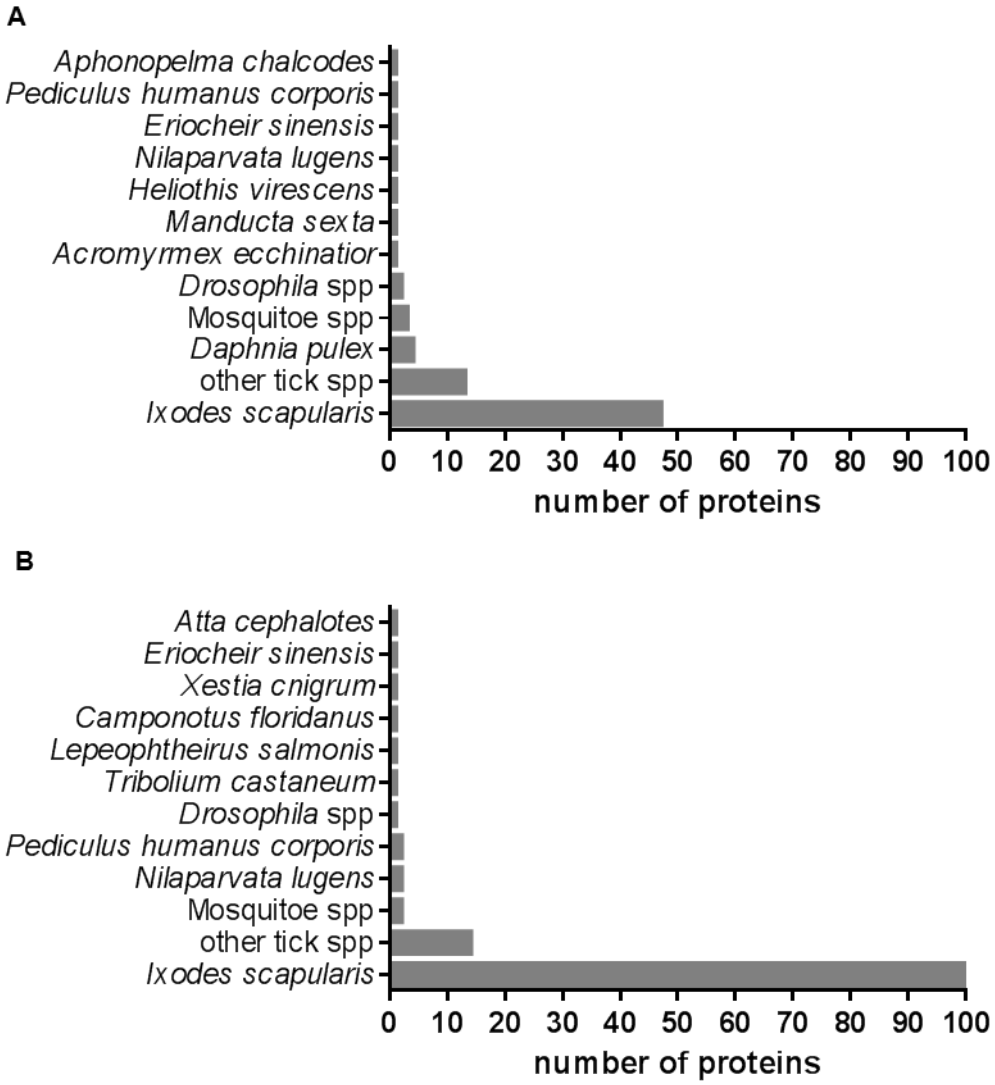

Figure 4.11 Blast hit species distribution for statistically significantly differentially represented proteins in TBEV-infected IDE8 and IRE/CTVM19 cells

Number of proteins identified by blast search against the arthropod UniProt database is shown on the x-axes for IDE8 (A) and IRE/CTVM19 (B). Protein numbers for each tick cell line include both time-points. Species to which the proteins showed the highest homology are indicated on the y-axes.

As mentioned in 4.4.4.1 for transcripts, several of the differentially represented proteins were homologues of proteins of other species. In the case of the protein datasets these were mostly insects. Insects and ticks are evolutionarily quite distant (Figure 1.5); thus identified homologues might have evolved different functions within ticks and insects. However, the lack of annotation based on experimental evidence within tick transcript/protein data makes it currently impossible to resolve

this issue. Thus inferring the biological role based on homology is a starting point useful for the identification of interesting targets; however these have to be experimentally investigated for their true biological role in ticks and tick cell lines.

All tick proteins which were statistically significantly differentially represented in TBEV-infected cells are separated into lists for IDE8 at days 2 (Table 4.13) and 6 p.i. (Table 4.14) and for IRE/CTVM19 at days 2 (Table 4.15) and 6 p.i. (Table 4.16). The lists include information about protein ontology and were sorted according to over- and underrepresentation in comparison to the corresponding mock-infected control. For statistically significantly differentially expressed transcripts, a brief discussion of the functional classes, such as nucleic acid processing, cell stress and immunity is provided at the end of this section.

In both cell lines proteins with unknown function included putative uncharacterised proteins, putative secreted proteins or those that could not be ontologically classified for other reasons, such as the lack of literature or protein names which could not be unequivocally allocated a specific function.

For IDE8 at day 2 (Table 4.13) the majority of proteins were underrepresented, whereas at day 6 (Table 4.14) the majority were overrepresented. The total number of proteins differentially represented was higher at day 2 p.i. than at day 6 p.i. (Table 4.14). For IRE/CTVM19 however more proteins were differentially represented at day 6 (Table 4.16) than at day 2 p.i. (Table 4.15). More proteins were underrepresented than overrepresented at day 6, in contrast to day 2 when equal numbers of proteins were under- and overrepresented.

Interestingly, a large proportion of the differentially represented proteins at both days in both cell lines were involved in nucleic acid processing and these will be highlighted later in 4.4.5.1.

The other differentially represented proteins in both cell lines were involved in a number of different biological processes. Those proteins involved in cell structure and/or transport belonged mainly to the tubulin family, but cortactin, dynactin and kinesin were also differentially represented in IDE8 (Table 4.13, Table 4.14), whereas in IRE/CTVM19 (Table 4.15, Table 4.16) tubulin, actin, cortactin, kinesin,

tropomyosin, paramyosin, coronin, alpha-actinin, alpha-parvin, vinculin and paxilin were differentially represented. These proteins are all part of or connected to the cytoskeleton. Proteins of the cytoskeleton are involved in cell trafficking and cellular cargo transport and can also traffic viral components and virions (Greber & Way, 2006). Studies using DENV in mosquito cells have indicated that actin and tubulin might be important for virus entry and transport (Chee & AbuBakar, 2004; Paingankar, Gokhale & Deobagkar, 2010). Up-regulation of alpha-tubulin at the protein level was observed upon WNV infection of Vero cells (Pastorino et al., 2009). The authors suggested a possible role for tubulin in trafficking of WNV. A recent study looking at the effect of LGTV infection on *I. scapularis* tick salivary glands reported down-regulation of transcripts coding for beta-tubulin (McNally et al., 2012). Furthermore, the motorprotein kinesin, important for the anterograde transport of cargo along microtubules, has been implicated in the transportation of WNV E protein (Chu & Ng, 2002), while dynactin, a 20 S complex protein connecting cellular cargo to dynein, responsible for retrograde transport, has been shown to be important in DENV E and C protein trafficking (Shrivastava et al., 2011). It is thus tempting to speculate that differential representation of these cytoskeletal proteins indicates a role for them in trafficking of TBEV components or virions within tick cells. It is also interesting to note that although the main role of the actin-binding vinculin is related to cell structure and integrity, it has also been implicated, together with paxillin, in modulating cellular signalling pathways involved in apoptosis (Subauste et al., 2004). Down-regulation of vinculin at the protein level, as in the present study, was also observed during DENV infection of a mammalian cell line and the authors hypothesised that the decrease in vinculin inhibits apoptosis, which would be beneficial for DENV replication (Pattanakitsakul et al., 2007).

For IDE8 five proteins involved in signalling were differentially represented at day 2 p.i. (Table 4.13), and only two at day 6 p.i. (Table 4.14). The proteins involved in signalling at day 2 p.i. include the overrepresented cell division cycle 42 (cdc42), also overrepresented in IRE/CTVM19 at day 6 p.i. (Table 4.16), which belongs to the Rho family of small GTPases, and the 14-3-3 zeta belonging to the family of 14-3-3

proteins. Both are involved in a variety of cellular activities which include cellular trafficking, regulation of the cytoskeleton and the control of other signalling pathways leading for example to cell-cycle progression and transcriptional activation (Aitken, 2006; Cerione, 2004; Hall, 1998; Wang & Shakes, 1996). Another protein with the UniProt accession number G3MQ03 (putative uncharacterised protein) of the 14-3-3 family is underrepresented at day 2.

The developmentally-regulated GTP-binding protein (DRG) 2, overrepresented at day 2 p.i., is another member of the GTPase superfamily which is highly conserved across eukaryotic species. Its molecular function is poorly understood but there are indications that DRGs have a role in the regulation of cell proliferation (Ko et al., 2004; Song et al., 2004) and translation (Daugeron et al., 2011). Another interesting protein which was underrepresented in IDE8 at day 2 and IRE/CTVM19 at day 6 is the ubiquitin carboxyl-terminal hydrolase which is part of the ubiquitination machinery. The ubiquitination machinery is involved in a plethora of functions from DNA transcription to protein degradation, and among these it has been recognised as a major signalling regulator of immunity in mammals. Although ubiquitination is probably also essential in regulation of arthropod immunity, a recent review highlighted the lack of knowledge about its role in arthropod immunology (Severo et al., 2013a). However, all major components of the ubiquitin machinery have been identified by a bioinformatics study in the tick *I. scapularis* (Choy et al., 2013), and differential representation of ubiquitin-related proteins has been described in the tick cell line IDE8 upon infection with *A. marginale* (de la Fuente et al., 2007a). It is also interesting to note that several other members of the ubiquitination machinery, including not only the ubiquitin carboxyl-terminal hydrolase mentioned above, but also the ubiquitin activating enzyme E1, a putative protein associated with the ubiquitin conjugating enzyme E2, and ubiquilin 1,2 were underrepresented in IRE/CTVM19 at day 6 p.i. (Table 4.16). Signalling molecules differentially represented in IDE8 at day 6 p.i. (Table 4.14) include ADP ribosylation factor (Arf) 79 and sorting nexin. Interestingly, the ubiquitous small Ras related GTPase Arf 79 containing an Arf1 domain was overrepresented in IDE8. An Arf1 homologue was also overrepresented in IRE/CTVM19 at days 2 (Table 4.15) and 6 p.i. (Table 4.16).

Arf1 is a class I Arf protein which is involved in vesicle formation, influences actin assembly at the Golgi apparatus and is important in regulation of trafficking along the secretory pathway (D'Souza-Schorey & Chavrier, 2006). By influencing traffic through the Golgi, Arf1 might have a role in the release of TBEV similar to that observed in the study of Kudelko (2012) in which knockdown of Arf1 resulted in a partial decrease of recombinant subviral particles during DENV infection (Kudelko et al., 2012). Sorting nexin, which was underrepresented at day 6 p.i., belongs to a family of proteins associated with the endocytic network. They are involved in a variety of processes including endocytosis, endosomal sorting and endosomal signalling (Cullen, 2008; Worby & Dixon, 2002).

Four proteins involved in transportation were underrepresented at day 2 p.i. (Table 4.13) while one was overrepresented at day 6 p.i. (Table 4.14). The latter protein, Arf 79 was described above for its role in signalling. The four proteins underrepresented at day 2 p.i. include two proteins, kinesin and dynactin, which were already described above for their connection to the cytoskeleton, two importin beta proteins which both belong to the karyopherin group of nuclear import factors and the adaptor protein-2 (AP-2) complex subunit alpha-1 (Table 4.13). Interestingly, the AP-2 protein is also differentially represented in IRE/CTVM19 at day 6 p.i. (Table 4.16). AP-2 is involved in clathrin-mediated endocytosis. Although TBEV has been shown to be taken up by clathrin mediated endocytosis (Heinz et al., 1991), involvement of AP-2 has not been shown. It is thus tempting to speculate that AP-2 might be involved in the endocytosis of TBEV in tick cells. Importin beta is a nuclear import factor involved in the nuclear localisation of host cell proteins and has also been implicated in the nuclear localisation of DENV NS5 (Johansson et al., 2001; Pryor et al., 2007). Nuclear localisation of the DENV NS5 protein has been shown to be an integral part of DENV infection; mutations preventing this nuclear localisation abolished virus production (Pryor et al., 2007). Although NS5 proteins of other flaviviruses such as JEV and WNV have been shown to localise to the nucleus (Uchil, Kumar & Satchidanandam, 2006), no study has so far demonstrated nuclear localisation of TBEV proteins.

Table 4.13 Statistically significantly differentially represented proteins in TBEV-infected IDE8 cells at day 2 p.i.

Annotated proteins, including their representation status, their p-values and their ontology: CC (cell cycle), CS (cell stress), D (development), IM (immunity), M (metabolism), NAP (nucleic acid processing), PF (protein folding), PR (proteolysis), SI (signal transduction), ST (structural), T (transport), UK (unknown).

IDE8 2d protein	Annotation	Protein levels in infected compared to mock-infected cells	P-value	Ontology
B4NIY4	GK14362 OS (alpha tubulin)	overrepresented	4.40E-05	ST
B7QP06	Alpha tubulin	overrepresented	4.40E-05	ST
Q4PMD4	60S ribosomal protein L9	overrepresented	2.90E-02	NAP
B0WN56	Histone H2A	overrepresented	2.90E-02	NAP
F4WQW1	Cdc42-like protein	overrepresented	1.46E-02	SI
F0J8X9	Exon-exon junction complex Magoh component	overrepresented	2.90E-02	NAP
B7P4I9	Cellular nucleic acid binding protein	overrepresented	2.90E-02	NAP
C4NFK6	14-3-3 zeta	overrepresented	3.87E-03	SI
B7QGL9	Splicing factor SC35	overrepresented	2.90E-02	NAP
Q5Q976	Putative secreted salivary gland peptide	overrepresented	1.46E-02	UK
G3MFC4	Putative uncharacterized protein (alpha tubulin)	overrepresented	2.01E-03	ST
A5Z1D9	Putative uncharacterized protein	overrepresented	2.90E-02	UK
G3MNE5	Eukaryotic translation initiation factor 3 subunit I	overrepresented	2.90E-02	NAP
B7PR90	Ribosomal protein L13A	overrepresented	2.90E-02	NAP
B4MA19	GJ15754 OS (peroxiredoxin domain)	overrepresented	2.90E-02	CS
B7PJS9	Splicing factor hnRNP-F	overrepresented	2.90E-02	NAP
B7PC94	Tryptophanyl-tRNA synthetase	overrepresented	1.46E-02	NAP
B7QH74	GTP-binding protein DRG2	overrepresented	2.90E-02	SI, CC
B7PG66	Protein Mo25	overrepresented	2.90E-02	D
E9GQY5	Putative uncharacterized protein (Dead box RNA helicase domain)	overrepresented	1.46E-02	NAP
G3MQ03	Putative uncharacterized protein (14-3-3 zeta family)	underrepresented	9.52E-03	SI
B7PH43	Alpha tubulin	underrepresented	6.01E-04	ST
B7PAB0	Secreted salivary gland peptide	underrepresented	2.48E-02	UK
B7PRY6	Golgi apparatus protein	underrepresented	2.12E-02	UK
Q4PMB9	40S ribosomal protein S5	underrepresented	2.48E-02	NAP

B7P4E1	Glutamate dehydrogenase	underrepresented	3.74E-03	M
B7QIP4	4SNc-Tudor domain protein	underrepresented	2.04E-02	IM, NAP
B7P872	Alpha tubulin	underrepresented	2.36E-03	ST
G3MF56	Putative uncharacterized protein (Kinesin)	underrepresented	4.60E-02	ST, T
B7Q5U5	Putative uncharacterized protein (helix hairpin DNA binding motif)	underrepresented	2.48E-02	NAP
E0V9N7	Heat shock protein 70kDa	underrepresented	1.49E-03	CS,PF
B7P4Q8	Inosine-5' monophosphate dehydrogenase	underrepresented	2.48E-02	M
G3MLR1	Putative uncharacterized protein	underrepresented	2.48E-02	UK
B7PL04	Pyruvate decarboxylase (E-1) alpha subunit	underrepresented	4.04E-02	M
B7P0V4	Cortactin,	underrepresented	1.53E-02	ST, T
G3MNC8	Putative uncharacterized protein	underrepresented	4.04E-02	UK
E9FRV3	Isocitrate dehydrogenase [NADP],	underrepresented	2.48E-02	M
B7QD28	Putative uncharacterized protein	underrepresented	1.53E-02	UK
B7QDY5	Protease,	underrepresented	4.04E-02	PR, M
B7QNR8	Importin beta, nuclear transport factor,	underrepresented	1.53E-02	T
B7PYP5	Heat shock protein 90	underrepresented	4.04E-02	CS, PF
B7PEY0	AP-2 complex subunit alpha-1	underrepresented	2.48E-02	T
B7PNE2	Cysteinyl-tRNA synthetase	underrepresented	1.53E-02	NAP
D0UNG5	Translational elongation factor-2	underrepresented	9.52E-03	NAP
B7PKH2	Mcm2/3	underrepresented	4.04E-02	NAP, CC
B7PEY9	Lysyl-tRNA ligase	underrepresented	4.04E-02	NAP
B7QCA1	RNA-binding translational regulator IRP	underrepresented	4.04E-02	M, NAP
B7PXZ9	Karyopherin (Importin) beta	underrepresented	2.48E-02	T
B7QDB1	Ubiquitin carboxyl-terminal hydrolase	underrepresented	2.48E-02	PR, SI
B7PTW9	DNA replication licensing factor, MCM4 component	underrepresented	4.04E-02	NAP, CC
B7QK02	SWI/SNF complex subunit SMARCC2	underrepresented	4.04E-02	NAP
B7PXJ8	Dynactin,	underrepresented	4.04E-02	ST, T

Other proteins differentially represented in IDE8 (Table 4.13 and Table 4.14) are involved in different metabolic processes such as carbohydrate metabolism (pyruvate decarboxylase E1), the citric acid cycle (isocitrate dehydrogenase, glutamate dehydrogenase), fatty acid metabolism (protease) and purine metabolism (inosine-5' monophosphate dehydrogenase).

Table 4.14 Statistically significantly differentially represented proteins in TBEV-infected IDE8 cells at day 6 p.i.

Annotated proteins, including their representation status, their p-values and their ontology: CS (cell stress), IM (immunity), M (metabolism), NAP (nucleic acid processing), PF (protein folding), SI (signal transduction), ST (structural), T (transport), UK (unknown).

IDE8 6d protein	Annotation	Protein levels in infected compared to mock-infected cells	P-value	Ontology
E9HEX5	Putative uncharacterized protein, DAPPUDRAFT_300845 (Beta tubulin)	overrepresented	2.48E-04	ST
B7PTQ4	ADP ribosylation factor 79F	overrepresented	3.45E-02	SI, T
B0WN56	Histone H2A	overrepresented	3.45E-02	NAP
B7PPR4	RSZp22 protein, putative	overrepresented	3.45E-02	NAP
B7PNN7	Attractin and platelet-activating factor acetylhydrolase	overrepresented	1.81E-02	IM
G3MHR0	Isocitrate dehydrogenase [NADP]	overrepresented	4.51E-04	M
B7QJ22	Putative uncharacterized protein	overrepresented	1.81E-02	UK
B7PYD1	ATP-dependent RNA helicase	overrepresented	3.45E-02	NAP
B7PG97	Transcription factor NFAT, subunit NF45	overrepresented	3.45E-02	IM, NAP
E9HNC6	Putative uncharacterized protein, DAPPUDRAFT_302452 (HSP90 domain)	overrepresented	8.23E-04	CS, PF
F5HL97	Elongation factor 1-alpha	overrepresented	9.59E-03	NAP
G3MNS8	Putative uncharacterized protein (EF-1A/Tu domain)	overrepresented	3.45E-02	NAP
B7Q7X2	Putative uncharacterized protein	overrepresented	3.45E-02	UK
G3MK99	Putative uncharacterized protein (Dead RNA helicase domain)	overrepresented	3.45E-02	NAP
O17449	Tubulin beta 1 chain	underrepresented	6.01E-04	ST
B7PA92	Beta tubulin	underrepresented	6.39E-04	ST
B7PGI8	Alpha tubulin	underrepresented	2.75E-03	ST
Q5Q976	Putative secreted salivary gland peptide	underrepresented	3.43E-02	UK
E2J6W0	40S ribosomal protein S2/30S ribosomal protein S5	underrepresented	3.43E-02	NAP
B7P4E1	Glutamate dehydrogenase	underrepresented	2.75E-03	M
B7Q8P2	Sorting nexin	underrepresented	3.43E-02	SI
G3MNE5	Putative uncharacterized protein (eIF-3 domain)	underrepresented	3.43E-02	NAP
D5KXW7	Heat shock protein 90	underrepresented	1.69E-03	CS, PF
C4MX30	90 kDa heat shock protein	underrepresented	2.75E-03	CS, PF

For differentially represented proteins in IRE/CTVM19 (Table 4.15 and Table 4.16) involved in metabolism, metabolic processes included those involved in energy metabolism such as the citric acid cycle (malic enzyme, 2-oxoglutarate dehydrogenase, ATP-citrate synthase), electron transport chain (NADH ubiquinone oxidoreductase) and glycolysis (phosphoglycerate kinase), those involved in carbohydrate metabolism (GDP-mannose pyrophosphorylase, phosphorylase, glucosidase II, protein kinase C substrate), iron metabolism (cytoplasmic aconitase/iron regulatory protein), purine metabolism (GMP synthase), lipid metabolism (saposin) and heme metabolism (heme lipoprotein). Of these, saposins, which are lipid degrading enzymes located in the lysosome, were found to be differentially represented at the transcript level in ticks infected with *Babesia* (Heekin et al., 2013) and mosquitoes infected with SINV (Sanders et al., 2005). Of special interest are the two proteins involved in carbohydrate metabolism, glucosidase II and the protein kinase C substrate. The first resembles the alpha subunit of glucosidase II exhibiting catalytic activity while the protein kinase C substrate resembles the glucosidase II beta subunit important for the ER localisation and enhancement of N-glycan trimming activity. Glucosidase II is important for the quality control of glycoprotein folding in the ER where, by glucose trimming, it regulates the entry of newly synthesised glycoproteins into the calnexin/calreticulin folding cycle (Deprez, Gautschi & Helenius, 2005; Trombetta, 2003). Glucose trimming by glucosidases was also shown to be important for DENV assembly, since inhibition of glucosidases prevented the processing of envelope glycoproteins (Courageot et al., 2000) resulting in reduced virus titers. Underrepresentation of glucosidase and calnexin in IRE/CTVM19 at day 6 (Table 4.16) could thus have an antiviral effect on TBEV.

Table 4.15 Statistically significantly differentially represented proteins in TBEV-infected IRE/CTVM19 cells at day 2 p.i.

Annotated proteins, including their representation status, their p-values and their ontology: CS (cell stress), M (metabolism), NAP (nucleic acid processing), PF (protein folding), PR (proteolysis), SI (signal transduction), ST (structural), T (transport), UK (unknown).

IRE/CTVM19 2d protein	Annotation	Protein levels in infected/mock-infected cells	P-value	Ontology
B7PA92	Beta tubulin	overrepresented	1.42E-04	ST
G3MGQ1	Putative uncharacterized protein (alpha tubulin)	overrepresented	1.42E-04	ST
B4JID3	GH19077 OS (actin-like)	overrepresented	8.48E-04	ST
B7PA03	ATP-dependent helicase (DEAD box)	overrepresented	1.84E-02	NAP
B7QCW2	ADP-ribosylation factor	overrepresented	3.49E-02	SI, T
C1BU48	Ras-related protein ORAB-1	overrepresented	3.49E-02	SI,T
F0J9Q3	26S proteasome regulatory complex subunit RPN3/PSMD3	overrepresented	3.49E-02	PR
G3MRB5	Putative uncharacterized protein (Tropomyosin)	overrepresented	3.49E-02	ST, T
B7PEL3	Protein tyrosine phosphatase	overrepresented	3.49E-02	SI
H9J5W8	Uncharacterized protein	overrepresented	3.49E-02	UK
B0LF74	Beta actin	underrepresented	1.01E-03	ST
E0V9N7	Heat shock 70kDa protein	underrepresented	1.01E-03	CS,PF
D5KXW7	Heat shock protein 90	underrepresented	2.69E-03	CS, PF
B7Q407	Heme lipoprotein	underrepresented	7.27E-03	M, T
G3MKJ8	Putative uncharacterized protein	underrepresented	1.21E-02	UK
Q4PMB9	40S ribosomal protein S5	underrepresented	2.01E-02	NAP
G3MP73	Putative uncharacterized protein	underrepresented	2.01E-02	UK
F5HL97	Elongation factor 1-alpha	underrepresented	2.01E-02	NAP
B7P1Y8	Translation initiation factor 3 and TGF-beta interacting protein	underrepresented	3.39E-02	NAP
B7Q6Z1	Saposin, putative	underrepresented	3.39E-02	M

Only four proteins involved in transport were differentially represented in IRE/CTVM19 at day 2 p.i. (Table 4.15) whereas 21 were differentially represented at day 6 p.i. (Table 4.16), with the majority of them underrepresented. Of those which were not previously mentioned, the ADP/ATP translocase, an antiporter resident in the inner mitochondrial membrane, is a key component of the respiratory chain in

eukaryotic cells whereas the antiporter Na^+/K^+ ATPase is involved in the ionic exchange mechanism. A study in human cells inhibiting the Na^+/K^+ ATPase, thus changing the potassium levels, resulted in a decrease of infectious DENV particles released from the cells, highlighting the fact that viruses often modulate the biochemistry of infected cells to optimise the conditions for different steps of their viral life cycle (Carvalho et al., 2012). Interestingly the other proteins (vacuolar protein sorting-associated protein 35, vesicle docking protein p115, signal recognition particle protein, coatomer subunit beta and gamma, AP-2 complex, dynamin, vacuolar v-ATPase (v-ATPase)) are involved in endocytosis, the endosomal pathway or vesicle-mediated transport along the secretory pathway. For example the proteins AP-2 complex and the GTPase dynamin could be involved in the clathrin-mediated endocytosis of TBEV which has been shown to be important for DENV and WNV uptake into mosquito cells (Acosta, Castilla & Damonte, 2008, 2011; Chu, Leong & Ng, 2006; Mosso et al., 2008) and TBEV in mammalian cells (Heinz et al., 1991). The v-ATPase then acidifies endosomal compartments allowing membrane fusion and uncoating which was shown to be the case for WNV in mosquito cells (Chu, Leong & Ng, 2006) where an inhibition of v-ATPase reduced WNV infection.

Several proteins involved in signalling were differentially represented in IRE/CTVM19 with three at day 2 p.i. (Table 4.15) and 11 at day 6 p.i. (Table 4.16). Of special interest apart from those already mentioned above are the Ras-related protein (Rab) ORAB-1 which was overrepresented at day 2 p.i. (Table 4.15) and the Rab-10 (Rab10) which was overrepresented at day 6 p.i. (Table 4.16). Rab proteins are Ras-related GTPases which are involved in regulating several steps of membrane traffic from the Golgi to plasma membranes, such as vesicle formation, vesicle trafficking along actin and tubulin networks and membrane fusion (Armstrong, 2000; Martinez & Goud, 1998). The Rab proteins Rab5 and Rab11, which are involved in trafficking from the plasma membrane to early endosomes and in recycling of endosomes to the plasma membrane, have been shown to be important for efficient virus production in HSV of mammalian cells (Hollinshead et al., 2012). Furthermore, Rab GTPases are also involved in the formation and maturation of phagosomes

(Flannagan, Jaumouillé & Grinstein, 2012; Rupper & Cardelli, 2001). Interestingly Rab6, a member of the the Rab GTPase family, has been shown to be required for the phagocytosis of *Drosophila* C virus in *Drosophila* S2 cells, highlighting a possible role of Rab GTPases in the cellular innate immune defence against virus infection in invertebrates (Ye, Tang & Zhang, 2012).

Several proteins involved in signalling were differentially represented in IRE/CTVM19 with three at day 2 p.i. (Table 4.15) and 11 at day 6 p.i. (Table 4.16). Of special interest apart from those already mentioned above are the Ras-related protein (Rab) ORAB-1 which was overrepresented at day 2 p.i. (Table 4.15) and the Rab-10 (Rab10) which was overrepresented at day 6 p.i. (Table 4.16). Rab proteins are Ras-related GTPases which are involved in regulating several steps of membrane traffic from the Golgi to plasma membranes, such as vesicle formation, vesicle trafficking along actin and tubulin networks and membrane fusion (Armstrong, 2000; Martinez & Goud, 1998). Furthermore, Rab GTPases are also involved in the formation and maturation of phagosomes (Flannagan, Jaumouillé & Grinstein, 2012; Rupper & Cardelli, 2001). Interestingly Rab6, a member of the the Rab GTPase family, has been shown to be required for the phagocytosis of *Drosophila* C virus in *Drosophila* S2 cells, highlighting a possible role of Rab GTPases in the cellular innate immune defence against virus infection in invertebrates (Ye, Tang & Zhang, 2012).

Table 4.16 Statistically significantly differentially represented proteins in TBEV-infected IRE/CTVM19 cells at day 6 p.i.

Annotated proteins, including their representation status, their p-values and their ontology: CA (cell ashesion), CC (cell cycle), CS (cell stress), D (development), IM (immunity), M (metabolism), NAP (nucleic acid processing), PF (protein folding), PR (proteolysis), SI (signal transduction), ST (structural), T (transport), UK (unknown).

IRE/CTVM19 6d protein	Annotation	Protein levels in infected/mock-infected cells	P-value	Ontology
B7P872	Alpha tubulin	overrepresented	4.37E-04	ST
B7Q4Q3	ADP/ATP translocase	overrepresented	5.03E-03	T
B7QER9	DEAD box ATP-dependent RNA helicase	overrepresented	5.03E-03	NAP
B7Q731	Malic enzyme	overrepresented	5.03E-03	M
B7PA01	ATP-dependent RNA helicase	overrepresented	9.41E-03	NAP
F5HL97	Elongation factor 1-alpha	overrepresented	9.41E-03	NAP
H9J9S0	T-complex protein 1 subunit alpha	overrepresented	9.41E-03	PF
B7PHY7	Cdc42 protein	overrepresented	1.78E-02	SI
G3MTB8	Putative uncharacterized protein	overrepresented	1.78E-02	UK
B7QE67	Proteasome subunit alpha type	overrepresented	3.40E-02	PR
B7QCW2	ADP-ribosylation factor	overrepresented	3.40E-02	SI, T
B7QEM6	NADH-ubiquinone oxidoreductase, NDUFS3/30 k Da	overrepresented	3.40E-02	M
G3MH11	Putative uncharacterized protein (ubiquitin conjugating enzyme E2)	overrepresented	3.40E-02	SI, PR
E2AT08	Ras-related protein Rab-10	overrepresented	3.40E-02	T, SI
B7PDV5	Putative uncharacterized protein	overrepresented	3.40E-02	UK
B7PVP0	Putative uncharacterized protein	overrepresented	3.40E-02	UK
G3MRC0	Putative uncharacterized protein	overrepresented	3.40E-02	UK
E3V0H8	Salivary protein antigen P40	overrepresented	3.40E-02	UK
G3MNU2	Putative uncharacterized protein (v-ATPase)	overrepresented	3.40E-02	T
B7PTB1	Initiation factor 2 subunit (eIF-2B)	overrepresented	3.40E-02	NAP
B7Q825	Transferase	overrepresented	3.40E-02	NAP
D2A5H8	Phosphoglycerate kinase	overrepresented	3.40E-02	M
B7QN92	GDP-mannose pyrophosphorylase	overrepresented	3.40E-02	M
H9IIV4	Uncharacterized protein (ABC Transporter like)	overrepresented	3.40E-02	T
B7QJH6	Alpha-actinin	underrepresented	2.40E-05	ST
B7P1Z8	Heat shock protein (HSP70)	underrepresented	9.90E-05	CS, PF
B7PQ21	DEAD box ATP-dependent RNA helicase	underrepresented	1.58E-04	NAP
B7P5Y3	Phosphorylase	underrepresented	1.58E-04	M

G3MGL5	Putative uncharacterized protein	underrepresented	1.58E-04	UK
B7Q5X7	Vinculin	underrepresented	2.55E-04	CA, SI, ST
B7QI53	Apoptosis-promoting RNA-binding protein TIA-1/TIAR	underrepresented	4.11E-04	NAP, CS
B7PDF5	Prolyl endopeptidase	underrepresented	6.63E-04	PR
B7PR84	Ubiquitin-activating enzyme E1	underrepresented	1.07E-03	PR, SI
B7PD93	Ran-binding protein	underrepresented	1.07E-03	CC, T, SI
G3MF56	Putative uncharacterized protein (kinesin)	underrepresented	1.07E-03	ST, T
B7PEY0	AP-2 complex subunit alpha-1, putative	underrepresented	1.07E-03	T
E0V9N7	Heat shock 70 kDa cognate	underrepresented	1.07E-03	CS, PF
D5KXW7	Heat shock protein 90	underrepresented	1.07E-03	CS, PF
B7QIP4	4SNc-Tudor domain protein	underrepresented	1.74E-03	IM
B7QC85	Tumor rejection antigen (Gp96)	underrepresented	1.74E-03	CS, IM, PF
B7Q3Z3	26S proteasome regulatory subunit rpn1	underrepresented	1.74E-03	PR
B7QMV1	Elongation factor (EF-2)	underrepresented	2.56E-03	NAP
G3MSX8	Putative uncharacterized protein (V-ATPase)	underrepresented	2.83E-03	T
B7P7C0	Fasciclin	underrepresented	2.83E-03	CA
B7QLI1	Vacuolar protein sorting-associated protein 35	underrepresented	2.83E-03	T
B7Q5I1	Cniwi prot	underrepresented	2.83E-03	IM, D
B7QAM0	Threonyl-tRNA synthetase	underrepresented	2.83E-03	NAP
B7QL56	DNA replication licensing factor	underrepresented	2.83E-03	NAP
B9UNL8	Cytoplasmic aconitase/iron-regulatory protein	underrepresented	2.83E-03	M
B7P8Q5	Hsp70	underrepresented	3.99E-03	CS, PF
B7QL12	Glycyl-tRNA synthetase	underrepresented	4.63E-03	NAP
B7QCH5	Coatomer subunit gamma	underrepresented	4.63E-03	T
B7QCA7	Glucosidase 2	underrepresented	4.63E-03	M
B7PRM5	DEAD-box protein	underrepresented	4.63E-03	NAP
B7PU84	Putative uncharacterized protein	underrepresented	4.63E-03	UK
B7P7M2	Signal recognition particle protein	underrepresented	4.63E-03	T
C4MX30	90 kDa heat shock protein	underrepresented	4.63E-03	CS, PF
B7PL25	Double-stranded RNA-specific editase B2	underrepresented	7.59E-03	NAP
B7PYD1	ATP-dependent RNA helicase	underrepresented	7.59E-03	NAP
B7PPP8	Dynamin,	underrepresented	7.59E-03	T
B7QAA7	Coatomer beta subunit	underrepresented	7.59E-03	T
B7Q355	Paramyosin	underrepresented	7.59E-03	ST
B7PWC4	Poly [ADP-ribose] polymerase	underrepresented	7.59E-03	NAP, CS

B7PCU5	2-oxoglutarate dehydrogenase	underrepresented	7.59E-03	M
B7P806	Vesicle docking protein P115	underrepresented	7.59E-03	T
B7PC82	Thimet oligopeptidase	underrepresented	7.59E-03	PR
B7P622	Ran-binding protein	underrepresented	7.59E-03	CC, T, SI
B7P5X4	tRNA synthetases class 1	underrepresented	7.59E-03	NAP
B7PSW5	Programmed cell death 6-interacting protein	underrepresented	7.59E-03	CS, T
B7PKA3	PDZ domain-containing protein	underrepresented	1.25E-02	SI
B7PEY5	Alanyl-tRNA synthetase	underrepresented	1.25E-02	NAP
B7QLE3	Protein kinase C substrate	underrepresented	1.25E-02	M
B7Q3D3	ATP-citrate synthase	underrepresented	1.25E-02	M
B7PX63	Zinc finger protein	underrepresented	1.25E-02	UK
B7PKH2	Mcm2/3	underrepresented	1.25E-02	NAP, CC
B7Q420	Ribonucleoside-diphosphate reductase	underrepresented	1.25E-02	NAP
B7P9E4	Na+/K+ ATPase	underrepresented	1.25E-02	T
B7P9L0	Tip120	underrepresented	1.25E-02	NAP
B7P8X1	Coronin	underrepresented	1.25E-02	ST, T
B7QD28	Putative uncharacterized protein	underrepresented	1.25E-02	UK
B7PGQ2	Calnexin,	underrepresented	1.25E-02	CS, IM, PF
B7QBM2	Dipeptidyl peptidase 3	underrepresented	1.47E-02	PR
B7PVR6	Villin	underrepresented	1.51E-02	ST
B7P839	DEK domain-containing protein	underrepresented	2.08E-02	UK
B7PZM7	Transmembrane protein	underrepresented	2.08E-02	UK
B7PUU3	Putative uncharacterized protein	underrepresented	2.08E-02	UK
B7PNE2	Cysteinyl-tRNA synthetase	underrepresented	2.08E-02	NAP
B7QEE0	Hypoxia up-regulated protein	underrepresented	2.08E-02	CS, PF
B7PEY9	Lysine-tRNA ligase	underrepresented	2.08E-02	NAP
B7PN34	KH domain RNA binding protein	underrepresented	2.08E-02	UK
B7QCA9	Calcium-dependent cysteine protease	underrepresented	2.08E-02	PR
B7PNU9	DnaJ domain and thioredoxin-containing protein	underrepresented	2.08E-02	PF, CS
B7P595	Proline and glutamine-rich splicing factor (SFPQ)	underrepresented	2.08E-02	NAP
B7QDB1	Ubiquitin carboxyl-terminal hydrolase	underrepresented	2.08E-02	SI, PR
B7PKN7	GMP synthase	underrepresented	2.30E-02	M
B7PM08	eIF2-interacting protein ABC50	underrepresented	3.48E-02	NAP
B7P9A9	HyFMR1 protein, putative	underrepresented	3.48E-02	NAP, D
B7P0V4	Cortactin	underrepresented	3.48E-02	ST, T
B7PB10	Putative uncharacterized protein	underrepresented	3.48E-02	UK
B7P6L0	GTP-binding protein mmr1	underrepresented	3.48E-02	UK

B7PKV6	Ubiquilin 1,2	underrepresented	3.48E-02	PR, SI
B7PAX0	Alpha-parvin	underrepresented	3.48E-02	ST, CA
B7QNV8	Putative uncharacterized protein	underrepresented	3.48E-02	UK
B7Q0A4	Paxillin,	underrepresented	3.48E-02	SI, CA, ST
G3MK99	Putative uncharacterized protein (Dead box RNA helicase domain)	underrepresented	3.48E-02	NAP
B7P9Z2	AP-2 complex subunit alpha-1, putative	underrepresented	3.48E-02	T
B7Q220	Structure-specific recognition protein	underrepresented	3.48E-02	NAP
B7PYP5	Heat shock protein 90	underrepresented	3.48E-02	CS, PF
B7QHT6	DNA replication licensing factor	underrepresented	3.48E-02	NAP

In addition to the processes already described above, several differentially represented proteins were involved in proteolysis. Interestingly these include components of the 26S proteasome such as the regulatory subunit rpn3, overrepresented at day 2 p.i. (Table 4.15), the proteasome subunit alpha overrepresented at day 6 p.i. (Table 4.16) and the regulatory subunit rpn1 underrepresented at day 6 p.i.. The 26S proteasome is tightly linked to the ubiquitin pathway, in which it degrades proteins targeted for destruction by polyubiquitin chains. Apart from playing a central role in degradation of misfolded or unnecessary proteins, including numerous regulatory proteins, it has also been found to be required for flavivirus infection in mammalian and insect cells (Fernandez-Garcia et al., 2011).

4.4.5.1 Nucleic acid processing

As already mentioned above in 4.4.4.2, proteins in this category are involved in nucleic acid replication, transcription, processing, alternative splicing and translation and have been found to be differentially expressed in a number of mosquito and tick transcriptome (Bartholomay et al., 2004; Colpitts et al., 2011a; Heekin et al., 2013; Sim, Ramirez & Dimopoulos, 2012) and tick, mosquito and mammalian proteome (de la Fuente et al., 2007a; Pastorino et al., 2009; Zhang et al., 2013) studies on pathogen infection. Many of these proteins may be participating in virus replication and translation. Histones and EF-1 alpha were differentially expressed at the transcript as well as at the protein level. Their possible roles during virus infection

have already been discussed above in 4.4.4.2. Interestingly, as observed during WNV infection in Vero cells (Pastorino et al., 2009), eukaryotic translation initiation factor (eIF) 3 was underrepresented in IDE8 at day 6 p.i. and in IRE/CTVM19 at day 2 p.i.. This is surprising since eIF3 together with the 40S ribosomal subunit, also underrepresented in the present study, are important in the first stage of protein synthesis and flaviviruses are thought to prevent host cell translation shutoff, at least in mammalian cells (Emara & Brinton, 2007). However a recent study using YFV in mammalian cells found that NS5 interacts with eIF3L, a subunit of eIF3, and that overexpression of this subunit facilitates translation of YFV but does not change global protein synthesis (Morais et al., 2013). This suggests that eIF3 is important for replication of flaviviruses. Down-regulation of this inititation factor might have an antiviral effect. Interestingly EF-2 and several participants in the translation of RNA such as t-RNA synthetasen, which loads t-RNAs with the respective amino acid, were also underrepresented in the present study which is in contrast to the findings of Pastorino et al. (2009).

Another interesting finding is the up-regulation of the DEAD-box RNA helicase in both cell lines at both time-points which was also seen at least at the transcriptional level for DENV in *Ae. aegypti* cells (Sim & Dimopoulos, 2010). This is a noteworthy finding since Dcr-2, a DExD/H-box helicase, was shown to be capable of sensing viral dsRNA in *Drosophila* leading to production of possibly antiviral molecules (Deddouche et al., 2008).

4.4.5.2 Cell stress and immunity

Several proteins possibly involved in the immune and cell stress responses of IDE8 (Table 4.17) and IRE/CTVM19 (Table 4.18) cells were differentially represented at day 2 or 6 p.i.. Of those involved in immunity, the 4SNc Tudor domain (Tudor-SN) protein was differentially represented in both cell lines, in IDE8 (Table 4.17) at day 2 and in IRE/CTVM19 (Table 4.18) at day 6 p.i.. The Tudor-SN protein is a multifunctional protein involved in transcription, processing of edited dsRNA, and splicing regulation. Interestingly it has also been implicated in the modulation of RNAi pathways by binding and possibly cleaving hyper-edited miRNAs (Scadden,

2005; Yang et al., 2006) and by being a part of the RISC complex (Caudy et al., 2003). Although Tudor-SN was also found to be expressed and suspected to be a part of the RISC complex within ticks (Kurscheid et al., 2009), the role of Tudor-SN within the RISC complex in arthropods is still unclear (Barnard et al., 2012b).

The other proteins possibly involved in the defence response in IDE8 include the attractin and platelet-activating factor acetylhydrolase (PAF-AH) and the transcription factor Nuclear factor of activated t-cells (NFAT) which were both overrepresented at day 6 p.i.. PAF-AH is a Ca^{2+} -independent phospholipase A2 which is involved in the inactivation of platelet-activating factor by deacetylation (McIntyre, Prescott & Stafforini, 2009; Stafforini et al., 1997). PAF-AH was identified in the saliva of the cat flea (Cheeseman, Bates & Crampton, 2001) where it is possibly involved in regulating the activation of host cells that are central to inflammation and haemostasis in vertebrate immunity (Prescott et al., 2000). Furthermore there is evidence that an increase in PAF-AH in the haemolymph upon pathogen infection of the insect *Rhodnius prolixus* interfered with the haemocyte-mediated immune responses phagocytosis and haemocyte microaggregation (Figueiredo et al., 2008; Garcia et al., 2009). The role of PAF-AH in the antimicrobial or antiviral defence response in ticks has not yet been examined.

The transcription factor NFAT belongs to a family of transcription factors present in cells of the adaptive and innate immune system in vertebrates. Upon activation it induces gene expression and thus regulates several innate and adaptive immune responses (Fric et al., 2012; Rao, Luo & Hogan, 1997; Wu et al., 2007; Zanoni & Granucci, 2012). In invertebrates however, only homologues of NFAT5 have been identified (Graef et al., 2001; Keyser, Borge-Renberg & Hultmark, 2007; Song et al., 2013) which have been shown to be activated upon osmotic stress (Keyser, Borge-Renberg & Hultmark, 2007). Furthermore the NFAT homologue in amphibians was shown to be up-regulated upon LPS stimulation and authors suggested a role for NFAT in LPS-stimulated immunity in invertebrates (Song et al., 2013). The role of NFAT in antiviral immunity in invertebrates has not yet been elucidated.

Interestingly the four proteins possibly involved in innate immunity in IRE/CTVM19 were all underrepresented at day 6 p.i. (4.4.5.2). These include the Tudor-SN protein (described above), gp96 (described in 4.4.4.3), the PIWI 1 protein Cniwi and the lectin-chaperone calnexin. PIWI proteins are part of the piRNA pathway which was initially thought to be only important for the protection of germline cells from transposable elements in *Drosophila*. The discovery of virus-specific piRNA molecules being expressed for a variety of different viruses in *Drosophila* as well as in mosquitoes (Léger et al., 2013; Morazzani et al., 2012; Schnettler et al., 2013a, 2013b; Vodovar et al., 2012; Wu et al., 2010), including for DENV (Hess et al., 2011), suggested an additional role of the piRNA pathway in the antiviral response. This suggestion was confirmed by knockdown of PIWI proteins in mosquito cells which led to an increase in SFV replication and production (Schnettler et al., 2013a). It would be tempting to speculate that this pathway might also be important for the antiviral response against TBEV in tick cells in addition to the exogenous siRNA pathway.

Calnexin is a membrane-bound ER chaperone similar to the soluble ER chaperone calreticulin, which was up-regulated at the transcript level in IRE/CTVM19 at day 2 p.i. (Table 4.12, 4.4.4.3). Both of these proteins interact with glycosylated proteins and are important for viral glycoprotein processing and maturation (Pieren et al., 2005) and have been shown to be important in Vero cells for the production of infectious DENV particles upon interaction with the glycosylated DENV E protein (Limjindaporn et al., 2009). Hypothesising that calnexin and calreticulin are also necessary for the production of infectious TBEV particles in tick cells, an underrepresentation at day 6 p.i. could be a tick cell response to reduce the number of infectious viruses produced.

As already observed at the transcript level for both cell lines (Table 4.11, Table 4.12) HSPs were generally down-regulated at the protein level. The possible role of HSP in the response to virus-infection was discussed in 4.4.4.3. Interestingly however, HSP90 was not statistically significantly differentially expressed at the transcript level but was statistically significantly underrepresented at the protein level. Underrepresentation at the protein level was also observed during WNV infection of

Vero cells (Pastorino et al., 2009). HSP90, which displays ATP-dependent folding capacity (Panaretou et al., 1998), seems to have in contrast to HSP70 a specific set of target proteins (Agashe & Hartl, 2000; Pratt & Toft, 2003). Interestingly, inhibition of HSP90 has been shown to block viral replication (Connor et al., 2007; Hung, Chung & Chang, 2002) and has been proposed to be an important factor for the replication of a wide spectrum of RNA viruses (Connor et al., 2007). Thus the down-regulation of HSP90 in tick cells upon TBEV infection might be an innate cellular protective response. Another protein involved in the cell stress response is peroxiredoxin, which was overrepresented in IDE8 at day 2 p.i.. Peroxiredoxins are antioxidant enzymes which protect cells from oxidative damage by removing excess ROS species. Upregulation of peroxiredoxins is a marker of cell stress and was observed in other proteomic studies of bacterial or viral infection (Heekin et al., 2013; Rachinsky, Guerrero & Scoles, 2007; Zhang et al., 2013).

Table 4.17 List of proteins involved in immunity and cell stress in TBEV-infected IDE8 cells

Colour code for differential expression: green = overrepresented, red = underrepresented, black = not statistically significantly differentially represented

Immunity

protein	transcript or species	annotation	2d	6d
B7QIP4	ISCW014289-RA	4SNc-Tudor domain protein		
B7PNN7	ISCW006386-RA	Attractin and platelet-activating factor acetylhydrolase		
B7PG97	ISCW017579-RA	Transcription factor NFAT, subunit NF45		

Cell stress

protein	transcript or species	annotation	2d	6d
E0V9N7	*Pediculus humanus corporis*	Heat shock protein 70kDa		
B4MA19	*Drosophila virilis*	GJ15754 OS (Peroxiredoxin)		
B7PYP5	ISCW009087-RA	Heat shock protein 90		
D5KXW7	*Nilaparvata lugens*	Heat shock protein 90		
E9HNC6	*Daphnia pulex*	Putative uncharacterized protein (HSP90 domain)		
C4MX30	*Eriocheir sinensis*	90 kDa heat shock protein		

Other proteins possibly involved in the cell stress response in IRE/CTVM19 such as the apoptosis-promoting RNA-binding protein TIA-1/TIAR, poly (ADP-ribose) polymerase (PARP), programmed cell death 6 interacting protein (referred to as Alix/AIP2), a DNAJ domain and thioredoxin containing protein and the hypoxia up-regulated protein (referred to as GRP170) were all down-regulated at day 6 p.i. (Table 4.18). Possible functions of each during virus infection will only be mentioned in brief. TIA-1/TIAR are involved in the formation of stress granules that are only formed in stressed cells and are possibly involved in the regulation and lifecycle of mRNA (Anderson & Kedersha, 2006, 2008). Many viruses interfere with the formation of stress granules as a means to support virus replication (Lloyd, 2013; Valiente-Echeverría, Melnychuk & Mouland, 2012). WNV for example is able to block stress granule formation (Emara & Brinton, 2007) by interacting with TIA-1/TIAR in mammalian cells (Li et al., 2002). This apparently supports viral replication since TIA-1/TIAR knock-out mice showed reduced WNV replication (Li et al., 2002). Alix/AIP1 is involved in promoting apoptosis but has an additional role in endolysosomal trafficking (Odorizzi, 2006). A study in mammalian cells suggested that Alix controls the release of VSV nucleocapsid from late endosomes into the cytoplasm (Le Blanc et al., 2005). In shrimp, no correlation between Alix and apoptosis could be identified upon WSSV infection and the authors concluded that Alix does not play a role in viral-induced cell death in shrimp (Sangsuriya et al., 2010). Similarly the nuclear enzyme PARP is involved in promotion of cell death and in DNA damage surveillance (Yu et al., 2002). The DNAJ domain and thioredoxin-containing protein was annotated to be involved in cell stress and protein folding but its exact function could not be discovered by literature search. On the other hand the hypoxia up-regulated protein grp170 is a large HSP70 protein resident in the ER where it functions as a chaperone of unfolded proteins (Behnke & Hendershot, 2013). The roles of PARP, DNAJ domain and thioredoxin-containing protein and grp170 during virus infection in arthropods have not been examined.

Table 4.18 List of proteins involved in immunity and cell stress in TBEV-infected IRE/CTVM19 cells

Colour code for differential expression: red = underrepresented, black = not statistically significantly differentially represented

Immunity

protein	transcript or species	annotation	2d	6d
B7QIP4	ISCW014289	4SNc-Tudor domain protein		
B7QC85	ISCW022766	Tumor rejection antigen (Gp96)		
B7Q5I1	ISCW011373	Cniwi prot		
B7PGQ2	ISCW003709	Calnexin,		

Cell stress

protein	transcript or species	annotation	2d	6d
E0V9N7	*Pediculus humanus corporis*	Heat shock 70kDa protein		
D5KXW7	*Nilaparvata lugens*	Heat shock protein 90		
B7P1Z8	ISCW016090	Heat shock protein 70		
B7QI53	ISCW014211	Apoptosis-promoting RNA-binding protein TIA-1/TIAR		
B7QC85	ISCW022766	Tumor rejection antigen (Gp96)		
B7P8Q5	ISCW017192	Hsp70		
C4MX30	*Eriocheir sinensis*	90 kDa heat shock protein		
B7PWC4	ISCW019519	Poly [ADP-ribose] polymerase		
B7PSW5	ISCW019764	Programmed cell death 6-interacting protein		
B7PGQ2	ISCW003709	Calnexin,		
B7QEE0	ISCW012646	Hypoxia up-regulated protein		
B7PNU9	ISCW018779	DnaJ domain and thioredoxin-containing protein		
B7PYP5	ISCW009087	Heat shock protein 90		

4.4.6 Correlation between transcript and protein profiles

In both cell lines at both time-points the majority of the statistically significantly differentially expressed transcripts (Figure 4.12 A) were down-regulated with the exception of IRE/CTVM19 at day 6 p.i. where all transcripts were up-regulated. However at the protein level (Figure 4.12 B), although the majority of proteins were underrepresented at day 2 in IDE8 and day 6 in IRE/CTVM19, equal numbers in IRE/CTVM19 at day 2 p.i. were differentially represented and in IDE8 slightly more proteins were overrepresented at day 6 p.i.. Furthermore, when comparing the transcript and protein profiles for each cell line at each time-point individually, there is little correlation at the biological process group level or at the individual transcript and protein level between transcripts and proteins. It is also interesting to note that substantially more proteins were significantly differentially represented than transcripts for each cell line at both time-points.

Correlation between transcripts and protein profiles can be observed for those involved in protein folding and cell stress, both of which were generally down-regulated in both cell lines at both time-points. These include the group of HSPs with HSP70 being the only one down-regulated at the same time point, day 2 p.i., in both IDE8 (Table 4.7, Table 4.13) and IRE/CTVM19 (Table 4.9, Table 4.15), at the transcript and protein level.

It is however interesting to note that a large proportion of the transcripts and/or proteins differentially expressed in both cell lines at both time-points were involved in nucleic acid processing (Figure 4.12), although their trends and the individual transcripts or proteins did not correlate. Of these only EF-1A was up-regulated in IRE/CTVM19 at both the transcript (Table 4.10) and protein (Table 4.16) levels at day 6 p.i..

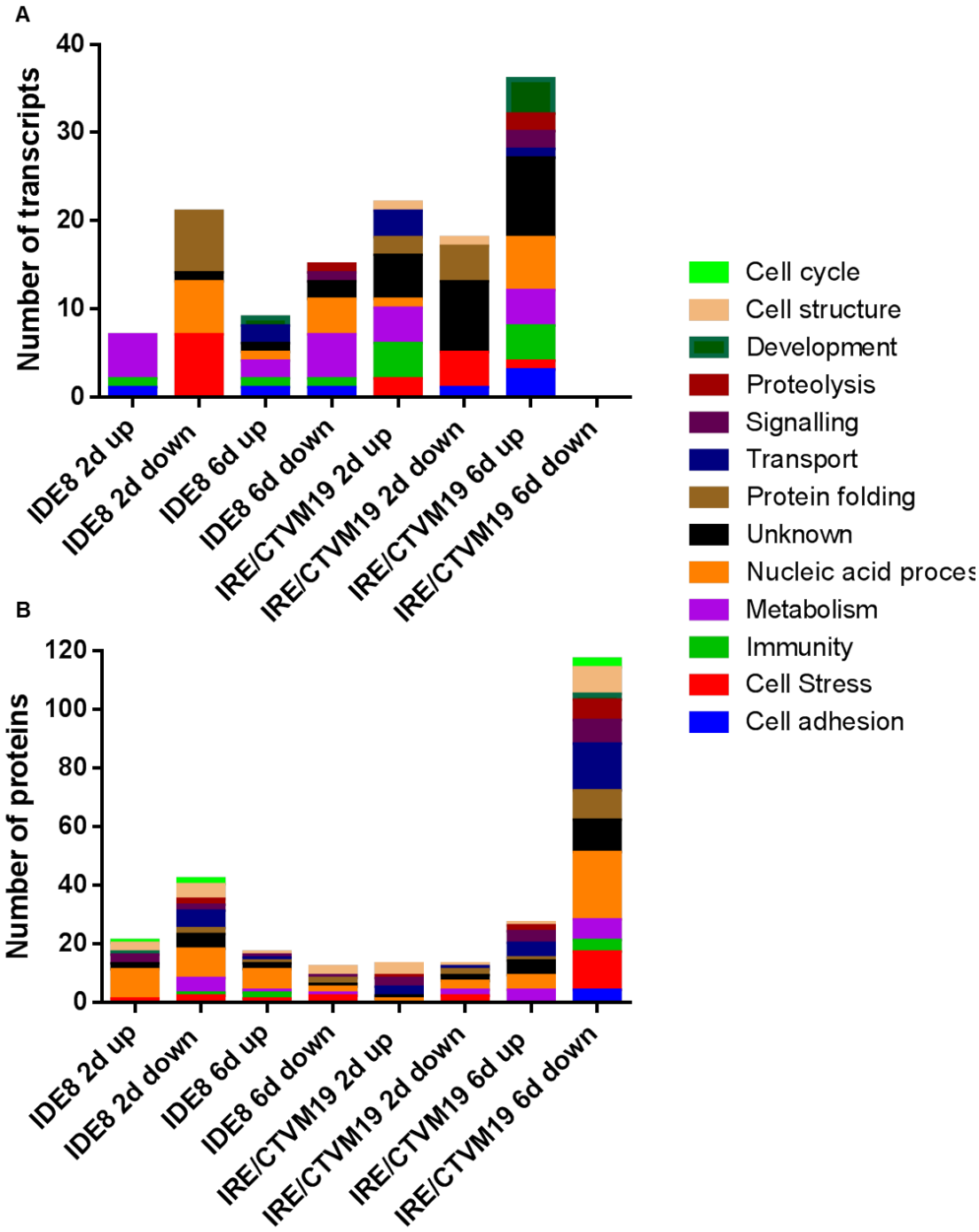

Figure 4.12 Profiles of up- and down-regulated transcripts and over- and under-represented proteins in TBEV-infected IDE8 and IRE/CTVM19 cells at days 2 and 6 p.i.

Each individual transcript (A) or protein (B) was grouped according to its regulation status and function. Ontology groups were assigned using information available on UniProt/Swiss-Prot database. Information was then curated manually according to gene function published in the literature.

Interestingly, a large proportion of the differentially represented proteins were down-regulated at day 6 p.i. in IRE/CTVM19 cells, whereas all the differentially expressed transcripts were up-regulated. This decrease in protein was accompanied by up-regulation of some proteases, such as proteasome subunit alpha and ubiquitin conjugating enzyme E2, which might suggest increased protein degradation at day 6 p.i.; however other proteases including Ubiquitin-activating enzyme E1 and the 26S proteasome regulatory subunit rpn1 were underrepresented which would not support this suggestion.

4.4.7 Verification of RNA-Seq data by qRT-PCR

To validate the HiSeq2000 sequencing data, 12 transcripts which were either differentially represented in the transcriptomics data and/or coding for differentially represented proteins in the proteomics data were selected for qRT-PCR analysis (2.4.10.2, 2.4.10.4). Preference was given to transcripts or proteins possibly involved in immunity or cell stress and included transcripts which were either up-regulated, or down-regulated or not statistically significantly differentially expressed. The primers used for validation (Table 2.3) were designed using species-specific sequences or identical regions from sequences common to both *I. scapularis* and *I. ricinus* obtained by HiSeq2000 as template. In brief, the same samples which were pooled for the transcriptome profiling were used individually for qRT-PCR analysis (2.4.10.2, 2.4.10.4) on the ViiA7 qPCR machine (2.4.10.4, Table 2.5).The fold change relative to mock-infected controls was then calculated using the ΔΔCT method as described in 2.4.10.4, using beta actin and the ribosomal protein L13A, which were not differentially expressed at the transcript level, as reference genes. Statistical significance of fold changes was calculated by an unpaired t-test with a FDR <5% using GraphPad Prism (version 6.00 for Windows, GraphPad Software, La Jolla California USA, www.graphpad.com). The average fold changes and statistical significance by qRT-PCR of two or three biological replicate samples per cell line per time-point were compared to the fold changes and statistical significance of pooled samples from sequencing data calculated by DESeq in R (Figure 4.13).

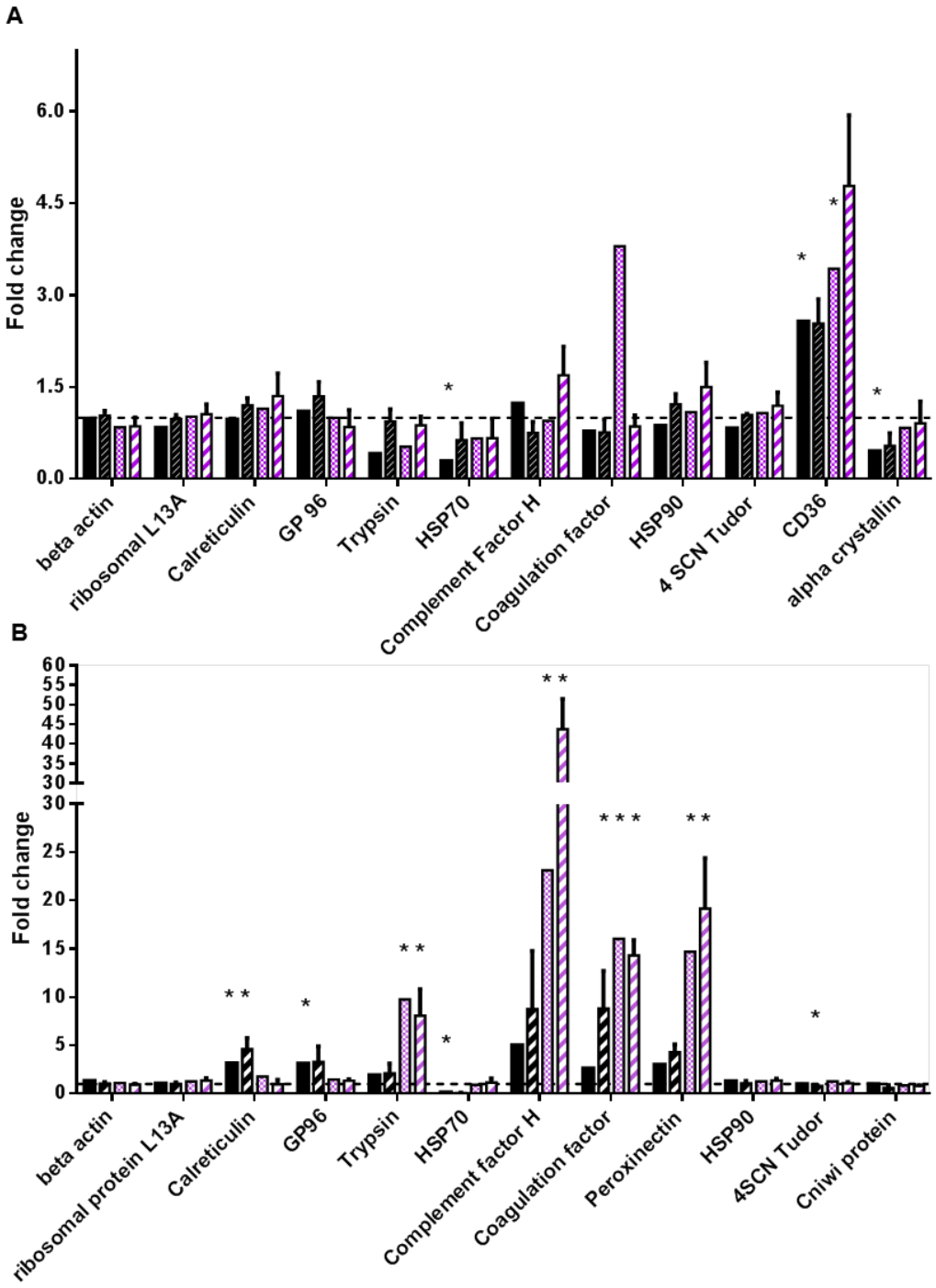

Figure 4.13 Verification of sequencing data for TBEV-infected IDE8 (A) and IRE/CTVM19 (B) cells by qRT-PCR

The average fold change of 2-3 biological replicate samples obtained by qRT-PCR for IDE8 (A) and IRE/CTVM19 (B) at day 2 ( ) and day 6 ( ) p.i. were compared to the fold change and statistical significance of pooled samples from sequencing data calculated by DESeq in R at day 2 ( )and day 6 ( ) p.i.. Error bars are standard error of mean and asterisks mark statistical significance with FDR <5%. The dotted line at fold change 1 represents the cut-off for differential expression.

For IRE/CTVM19 (Figure 4.13 B) the results obtained by qRT-PCR agreed well with those seen in the HiSeq2000 sequencing analysis and showed at least the same pattern of expression. In IDE8 however, some transcripts showed down-regulation (trypsin and HSP70) or up-regulation (complement Factor H and coagulation factor) by sequencing but no differential expression by qRT-PCR. The same is true for statistical significance: in IRE/CVTM19 statistical significance agreed well with the HiSeq2000 sequencing analysis whereas in IDE8 none of the transcripts were statistically significantly expressed by qRT-PCR analysis. Overall, with the exception of only a few transcripts, qRT-PCR analysis confirmed differential expression patterns detected by the HiSeq2000 sequencing analysis.

4.5 Summary of findings

- The RNA quality check on heat-denatured RNA isolates using the Agilent Bioanalyzer revealed the lack of a 28S rRNA peak in the electropherogram of all tested tick cell samples.
- TBEV infection was verified in infected samples used for transcriptomic and proteomic analysis. Mock-infected samples were verified as non-infected prior to transcriptomic and proteomic analysis. Infection status was further verified by the presence of reads, approximately 3% in IDE8 and 4-8% in IRE/CTVM19, mapping to TBEV in TBEV-infected samples only. Furthermore, TBEV proteins were identified in TBEV-infected samples in both cell lines at both days 2 and 6 p.i..
- Only a small number of cellular transcripts (IDE8 2d: 22, 6d: 21; IRE/CTVM19 2d: 40, 6d: 43) and cellular proteins (IDE8 2d: 52, 6d: 24; IRE/CTVM19 2d: 20, 6d: 109) were statistically significantly differentially regulated upon TBEV infection. Of these, at both time-points, more transcripts were down-regulated than up-regulated in IDE8 cells while more transcripts were up-regulated than down-regulated in IRE/CTVM19 cells. At the protein level, more proteins were underrepresented than overrepresented in IDE8 at day 2 and IRE/CTVM19 at day 6 p.i..

- Transcripts statistically significantly up-regulated upon TBEV infection are involved in a variety of cellular processes. In IDE8 cells most transcripts are possibly involved in metabolism and transport. Those statistically significantly up-regulated in IRE/CTVM19 cells upon TBEV infection are mostly involved in metabolism, innate immunity and nucleic acid processing.
- Transcripts statistically significantly down-regulated upon TBEV infection are involved in a variety of cellular processes. In IDE8 cells most transcripts are possibly involved in cell stress, nucleic acid processing, protein folding and metabolism. Those statistically significantly down-regulated in IRE/CTVM19 cells upon TBEV infection are mostly involved in cell stress and protein folding.
- Proteins statistically significantly overrepresented in tick cells infected with TBEV are involved in a variety of cellular processes. In IDE8 cells the biggest group are involved in nucleic acid processing. In IRE/CTVM19 the biggest groups of proteins are possibly involved in nucleic acid processing, transport, signalling, proteolysis and cell structure.
- Proteins statistically significantly underrepresented in tick cells infected with TBEV are involved in a variety of cellular processes. In IDE8 cells the biggest groups of proteins are involved in cell stress, nucleic acid processing, transport and cell structure. In IRE/CTVM19 the biggest groups of proteins are possibly involved in cell stress, nucleic acid processing and transport.
- qRT-PCR analysis confirmed the differential expression detected by the HiSeq2000 sequencing analysis, with most transcripts showing similar expression levels in both analyses or at least the same pattern of expression.
- Several transcripts and proteins with a possible role in cell stress and the antiviral innate immune response were identified in the present study. Some of these were chosen for evaluation of their role during TBEV infection, results of which are presented in Chapter 5.

4.6 Discussion

Ticks are known to transmit an enormous variety of pathogens but knowledge about the vector-pathogen relationship in respect to immunity is very restricted. There are several transcriptomics (Heekin et al., 2013; Mercado-Curiel et al., 2011; Nene et al., 2004; Zivkovic et al., 2010b), functional genomics (Antunes et al., 2012; de la Fuente et al., 2007a) and proteomics studies (Cotté et al., 2014; Rachinsky, Guerrero & Scoles, 2007, 2008; Stopforth, Neitz & Gaspar, 2010; Villar et al., 2010a, 2010b) looking at the response of ticks to parasites and bacteria, but with regard to viruses to date only one transcriptomics study examined differential gene expression by microarray upon LGTV infection in *I. scapularis* salivary glands (McNally et al., 2012). The purpose of the present study was therefore to identify genes and proteins which might possibly be involved in the antiviral defence response based on the hypothesis that TBEV infection of tick cells leads to changes in their transcriptome and proteome profiles which will elucidate novel pathways possibly involved in the defence response against viruses. To achieve this goal, cell lines derived from two *Ixodes* spp. ticks, IRE/CTVM19 derived from the TBEV vector *I. ricinus* and IDE8 derived from *I. scapularis* which, although a closely related species, is not known to be a vector of TBEV but is the only tick with a sequenced and partially annotated genome, were infected with TBEV strain Neudoerfl. RNA and proteins were then extracted at days 2 and 6 p.i. and, after testing their quantity, quality (4.4.1.1) and infection status (4.4.1.2), were subjected to deep sequencing or MS analysis respectively. Interestingly the RNA quality check using the Agilent Bioanalyzer revealed only one peak corresponding to the 18S rRNA, whereas the 28S rRNA peak was missing. Since the RNA was heat-denatured prior to testing its quality, the absence of the 28S rRNA peak suggested that ticks might have a “hidden break” in the 28S rRNA similar to that observed in insects and other arthropods (Winnebeck, Millar & Warman, 2010) preventing the calculation of an RIN number, usually calculated by the Agilent software, for assessment of RNA quality. Upon heat-denaturation this “hidden break” in the 28S rRNA causes its disintegration resulting in two similar sized fragments which migrate close to the 18S rRNA peak and could be misinterpreted as degradation (Winnebeck, Millar & Warman, 2010). This was

however not reported by another tick transcriptomics study which also used the Agilent Bioanalyzer (McNally et al., 2012). A possible explanation for the different observations might be that, in contrast to the present study, McNally and co-workers did not heat-denature their RNA prior to testing RNA quality on the Agilent Bioanalyzer. The quality of RNA in the present study was therefore assessed by judging the gel-like image and electropherogram (Figure 4.4) produced by the Agilent analyser software as described in 4.4.1.1 and samples which showed degradation were excluded from further analysis.

Two or three samples from each cell line and time-point passed all quality checks at both the RNA and protein level. Pooled RNA samples were then sequenced by ARK-Genomics who provided the reference assembled IDE8 and the *de novo* assembled IRE/CTVM19 transcriptome together with raw count data for differential expression analysis using DESeq and sequences for annotation. The sequenced, annotated and differentially represented proteome was provided by Dr. Margarita Villar-Rayo. Although the study was able to reveal possible immune-related genes and proteins in both tick cell lines at both time-points, several weaknesses in the study design and methodology have to be addressed.

A major limitation of the present study was the lack of biological replicates, due to funding constraints, since although samples were derived from several individual samples only one pooled aliquot per time-point per cell line was subjected to transcriptomic and proteomic analysis which makes the interpretation of biological relevance difficult. A higher number of biological replicates would have provided more confidence in the p-values obtained using DESeq in the case of RNA, and X^2 test in the case of protein. In the case of DESeq, the protocol allows for calling significance in samples without replicates (Anders & Huber, 2010), and has been used as such in another published study (Bonizzoni et al., 2012). It uses the assumption that only a few genes will be differentially expressed between conditions, which makes it valid to use the two samples as replicates of each other. This assumption leads to a very conservative estimation of variance and reduces the number of transcripts which will be called statistically significant in comparison to experiments with more replicates (Anders & Huber, 2010). This means that, by

focusing on only statistically significantly differentially expressed transcripts, some which might be important in the antiviral defence response in ticks will certainly be excluded but all included transcripts are strongly supported by this analysis.

Programmes used for estimating differential expression of RNA-Seq data are constantly evolving and some of these have recently been found to be better suited for the task of calling differentially expressed transcripts by taking into account that some genes encode a number of differentially expressed isoforms which might hide or overestimate the true differential expression (Trapnell et al., 2013). The count data used for differential gene expression analysis in the present study was provided by ARK-Genomics, who generated the count data by only counting reads which mapped unambiguously to one transcript. This approach is more likely to lead to an underestimation of the true transcript expression since only a few reads will map unambiguously to different transcript isoforms which share a common part. It has to be noted though, that in the present study the majority of reads mapped unambiguously, so only a very few transcripts should be affected by underestimation. Nevertheless, this would affect both conditions, the mock-infected and TBEV-infected samples, and only create a problem if there was a true shift of isoforms between the different conditions. A comparison of DESeq and cuffdiff2 data with qRT-PCR data revealed that fold changes produced by both were accurate and that sensitivity of DESeq is similar to cuffdiff2 when no isoform switching occurs (Trapnell et al., 2013). There is however no knowledge about how many genes in ticks are affected by alternative splicing resulting in several transcript isoforms, thus the impact of analysing the data with only DESeq is difficult to estimate. Interestingly, the use of both Cuffdiff and DESeq at the gene level in a transcriptomics study without biological replicates resulted in very different numbers of genes called statistically significant by each of the programmes (Bonizzoni 2012) with DESeq applying a more conservative approach. This study highlights the fact that it might be useful and necessary to use several differential expression tools and to focus on those transcripts common to both; however this was not done in the present study because of time constraints.

To verify sequencing data, 12 transcripts were chosen from the list of statistically differentially expressed transcripts and proteins for qRT-PCR analysis (4.4.7). Most of the 12 transcripts showed similar fold changes when compared to the results obtained by RNA-Seq (Figure 4.13) in both cell lines at both time-points, with five out of seven transcripts confirmed as statistically significant in IRE/CTVM19. In IDE8, although fold changes were similar none of the four transcripts that were statistically significant by sequencing were confirmed as statistically significant by qRT-PCR. This was surprising in the case of CD36, which showed a high fold change, 2.6 at day 2 and 3.4 at day 6, during qRT-PCR. A possible explanation at least for the sample from day 2 might be that due to the number of biological replicates, with only two in the control group but three in the infected group, replicate numbers might have been too low for the statistical test used or that the variation between individual samples, as indicated by the standard error, was too high. Another possibility is that the transcripts called statistically significant by DESeq were false positives. Most of the transcripts as already mentioned above showed similar fold changes or at least confirmed the trend seen in the sequencing data. Complement Factor H however showed in both cell lines a much higher fold change during qRT-PCR than during the RNA-Seq. This discrepancy could be explained if this gene results in alternative splice variants which might have been underestimated in the RNA-Seq experiment by the count method applied, as described above. This however does not explain the difference in fold change for coagulation factor in IDE8 at day 6 p.i. which was higher in the sequencing data than in the qRT-PCR, unless a complete shift of transcript isoforms occurred with only one isoform present in the infected sample and several in the uninfected sample. If such a complete shift occurred, sequencing data would underestimate the number of this isoform in the mock-infected control. However, there is currently no information about different splice variants for either of these genes. Apart from splice variants, other factors such as preparation methods, primer design, reference genes and different normalisation methods can influence the correlation between these two methods (Devonshire et al., 2013). However, overall there was good agreement between the RNA-Seq data and the qRT-PCR data as the fold change usually showed

the same direction. Similar observations were also reported in other transcriptomics studies (Hegedus et al., 2009; Zeng et al., 2013; Zhu et al., 2013).

The transcript data also revealed several contigs/transcripts which did not show any homology to existing tick, arthropod or mammalian datasets. This lack of homology has also been reported in other tick studies (Gibson et al., 2013; de la Fuente et al., 2007a; McNally et al., 2012) and could be attributed to different factors such as low sequence quality, low assembly quality, that these sequences are novel transcripts which are tick species-specific or that the lack of homology to the *I. scapularis* genome is due to the fragmented state of the current genome assembly where gene regions are split across scaffolds (Gibson et al., 2013). The possible reasons for the high proportion of non-annotated contigs in the present dataset were however not analysed further and contigs without sequence hits were ignored since their analysis would fall outside the scope of the present study. However further analysis of the non-annotated contigs might reveal novel transcripts which could be used to update the current *I. scapularis* genome and augment the available tick transcriptome data for other researchers.

Although the transcript data presented in the present study is not without limitations, by annotating all the transcripts which are more than $\log_2$ 2-fold differentially expressed, but only focusing on those which are statistically significantly differentially expressed it was possible to narrow down the transcript list to a manageable size. From this list of statistically significantly differentially expressed transcripts, target genes with a possible role in antiviral immunity of ticks such as HSPs, calreticulin, ER based chaperones, CD36, complement Factor H, serine protease (trypsin), peroxinectin and a coagulation factor could be identified. Differential expression of some of these was also verified by qRT-PCR.

The isolated protein extracts, as assessed by SDS-PAGE and Coomassie staining (Figure 4.5), showed no obvious protein degradation but clear and distinct bands and were assumed to be suitable for quantitative MS analysis.

The protein dataset revealed that slightly more proteins were identified for IRE/CTVM19 than for IDE8 which suggests a tick species-specific difference in

response to TBEV rather than an influence of the database on identification. Although more protein sequences are available for *I. scapularis* than for *I. ricinus* in the UniProt database, the majority of hits obtained for *I. ricinus* were to *I. scapularis*. Furthermore the number of peptides used for the identification of both was almost identical which further excludes the influence of a bias introduced by the database composition, thus allowing comparative quantitative proteomics.

Due to the limited amount of protein, only IRE/CTVM19 samples were subjected to differential representation by both 2D-DIGE and label-free quantitative MS, whereas IDE8 samples were only subjected to MS analysis. Interestingly, only label-free quantitative MS analysis was able to detect differentially represented proteins whereas none of the proteins were differentially represented in 2D-DIGE. Possible explanations could be the lower sensitivity of 2D-DIGE compared to MS (Bantscheff et al., 2007; Patterson & Aebersold, 2003; Zhu, Smith & Huang, 2010), since proteins with low abundance or high molecular weight, hydrophobic proteins and proteins with extreme isoelectric points will be poorly represented on a 2D-DIGE gel (Lilley & Friedman, 2004; Villar et al., 2012). Another possible explanation would be that some proteins co-migrate because they have similar isoelectric points and molecular weights (Lilley & Friedman, 2004; Zhu, Smith & Huang, 2010) and thus resolve within the same spot on the 2D-DIGE gel, thereby masking differential representation. Furthermore, TBEV might only lead to subtle changes in protein expression between mock-infected and infected cells which were missed by DIGE but detected by MS analysis. Possibly a combination of all the above-mentioned factors might be involved in the present study, although other studies carried out on ticks infected with bacteria were able to detect differential expression by 2D-DIGE. Further repetitions of the 2D-DIGE test would be required, to exclude other possible influences such as sample preparation procedures.

A definite strength of this study is the use of both transcriptomic and proteomic data, and although the two datasets did not necessarily correlate well at the transcript and protein level this was not really surprising since it was also seen in previous studies (de la Fuente et al., 2007a; Villar et al., 2010a, 2010b). In those studies, as in the present study, the numbers, types and levels of mRNA and proteins were different in

response to pathogen infection. This difference might be explained by the different half-lives of mRNA and proteins, variation in the sensitivities of each method (de la Fuente et al., 2007a; Villar et al., 2010a, 2010b) and post-transcriptional regulation of some proteins (Villar et al., 2010a, 2010b).

By integrating these two approaches however, it was obvious that TBEV was not only infecting both tick cell lines, as seen by TBEV RNA present before (Figure 4.6) and after sequencing (4.4.2.2) but the TBEV RNA was also translated as seen by the presence of TBEV proteins (4.4.3.1) in the proteomic data set. Lower amounts of viral RNA and protein were present in IDE8 cells compared to IRE/CTVM19 cells, which was in accordance with the lower amount of infectious viral particles produced by IDE8 (Figure 3.10). Interestingly the percentage of TBEV RNA increased from day 2 to day 6, whereas the amount of TBEV protein stayed similar. This might suggest that translation of TBEV RNA in IRE/CTVM19, but not in IDE8, is the limiting factor leading to a reduction of infectious virus particles observed in the TBEV growth curve from day 3 to day 10 (Figure 3.10). This was also accompanied by the underrepresentation in IRE/CTVM19 of several proteins involved in the translation process such as EF-1 alpha and translation initiation factor 3 at day 2 and EF-2, t-RNA synthasen and EF-2 interacting protein at day 6 p.i.. This underrepresentation suggests a role for these proteins either directly or indirectly in the antiviral immune response of tick cells. However it has to be mentioned that some proteins involved in translation such as EF-1 alpha and initiation factor 2 subunit are overrepresented at day 6 p.i.. Further research would be required to elucidate the true meaning of differential expression of these proteins in the antiviral response. Nevertheless this highlights another strength of this study, that using two time-points for each cell line helps to elucidate intricate patterns of cell response at both mRNA and protein levels caused by different stages of the virus life-cycle such as early and late infection. However this was not the main focus of the present study and would require more research to elucidate the possible role of each transcript during virus infection. It would also be interesting to test whether this difference in response between IRE/CTVM19 and IDE8 cells is due to the fact that the former is derived from a vector tick species whereas the latter is derived from a tick species

not known to naturally transmit TBEV. To draw any conclusions in respect to vector/non-vector response both transcriptomes should be assembled in the same way and annotated completely to reduce any biases in transcript selection by applying different techniques to both, which was not done in the present study. Unfortunately due to the lack of similiarity between the *I. ricinus* and *I. scapularis* genomes whereby only approximately 30% of the reads from *I. ricinus* mapped to *I. scapularis*, it was decided to *de novo* assemble the transcriptome of IRE/CTVM19 while the IDE8 transcriptome was assembled by mapping to the *I. scapularis* genome. Furthermore only the differentially expressed transcripts were annotated and not the whole transcriptome because of time constraints. It is also interesting to note that, in tick cells, virus RNA and protein made up only a small percentage of the total RNA (2.84% - 7.7%) and protein (1.64% - 2.03%) within the cell. This is in contrast to what was observed in mammalian cells upon influenza virus infection, where viral RNA made up 20 - 40% of the total RNA content (Varich et al., 1981), but similar to what was observed in mosquitoes in which SFV made up approximately 1.65% of the total RNA (Rodriguez, 2012).

By combining the results of protein and transcript data from both cell lines at both time-points, the present study was able to reveal intriguing patterns of differential expression that suggest a broad impact of TBEV infection on tick cells. Differentially represented proteins were involved in a variety of biological processes including metabolism, cell structure, transportation, immunity, protein folding, cell stress and nucleic acid processing. A majority of these transcripts and proteins identified as differentially expressed in the present study were also differentially represented in studies of mosquitoes upon virus infection (Bonizzoni et al., 2012; Sim & Dimopoulos, 2010; Zhang et al., 2013). Although some of these studies showed different directions of representation, this might be attributed to different sampling times, different species and/or *in vivo* versus cell line usage. Nevertheless, some of the differentially expressed transcripts or represented proteins identified in the present study have been implicated, as discussed above, to be important during different processes of the viral life cycle, including endocytosis, trafficking, maturation and RNA replication and translation.

Furthermore, some transcripts and/or proteins possibly involved in immune-related pathways such as the ubiquitin-proteasome pathway, phagocytosis, complement system, RNAi with the piRNA pathway, or the UPR, were differentially represented. Of these pathways phagocytosis, the complement system and the ubiquitin-proteasome pathway have been shown to be important for the antimicrobial defence response in ticks (Choy et al., 2013; Hajdušek et al., 2013; Kopácek et al., 2010; Kopacek, Hajdusek & Buresova, 2012; Severo et al., 2013a; Taylor, 2006); however nothing is known about their role in the antiviral response in ticks. Inhibition of the ubiquitin-proteasome pathway in mammalian and mosquito cells revealed that flaviviruses require a functional ubiquitin-proteasome pathway for the amplification of viral RNA (Fernandez-Garcia et al., 2011); thus the down-regulation of several components of this pathway at day 6 p.i. in IRE/CTVM19 might suggest a host cell response trying to prevent further TBEV replication. Phagocytosis on the other hand has been shown to be a key innate immune pathway involved in protecting shrimps from virus infection (Wang & Zhang, 2008) and since several components possibly regulating phagocytosis, as mentioned above, were differentially represented in the present study, phagocytosis might also be important in the antiviral response in ticks. The complement system in mammals is a crucial component of the innate and adaptive immunity shown to be active against viruses, and viruses have also evolved to evade it (Blue, Spiller & Blackbourn, 2004; Favoreel, 2003; Hirsch, 1982; Lachmann & Davies, 1997). Although a primitive complement system with a role in antimicrobial defence in ticks and other arthropods has been found, there is no knowledge available on its antiviral function. Similarly, nothing is known about the antiviral role of the UPR or ER stress in ticks or mosquitoes, but studies on mammalian cells suggest a possible role of ER stress and the UPR during SFV and DENV infection (Barry et al., 2010; Doolittle & Gomez, 2011). Since several ER resident chaperones and proteasome subunits, but no homologues to other members of the UPR pathway, were differentially expressed this pathway might or might not play a role in ticks.

Though RNAi is probably one of the most important antiviral pathways in arthropods, and many of the components are present in ticks (Kurscheid et al., 2009),

none apart from the Tudor-SN protein were differentially represented in the present study. The reason might be that either RNAi components are not differentially represented upon TBEV infection or just not at the two time-points chosen in the present study. However, this lack of differential expression of RNAi components is in accordance with studies in other arthropods, such as mosquitoes (Waldock, Olson & Christophides, 2012; Xi, Ramirez & Dimopoulos, 2008) and *Drosophila* (Dostert et al., 2005), which concluded that components of the RNAi defence systems are likely to be constitutively expressed and thus do not require transcriptional induction upon viral challenge, or that viruses actively suppress transcription of such transcripts as a defence mechanism (Waldock, Olson & Christophides, 2012; Xi, Ramirez & Dimopoulos, 2008). Interestingly Cniwi, a protein of the RNAi piRNA pathway which has recently been shown to be involved in the antiviral response in mosquito cells upon SFV infection (Schnettler et al., 2013a), was differentially represented in IRE/CTVM19 at day 6 p.i..

It is obvious from the present study that virus infection changes gene expression and protein representation in tick cells and that RNAi is not the only mechanism involved in the antiviral response in ticks. However to elucidate the functional role of the differentially expressed transcripts and proteins identified in this study further experiments and research are required. The present study however could be used as starting point to elucidate the cellular mechanisms behind virus infection in tick cell lines and ticks.

To start to elucidate the role of some of the differentially expressed transcripts and/or differentially represented proteins during virus infection in tick cells, a small selection of genes/proteins involved in cell stress and immunity were selected for knockdown experiments. Results of knockdown experiments for the selected genes/proteins, which include calreticulin, gp96, HSP70, HSP90, peroxinectin, trypsin, coagulation factor and complement Factor H, are presented in the next chapter.

5 Chapter 5 Functional role of genes differentially regulated in tick cells during arbovirus infection

5.1 Introduction

RNAi is a popular reverse-genetics tool for post-transcriptional gene silencing in a number of different species of plants, fungi, vertebrates and invertebrates (Cogoni & Macino, 2000; Shi, 2003). Gene silencing by the RNAi pathway is triggered by exogenous dsRNA molecules which are cleaved by the enzyme Dcr into siRNAs (Bernstein et al., 2001; Lee et al., 2004). These siRNAs are loaded into the RISC which then, using the siRNA as a guide, sequence-specifically cleaves target mRNAs (Rand et al., 2004) resulting in gene silencing.

Since the first successful application of RNAi in ticks (Aljamali, Sauer & Essenberg, 2002), it has become a valuable research tool for studying tick gene function, characterising the tick-pathogen interface and screening for tick-protective antigens (de la Fuente et al., 2007b). Different techniques such as manual injection, immersion, artificial feeding (de la Fuente et al., 2007) and electroporation (Karim, Troiano & Mather, 2010) have been exploited for the introduction of dsRNA into whole ticks through which comprehensive and relatively long-term gene silencing, for several weeks (Nijhof et al., 2007), can be achieved. Furthermore it has also been shown that silencing in female ticks can be carried over to their progeny (Kocan, Manzano-Roman & de la Fuente, 2007; Nijhof et al., 2007). RNAi has been successfully applied not only to whole ticks but also for determining the functional role of tick genes during pathogen infection in tick cell lines derived from *I. scapularis* (de la Fuente et al., 2007a), *I. ricinus* (Pedra et al., 2010) and *R. microplus* (Zivkovic et al., 2010b). A recent study established optimised parameters for RNAi-based gene silencing in a panel of different tick cell lines (Barry et al., 2013). Overall, previous studies showed that RNAi is a powerful tool for elucidating the role of gene function in ticks and tick cell lines. In the present study RNAi will therefore be used to silence some of the differentially-represented genes identified by transcriptomics and proteomics to further characterise their possible role during the antiviral defence response in tick cell lines.

5.2 Objective

- To determine the functional role of genes differentially regulated during arbovirus infection.

5.3 Experimental set-up

To evaluate the role of some of the differentially-regulated genes described in Chapter 4, knockdown experiments were carried out during virus infection. In brief, dsRNA molecules were produced with a T7 RNA polymerase *in vitro* transcription kit using PCR products (2.4.11), specific for each cell line, as template. Since adding any dsRNA might trigger RNAi and potentially additional immune responses, as observed in other arthropods (Flenniken & Andino, 2013; Pitaluga, Mason & Traub-Cseko, 2008; Robalino et al., 2007), dsRNA derived from an eGFP (615 bp) PCR product was used as a negative control, to provide a baseline level of activation above which the effect of the specific exogenous dsRNA was measured. Knockdown experiments were optimised by using species-specific primer sets for generating dsRNA (407-555 bp). These were tested in both cell lines, and only those dsRNAs resulting in knockdowns were used in subsequent experiments.

Both cell lines, IDE8 and IRE/CTVM19, were seeded at a density of $5x10^5$ cells per well in 24-well plates. To achieve a good knockdown in IDE8, 300 ng of dsRNA was added twice to the supernatant, at 8 h and 48 h post-seeding. Approximately 72 h after seeding, cells were transfected with either LGTV replicon E5repRluc2B/3 or TBEV replicon C17Fluc-TAV2A (2.5.3, 2.5.5). Growth curves for both replicons were established previously (Figure 3.15). At 24 h p.t. the supernatant was discarded and the cells lysed for luciferase assay (2.6). Negative controls were either transfected with replicon without dsRNA treatment or were treated with dsRNA coding for eGFP and transfected with replicon. For infection experiments, IDE8 cells were infected with wild-type LGTV at MOI 0.5 or 0.01 and at 24 or 48 h p.i. respectively, supernatant was collected for plaque assay and cells were harvested for RNA extraction using TRI Reagent (2.4.7).

For IRE/CTVM19 cells, knockdowns were only achieved by transfecting dsRNA into cells (Barry et al., 2013), which prevented the use of replicons since the cells did not tolerate a second transfection. In brief, IRE/CTVM19 cells were seeded and 24 h later were transfected with 400 ng dsRNA using Lipofectamine2000 as transfection reagent. After incubation for a further 48 h, cells were infected with LGTV at MOI 0.5. At 24 h p.i supernatant was collected for plaque assay and RNA was extracted using TRI Reagent.

Aliquots of extracted RNA samples, corresponding to 1 µg each, were reverse-transcribed (2.4.10.2), and the resulting cDNA was diluted 1:5 for knockdown validation and determination of LGTV NS5 expression by qPCR. cDNA derived from samples in which dsRNA coding for Ago (Ago-16, Ago-30), Dcr-90 or peroxinectin (IDE8 only) were used was divided in half. One half was diluted 1:5 for the determination of LGTV NS5 by qPCR (2.4.10.4; Table 2.5); the other half was kept undiluted and 2 µl of the undiluted sample was used for conventional PCR (2.4.10.1) using 30 cycles to establish if genes were knocked down.

5.4 Results

5.4.1 Why use LGTV instead of TBEV?

Since the Neudoerfl strain of TBEV, propagated in suckling mouse brain, was only available for experiments that I carried out in the Czech Republic, TBEV was grown from the plasmid pTND/c, kindly provided by Professor Franz X. Heinz as described in 2.5.2. The supernatant of plasmid-derived TBEV, passaged twice through BHK-21 cells, was used in attempts to titrate the virus in BHK-21, BSR and PS cells. However, none of the plaque assays resulted in countable plaques.

To test whether the supernatant actually contained infectious virus particles, BHK-21 cells were immunostained for TBEV. In brief, cells were seeded at a density of $3x10^5$ cells per well on coverslips in a 6-well plate 24 h prior to infection. 500 µl of supernatant of the second passage in BHK-21 cells was then used to infect new BHK-21 cells, which were incubated for a further 24 h prior to removing the

supernatant and fixing in neutral buffered paraformaldehyde for 4 h. Uninfected cells were treated in the same way. The fixed cells were immunostained with TBEV E or NS1 protein antibodies using the protocol described in 2.7, without the SDS permeabilisation step, before images were taken on the Axiovert Observer D1 inverted microscope (Figure 5.1).

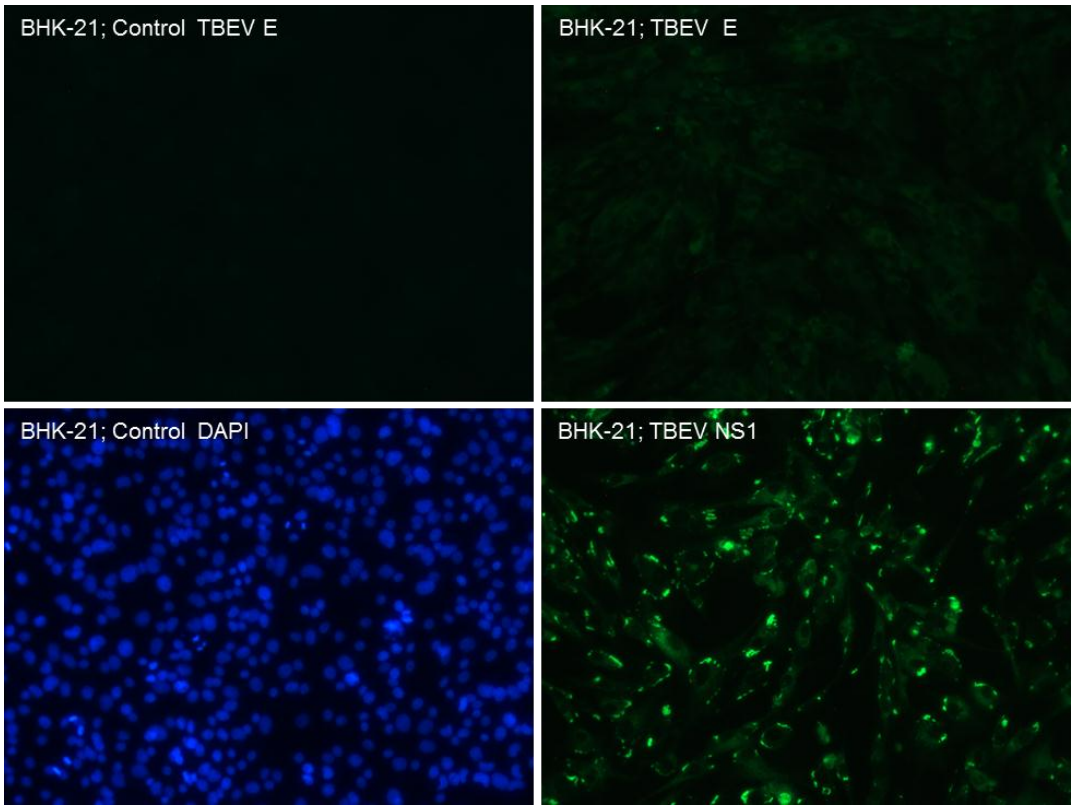

Figure 5.1 Immunostaining of plasmid-derived TBEV-infected BHK-21 cells with TBEV E protein or NS1 protein antibodies

BHK-21 cells were infected with supernatant containing plasmid-derived TBEV passaged twice through BHK-21 cells. Uninfected control cells (left panel) and infected cells (right panel) were fixed in neutral-buffered formaldehyde 24 h p.i. and immunostained with either TBEV E protein (top panel) or TBEV NS1 protein (bottom panel) antibodies and then with DyLight 488 secondary antibody (green). Nuclei were stained with DAPI (blue). Images were taken using the Axiovert Observer D1 inverted microscope at 200x magnification with UV illumination.

Both TBEV E protein and NS1 protein staining revealed the presence of TBEV proteins in infected BHK-21 cells in contrast to the uninfected controls which did not show any green fluorescence (Figure 5.1).

Another round of plaque assays done in BHK-21, BSR and PS cells, testing different overlays such as agar, Avicel and agarose, were however still unsuccessful in

revealing any virus plaques. Due to the inability to quantify TBEV particles by plaque assay and time constraints, it was decided to use LGTV instead of TBEV for evaluating the role of the differentially-expressed transcripts identified in the previous chapter. LGTV is a naturally attenuated virus (Price et al., 1963; Smith, 1956), which shares a high homology with the CL3 pathogen TBEV and is likely to be regulated by the same immune responses. It has the advantage over TBEV that it can be used at CL2.

5.4.2 Effect of gene knockdown on virus replication using virus replicons

To elucidate the role of differentially-expressed transcripts during virus replication, transcripts coding for complement Factor H, coagulation factor, HSP90, HSP70, peroxinectin, trypsin, calreticulin and gp96 were silenced using dsRNA and subsequently transfected with reporter (luciferase) replicons of LGTV or TBEV. Furthermore, Ago-16 and Ago-30, orthologues of insect-Ago-2 proteins (Schnettler et al., 2014) involved in the antiviral exogenous siRNA pathway in insects (Keene et al., 2004; van Rij et al., 2006), were included as positive controls for silencing while dsRNA coding for eGFP was used as a negative control. Silencing could not be verified for each well due to the requirement to lyse the cells for luciferase assay, but subsequent experiments involving knockdown of these transcripts (Figure 5.3, Figure 5.5) revealed a consistent knockdown, at least for some of them.

When the LGTV replicon was transfected into silenced IDE8 cells, a significant increase in replicon Rluc activity (Figure 5.2 A) was seen in cultures treated with dsRNA specific for Ago-30, coagulation factor, trypsin, calreticulin, HSP90 and gp96-2. The greatest increases in Rluc expression, more than 2-fold relative to the negative controls, were observed for calreticulin, HSP90 and trypsin. Silencing of peroxinectin on the other hand resulted in a significant decrease in Rluc expression compared to control dsRNA.

In contrast, when the TBEV replicon was transfected into silenced IDE8 cells, a significant increase in Fluc expression was only observed for Ago-30 and Ago-16 (Figure 5.2 B).

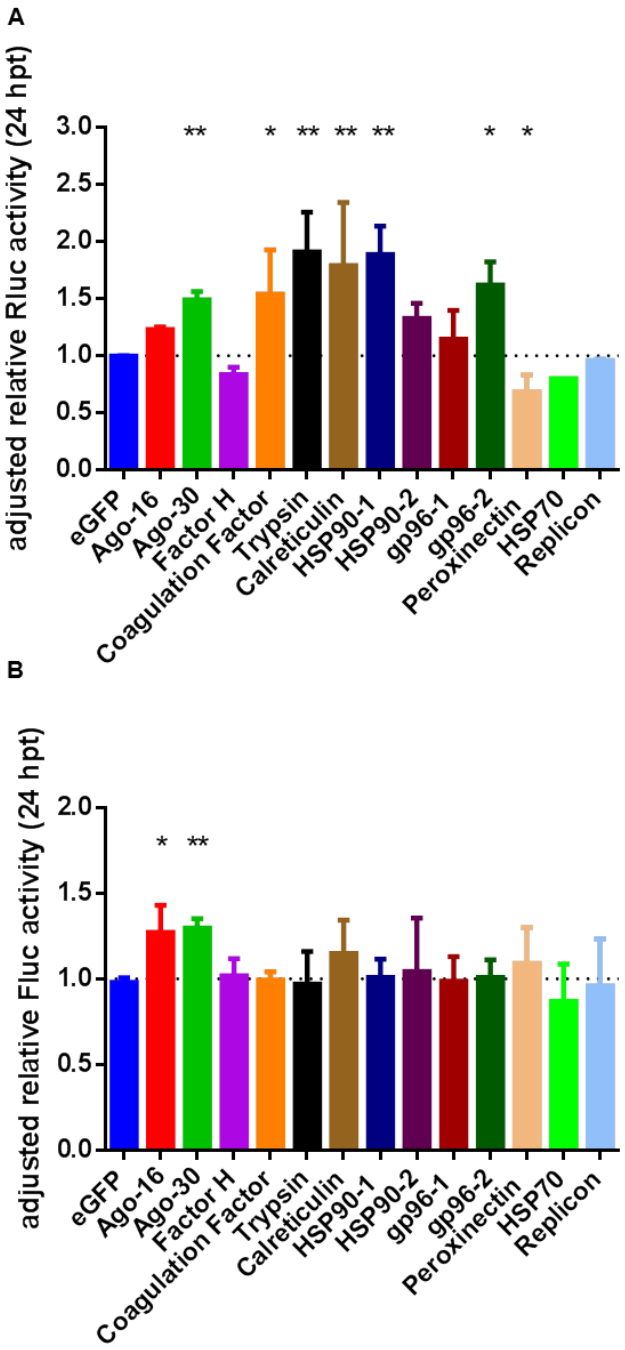

Figure 5.2 Effects of transcript knockdown on LGTV and TBEV replicon replication in IDE8 cells

Silenced IDE8 cells were transfected with capped *in vitro*-transcribed LGTV E5repRluc2B/3 replicon (A) or TBEV C17Fluc-TAV2A replicon RNA (B), and luciferase activity was determined 24 h p.t.. Adjusted light units represent light units minus background luminescence calculated from uninfected control cultures. The mean fold change with standard error of two independent experiments performed in triplicate or quadruplicate is shown. HSP70 was only tested once in quadruplicate. The data was normalised to cells treated with eGFP-specific control dsRNA. Statistical significance was calculated using a two-way ANOVA Fisher's LSD test (* $p<0.05$ ** $p<0.001$)

5.4.3 Effect of gene knockdown on LGTV replication and production in IDE8 cells

In order to further investigate the effect of silencing of the above-mentioned transcripts on virus infection, IDE8 cells were infected with wild type LGTV at MOI 0.5 (Figure 5.3, Figure 5.4) or 0.01 (Figure 5.5, Figure 5.6). These two low MOIs were chosen to allow virus spread through the culture. As previously established by immunostaining, approximately 97% of cells were positive for LGTV NS5 protein at day 2 p.i. (3.4.1), and LGTV replication as determined by qRT-PCR was detected at 24 h p.i. in IDE8 cells infected with MOI 1 and at 48 h in IDE8 cells infected with MOI 0.05 (3.4.3, Figure 3.11). With both MOIs replication increased up to day 2 before levelling off. An MOI of 0.5 or 0.01 should thus allow virus spread and the detection of LGTV replication at 24 h p.i. or 48 h p.i., respectively.

In the case of IDE8 cells infected with MOI 0.5, supernatant and cells for RNA extraction were collected at 24 h p.i.. After reverse-transcription (2.4.10.2), aliquots of cDNA were used to determine the efficiency of gene silencing (Figure 5.3) by semi-quantitative PCR (2.4.10.1) or qPCR (2.4.10.4). Data were normalised against beta actin and efficiency was quantified relative to cells treated with control dsRNA. Cells treated with Ago-16, Ago-30, trypsin, calreticulin, HSP90-1 and -2 and gp96-1 and -2 showed a reduction in target transcript levels (30-97%) in all replicates. Complement Factor H, however, showed a reduction in transcript levels (38-46%) in three out of four replicates, while coagulation factor (28-36%) and peroxinectin (7-28%) only showed a reduction in two replicates out of four. In Figure 5.3 all 4 replicates are plotted, independent of whether knockdown was achieved or not, thus the apparent increases in gene expression compared to control dsRNA (eGFP) treatment measured for complement Factor H (x 1.14 ± 0.6) and coagulation factor (x 4.4 ± 3.7) were caused by the replicates in which no knockdown was achieved, indicated by the high standard error of the mean. This increase might result from detecting dsRNA which was introduced into cells for silencing, since this dsRNA might be less efficiently degraded than other dsRNAs. Additional explanations could be that complement Factor H and coagulation factor have efficient feedback

mechanisms within tick cells that counteract the RNAi response by increasing transcription, or that their mRNAs are more efficiently protected from RNases than those of other mRNAs which were targeted by dsRNA.

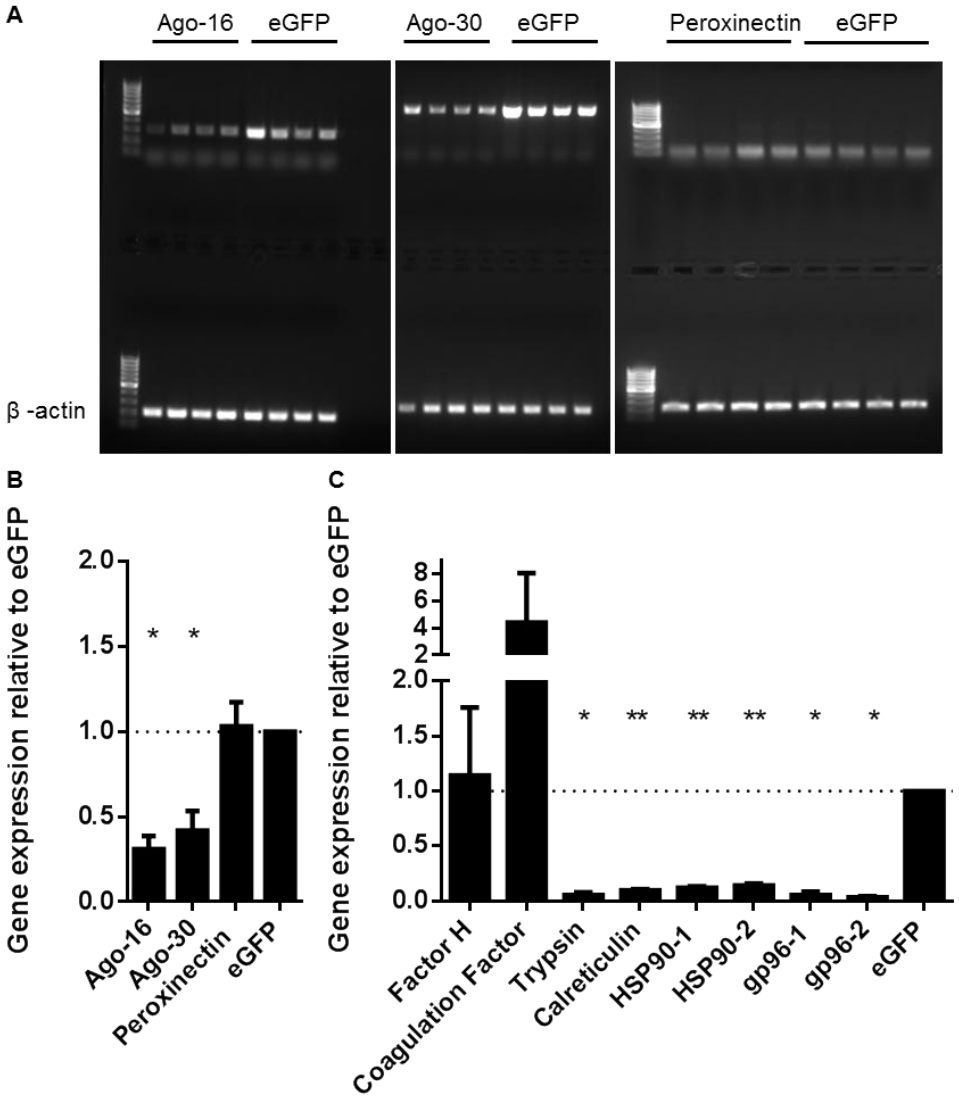

Figure 5.3 Knockdown of differentially-expressed tick gene transcripts in IDE8 cultures infected with LGTV at MOI 0.5

dsRNA-based silencing of differentially-expressed transcripts in IDE8 cells. Quantification was done by RT-PCR (A,B) or qRT-PCR (C). (A,B) Transcripts coding for Ago (Ago-16 and Ago-30) or peroxinectin were detected by RT-PCR using dsT7-Ago-16-2, dsT7-Ago-30 and peroxinectin primers. Gel-electrophoresis images were used to quantify mRNA knockdown with Image Lab software (BioRad) normalised to beta actin control. (C) mRNA knockdown quantification of transcripts by qRT-PCR. Gene expression levels were normalised to beta actin and relative to eGFP-dsRNA controls (B,C). Error bars indicate standard error of the mean for one experiment done in quadruplicate. Statistical significance was calculated using t-test with FDR < 5% (* $p<0.05$ ** $p<0.001$).

After validating knockdown, cDNAs of only those samples in which gene silencing was observed were used for determining LGTV RNA levels by qPCR relative to LGTV NS5 levels in cells treated with control dsRNA. No statistically significant changes in LGTV RNA levels were observed in any of the samples (Figure 5.4 A).

To test if knockdown might have an effect on LGTV production, supernatants containing virus, corresponding to tested RNA samples, were titrated by plaque assay. A statistically significant increase, although less than 1.5-fold, was observed in IDE8 cells silenced with HSP90-2 (Figure 5.4 B).

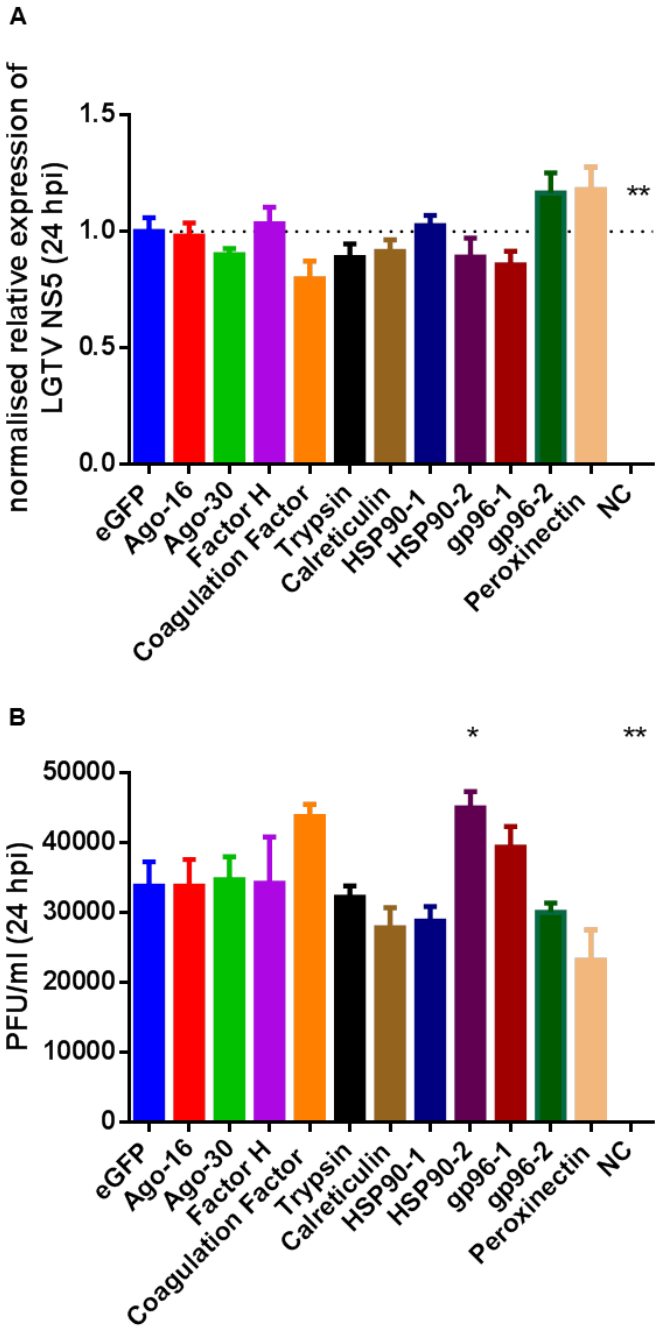

Figure 5.4 Effect of transcript knockdown on wild-type LGTV replication and production in IDE8 cells infected at MOI 0.5

Silenced IDE8 cells were infected with wild-type LGTV at MOI 0.5. (A) Viral RNA levels were determined by qRT-PCR using LGTV NS5 primers at 24 h p.i.. The data was normalised against beta actin and is presented as fold changes relative to eGFP dsRNA controls. (B) Infectious virus particles present in supernatant were titrated by plaque assay at 24 h p.i..The means with standard error are shown for one experiment, including only those samples in which knockdown was validated. (duplicate: coagulation factor, peroxinectin; triplicate: Factor H; quadruplicate: all others). Statistical significance was calculated using t-test with Welch correction (* $p<0.05$ ** $p<0.001$). NC: negative control.

Since knockdown of none of the above mentioned-transcripts apart from HSP90-2, not even the positive controls Ago-16 and Ago-30, showed any effect on virus replication and production , a lower MOI of 0.01 was tested at a later time-point . A lower MOI and later time-point should ensure that cells are not overloaded with virus at the beginning of the experiment and allow the virus to spread through the culture. Therefore if silencing of genes interferes with any step during virus infection, such as entry, replication, maturation or exit, changes should be more pronounced. Supernatants and RNA samples from LGTV-infected (MOI 0.01) IDE8 cells were collected at 48 h p.i. and processed as mentioned above.

Knockdown validation (Figure 5.5) revealed that, in cells treated with Ago-16, Ago-30, coagulation factor, trypsin, HSP90-1 and -2, gp96-1 and -2 or calreticulin, all four replicates showed silencing of target transcripts with an efficiency between 51 and 97%. In samples silenced with dsRNA coding for complement Factor H, target transcript reduction (43- 64%) was observed in three replicates, while only one replicate showed a reduction in target transcript expression for peroxinectin (34%) and HSP70 (33%). In Figure 5.5 all four replicates are plotted independent of whether knockdown was achieved or not, thus the apparent increases in gene expression compared to control dsRNA (eGFP) treatment measured for peroxinectin (x 1.1 ± 0.19) and HSP70 (x 9.28 ± 7.3) were caused by the replicates in which no knockdown was achieved, indicated by the high standard error of the mean. This increase might result from detecting dsRNA which was introduced into cells for silencing.

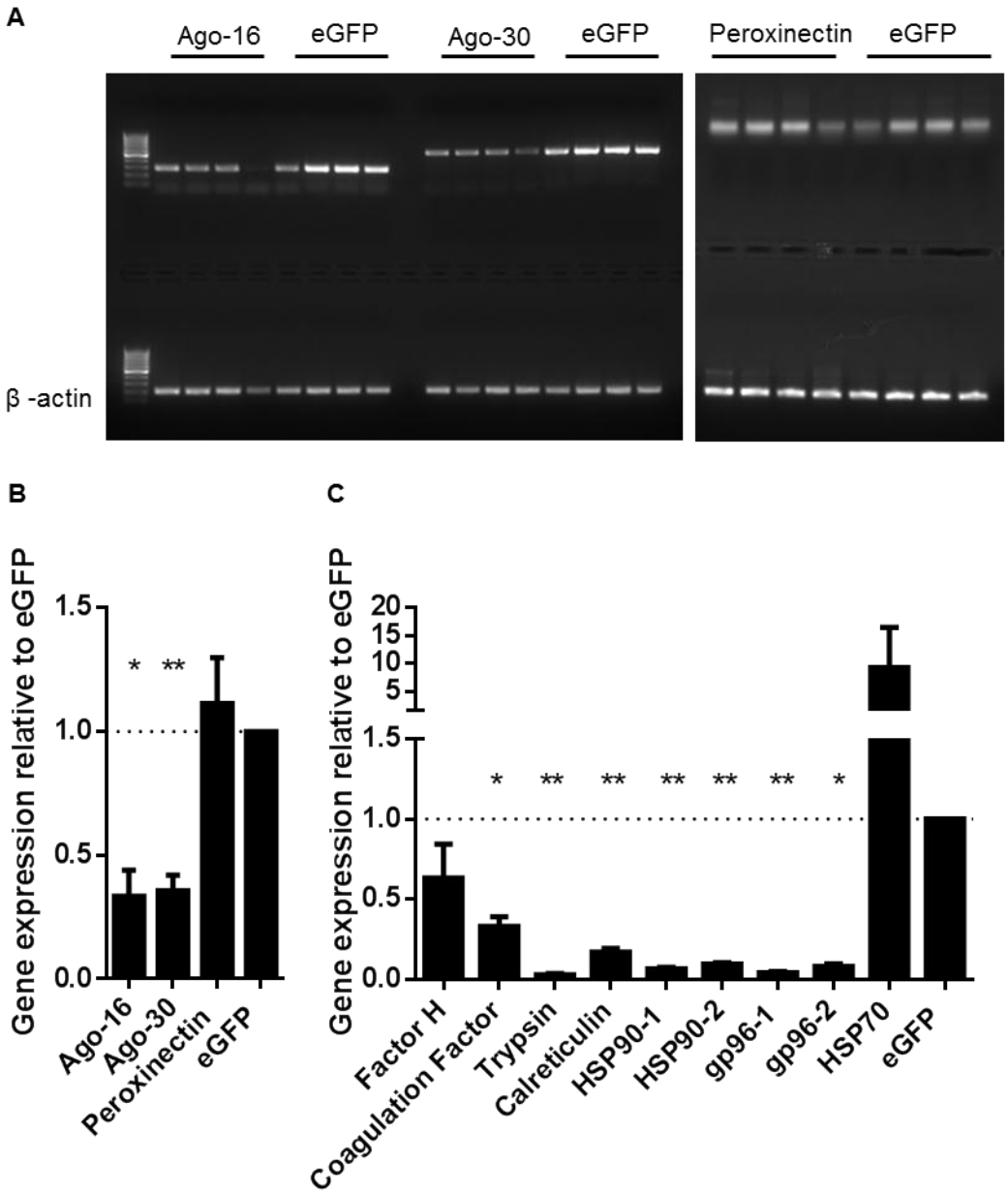

Figure 5.5 Knockdown of differentially-expressed tick gene transcripts in IDE8 cells infected with LGTV MOI 0.01

dsRNA-based silencing of differentially-expressed transcripts in IDE8 cells. Quantification was done by RT-PCR (A,B) or qRT-PCR (C). (A,B) Transcripts coding for Ago (Ago-16 and Ago-30) or peroxinectin were detected by RT-PCR using dsT7-Ago-16-2, dsT7-Ago-30 and peroxinectin primers. Gel-electrophoresis images were used to quantify mRNA knockdown with the Image Lab software (BioRad) normalised to beta actin control. (C) mRNA knockdown quantification of transcripts by qRT-PCR. Gene expression was normalised to beta actin and relative to eGFP-dsRNA controls (B,C). Error bars indicate standard error of the mean for one experiment done in quadruplicate. Statistical significance was calculated using t-test with FDR < 5% (* $p<0.05$ ** $p<0.001$).

Focusing on only those samples in which gene silencing was observed, LGTV RNA levels (Figure 5.6 A) significantly increased in cells treated with dsRNA coding for complement Factor H and gp96-2; this increase was accompanied by an increase in virus production (Figure 5.6 B). Interestingly, in this experiment untreated cells which were only infected with virus showed a significant increase in RNA levels (Figure 5.6 A) but not in virus production levels (Figure 5.6 B) compared to those treated with control dsRNA coding for eGFP, suggesting that dsRNA addition alone triggers RNAi or that cells which have taken up dsRNA are not as susceptible to infection as those which have not taken up dsRNA.

Virus production was also significantly increased in cells treated with dsRNA coding for Ago-16, Ago-30, calreticulin, trypsin and HSP90 (Figure 5.6 B); this was however not accompanied by an increase in virus RNA levels.

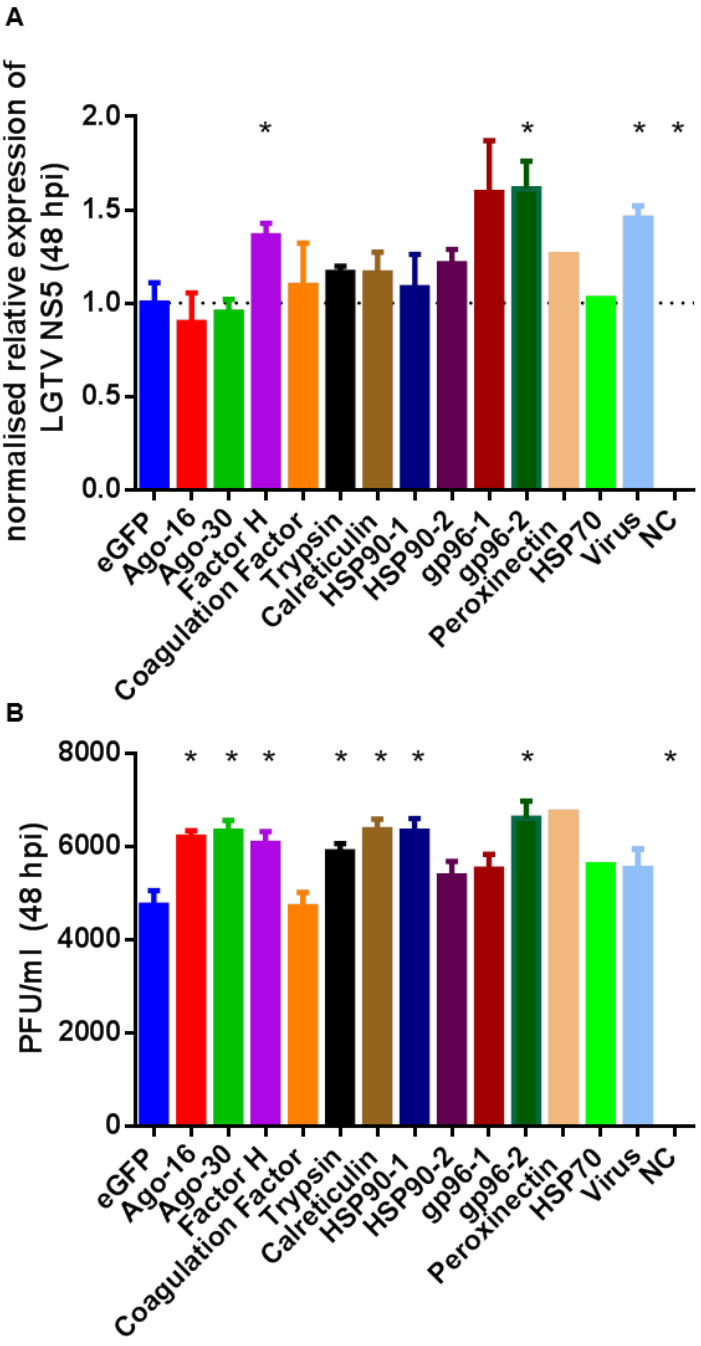

Figure 5.6 Effect of transcript knockdown on wild-type LGTV replication and production in IDE8 cells infected at MOI 0.01

Silenced IDE8 cells were infected with wild-type LGTV at MOI 0.01. (A) Viral RNA levels were determined by qRT-PCR using LGTV NS5 primers at 48 h p.i.. The data was normalised against beta actin and is presented as fold changes relative to eGFP dsRNA controls. (B) Infectious virus particles present in supernatant were titrated by plaque assay at 48 h p.i..The mean with standard error is shown for one experiment, including only those samples in which knockdown was validated. (singleton: peroxinectin and HSP70; triplicate: Factor H, virus and NC; quadruplicate: all others). Statistical significance was calculated using t-test with Welch correction (* $p<0.05$). NC: negative control

5.4.4 Effect of gene knockdown on LGTV replication and production in IRE/CTVM19 cells

For IRE/CTVM19 cells the effect of silencing of transcripts coding for Ago-30, Dcr-90, complement Factor H, calreticulin, peroxinectin, gp96, HSP90 and HSP70 during virus infection was investigated. Dcr-90 was included as a positive control, since it is an orthologue of Dcr proteins (Schnettler et al., 2014) that are known to be involved in the miRNA and siRNA pathways in insects. Due to the lack of sufficient sequences for Dcr proteins from different arthropod species it was not possible to determine if Dcr-90 is an orthologue of Dcr-1 (miRNA pathway) or the antiviral Dcr-2 (siRNA pathway). Some of the transcripts for which silencing was achieved in IDE8, such as coagulation factor, Ago-16 and trypsin, were not included in the experiments with IRE/CTVM19 since dsRNA designed for the respective IRE/CTVM19 sequences did not result in any measurable knockdown.

In brief, IRE/CTVM19 cells were infected with LGTV at MOI 0.5, supernatant was collected at 24 h p.i. and cells were harvested for plaque assay or RNA isolation. RNA samples and supernatant were processed and analysed as described for IDE8 (5.4.3). The experiment was repeated twice in quadruplicate.

Experiments in IRE/CTVM19 cells (Figure 5.7) revealed an overall lower knockdown efficiency compared to those achieved in both IDE8 experiments (Figure 5.3, Figure 5.5). Cells treated with Ago-30, HSP90, gp96 and peroxinectin showed a reduction in target transcript levels (16-85%) in all replicates (Figure 5.7). Dcr-90 however showed a reduction in transcript levels (5-36%) in three out of four replicates in both experiments, while calreticulin (15-33%) and complement Factor H (33-73%) showed a reduction in four replicates in one experiment and two replicates in the other. In cells treated with HSP70 dsRNA, silencing was only observed in two replicates in the first and one replicate in the second experiment with an efficiency of 8 - 30%.

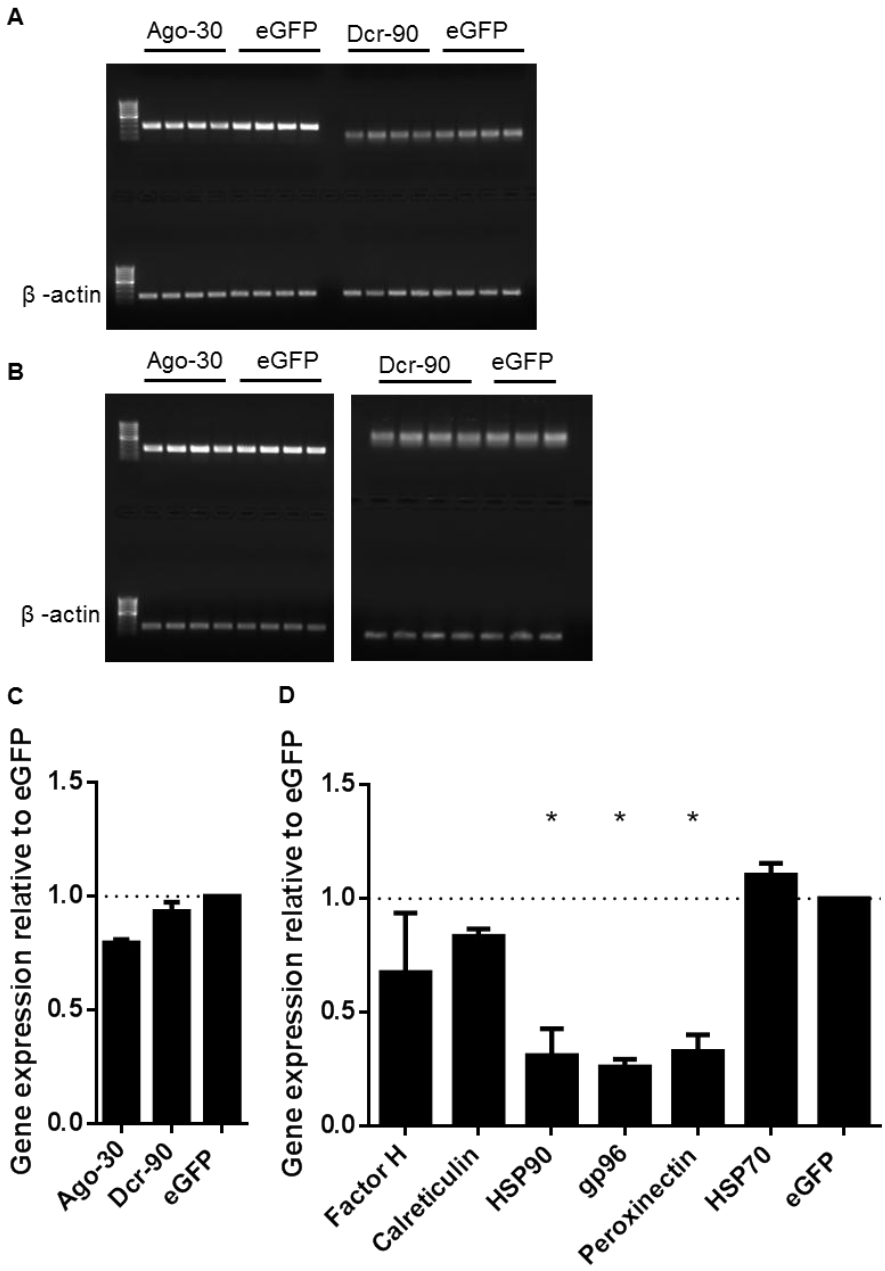

Figure 5.7 Knockdown of differentially-expressed tick gene transcripts in IRE/CTVM19 cultures infected with LGTV at MOI 0.5

dsRNA-based silencing of differentially-expressed transcripts in IRE/CTVM19 cells. Quantification was done by RT-PCR (A,B) or qRT-PCR (D). (A,B,C) Transcripts coding for Ago (Ago-30 and Dcr-90) were detected by RT-PCR using dsT7-Ago-30 or dsT7-Dcr-90 primers. Gel-electrophoresis images were used to quantify mRNA knockdown with the Image Lab software (BioRad) normalised to beta actin control. (D) mRNA knockdown quantification of transcripts by qRT-PCR. Gene expression was normalised to beta actin and relative to eGFP-dsRNA controls (C, D). Error bars indicate standard error of the mean for two independent experiments done in quadruplicate (gp96 triplicates in 2nd experiment) are shown. Statistical significance was calculated using two-way ANOVA Fisher's LSD test (* $p<0.05$, ** $p<0.001$).

Focusing on only those samples in which silencing was validated, knockdown of Ago-30 and Dcr-90 resulted in a significant increase in LGTV RNA levels as well as virus production (Figure 5.8). Interestingly, silencing of calreticulin resulted in a significant increase in virus RNA levels which was accompanied by, although not significant, a decrease in infectious virus particle production. As observed in IDE8 cells (Figure 5.6), IRE/CTVM19 cells treated with HSP90 and gp96 showed an increase in virus production.

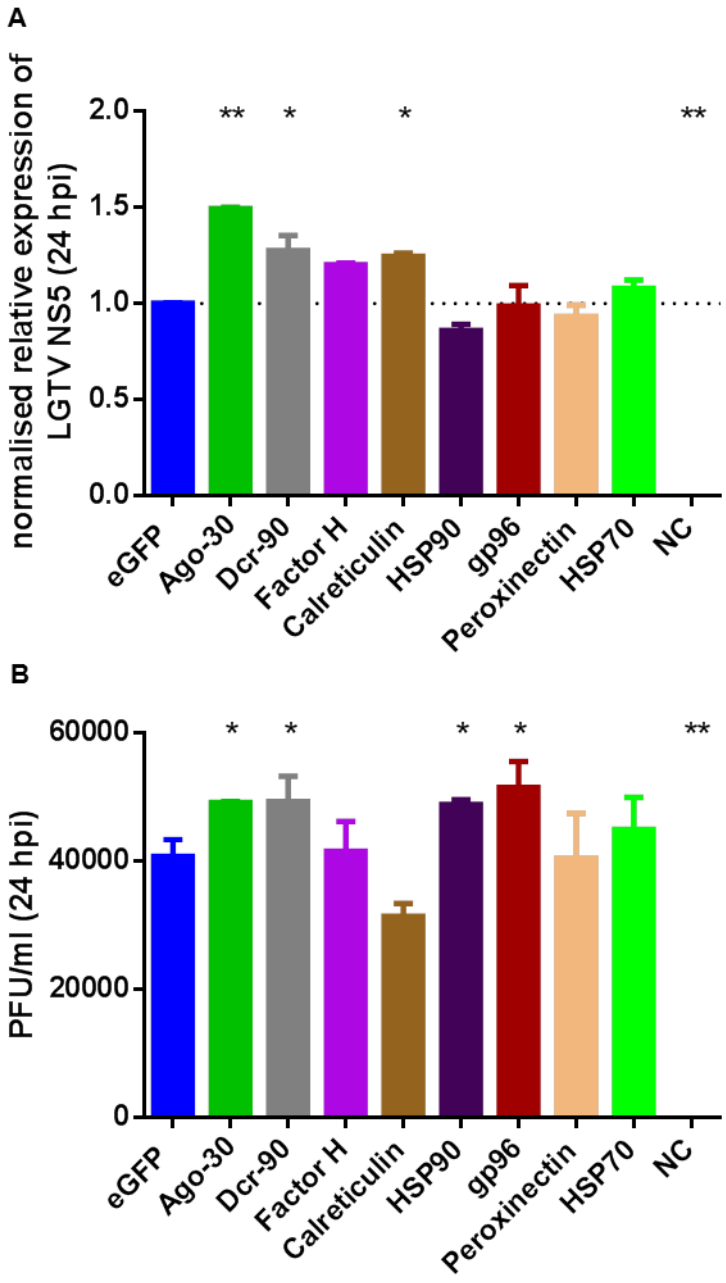

Figure 5.8 Effect of transcript knockdown on wild-type LGTV replication and production in IRE/CTVM19 cultures infected with MOI 0.5

Silenced IRE/CTVM19 cells were infected with wild type LGTV at MOI 0.5. (A) Viral RNA levels were determined by qRT-PCR using LGTV NS5 primers at 24 h p.i.. The data was normalised against beta actin and is presented as fold changes relative to eGFP dsRNA controls. (B) Infectious virus particles present in supernatant were titrated by plaque assay at 24 h p.i.. The mean with standard error is shown for two experiments, including only those samples in which knockdown was validated. (Dcr-90: triplicate in both experiments; Factor H: quadruplicate and duplicate; Calreticulin: quadruplicate and duplicate; gp96: quadruplicate and triplicate; HSP70: duplicate and singleton; all others: quadruplicate in both). Statistical significance was calculated using the two-way ANOVA Fisher's LSD test (* $p<0.05$, ** $p<0.001$). NC: negative control

5.5 Summary of findings

- Plasmid-derived TBEV infected tick cells as established by immunostaining; however plaque assay and endpoint dilution assay did not reveal any countable plaques. Since TBEV could not be quantified by either assay, LGTV was used instead.
- Silencing of tick genes was more efficient and consistent in IDE8 than in IRE/CTVM19. Efficient and consistent knockdown in IDE8 was achieved for 6 out of 12 transcripts (trypsin, calreticulin, HSP90-1, HSP90-2, gp96-1 and gp96-2). Consistent but slightly less efficient knockdown was achieved for Ago-16 and Ago-30 in IDE8. In IRE/CTVM19 efficient and consistent knockdown was obtained for HSP90, gp96 and peroxinectin. Silencing of Ago-30 was consistent but showed a low efficiency. Knockdown of calreticulin and complement Factor H was slightly less efficient and consistent than all the above-mentioned transcripts in IRE/CTVM19 cells.
- Knockdown of Ago-16 and Ago-30 resulted in increased Fluc activity in IDE8 cells transfected with TBEV C17Fluc-TAV2A suggesting an antiviral effect of Ago-16 and Ago-30 on TBEV replicon replication. In contrast to IRE/CTVM19 cells, silencing of several transcripts (Ago-30, coagulation factor, trypsin, calreticulin, HSP90-1 and gp96-2) in IDE8 cells transfected with LGTV E5repRluc2B/3 resulted in increased Rluc activity suggesting an antiviral effect of these on replication and/or translation. Knockdown of peroxinectin in IDE8 cells, on the other hand, decreased Rluc activity suggesting a proviral role for peroxinectin.
- In IDE8 cells infected with LGTV at MOI 0.01, prior treatment with nonspecific control dsRNA resulted in lower LGTV RNA levels compared to those in cells infected with LGTV without prior dsRNA treatment.

- Silencing of transcripts in IDE8 cells infected with LGTV at MOI 0.5 did not show any effect on LGTV replication and production, with the exception of HSP90-2, whereas silencing in cells infected at MOI 0.01 implicated several transcripts, including complement Factor H, gp96, HSP90, Ago-16 and Ago-30, but not HSP90-2, for an antiviral role in IDE8 cells.
- In IRE/CTVM19 cells infected with LGTV at MOI 0.5, silencing of Ago-30 and Dcr-90 resulted in increased viral RNA levels as well as virus titres suggesting an antiviral role during LGTV infection. An antiviral role in IRE/CTVM19 during virus infection was also seen for HSP90 and gp96, silencing of which led to increased virus production. Calreticulin knockdown on the other hand resulted in increased RNA levels accompanied by a reduction in virus titres implicating calreticulin as possibly proviral at the post-replication and/or post-translation stages.

5.6 Discussion

Several transcripts and proteins with a possible role in the tick cell antiviral immune response to TBEV (Neudoerfl strain) were identified by transcriptomic and proteomic analysis as described in the previous chapter. As these molecules have not previously been reported to have antiviral activity in ticks, their putative role in tick cell innate immunity was inferred by comparing results reported for different viruses in vertebrate and arthropod species. In order to elucidate their actual role in the response to virus infection in tick cells, some transcripts/proteins were selected for *in vitro* knockdown experiments, namely calreticulin, gp96, HSP70, HSP90, complement Factor H, coagulation factor, peroxinectin and trypsin, and the cultures were subsequently transfected with viral replicons or infected with wild-type virus.

Since TBEV is a CL3 pathogen in the UK, the transportation of wild-type TBEV from the Czech Republic, where it is classed as a CL2 pathogen, was not attempted due to administrative, biorisk and financial issues. Nonetheless, a plasmid encoding the full-length cDNA clone of TBEV Neudoerfl (Mandl et al., 1997) was used to

propagate TBEV as described in 2.5.2. The virus was passaged twice in BHK-21 cells and the supernatant was titrated on PS cells according to the established TBEV plaque assay protocol (De Madrid & Porterfield, 1969), with the only difference being the use of Avicel instead of CMC as an overlay. Avicel is a combination of microcrystalline cellulose and CMC forming a viscous overlay, which was shown to form better plaques with influenza virus than conventional methylcellulose (Matrosovich et al., 2006). However, in the present study no countable plaques for TBEV were visible after an incubation period of five to six days, not even by microscopy. In an attempt to optimise the protocol, the plaque assay was repeated on BHK-21 cells, PS cells and BSR cells, using the different overlays agar, agarose and Avicel, to exclude any influence of the overlay on virus spread and thus plaque formation; however again none of the plaque assays resulted in countable plaques. Furthermore the use of an end-point titration assay on BHK-21 cells also failed. This is in contrast to the immunofluorescence results (Figure 5.1.), in which immunostaining of BHK-21 cells inoculated with supernatant from TBEV-infected cultures confirmed the presence of infectious virus by positive staining for TBEV NS1 and E proteins.

Several viruses or virus strains cannot be titrated by plaque assay since they either do not form any countable plaques or do not show any cytopathic effect and thus do not lead to plaque formation (Enders, 1954). However this should not be the case for TBEV, and specifically not for the plasmid-derived TBEV, since Mandl and co-workers showed that it could be titrated on PS cells and was also able to induce a cytopathic effect in BHK-21 cells upon endpoint dilution experiments (Mandl et al., 1997, 2001). An explanation for the lack of cytopathic effect during virus titration might be that no infectious virus was present in the inoculum; however this was contradicted by the immunostaining results (Figure 5.1). The plasmid cDNA used for generating the virus might have acquired mutations which prevented cell death, thus inhibiting plaque formation. This is unlikely to be the case, since cell death was observed in BHK-21 cells during propagation of TBEV, although at a low level. Some viruses can only infect or replicate efficiently in certain cell types since some cell types can specifically restrict viral infection, however in the case of TBEV, PS

cells are commonly used (De Madrid & Porterfield, 1969) and also BHK-21 cells, which lack a functional interferon system (Andzhaparidze et al., 1981; Clarke & Spier, 1983; Habjan et al., 2008; Otsuki et al., 1978), were shown to die upon TBEV infection (Mandl et al., 1997, 2001). It might also have been possible that the batch of BHK-21 cells were growing too fast, which in combination with a low titre of TBEV in the supernatant used for infection might cause overgrowing of plaques rendering them visually undetectable. However, the same batch of BHK-21 cells with a similar passage number was successfully used to titrate LGTV (Claudia Rückert, personal communication). Other methods of titrating the virus, such as focus-forming assay (Ishimine et al., 1987; Matrosovich et al., 2006; Overby et al., 2010; Pletnev, Bray & Hanley, 2001) were not attempted, and CMC was not tested as an overlay, due to time constraints. Since no reliable method for titrating plasmid-derived TBEV could be established in the time available, LGTV strain TP21, a CL2 pathogen and close relative of TBEV, was used instead for subsequent knockdown experiments.

Silencing of 11 different transcripts was carried out. dsRNA coding for eGFP was used as a negative control to account for the fact that dsRNA addition alone might trigger an immune response which would mask possible specific transcript-derived effects on virus replication or production. In the case of subsequent transfection of silenced IDE8 cells with LGTV or TBEV replicon, dsRNA addition did not seem to have an effect on either replication or translation as measured by luciferase activity (Figure 5.2). For LGTV-infected samples however, higher LGTV RNA levels were observed in control samples without prior dsRNA treatment as compared to those treated with control dsRNA (Figure 5.6), suggesting that dsRNA treatment alone triggers an antiviral immune response. This was however only tested once in IDE8 cells infected with an MOI of 0.01, and additional experiments would be required to confirm this observation. In contrast to mosquitoes and *Drosophila* in which RNAi is a sequence-specific antiviral response, which was shown to be triggered only by virus-specific but not non-specific dsRNA (Keene et al., 2004; Saleh et al., 2009), the reduction seen in the present study was triggered by non-specific dsRNA coding for eGFP. Similar observations, in which non-specific dsRNA triggers an antiviral

state affecting virus infection, were also made in other arthropod systems including sandfly cells (Pitaluga, Mason & Traub-Cseko, 2008), shrimp (Robalino et al., 2007) and honey bees (Flenniken & Andino, 2013).

Interestingly, dsRNA coding for eGFP resulted in an increase of Dcr-2 levels in *Bombyx mori* (Liu, Smagghe & Swevers, 2013), suggesting that Dcr-2 recognises non-specific dsRNA as PAMP, which might result as described in *Drosophila* and mosquitoes in the expression of Vago (Deddouche et al., 2008; Dostert et al., 2005; Paradkar et al., 2012). Vago is an interferon-like molecule which induces an antiviral state in neighbouring cells, independent of other components of the RNAi pathway (Deddouche et al., 2008; Dostert et al., 2005; Paradkar et al., 2012). This might be an explanation for the observed influence of dsRNA addition as opposed to virus infection alone in IDE8 cells infected with LGTV at MOI 0.01 in the present study (Figure 5.6). If Vago or Dcr-2 expression is induced upon addition of non-specific dsRNA to tick cells, possibly leading to an antiviral state in neighbouring uninfected cells and resulting in reduced virus infection levels in the culture as a whole as observed in the present study, this could suggest the presence of a non-specific antiviral response in tick cells which recognises dsRNA as foreign. However, this experiment was only done once and Vago and Dcr-2 differential expression upon dsRNA addition would have to be confirmed in further experiments.

Previous studies on gene knockdown in tick cells identified variability in efficiency and consistency of gene silencing which depends not only on the cell line but also on the genes chosen for knockdown (Barry et al., 2013; de la Fuente et al., 2007a; Sim, Ramirez & Dimopoulos, 2012). Knockdown variability was also observed in other arthropods (Bellés, 2010; Sim, Ramirez & Dimopoulos, 2012; Terenius et al., 2011). In the present study similar observations were made. A very efficient and consistent knockdown, with more than 84% silencing, for all four replicates and across two independent experiments (Figure 5.3, Figure 5.5) was achieved for six transcripts (trypsin, calreticulin, HSP90-1, HSP90-2, gp96-1 and gp96-2) out of 12 in IDE8 cells. Consistent but slightly less efficient silencing, between 53 and 70%, was observed for Ago-16 and Ago-30 in IDE8 cells.

Knockdown results in IRE/CTVM19, however, were much more variable and less efficient than in IDE8, but were probably not due to a lack of Dcr functionality as suggested by Barry et al (2013). If a functional Dcr was missing from IRE/CTVM19 cells they should be unable to recognise and process any long dsRNA, as observed in the mosquito cell lines C6/36 and C7-10 (Brackney et al., 2010; Morazzani et al., 2012; Scott et al., 2010), but knockdown of some genes in these cells using dsRNA, such as HSP90, gp96 and peroxinectin, resulted in 60-85% silencing in all four replicates in each of the two independent experiments (Figure 5.7). Therefore a possible explanation for the less efficient knockdown in IRE/CTVM19 compared to IDE8 might be that, since both cell lines are heterogeneous, some of the cells in IRE/CTVM19 may not express Dcr-2 or other components of the RNAi pathway while others do, which would impair overall knockdown efficiency and consistency. Other explanations, at least for the three transcripts for which no knockdown was achieved in IRE/CTVM19 (coagulation factor, Ago-16 and trypsin), could be that the dsRNA produced did not efficiently target IRE/CTVM19 transcripts. For the three transcripts mentioned, primers were designed against the IDE8 genome sequence, and subsequent sequencing revealed major sequence differences between dsRNA derived from IDE8 and IRE/CTVM19 for Ago-16 (Dr. Esther Schnettler, personal communication), and 6-8 nucleotide differences for the other two transcripts. These differences could possibly lead to the lack of transcript knockdown in IRE/CTVM19 as opposed to IDE8. Furthermore, the intracellular turnover time of specific transcripts can vary depending on the cell line, and the ability to take up dsRNA could be better in one line than in the other (Barry et al., 2013) and thus influence knockdown efficiency. It would be interesting to sequence the small RNA profile produced by infected IRE/CTVM19 cells and to test if the cells target virus by RNAi.

For the experiment in which transcripts were knocked down and subsequently transfected with replicons it was not possible to determine the knockdown in each well due to the sample preparation procedure which required the lysis of cells. This might have led to the inclusion of replicates which did not show any knockdown and raises the possibility of either reducing, thus hiding, or increasing, thus amplifying, the true effect on virus replication or translation measured by luciferase expression.

This would possibly result in large standard errors as seen for coagulation factor and calreticulin in LGTV replicon-transfected cells and for HSP90-2 in TBEV replicon-transfected cells. At least for coagulation factor this inconsistency in knockdown would correlate with the results obtained in subsequent knockdown experiments (Figure 5.3, Figure 5.5).

Possibly the most important antiviral response in insects discovered to date is RNAi (Blair, 2011) which is also suspected to be of importance in ticks, since the production of specific viRNAs has been detected in tick cells infected with LGTV (Schnettler et al., 2014) and in tick cells infected with recombinant SFV containing Hazara virus S segment sequence (Garcia et al., 2005). Furthermore, gene-specific dsRNA treatment of tick cells is able to restrict viral infection (Barry et al., 2013; Garcia et al., 2005) and viral proteins acting as suppressors of RNAi in plants and insect cells were able to abrogate RNA silencing in tick cells (Garcia et al., 2006). In a recent study in tick cells (Schnettler et al., 2014) several orthologues of Ago-2, which is a key member of the exogenous siRNA pathway in insects, were identified and of these orthologues Ago-16 and Ago-30 mediated an antiviral effect against wild-type LGTV and a LGTV replicon. Dcr-90 also exhibited an antiviral effect, at least when transfected alongside the LGTV replicon. In the present study, Ago-16, Ago-30 and Dcr-90 were included as positive controls, although they were not found to be significantly differentially expressed upon TBEV infection in either the transcript or the protein data. This lack of differential expression of RNAi components is in accordance with studies in other arthropods such as mosquitoes (Waldock, Olson & Christophides, 2012; Xi, Ramirez & Dimopoulos, 2008) and *Drosophila* (Dostert et al., 2005), which indicated that components of the RNAi defence systems are likely to be constitutively expressed and thus do not require transcriptional induction upon viral challenge, or that viruses actively suppress transcription of such transcripts as a defence mechanism (Waldock, Olson & Christophides, 2012; Xi, Ramirez & Dimopoulos, 2008).

In general, all the experiments carried out within the present study, including virus RNA levels versus virus production, infection of IDE8 cells with MOI 0.5 versus MOI 0.01, IDE8 cells versus IRE/CTVM19 cells, replicon versus virus and

transfection with LGTV replicon versus TBEV replicon showed inconsistent results. Parameters which could have an influence on the observed results will be briefly discussed below.

An important observation from the present study was the influence of the MOI used on the results of experiments elucidating the functional role of transcripts during virus infection. IDE8 cells infected with LGTV at an MOI of 0.5 did not show any significant changes on virus infection following silencing of specific transcripts, with the exception of HSP90 (Figure 5.4), whereas cells infected with a lower MOI of 0.01 revealed a possible antiviral role for several transcripts, including complement Factor H, gp96, Ago-16 and Ago-30 (Figure 5.6). A possible explanation for this observation is that with a low MOI, virus will not have infected all the cells at the beginning of the experiment, thus allowing virus to spread from cell to cell which might multiply the observed effect of transcript knockdown on virus replication and/or production. For example, if only some cells have an efficient knockdown but others have not, and the virus infects all the cells at the beginning, virus production will not be inhibited in those cells without knockdown, possibly masking the effect of those cells in which silencing reduces virus infection. It might also be that by overloading the cells, using a higher MOI, antiviral effects might be less efficient due to saturation and thus not as easily detectable. Furthermore, overloading the cells might inhibit factors which are associated with cell-to-cell spread of, for example dsRNA, siRNA or any other antiviral effector molecules thus reducing the innate defence response of the whole culture to the virus. Additionally, if some of the transcripts chosen for knockdown are involved in cell-to-cell spread of the virus, thus having a proviral role during virus infection, a high MOI in which most of the cells are already infected with virus would mask the proviral role since cell-to-cell spread would only be observable with a low MOI. With an MOI of 1, 97% of the cells were infected by LGTV, as shown in 3.4.1, and virus replication and production could be detected at 24 h p.i. (Figure 3.11); with an MOI lower than 1 it was assumed that virus had not infected all the cells at the start of the experiment, since virus replication in IDE8 cells infected with MOI 0.05 was only detectable at day 2 p.i. (Figure 3.11). However due to time constraints, immunostaining to see how many

cells were infected at 24 h or 48 h p.i. with different MOIs was not conducted to confirm this assumption.

Interestingly, for some transcripts LGTV production increased (< 20%) whereas no differences were observed in the viral RNA levels. This observation could be explained if the transcript knockdown affected a process after viral RNA replication, such as translation, maturation or virus release. However, in the case of Ago-16 and Ago-30 in IDE8 cells infected at MOI 0.01 (Figure 5.6), both knockdowns were expected to lead to an increase in viral RNA levels as well as virus production, since both homologues of Ago-2 have been shown to be involved in RNAi affecting virus replication in tick cells (Schnettler et al., 2014). A possible explanation is that the time-points chosen did not permit detection of changes in both virus replication and production. Flavivirus replication in mammalian cells starts as early as 3 to 6 h p.i. but the first infectious virus release takes approximately 12 h (Chambers et al., 1990). The metabolism and growth of tick cells is slower than that of mammalian cells (Bell-Sakyi et al., 2007), which might affect the timing of the virus replication cycle. LGTV replication and production in IDE8 cells infected at a slightly higher MOI of 0.05 (Figure 3.11), compared to MOI 0.01, was detectable between days 1 and 2. Thus an additional time-point later during infection might be necessary to detect changes in both virus replication and virus production levels.

Interestingly knockdown of some transcripts, including complement Factor H and coagulation factor, resulted in different responses in cells transfected with LGTV replicon (Figure 5.2) and cells infected with wild-type LGTV (Figure 5.4, Figure 5.6). These different responses could reflect differences either between the two viral systems, replicon versus whole virus, or between the methods used for detection, luciferase assay versus plaque assay or qRT-PCR. In respect to the first point, LGTV replicon is able to replicate within cells (Schnettler et al., 2014) and is translated and processed as measured by Rluc activity; however, since the structural proteins are missing, in contrast to wild-type virus, the replicon is unable to produce infectious virions, thus is unable to spread from cell to cell. Transcripts affecting replication and some aspects of translation should thus be detected with both systems, whereas transcripts influencing translation of a glycoprotein (at the ER) or post-translational

steps, such as packaging, maturation, transport or release of infectious virus particles would only be detected using wild-type virus. Transcripts may also be able to influence more than one step within a virus life cycle. Differences observed between replicon and wild-type virus could also be caused by the different assays used, which detect different parameters with different sensitivities. The luciferase assay is able to detect effects on virus replication and translation, whereas qRT-PCR detects viral RNA levels. Plaque assays should detect differences during any step within the replication cycle of a virus including the production of infectious virus particles, but are possibly the least precise of the assays used.

An interesting observation was that knockdown of transcripts seemed to have different effects on the LGTV and TBEV replicons. In IDE8 cells transfected with the former, most knockdowns apart from Ago-16, complement Factor H, HSP90-2 and gp96-1 resulted in an increase in luciferase activity. In contrast in IDE8 cells transfected with TBEV replicon, only knockdown of Ago-16 and Ago-30 resulted in an increase in luciferase activity. The differences between the LGTV and TBEV replicons could result from a virus species-specific effect. Small changes, such as that seen in CHIKV in which one mutation enabled the virus to be transmitted better by *Ae. albopictus* (Vazeille et al., 2007), can lead to differential responses. Another possible explanation could be that the host cell transcripts and/or proteins differentially expressed upon TBEV infection were not differentially expressed upon LGTV infection which could possibly indicate that they are not involved in the antiviral response towards LGTV.

The TBEV and LGTV replicons were designed in a similar way (Schnettler et al., 2014), with the only differences being that the LGTV replicon encodes Rluc followed by the recognition sequence for the LGTV NS2B/3 protease, whereas the TBEV replicon encodes Fluc followed by a TAV2A cleavage site (Hoenninger et al., 2008). Since both were designed similarly and the LGTV replicon was shown to replicate within IDE8 cells by antigenome specific RT-PCR (Schnettler et al., 2014), lack of replication of the TBEV replicon as a reason for the lack of effect seems rather unlikely though replication of the TBEV replicon was not verified by antigenome specific RT-PCR in the present study. The observed differences could be

caused by the different cleavage sites introduced into the LGTV and TBEV replicons. In the TBEV replicon the TAV2A cleavage site resulted in more efficient release of Fluc than the NS2B/3 cleavage site (Figure 3.15), which confirms the observation of Hoenninger et al. (2008) who compared different TBEV replicons transfected into BHK-21 cells. Comparing the release from the polyprotein of Fluc from the TBEV replicon and Rluc from the LGTV replicon via the TAV2A and NS2B/3 cleavage sites, respectively, 20 times lower luciferase activity levels were observed in the peak of luciferase activity in the TBEV replicon growth curve compared to the LGTV replicon growth curve (Figure 3.15). This could partially be explained by the known differences in signal intensities between Fluc and Rluc but it might additionally have been caused by less efficient cleavage from the TBEV replicon. This suggests that the LGTV protease is possibly more efficient in cutting than the TBEV protease, resulting in higher luciferase levels and making the LGTV replicon system more sensitive to subtle changes. Therefore the differences in effect observed between the TBEV and LGTV replicons could be caused by lower sensitivity of the former. Another reason for differences in the expression levels of luciferase could be the different promoters in the plasmids coding for the TBEV and LGTV replicons, respectively T7 and SP6. Compared to the T7 promoter, the SP6 promoter is generally more efficient and produces higher yields of RNA during *in vitro* transcription (Stump & Hall, 1993). Therefore more LGTV replicon (SP6 promoter) than TBEV replicon (T7 promoter) could have been introduced into cells, since despite using the same starting amount before *in vitro* transcription, more RNA might have been produced by the former during *in vitro* transcription, thus explaining the higher luciferase activity measured for the former. Additional experiments using wild-type TBEV and possibly replicons with the same promoters and same cleavage sites would be required to determine if any of these factors, separately and/or combined, are the explanation for the differences in response or if the difference is virus-specific.

Another possibility for the lack of effect of transcript knockdown on the TBEV replicon could be that it was not replicating efficiently within the cells. Although replication was not determined, the ability to detect Fluc activity for more than 5

days p.t. (Figure 3.15), with the half-life of luciferase usually being 2 h (Technical Manual for Dual-Glo® Luciferase Assay System; Promega), suggests that the detected luciferase activity is due to newly-produced rather than residual luciferase activity. Additionally, knockdown of Ago-16 and Ago-30 resulted in an increase in luciferase activity, suggesting that the TBEV replicon is able to replicate within the cell, making this a less likely explanation.

Surprisingly none of the transcripts, apart from HSP90, showed any effect on virus replication or virus production in IDE8 cells infected with LGTV at MOI 0.5 (Figure 5.4). Possible explanations could be that the time-point of 24 h was too early to see any effect on virus replication and production or that transcript knockdown made no difference to virus infection in IDE8 cells. However, knockdown experiments using IRE/CTVM19 cells infected with the same MOI showed an effect on virus replication and production (Figure 1.8). The observed difference could reflect a cell-specific effect caused by differences in the number of cells infected or be due to differences in metabolism leading to a faster virus life cycle in IRE/CTVM19 cells. To test this hypothesis, the establishment of a LGTV growth curve in IRE/CTVM19 cells would be required. Another possible explanation could be that an MOI of 0.5 was too high, overloading the cells and the respective immune response with virus thus hiding the effect of transcript knockdown. Results obtained in IDE8 cells infected with LGTV at MOI 0.5 will thus not be included in subsequent discussion of possible effects of transcript knockdown on virus infection.

Some transcripts (Ago-30, HSP90 and gp96) showed an effect in all of the experiments in both cell lines suggesting that they play an important role in the antiviral response of tick cells towards LGTV infection.

Ago-16, Ago-30 and Dcr-90, which have been shown to be important in the antiviral response of tick cells against LGTV (Schnettler et al., 2014), were included in the present study as positive controls. However, they only partially fulfilled this function. As expected, knockdown of Ago-30 revealed an antiviral role in LGTV replicon- and TBEV replicon-transfected IDE8 cells (Figure 5.2) and in LGTV-infected IRE/CTVM19 cells (Figure 5.8) but not in LGTV-infected IDE8 cells. Ago-

16 knockdown only resulted in an increase in luciferase activity in TBEV replicon-transfected IDE8 cells (Figure 5.2 B). In the case of LGTV replicon this could be due to inconsistent silencing of Ago-16; however knockdown was consistent in other experiments in the present study and higher than achieved in Schnettler's study, making inefficient knockdown an unlikely explanation. The lack of an effect of silencing of Ago-16 and Ago-30 in IDE8 cells, compared to the antiviral effect observed in IRE/CTVM19 cells upon Ago-30 silencing, could be caused by the different MOIs used for infection, MOI 0.01 and MOI 0.5 respectively, or be due to the application of dsRNA with or without transfection reagent. In contrast to the present study, Schnettler et al. (2014) were able to detect an influence of Ago-16 and Ago-30 knockdown on LGTV replication. The observed differences between the two studies could also be explained by differences in knockdown protocols. Schnettler et al. transfected dsRNA into cells, thereby increasing the amount of dsRNA per cell and possibly the number of cells containing dsRNA (Barry et al., 2013), whereas in the present study dsRNA was added to the medium of IDE8 cells possibly resulting in less dsRNA per cell and fewer cells taking up the dsRNA. This could reduce the chance of a virus encountering a cell containing dsRNA, and a later time-point allowing further virus spread might have given better results. Repetition of experiments in IDE8 cells would be necessary to verify the antiviral role of Ago-30 and Ago-16, since the experiment was done only once.

In IRE/CTVM19 cells infected with LGTV at MOI 0.5, both Ago-30 and Dcr-90 knockdowns resulted in significantly increased LGTV RNA levels and production, suggesting their involvement in the antiviral RNAi response in IRE/CTVM19 cells, as found by Schnettler et al. (2014) in IDE8. Although further experiments are necessary, Schnettler's study and the present study confirm that RNAi mediated by Ago-2 orthologues and Dcr-90 is an important and effective antiviral response in tick cells.

An interesting observation in the present study was that some heat-shock proteins, including HSP90 and HSP70, were down-regulated/underrepresented, whereas others such as gp96 were up-regulated/overrepresented at the transcript and/or protein level upon TBEV infection (Table 4.6, Table 4.8, Table 4.13, Table 4.15) in both cell

lines. HSPs are conserved molecules with chaperone or protease function, that are induced under stress conditions such as heat-shock, toxicity and pathogen infection (Pockley, 2003; Zhao & Jones, 2012). For several RNA viruses, HSPs are important host factors exploited for virus multiplication through regulation of translation, replication and virion assembly and as a defence against premature cell apoptosis (Nagy et al., 2011).

Under-representation of HSP90 was observed at days 2 and 6 p.i. at the protein level in the present study. Under-representation of the same protein was also seen upon WNV infection of Vero cells (Pastorino et al., 2009). One possible explanation is that the virus actively down-regulates the translation of HSP90 allowing for better virus infection. It is however more likely that HSP90 down-regulation results from some other change in the cell initiated by the virus infection. In the present study, knockdown of HSP90 resulted in an increase in luciferase activity in cells transfected with the LGTV replicon (Figure 5.2 A) and in LGTV production in IDE8 and IRE/CTVM19 cells, suggesting an antiviral role for HSP90, possibly at the translational level. Interestingly, HSP90 was shown to be required for the loading of siRNA duplexes into Ago-2 in *Drosophila* (Iwasaki et al., 2010; Miyoshi et al., 2010); thus inhibition of HSP90 would lead to impairment of RNAi which should subsequently lead to a reduction in the degradation of viral RNA. This was not observed in the present study. The findings of the present study instead suggest an antiviral role for HSP90 during viral RNA translation. Further studies would be required to determine the exact role(s) of HSP90 in the RNAi response in tick cells and its possible role during viral RNA translation, assembly, maturation or virus budding; these should include the overexpression of HSP90 since it is usually down-regulated during viral infection. Overall, the results obtained for HSP90 in the present study are intriguing and encourage further elucidation of the antiviral role of HSP90 in tick cells

Interestingly the tumor-rejection antigen gp96, belonging to the family of HSP90 proteins, was up-regulated at day 2 p.i. at the transcript level (Table 4.8) and underrepresented at day 6 p.i. at the protein level (Table 4.15) in TBEV-infected IRE/CTVM19 cells. This would suggest either that the translation of gp96 is

inhibited, since a higher amount of transcripts does not result in more protein being produced, or that the protein is degraded more quickly, in TBEV-infected cells compared to uninfected cells. Gp96 is an ubiquitious ER-based chaperone which in mammals is involved in the folding of a limited clientele of proteins, including TLRs and integrins, and exhibits similar functions in *Drosophila* (Morales et al., 2009). In the present study, knockdown of gp96 in IDE8 cells resulted in increased Rluc activity upon transfection with LGTV replicon (Figure 5.2), as well as increased levels of LGTV RNA and infectious virus particles in cells infected (MOI 0.01) with LGTV (Figure 5.6). Furthermore, knockdown of gp96 also resulted in increased LGTV production in IRE/CTVM19 cells (Figure 5.8). This suggests an antiviral role for gp96 during LGTV infection. The antiviral role of gp96 might be due to its capacity for folding TLRs (Randow & Seed, 2001) or other client proteins involved in the antiviral response. In contrast to the present study, gp96 was shown to be essential for infection with VSV suggesting a proviral role during VSV infection of mammals (Bloor et al., 2010). The authors showed that gp96 is indirectly involved in the entry of VSV into cells through chaperoning a client protein that is required for the generation of a functional VSV receptor.

Up-regulation of ER chaperones such as gp96 or calreticulin, as seen in the present study, is often considered in mammalian cells to be a marker of ER stress accompanying the UPR (Hetz et al., 2011; Kim et al., 2006). Upon continuous ER stress, translation is inhibited at the initiation step which prevents the further accumulation of misfolded protein and, if not reduced, can lead to apoptosis. Some flaviviruses such as JEV trigger the UPR leading to cell death by translation inhibition (Su, Liao & Lin, 2002), DENV-2 infection does not rapidly trigger apoptosis but manipulates the UPR to prolong cell survival and its own replication cycle (Peña & Harris, 2011). This might suggest that, as a consequence of TBEV infection in tick cells, gp96 is up-regulated possibly by the induction of ER stress through the viral protein load in the ER, and this up-regulation might exert a direct and/or indirect antiviral role by chaperoning TBEV proteins and/or an important antiviral client protein which diminishes virus infection and ER stress in tick cells. However, additional experiments elucidating the presence of the UPR in tick cells,

for example by identifying homologues of the mammalian pathway components, would be required as well as knockdown and expression studies. Nevertheless, the possibility of gp96 acting as a direct or an indirect antiviral molecule in the tick cell response as suggested in the present study encourages additional experiments.

For all other transcripts, interpretation of results is difficult due to inconsistency, such as effect on virus production but not on RNA levels, and because they differ between the two different cell lines. Therefore more experiments would be required to give a final conclusion. However, possible roles for each transcript will be briefly discussed.

As with gp96, calreticulin, another ER based chaperone up-regulated in mammalian cells during the UPR, was up-regulated in the present study at day 2 p.i. at the transcript level in response to TBEV infection (Chapter 4). Calreticulin is a lectin-like chaperone with multiple functions inside and outside of the ER, including wound healing, immunity, quality control of newly synthesised proteins and glycoproteins and Ca^{2+} homeostasis (Wang, Groenendyk & Michalak, 2012). In the present study the results for calreticulin knockdown were not consistent between IDE8 and IRE/CTVM19 cells. In IDE8 cells, calreticulin silencing resulted in increased Rluc activity upon transfection with the LGTV replicon (Figure 5.2) and in an increase in virus production in IDE8 cells infected (MOI 0.01) with LGTV (Figure 5.6), which suggests an antiviral role for calreticulin at the translational level. However, since the experiment was only done once in IDE8 cells, a repetition of the experiment would be required to confirm this function.

Interestingly, in contrast to IDE8 cells, levels of LGTV RNA in IRE/CTVM19 cells were significantly increased following calreticulin silencing, while virus production may have decreased (Figure 5.8); this was not statistically significant but low enough to warrant further investigation. A possible explanation for this observation would be that virus production was impaired by knockdown of calreticulin while replication was unaffected. If this was the case, viral RNA would not be transported out of the cell within virus particles thus resulting in accumulation of viral RNA within the cell. Therefore calreticulin would be implicated as proviral during LGTV infection of

IRE/CTVM19 cells. A similar observation, where knockdown of calreticulin resulted in decreased production of DENV infectious virus particles was made in Vero cells (Limjindaporn et al., 2009). The authors showed by co-immunoprecipitation that calreticulin interacts directly with the DENV E glycoprotein (Limjindaporn et al., 2009), implicating calreticulin in the processing and maturation of viral glycoproteins (Pieren et al., 2005). It is therefore tempting to speculate that calreticulin is involved in processing and maturation of the TBEV and LGTV E protein, and that calreticulin knockdown impairs the production of infectious virus particles resulting in an accumulation of viral RNA which is not packaged into the virion and cannot exit the cell. Correct folding of the envelope protein is important for virus budding.

In contrast to knockdown of gp96, knockdown of the complement Factor H homologue resulted in a significant increase in both virus RNA levels and virus production in IDE8 cells infected with LGTV (MOI 0.01) (Figure 5.6). There was no effect on the LGTV replicon. In mammalian cells, Factor H is an important negative regulator of the alternative pathway of the complement system where it leads to accelerated decay of C3 convertase and, together with its cofactor, Factor-I, accelerates cleavage of C3b (Makou, Herbert & Barlow, 2013). Factor H is a pattern-recognition molecule which is able to bind with a high efficiency to host-specific molecular signatures, such as heparin and sialic acid, protecting uninfected cells from the complement system (Makou, Herbert & Barlow, 2013). It does not bind if these signatures are not present, which might be the case for the surfaces of some bacterial cells and certain virus-infected cells (Favoreel, 2003). Virus infection might lead to a decrease of molecular signatures recognised by complement Factor H on the cell surface, allowing the complement system to target these cells for degradation (Blue, Spiller & Blackbourn, 2004). Interestingly, the NS1 protein of WNV was shown to directly interact with complement Factor H in solution promoting the Factor-I mediated cleavage of C3b, and/or with complement Factor H bound to cell surfaces inhibiting the deposition of C3b and the membrane attack complex, thereby protecting virus-infected cells from complement-dependent cell lysis (Chung et al., 2006). In the present study, complement Factor H was up-regulated at the transcript

level in TBEV-infected IRE/CTVM19 cells at day 6 p.i.. If complement Factor H exhibits the same mechanism in tick cells as in mammalian cells, and if the complement system is active against TBEV, knocking down complement Factor H should have resulted in decreased virus replication and/or production. The opposite was observed in the present study. In tick cells Factor H may not be a negative regulator of the complement system. It could be a positive regulator or an important component of the complement system with an antiviral effect. It would be interesting to elucidate the role in virus infections of complement Factor H and other components effective against bacteria in tick cells, including α_2-macroglobulin, C3 complement components, insect TEP and macroglobulin-complement related molecules (Buresova et al., 2009, 2011; Hajdušek et al., 2013; Kopacek, Hajdusek & Buresova, 2012).

The different responses in the two tick cell lines used could represent a cell-specific response towards flavivirus infection since calreticulin was not differentially expressed at the transcript level in TBEV-infected IDE8 cells but was up-regulated in IRE/CTVM19 upon TBEV infection, a vector-specific response since the cell lines are derived from different tick species or an artefact since the experiment in IDE8 cells infected with LGTV was only done once whereas the experiment in IRE/CTVM19 was repeated twice. Furthermore, differences in responses could also result from the fact that both cell lines are heterogenous and thus might contain different cell types, or be due to their infection with endogenous viruses. Both IDE8 and IRE/CTVM19 cells are persistently infected with endogenous viruses, SCRV and reovirus-like particles respectively (Alberdi et al., 2012; Attoui et al., 2001; Bell-Sakyi et al., 2007), which could affect the innate immune response towards the virus used for superinfection (Bell-Sakyi & Attoui, 2013). A repetition of the experiment in both cell lines using identical parameters, in addition to *in vivo* experiments, might help to elucidate the role of calreticulin during LGTV and TBEV infection.

The serine-protease trypsin was up-regulated at the transcript level at day 6 p.i. in IRE/CTVM19 cells upon TBEV infection. Up-regulation of trypsin was also observed in a transcriptomic study on *Ae. aegypti* mosquitoes infected with SINV (Sanders et al., 2005). In the present study, knockdown of trypsin resulted in an

increase in Rluc activity upon replicon transfection (Figure 5.2) and an increase in LGTV production in IDE8 cells infected at MOI 0.01 (Figure 5.6). No knockdown of trypsin could be achieved in IRE/CTVM19 cells.

The effect observed in IDE8 cells suggests an antiviral role for trypsin during LGTV infection, possibly at the translational level. The antiviral effect of trypsin might be due to its serine protease activity, since serine proteases are involved in the modulation of several immune signalling pathways (De Gregorio et al., 2001, 2002; Ligoxygakis et al., 2002) and, of these, one or more might mediate an antiviral role. For establishing the exact role of trypsin, and the pathway through which it might exert its antiviral function, additional experiments are required.

The degree of silencing of coagulation factor, which was up-regulated at day 6 p.i. at the transcript level in IRE/CTVM19 cells, showed high variability between different experiments in IDE8 and was not achieved at all in IRE/CTVM19 cells, making interpretation of results difficult. No change was observed in either RNA levels or virus titres in IDE8 cells infected with LGTV at an MOI of 0.01 (Figure 5.6), although all four replicates showed a mean silencing efficiency of 78%, suggesting that coagulation factor is not involved in the antiviral response in tick cells. However the increase in Rluc activity from the LGTV replicon would suggest a role for coagulation factor in either replication or translation, but since silencing could not be measured and was generally highly variable between experiments, and a high standard error of mean was observed, it is not possible to draw any definite conclusions from this observation.

Peroxinectin, a cell adhesive and opsonic peroxidase, was shown to be up-regulated during the first 48 h of WSSV infection of the mud crab *Scylla paramamosain* (Du et al., 2013). Since the proliferation profile of WSSV infection showed a latent period of 48 h with an increase in virus RNA levels only when peroxinectin RNA levels decreased, the authors concluded that peroxinectin has an antiviral role controlling WSSV during early infection. Interestingly, in the present study peroxinectin was also increased at the transcript level, however only at day 6 p.i. in IRE/CTVM19 cells upon TBEV infection. To elucidate if peroxinectin exhibits an antiviral function

in tick cells, as seen in the mud crab, knockdown experiments were conducted. Unfortunately, knockdown of peroxinectin was not very consistent and efficient in IDE8 cells and results can therefore not be interpreted reliably. Interestingly, the knockdown of peroxinectin in IRE/CTVM19 cells was consistent with high silencing efficiency (Figure 5.7). However, peroxinectin knockdown did not show any effect on LGTV replication or production in these cells suggesting that, although peroxinectin was up-regulated at the transcript level upon TBEV infection, it does not have any effect on LGTV virus infection in the experimental set-up used.

As with coagulation factor and peroxinectin, knockdown of HSP70 was not very efficient and reproducible in IDE8 cells; no conclusions can be drawn as to the role of HSP70 during LGTV infection. As mentioned above, the heat-shock protein HSP70 was down-regulated/underrepresented during TBEV infection at the transcript and protein levels in IDE8 and IRE/CTVM19 cells; thus infection with LGTV leading to down-regulation of HSP70 at the transcript level might mask the knockdown of HSP70 by dsRNA. Thus it might have been better, in the case of HSP70, to verify the knockdown prior to infection or to overexpress HSP70 in order to determine its effect on virus infection. Additional experiments with verified knockdowns as well as experiments in which HSP70 is overexpressed might be useful to elucidate its role during virus infection.

Overall, the observed effect of transcript knockdown on LGTV infection was rather low compared to that seen with bacterial infection *in vitro* in tick cells (de la Fuente et al., 2007a; Pedra et al., 2010; Zivkovic et al., 2010b), with a maximum of 2-fold difference at the LGTV RNA level and a maximum of 1500 PFU/ml difference in viral titres compared to cultures treated with control dsRNA. The slight effect of transcript knockdown on virus infection compared to bacterial infection could reflect the difference in pathogenicity between the two microorganism groups, since bacterial infection usually leads to the death of tick cells *in vitro* (Bell-Sakyi & Attoui, 2013) whereas viruses persistently infect tick cells without causing any obvious cytopathic effect (Pudney, 1987). Another explanation could be that some of the transcripts might have an effect on the outcome of virus infection, such as whether or not a persistent infection develops, since most of the targets were up-

regulated at day 6 p.i.. Therefore, it might have been necessary to observe the effects of knockdowns at time-points later than 24-48 h. Other possible explanations might be that viruses are able to interfere with the RNAi response either inducing or inhibiting the response (Donald, Kohl & Schnettler, 2012; Kingsolver, Huang & Hardy, 2013). For LGTV and TBEV it was recently shown that they produce subgenomic flavivirus RNA which weakly suppresses the RNAi response in tick cells (Schnettler et al., 2014) and might thus lead to less dramatic effects of transcript knockdown on virus infection compared to bacterial infection. However, if the virus was interfering with the knockdowns, this should have been detected during knockdown validation.

Furthermore, the endogenous viruses chronically infecting both tick cell lines used in the present study might have interfered with the tick cell innate immune system, by either pre-activating or overloading antiviral pathways, since SCRV-specific siRNAs were detected in IDE8 cells suggesting an active RNAi response against this virus (Schnettler et al., 2014), or by inhibiting certain immune pathways thus making it more difficult either to knock down transcripts involved in the pre-activated pathways or to detect subtle changes in virus infection upon knockdown. Changes in the level of SCRV upon knockdown of target genes might indicate if a specific transcript is involved in controlling SCRV and thus indicate if SCRV is possibly involved in modulating a particular pathway. Changes in SCRV levels were not examined in the present study.

Furthermore, it has to be mentioned that the RNAi technique does not normally abolish target transcripts completely, thus allowing residual expression of target genes and subsequent protein expression making it more difficult to distinguish control groups from knockdown groups. However, for some transcripts knockdown was sufficient to allow detection of an effect, which might be increased by permanently knocking out genes coding for respective transcripts. However, no knock-out model is currently available for ticks or tick cell lines. Since some proteins have a long turn-over time, efficient silencing at the transcript level does not necessarily mean that protein levels are reduced. Testing knockdowns at both transcript and protein levels would be required to validate efficient silencing;

however, because suitable tick protein antibodies were not available, it was only possible to detect knockdowns at the transcript level.

Of the transcripts investigated within the present study, only calreticulin and HSP70 have been functionally analysed for their role during microbial infection of ticks or tick cell lines. In *R. microplus* ticks, knockdown of calreticulin resulted in a 73% reduction in *B. bigemina* infection levels compared to the controls, suggesting that calreticulin is required for *Babesia* infection (Antunes et al., 2012). Similarly in the present study, a proviral effect was hypothesised for calreticulin in IRE/CTVM19 cells infected with LGTV (Figure 5.8). With respect to HSP70, a study by Busby et al (2012) reported that HSP70 mRNA levels were not differentially expressed upon *A. phagocytophilum* infection in ISE6 cells but were down-regulated in *I. scapularis* whole ticks, guts and salivary glands. They showed that knockdown of HSP70 did not cause any changes in the *A. phagocytophilum* infection levels in tick cells, but resulted in increased infection levels in the salivary glands of *I. scapularis* ticks, suggesting that HSP70 may be down-regulated by the pathogen to promote infectivity (Busby et al., 2012). Although down-regulation of HSP70 following TBEV infection was also observed at the mRNA level in both tick cell lines in the present study, the failure to achieve knockdown of this gene prevented interpretation of the results obtained. These observations suggest that transcripts of interest should also be tested in whole ticks to detect any effect on virus infection.

Overall, more experiments are required to further elucidate and confirm the roles of the examined transcripts during LGTV and TBEV infection. However HSP90, gp96, Ago-30 and Dcr-90 seem to be important during LGTV infection at either the translational or post-translational level for the first two transcripts or during LGTV replication for the latter two. Furthermore, the increase in both virus replication and virus production upon Factor H knockdown suggests a role for the complement system during LGTV infection which deserves further examination for its antiviral role in tick cells.

6 Chapter 6 Concluding Remarks

Current research on the innate immune response of ticks or tick cells is mainly focused on bacterial infections, and has successfully identified important antimicrobial effectors and pathways (Hajdušek et al., 2013; Kopácek et al., 2010; Taylor, 2006) including the complement system (Buresova et al., 2009, 2011; Kopacek, Hajdusek & Buresova, 2012) and JAK/STAT pathway (Liu et al., 2012b) in the antibacterial response. However, not much is known about the response of ticks and tick cells to virus infection and no pathways except the RNAi pathway have been implicated in the tick antiviral defence to date (Barry et al., 2013; Schnettler et al., 2014; Garcia et al., 2005, 2006). This thesis, with the major aim of identifying novel antiviral defence strategies, reports the first study using transcriptomic and proteomic techniques to investigate the defence response of tick cells to virus infection.

The tick cell lines used in the present study are phenotypically and genetically heterogeneous, having been derived from eggs, and contain several different cell types (Bell-Sakyi et al., 2007). Thus some of these cell types within a culture might not become infected, might not support virus replication and production or might vary in the type of antiviral defence response they mount. Furthermore some cell types, since they are derived from eggs, might still be undifferentiated and might undergo differentiation during passaging of cultures or during infection. The results presented within this thesis are therefore rather the response of a whole culture than the response of a specific tick cell type, and slight but important changes in differential expression and/or antiviral defence response might be missed.

Previous studies investigating virus infection in tick cells were focused on determining the capability to propagate different viruses (Bhat & Yunker, 1979; Lawrie et al., 2004; Leake, Pudney & Varma, 1980; Pudney, 1987; Rehacek, 1987; Ruzek et al., 2008; Varma, 1989; Varma, Pudney & Leake, 1975; Yunker, Cory & Meibos, 1981), investigating persistence (Bhat & Yunker, 1979; Leake, Pudney & Varma, 1980; Pudney, 1987; Rehacek, 1987; Varma, 1989; Varma, Pudney & Leake, 1975) and super-infection (Kopecký & Stanková, 1998; Rehacek, 1987), establishing

a role for RNAi as an antiviral response (Barry et al., 2013; Schnettler et al., 2014; Garcia et al., 2005, 2006) and elucidating the viral life cycle employing immunostaining and EM techniques (Offerdahl et al., 2012; Senigl, Grubhoffer & Kopecký, 2006; Senigl, Kopecký & Grubhoffer, 2004). These studies, especially the earlier studies looking at virus propagation, revealed that the kinetics of virus infection vary depending on the cell lines used; thus to be able to identify suitable parameters for conducting experiments characterisation of viral infection must be established first for the virus and cell line of interest.

In Chapter 3, previous findings of tick cells being able to support and produce infectious virus particles upon tick-borne (LGTV and TBEV) and mosquito-borne virus (SFV) infection were confirmed and expanded by identifying the number of cells permissive for virus infection using different MOIs (LGTV, TBEV and SFV) and by determining replication kinetics (SFV and LGTV) in different tick cell lines. These basic parameters were used to identify a suitable MOI and suitable time-points for subsequent experiments and could be useful for other researchers planning experiments using the same viruses in the same tick cell lines. Additional important parameters were established, such as that long term experiments in tick cells, especially IRE/CTVM19, should be conducted in sealed culture tubes rather than in multiwell plates, since cell growth and thus possibly viability is impaired in multiwell plates. However short term experiments of up to 5 days are still possible in multiwell plates. Furthermore, as observed in mosquito cells (Finkelstein et al., 1999; Guerbois et al., 2013; Volkova et al., 2008), tick cells were found to be unable to support EMCV IRES-driven expression of reporter genes, thus either a different IRES (Woolaway et al., 2001; Wu et al., 2008) or other promoters suitable for tick cells need to be identified.

As part of a published study which established optimised parameters for RNAi-mediated gene silencing for different tick cell lines (Barry et al., 2013), the uptake of dsRNA and siRNAs with or without transfection reagent was investigated. In that study it was shown that for the uptake of siRNA a transfection reagent is required, whereas dsRNA alone was taken up from the medium by IDE8, ISE6 and

IRE/CTVM19 cells. However, more efficient and consistent gene silencing was observed in IRE/CTVM19 when dsRNA was transfected into the cells.

All the experimental designs and infection parameters established within the present study will be of use to other researchers working with tick cells and/or viruses, by pointing out important considerations for planning their experiments.

One of the most important findings reported in Chapter 3 of the present study was that all three tick cell lines used (ISE6, IDE8 and IRE/CTVM19), already carried endogenous viruses which by EM resemble reovirus-like particles. While the endogenous virus in the IDE8 cell line is known to be the orbivirus SCRV (Attoui et al., 2001; Bell-Sakyi et al., 2007), the viruses infecting IRE/CTVM19 and ISE6 cells are still unidentified (Alberdi et al., 2012; Bell-Sakyi & Attoui, 2013). However, the transcriptomic and proteomic information obtained within this study might be useful in identifying these endogenous viruses, depending on sequence similarities. It is unclear if these endogenous viruses moderate or even suppress the innate immune response to infection with other arboviruses and if they are perhaps an explanation for the low-level persistent infection without any cytopathic effect in tick cells. However, they do not seem to interfere with infection of tick cells with another virus since virus infection, replication and production of TBEV, LGTV and SFV was still possible, which is in agreement with previous studies (Leake, Pudney & Varma, 1980). The recent study by Schnettler et al. (2014) identified SCRV-specific viRNAs in the IDE8 cell line, suggesting that the RNAi pathway actively suppresses SCRV. This implicates the endogenous viruses in interaction with the innate immune system in tick cells. It would have been interesting to test whether the RNA levels of the endogenous viruses change upon infection with another virus, and if silencing of target genes has an effect on the endogenous viruses, which might indicate if these are involved in modulating a particular pathway. Furthermore, it would be interesting to investigate how curing these tick cell lines of endogenous virus infection (Bell-Sakyi & Attoui, 2013) would affect the tick cells, as well as newly-introduced viruses and the immune response towards virus infection. Investigating the interaction of endogenous viruses with ticks and/or tick cell lines and their influence on virus infection might be an interesting future research topic. It might reveal if

these endogenous viruses could be exploited as tools, similar to the obligate intracellular gram-negative bacterium *Wolbachia* which is able to protect *Drosophila* and mosquitoes from arbovirus infection (Merkling & van Rij, 2012), to control tick infection and virus transmission in nature.

In Chapter 4, the hypothesis that viral infection of tick cells leads to differential expression and/or representation of mRNA transcripts and/or proteins involved in the viral defence response was addressed. To identify possible antiviral immune-related molecules, IDE8 and IRE/CTVM19 cells were infected with TBEV, processed for transcriptomic and proteomic analysis, and differentially expressed/represented transcripts and proteins, respectively, were identified. These were involved in a variety of different biological processes, including metabolism, transport, protein folding, nucleic acid processing, signalling, cell stress and immunity, confirming that tick cells react towards virus infection at the transcriptome and proteome level, as observed in other arthropods upon viral infection (Bartholomay et al., 2004; Bonizzoni et al., 2012; Colpitts et al., 2011a; McNally et al., 2012; Pastorino et al., 2009; Sim & Dimopoulos, 2010; Sim, Ramirez & Dimopoulos, 2012; Waldock, Olson & Christophides, 2012; Xi, Ramirez & Dimopoulos, 2008; Zhang et al., 2013). Some of these transcripts and/or proteins, such as those involved in nucleic acid processing, transport, metabolism, protein folding and cell stress, have also been identified in other species as important host cell factors exploited by viruses to support their life cycle, including endocytosis, trafficking, viral RNA transcription and translation and maturation. Further analysis of these, which was however not done in the present study due to time constraints, might help to elucidate the specific factors required for successful infection, replication and production of viruses by ticks and tick cell lines. This dataset therefore presents an important starting point which could be successfully used by other researchers as a basis for elucidating the viral life-cycle and virus-vector relationships.

Additionally, the dataset was able to reveal transcripts and/or proteins with a possible role in immune-related pathways such as the ubiquitin-proteasome pathway, phagocytosis, the complement system, RNAi with the piRNA pathway, and the UPR. It is obvious from the present study that virus infection changes gene expression and

protein representation in tick cells and that RNAi is not the only mechanism involved in the antiviral response in ticks. The present study highlights the view that the antiviral response in tick cells, and by extrapolation ticks, is more complex than previously thought and encourages further research into elucidating the cellular mechanisms behind virus infection in tick cell lines and ticks, for which the generated datasets might be used as a starting point.

As presented in Chapter 5, the influence on virus infection of a subset of these differentially represented transcripts/proteins, was elucidated by knockdown experiments. The most convincing results were obtained upon knockdown of Ago-30, Dcr-90, HSP90 and gp96, as well as possibly complement Factor H, which suggests a role for these in the antiviral response in tick cells. In contrast, calreticulin seems to have a proviral role during virus infection in tick cells. These findings are encouraging and warrant further experiments to pinpoint the possible mechanisms and pathways behind their antiviral function. Further knockdown experiments *in vitro* and *in vivo*, as well as overexpression studies, should be conducted to prove their functional role in tick cells and ticks.

This study was able to identify important parameters required for successfully conducting experiments in tick cells as well as elucidating the kinetics of viral infection in specific tick cell lines. Important results were obtained in tick cells, despite their heterogeneity, slow growth and chronic infection with endogenous viruses, which encourages the use of tick cells for preliminary experiments, instead of the much more difficult-to-handle ticks *in vivo*. This might furthermore reduce the number of animals required for tick feeding experiments, thus benefiting animal welfare. Furthermore, this was the first study applying transcriptomic and proteomic techniques to investigate the response of tick cells to virus infection. This study enhances the understanding of viral infection of tick cells by revealing the identity of transcripts and proteins with a possible role in the viral lifecycle as well as the innate antiviral defence response. The generated datasets can be used as a basis for additional studies investigating the identity of endogenous viruses, identifying important host cell factors required for viral infection as well as elucidating the innate immune response of tick cells to virus infection.

Reference list

Abdallah, C., Dumas-Gaudot, E., Renaut, J., and Sergeant, K. (2012). Gel-based and gel-free quantitative proteomics approaches at a glance. *Int. J. Plant Genomics* 2012, 494572.

Ackermann, M., and Padmanabhan, R. (2001). *De novo* synthesis of RNA by the dengue virus RNA-dependent RNA polymerase exhibits temperature dependence at the initiation but not elongation phase. *J. Biol. Chem.* 276, 39926–39937.

Acosta, E.G., Castilla, V., and Damonte, E.B. (2008). Functional entry of dengue virus into *Aedes albopictus* mosquito cells is dependent on clathrin-mediated endocytosis. *J. Gen. Virol.* 89, 474–484.

Acosta, E.G., Castilla, V., and Damonte, E.B. (2011). Infectious dengue-1 virus entry into mosquito C6/36 cells. *Virus Res.* 160, 173–179.

Agarwala, K., Kawabata, S., Hirata, M., Miyagi, M., Tsunasawa, S., and Iwanaga, S. (1996). A cysteine protease inhibitor stored in the large granules of horseshoe crab hemocytes: purification, characterization, cDNA cloning and tissue localization. *J. Biochem.* 119, 85–94.

Agashe, V.R., and Hartl, F.U. (2000). Roles of molecular chaperones in cytoplasmic protein folding. *Semin. Cell Dev. Biol.* 11, 15–25.

Ahn, A., Klimjack, M., Chatterjee, P., and Kielian, M. (1999). An epitope of the Semliki Forest virus fusion protein exposed during virus-membrane fusion. *J. Virol.* 73, 10029–10039.

Ai, H.-S., Huang, Y.-C., Li, S.-D., Weng, S.-P., Yu, X.-Q., and He, J.-G. (2008). Characterization of a prophenoloxidase from hemocytes of the shrimp *Litopenaeus vannamei* that is down-regulated by white spot syndrome virus. *Fish Shellfish Immunol.* 25, 28–39.

Ai, H.-S., Liao, J.-X., Huang, X.-D., Yin, Z.-X., Weng, S.-P., Zhao, Z.-Y., Li, S.-D., Yu, X.-Q., and He, J.-G. (2009). A novel prophenoloxidase 2 exists in shrimp hemocytes. *Dev. Comp. Immunol.* 33, 59–68.

Aitken, A. (2006). 14-3-3 proteins: A historic overview. *Semin. Cancer Biol.* 16, 162–172.

Alberdi, M.P., Dalby, M.J., Rodriguez-Andres, J., Fazakerley, J.K., Kohl, A., and Bell-Sakyi, L. (2012). Detection and identification of putative bacterial endosymbionts and endogenous viruses in tick cell lines. *Ticks Tick-borne. Dis.* 3, 137–146.

Alekseev, A.N., and Chunikhin, S.P. (1990). The experimental transmission of the tick-borne encephalitis virus by ixodid ticks (the mechanisms, time periods, species and sex differences). *Parazitologiia* 24, 177–185.

Aliperti, G., and Schlesinger, M. (1978). Evidence for an autoprotease activity of Sindbis virus capsid protein. *Virology* 369, 366–369.

Aljamali, M.N., Sauer, J.R., and Essenberg, R.C. (2002). RNA interference: applicability in tick research. *Exp. Appl. Acarol.* 28, 89–96.

Amparyup, P., Charoensapsri, W., and Tassanakajon, A. (2013). Prophenoloxidase system and its role in shrimp immune responses against major pathogens. *Fish Shellfish Immunol.* 34, 990–1001.

Anders, S., and Huber, W. (2010). Differential expression analysis for sequence count data. *Genome Biol.* 11, R106.

Anderson, P., and Kedersha, N. (2006). RNA granules. *J. Cell Biol.* 172, 803–808.

Anderson, P., and Kedersha, N. (2008). Stress granules: the Tao of RNA triage. *Trends Biochem. Sci.* 33, 141–150.

Andrew, D.R. (2011). A new view of insect-crustacean relationships II. Inferences from expressed sequence tags and comparisons with neural caldistics. *Arthropod Struct Dev.*40, 289-302.

Andzhaparidze, O.G., Bogomolova, N.N., Boriskin, Y.S., Bektemirova, M.S., and Drynov, I.D. (1981). Comparative study of rabies virus persistence in human and hamster cell lines. *J. Virol.* 37, 1–6.

Angelo, I.C., Gôlo, P.S., Perinotto, W.M.S., Camargo, M.G., Quinelato, S., Sá, F.A., Pontes, E.G., and Bittencourt, V.R.E.P. (2013). Neutral lipid composition changes in the fat bodies of engorged females *Rhipicephalus microplus* ticks in response to fungal infections. *Parasitol. Res.* 112, 501–509.

Antunes, S., Galindo, R.C., Almazán, C., Rudenko, N., Golovchenko, M., Grubhoffer, L., Shkap, V., do Rosário, V., de la Fuente, J., and Domingos, A. (2012). Functional genomics studies of *Rhipicephalus (Boophilus) annulatus* ticks in response to infection with the cattle protozoan parasite, *Babesia bigemina*. *Int. J. Parasitol.* 42, 187–195.

Armstrong, J. (2000). How do Rab proteins function in membrane traffic? *Int. J. Biochem. Cell Biol.* 32, 303–307.

Arnot, C.J., Gay, N.J., and Gangloff, M. (2010). Molecular mechanism that induces activation of Spätzle, the ligand for the *Drosophila* Toll receptor. *J. Biol. Chem.* 285, 19502–19509.

Asgari, S. (2013). MicroRNA functions in insects. *Insect Biochem. Mol. Biol.* 43, 388–397.

Atrasheuskaya, A.V., Fredeking, T.M., and Ignatyev, G.M. (2003). Changes in immune parameters and their correction in human cases of tick-borne encephalitis. *Clin. Exp. Immunol.* 131, 148–154.

Attoui, H., Stirling, J.M., Munderloh, U.G., Billoir, F., Brookes, S.M., Burroughs, J.N., de Micco, P., Mertens, P.P., and de Lamballerie, X. (2001). Complete sequence characterization of the genome of the St Croix River virus, a new orbivirus isolated from cells of *Ixodes scapularis*. *J. Gen. Virol.* 82, 795–804.

Aung, K.M., Boldbaatar, D., Umemiya-Shirafuji, R., Liao, M., Xuenan, X., Suzuki, H., Galay, R.L., Tanaka, T., and Fujisaki, K. (2011). Scavenger receptor mediates systemic RNA interference in ticks. *PLoS One* 6, e28407.

Aung, K.M., Boldbaatar, D., Umemiya-Shirafuji, R., Liao, M., Tsuji, N., Xuenan, X., Suzuki, H., Kume, A., Galay, R.L., Tanaka, T., and Fujisaki, K. (2012). HlSRB, a Class B scavenger receptor, is key to the granulocyte-mediated microbial phagocytosis in ticks. *PLoS One* 7, e33504.

Avadhanula, V., Weasner, B.P., Hardy, G.G., Kumar, J.P., and Hardy, R.W. (2009). A novel system for the launch of alphavirus RNA synthesis reveals a role for the Imd pathway in arthropod antiviral response. *PLoS Pathog.* 5, e1000582.

Balogh, Z., Ferenczi, E., Szeles, K., Stefanoff, P., Gut, W., Szomor, K.N., Takacs, M., and Berencsi, G. (2010). Tick-borne encephalitis outbreak in Hungary due to consumption of raw goat milk. *J. Virol. Methods* 163, 481–485.

Bantscheff, M., Schirle, M., Sweetman, G., Rick, J., and Kuster, B. (2007). Quantitative mass spectrometry in proteomics: a critical review. *Anal. Bioanal. Chem.* 389, 1017–1031.

Barker, S.C., and Murrell, A. (2004). Systematics and evolution of ticks with a list of valid genus and species names. *Parasitology* 129, S15–S36.

Barnard, A.-C., Nijhof, A.M., Gaspar, A.R.M., Neitz, A.W.H., Jongejan, F., and Maritz-Olivier, C. (2012a). Expression profiling, gene silencing and transcriptional networking of metzincin metalloproteases in the cattle tick, *Rhipicephalus (Boophilus) microplus*. *Vet. Parasitol.* 186, 403–414.

Barnard, A.-C., Nijhof, A.M., Fick, W., Stutzer, C., and Maritz-Olivier, C. (2012b). RNAi in arthropods: Insight into the machinery and applications for understanding the pathogen-vector interface. *Genes (Basel).* 3, 702–741.

Barrero, R. A., Keeble-Gagnère, G., Zhang, B., Moolhuijzen, P., Ikeo, K., Tateno, Y., Gojobori, T., Guerrero, F.D., Lew-Tabor, A., and Bellgard, M. (2011). Evolutionary conserved microRNAs are ubiquitously expressed compared to tick-specific miRNAs in the cattle tick *Rhipicephalus (Boophilus) microplus*. *BMC Genomics* 12, 328.

Barrett, A.D.T., and Higgs, S. (2007). Yellow fever: a disease that has yet to be conquered. *Ann. Rev. Entomol.* 52, 209–229.

Barry, G., Fragkoudis, R., Ferguson, M.C., Lulla, A., Merits, A., Kohl, A., and Fazakerley, J.K. (2010). Semliki forest virus-induced endoplasmic reticulum stress accelerates apoptotic death of mammalian cells. *J. Virol.* 84, 7369–7377.

Barry, G., Alberdi, P., Schnettler, E., Weisheit, S., Kohl, A., Fazakerley, J.K., and Bell-Sakyi, L. (2013). Gene silencing in tick cell lines using small interfering or long double-stranded RNA. *Exp. Appl. Acarol.* 59, 319–338.

Barth, O. (1999). Ultrastructural aspects of the dengue virus (flavivirus) particle morphogenesis. *J. Submicrosc. Cytol. Pathol.* 31, 407–412.

Bartholomay, L., Cho, W., Rocheleau, T., Boyle, J.P., Beck, E.T., Fuchs, J.F., Liss, P., Rusch, M., Butler, K.M., Wu, R.C.-C., Lin, S.-P., Kuo, H.-Y., Tsao, I.-Y., Huang, C.-Y., Liu, T.-T., Hsiao, K.-J., Tsai, S.-F., Yang, U.-C., Nappi, A. J., Perna, N. T., Chen, C.-C., and Christensen, B.M.(2004). Description of the transcriptomes of immune response-activated hemocytes from the mosquito vectors *Aedes aegypti* and *Armigeres subalbatus*. *Infect. Immun.* 72, 4114–4126.

Bazlikova, M., Kazar, J., and Schramek, S. (1984). Phagocytosis of *Coxiella burnetti* by *Hyalomma dromedarii* tick haemocytes. *Acta Virol.* 28, 48–52.

Behnke, J., and Hendershot, L.M. (2013). The large Hsp70 Grp170 binds to unfolded protein substrates in vivo with a regulation distinct from conventional Hsp70s. *J. Biol. Chem.* 0–20.

Bellés, X. (2010). Beyond *Drosophila*: RNAi in vivo and functional genomics in insects. *Ann. Rev. Entomol.* 55, 111–128.

Bell-Sakyi, L., and Attoui, H. (2013). Endogenous tick viruses and modulation of tick-borne pathogen growth. *Front. Cell. Infect. Microbiol.* 3, 25.

Bell-Sakyi, L., Zweygarth, E., Blouin, E.F., Gould, E. A, and Jongejan, F. (2007). Tick cell lines: tools for tick and tick-borne disease research. *Trends Parasitol.* 23, 450–457.

Bell-Sakyi, L., Růzek, D., and Gould, E. A. (2009). Cell lines from the soft tick *Ornithodoros moubata*. *Exp. Appl. Acarol.* 49, 209–219.

Bell-Sakyi, L., Kohl, A., Bente, D. A., and Fazakerley, J.K. (2012). Tick cell lines for study of Crimean-Congo hemorrhagic fever virus and other arboviruses. *Vector-borne Zoonot. Dis.* 12, 138–150.

Belova, O. A., Burenkova, L. A., and Karganova, G.G. (2012). Different tick-borne encephalitis virus (TBEV) prevalences in unfed versus partially engorged ixodid ticks – evidence of virus replication and changes in tick behavior. *Ticks Tick-borne. Dis.* 3, 240–246.

Berezikov, E. (2011). Evolution of microRNA diversity and regulation in animals. *Nat. Rev. Genet.* 12, 846–860.

Bernstein, E., Caudy, A. A., Hammond, S. M., and Hannon, G. J. (2001). Role for a bidentate ribonuclease in the initiation step of RNA interference. *Nature* 409, 363–366.

Best, S. M., Morris, K. L., Shannon, J. G., Robertson, S. J., Mitzel, D. N., Park, G. S., Boer, E., Wolfinbarger, J.B., and Bloom, M. E. (2005). Inhibition of interferon-stimulated JAK-STAT signaling by a tick-borne flavivirus and identification of NS5 as an interferon antagonist. *J. Virol.* 79, 12828.

Bhat, B.K.M., and Yunker, C.E. (1979). Susceptibility of a tick cell line (*Dermacentor parumapertus* Neumann) to infection with arboviruses. In Arctic and Tropical Arboviruses, E. Kurstak, ed. (New York, NY: Academic Press), pp. 263–275.

Bissinger, B.W., Donohue, K. V, Khalil, S.M.S., Grozinger, C.M., Sonenshine, D.E., Zhu, J., and Roe, R.M. (2011). Synganglion transcriptome and developmental global gene expression in adult females of the American dog tick, *Dermacentor variabilis* (Acari: Ixodidae). *Insect Mol. Biol.* 20, 465–491.

Blackwell, J.L., and Brinton, M.A. (1997). Translation elongation factor-1 alpha interacts with the 3'stem-loop region of West Nile virus genomic RNA. *J. Virol.* 71, 6433–6444.

Blair, C.D. (2011). Mosquito RNAi is the major innate immune pathway controlling arbovirus infection and transmission. *Future Microbiol.* 6, 265–277.

Le Blanc, I., Luyet, P.-P., Pons, V., Ferguson, C., Emans, N., Petiot, A., Mayran, N., Demaurex, N., Fauré, J., Sadoul, R., et al. (2005). Endosome-to-cytosol transport of viral nucleocapsids. *Nat. Cell Biol.* 7, 653–664.

Bloor, S., Maelfait, J., Krumbach, R., Beyaert, R., and Randow, F. (2010). Endoplasmic reticulum chaperone gp96 is essential for infection with vesicular stomatitis virus. *Proc. Natl. Acad. Sci. USA.* 107, 6970–6975.

Blouin, E.F., Manzano-Roman, R., de la Fuente, J., and Kocan, K.M. (2008). Defining the role of subolesin in tick cell culture by use of RNA interference. *Ann. N. Y. Acad. Sci.* 1149, 41–44.

Blue, C.E., Spiller, O.B., and Blackbourn, D.J. (2004). The relevance of complement to virus biology. *Virology* 319, 176–184.

Bonatti, S., Migliaccio, G., Blobel, G., and Walter, P. (1984). Role of signal recognition particle in the membrane assembly of Sindbis viral glycoproteins. *Eur. J. Biochem.* 140, 499–502.

Bonizzoni, M., Dunn, W.A., Campbell, C.L., Olson, K.E., Marinotti, O., and James, A. A. (2012). Complex modulation of the *Aedes aegypti* transcriptome in response to dengue virus infection. *PLoS One* 7, e50512.

Booth, T.F., Gould, E. A. and Nuttall, P.A. (1991). Structure and morphogenesis of Dugbe virus (*Bunyaviridae*, *Nairovirus*) studied by immunogold electron microscopy of ultrathin cryosections. *Virus Res.* 21, 199–212.

Borovičková, B., and Hypša, V. (2005). Ontogeny of tick hemocytes: a comparative analysis of *Ixodes ricinus* and *Ornithodoros moubata*. *Exp. Appl. Acarol.* 35, 317–333.

Van Bortel, W., Dorleans, F., Rosine, J., Blateau, A., Rousset, D., Matheus, S., Leparc-Goffart, I., Flusin, O., Prat, C., Cesaire, R., Najioullah, F., Ardillon, V., Balleydier, E., Carvalho, L., Lemaître, A., Noel, H., Servas, V., Six, C., Zurbaran, M., Leon, L., Guinard, A., van den Kerkhof, J., Henry, M., Fanoy, E., Braks, M., Reimerink, J., Swaan, C., Georges, R., Brooks, L., Freedman, J., Sudre, B., and Zeller, H. (2014). Chikungunya outbreak in the Caribbean region, December 2013 to March 2014, and the significance for Europe. *Eurosurveillance* 19, 1–11.

Brackney, D.E., Scott, J.C., Sagawa, F., Woodward, J.E., Miller, N. A., Schilkey, F.D., Mudge, J., Wilusz, J., Olson, K.E., Blair, C.D., and Ebel, G.D. (2010). C6/36 *Aedes albopictus* cells have a dysfunctional antiviral RNA interference response. *PLoS Negl. Trop. Dis.* 4, e856.

Bray, S.J. (2006). Notch signalling: a simple pathway becomes complex. *Nat. Rev. Mol. Cell Biol.* 7, 678–689.

Breakwell, L., Dosenovic, P., Karlsson Hedestam, G.B., D'Amato, M., Liljeström, P., Fazakerley, J., and McInerney, G.M. (2007). Semliki Forest virus nonstructural protein 2 is involved in suppression of the type I interferon response. *J. Virol.* 81, 8677–8684.

Brennecke, J., Aravin, A. a, Stark, A., Dus, M., Kellis, M., Sachidanandam, R., and Hannon, G.J. (2007). Discrete small RNA-generating loci as master regulators of transposon activity in *Drosophila*. *Cell* 128, 1089–1103.

Brinton, M.A., and Dispoto, J.H. (1988). Sequence and secondary structure analysis of the 5 ' -terminal region of flavivirus genome RNA. *Virology* 162, 290–299.

Broehan, G., Kroeger, T., Lorenzen, M., and Merzendorfer, H. (2013). Functional analysis of the ATP-binding cassette (ABC) transporter gene family of *Tribolium castaneum*. *BMC Genomics* 14, 6.

Buresova, V., Hajdusek, O., Franta, Z., Sojka, D., and Kopacek, P. (2009). IrAM – An α_2-macroglobulin from the hard tick *Ixodes ricinus*: characterization and function in phagocytosis of a potential pathogen *Chryseobacterium indologenes*. *Dev. Comp. Immunol.* 33, 489–498.

Buresova, V., Hajdusek, O., Franta, Z., Loosova, G., Grunclova, L., Levashina, E. A, and Kopacek, P. (2011). Functional genomics of tick thioester-containing proteins reveal the ancient origin of the complement system. *J. Innate Immun.* 3, 623–630.

Buresová, V., Franta, Z., and Kopácek, P. (2006). A comparison of *Chryseobacterium indologenes* pathogenicity to the soft tick *Ornithodoros moubata* and hard tick *Ixodes ricinus*. *J. Invertebr. Pathol.* 93, 96–104.

Busby, A. T., Ayllón, N., Kocan, K.M., Blouin, E.F., de la Fuente, G., Galindo, R.C., Villar, M., and de la Fuente, J. (2012). Expression of heat shock proteins and subolesin affects stress responses, *Anaplasma phagocytophilum* infection and questing behaviour in the tick, *Ixodes scapularis*. *Med. Vet. Entomol.* 26, 92–102.

Calisher, C.H., and Gould, E.A. (2003). Taxonomy of the virus family *Flaviviridae*. *Adv. Virus Res.* 59, 1–19.

Cannon, J., Dishaw, L., Haire, R. Litman, R. T., Ostrov, D. A., and Litman, G. W. (2010). Recognition of additional roles for immunoglobulin domains in immune function. *Semin. Immunol.* 22, 17–24.

Carpenter, J., Hutter, S., Baines, J.F., Roller, J., Saminadin-Peter, S.S., Parsch, J., and Jiggins, F.M. (2009). The transcriptional response of *Drosophila melanogaster* to infection with the sigma virus (*Rhabdoviridae*). *PLoS One* 4, e6838.

Carr, S., Aebersold, R., Baldwin, M., Burlingame, A., Clauser, K., and Nesvizhskii, A. (2004). The need for guidelines in publication of peptide and protein identification data. *Mol. Cell. Proteomics* 3, 531–533.

Carvalho, F. A., Carneiro, F.A., Martins, I.C., Assunção-Miranda, I., Faustino, A.F., Pereira, R.M., Bozza, P.T., Castanho, M.A.R.B., Mohana-Borges, R., Da Poian, A.T., and Santos,N.C. (2012). Dengue virus capsid protein binding to hepatic lipid droplets (LD) is potassium ion dependent and is mediated by LD surface proteins. *J. Virol.* 86, 2096–2108.

Caudy, A. A, Ketting, R.F., Hammond, S.M., Denli, A.M., Bathoorn, A.M.P., Tops, B.B.J., Silva, J.M., Myers, M.M., Hannon, G.J., and Plasterk, R.H.A. (2003). A micrococcal nuclease homologue in RNAi effector complexes. *Nature* 425, 411–414.

Ceraul, S.M., Sonenshine, D.E., and Hynes, W.L. (2002). Resistance of the tick *Dermacentor variabilis* (Acari: Ixodidae) following challenge with the bacterium *Escherichia coli* (Enterobacteriales: Enterobacteriaceae). *J. Med. Entomol.* 39, 376–383.

Cerenius, L., Lee, B.L., and Söderhäll, K. (2008). The proPO-system: pros and cons for its role in invertebrate immunity. *Trends Immunol.* 29, 263–271.

Cerione, R.A. (2004). Cdc42: new roads to travel. *Trends Cell Biol.* 14, 127–132.

Chambers, T.J., Hahn, C.S., Galler, R., and Rice, C.M. (1990). Flavivirus Genome organization, expression, and replication. *Ann. Rev. Microbiol.* 44, 649–688.

Charrel, R.N., and de Lamballerie, X. (2008). Chikungunya virus in north-eastern Italy: a consequence of seasonal synchronicity. *Eurosurveillance* 13, 8003.

Charrel, R.N., de Lamballerie, X., and Raoult, D. (2007). Chikungunya outbreaks-the globalization of vectorborne diseases. *N. Engl. J. Med.* 356, 769–771.

Charrel, R.N., Attoui, H., Butenko, A.M., Clegg, J.C., Deubel, V., Frolova, T. V, Gould, E.A, Gritsun, T.S., Heinz, F.X., Labuda, M., Lashkevich, V.A., Loktev, V., Lundkvist, A., Lvov, D.V., Mandl, C.W., Niedrig, M., Papa, A., Petrov, V.S., Plyusnin, A., Randolph, S., Süss, J., Zlobin, V.I., de Lamballerie, X. (2004). Tick-borne virus diseases of human interest in Europe. *Clin. Microbiol. Infect.* 10, 1040–1055.

Chee, H.-Y., and AbuBakar, S. (2004). Identification of a 48kDa tubulin or tubulin-like C6/36 mosquito cells protein that binds dengue virus 2 using mass spectrometry. *Biochem. Biophys. Res. Commun.* 320, 11–17.

Cheeseman, M.T., Bates, PA., and Crampton, J.M. (2001). Preliminary characterisation of esterase and platelet-activating factor (PAF)-acetylhydrolase activities from cat flea (*Ctenocephalides felis*) salivary glands. *Insect Biochem. Mol. Biol.* 31, 157–164.

Chelius, D., and Bondarenko, P. (2002). Quantitative profiling of proteins in complex mixtures using liquid chromatography and mass spectrometry. *J. Proteome Res.* 1, 317–323.

Chen, C., Munderloh, U.G., and Kurtti, T.J. (1994). Cytogenetic characteristics of cell lines from *Ixodes scapularis* (Acari: Ixodidae). *J. Med. Entomol.* 31, 425–434.

Chen, W.Y., Ho, K.C., Leu, J.H., Liu, K.F., Wang, H.C., Kou, G.H., and Lo, C.F. (2008). WSSV infection activates STAT in shrimp. *Dev. Comp. Immunol.* 32, 1142–1150.

Cherry, S. (2009). VSV infection is sensed by *Drosophila*, attenuates nutrient signaling, and thereby activates antiviral autophagy. *Autophagy* 5, 1062–1063.

Chiang, Y.-A., Hung, H.-Y., Lee, C.-W., Huang, Y.-T., and Wang, H.-C. (2013). Shrimp Dscam and its cytoplasmic tail splicing activator serine/arginine (SR)-rich protein B52 were both induced after white spot syndrome virus challenge. *Fish Shellfish Immunol.* 34, 209–219.

Choi, I.K., and Hyun, S. (2012). Conserved microRNA miR-8 in fat body regulates innate immune homeostasis in *Drosophila*. *Dev. Comp. Immunol.* 37, 50–54.

Choy, A., Severo, M.S., Sun, R., Girke, T., Gillespie, J.J., and Pedra, J.H.F. (2013). Decoding the ubiquitin-mediated pathway of arthropod disease vectors. *PLoS One* 8, e78077.

Christensen, B.M., Li, J., Chen, C.-C., and Nappi, A.J. (2005). Melanization immune responses in mosquito vectors. *Trends Parasitol.* 21, 192–199.

Chu, J.J.H., and Ng, M.L. (2002). Trafficking mechanism of West Nile (Sarafend) virus structural proteins. *J. Med. Virol.* 136, 127–136.

Chu, J.J.H., and Ng, M.L. (2004). Infectious entry of West Nile virus occurs through a clathrin-mediated endocytic pathway. *J. Virol.* 78, 10543–10555.

Chu, P.W., and Westaway, E.G. (1985). Replication strategy of Kunjin virus: evidence for recycling role of replicative form RNA as template in semiconservative and asymmetric replication. *Virology* 140, 68–79.

Chu, J.J.H., Leong, P.W.H., and Ng, M.L. (2006). Analysis of the endocytic pathway mediating the infectious entry of mosquito-borne flavivirus West Nile into *Aedes albopictus* mosquito (C6/36) cells. *Virology* 349, 463–475.

Chung, K.M., Liszewski, M.K., Nybakken, G., Davis, A.E., Townsend, R.R., Fremont, D.H., Atkinson, J.P., and Diamond, M.S. (2006). West Nile virus nonstructural protein NS1 inhibits complement activation by binding the regulatory protein factor H. *Proc. Natl. Acad. Sci. U. S. A.* 103, 19111–19116.

Ciota, A.T., and Kramer, L.D. (2010). Insights into arbovirus evolution and adaptation from experimental studies. *Viruses* 2, 2594–2617.

Clarke, J.B., and Spier, R.E. (1983). An investigation into causes of resistance of a cloned line of BHK cells to a strain of foot-and-mouth disease virus. *Vet. Microbiol.* 8, 259–270.

Cleaves, G.R., and Dubin, D.T. (1979). Methylation status of intracellular dengue type 2 40 S RNA. *Virology* 96, 159–165.

Cleaves, G.R., Ryan, T.E., and Schlesinger, R.W. (1981). Identification and characterization of type 2 dengue virus replicative intermediate and replicative form RNAs. *Virology* 111, 73–83.

Coffey, L., Forrester, N., Tsetsarkin, K., Vasilakis, N., Weaver, S.C. (2013). Factors shaping the adaptive landscape for arboviruses: implications for the emergence of disease. *Future Microbiol.* 8, 155–176.

Cogoni, C., and Macino, G. (2000). Post-transcriptional gene silencing across kingdoms. *Curr. Opin. Genet. Dev.* 10, 638–643.

Colpitts, T.M., Cox, J., Vanlandingham, D.L., Feitosa, F.M., Cheng, G., Kurscheid, S., Wang, P., Krishnan, M.N., Higgs, S., and Fikrig, E. (2011a). Alterations in the *Aedes aegypti* transcriptome during infection with West Nile, Dengue and Yellow Fever viruses. *PLoS Pathog.* 7, e1002189.

Colpitts, T.M., Barthel, S., Wang, P., and Fikrig, E. (2011b). Dengue virus capsid protein binds core histones and inhibits nucleosome formation in human liver cells. *PLoS One* 6, e24365.

Conesa, A., Götz, S., García-Gómez, J.M., Terol, J., Talón, M., and Robles, M. (2005). Blast2GO: a universal tool for annotation, visualization and analysis in functional genomics research. *Bioinformatics* 21, 3674–3676.

Connor, J.H., McKenzie, M.O., Parks, G.D., and Lyles, D.S. (2007). Antiviral activity and RNA polymerase degradation following Hsp90 inhibition in a range of negative strand viruses. *Virology* 362, 109–119.

Cook, S., Moureau, G., Kitchen, A., Gould, E. A, de Lamballerie, X., Holmes, E.C., and Harbach, R.E. (2012). Molecular evolution of the insect-specific flaviviruses. *J. Gen. Virol.* 93, 223–234.

Cordes, E.J., Licking-Murray, K.D., and Carlson, K. A. (2013). Differential gene expression related to Nora virus infection of *Drosophila melanogaster*. *Virus Res.* 175, 95–100.

Costa, A., Jan, E., Sarnow, P., and Schneider, D. (2009). The Imd pathway is involved in antiviral immune responses in *Drosophila*. *PLoS One* 4, e7436.

Cotté, V., Sabatier, L., Schnell, G., Carmi-Leroy, A., Rousselle, J.-C., Arsène-Ploetze, F., Malandrin, L., Sertour, N., Namane, A., Ferquel, E., and Choumet, V. (2014). Differential expression of *Ixodes ricinus* salivary gland proteins in the presence of the *Borrelia burgdorferi* sensu lato complex. *J. Proteomics* 96, 29–43.

Courageot, M., Frenkiel, M., Santos Duarte Dos, C., Deubel, V., and Desprès, P. (2000). α -glucosidase inhibitors reduce dengue virus production by affecting the initial steps of virion morphogenesis in the endoplasmic reticulum. *J. Virol.* 74, 564–572.

Crochu, S., Cook, S., Attoui, H., Charrel, R.N., De Chesse, R., Belhouchet, M., Lemasson, J.-J., de Micco, P., and de Lamballerie, X. (2004). Sequences of flavivirus-related RNA viruses persist in DNA form integrated in the genome of *Aedes* spp. mosquitoes. *J. Gen. Virol.* 85, 1971–1980.

Cruz, C.E., Fogaça, A.C., Nakayasu, E.S., Angeli, C.B., Belmonte, R., Almeida, I.C., Miranda, A., Miranda, M.T.M., Tanaka, A.S., Braz, G.R., Craik, C.S., Schneider, E., Caffrey, C.R., Daffre, S. (2010). Characterization of proteinases from the midgut of *Rhipicephalus (Boophilus) microplus* involved in the generation of antimicrobial peptides. *Parasit. Vectors* 3, 63.

Cullen, P.J. (2008). Endosomal sorting and signalling: an emerging role for sorting nexins. *Nat. Rev. Mol. Cell Biol.* 9, 574–582.

D'Souza-Schorey, C., and Chavrier, P. (2006). ARF proteins: roles in membrane traffic and beyond. *Nat. Rev. Mol. Cell Biol.* 7, 347–358.

Danielová, V., and Kliegrová, S. (2008). Influence of climate warming on tick-borne encephalitis expansion to higher altitudes over the last decade (1997-2006) in the highland region (Czech Republic). *Cent. Eur. J. Heal.* 16, 4–11.

Danielová, V., Holubová, J., Pejcoch, M., and Daniel, M. (2002). Potential significance of transovarial transmission in the circulation of tick-borne encephalitis virus. *Folia Parasitol. (Praha).* 49, 323–325.

Daugeron, M.-C., Prouteau, M., Lacroute, F., and Séraphin, B. (2011). The highly conserved eukaryotic DRG factors are required for efficient translation in a manner redundant with the putative RNA helicase Slh1. *Nucleic Acids Res.* 39, 2221–2233.

Davis, W.G., Blackwell, J.L., Shi, P.-Y., and Brinton, M.A. (2007). Interaction between the cellular protein eEF1A and the 3'-terminal stem-loop of West Nile virus genomic RNA facilitates viral minus-strand RNA synthesis. *J. Virol.* 81, 10172–10187.

De Cedrón, G.M., Ehsani, N., Mikkola, M.L., García, J.A., and Kääriäinen, L. (1999). RNA helicase activity of Semliki Forest virus replicase protein NSP2. FEBS Lett. 448, 19–22.

Deddouche, S., Matt, N., Budd, A., Mueller, S., Kemp, C., Galiana-Arnoux, D., Dostert, C., Antoniewski, C., Hoffmann, J. A., and Imler, J.-L. (2008). The DExD/H-box helicase Dicer-2 mediates the induction of antiviral activity in *Drosophila*. *Nat. Immunol.* 9, 1425–1432.

De Gregorio, E., Spellman, P.T., Rubin, G.M., and Lemaitre, B. (2001). Genome-wide analysis of the Drosophila immune response by using oligonucleotide microarrays. Proc. Natl. Acad. Sci. USA. 98, 12590–12595.

De Gregorio, E., Han, S.-J., Lee, W.-J., Baek, M.-J., Osaki, T., Kawabata, S.-I., Lee, B.-L., Iwanaga, S., Lemaitre, B., and Brey, P.T. (2002). An immune-responsive Serpin regulates the melanization cascade in Drosophila. Dev. Cell 3, 581–592.

De Groot, R.J., Hardy, W.R., Shirako, Y., and Strauss, J.H. (1990). Cleavage-site preferences of Sindbis virus polyproteins containing the non-structural proteinase. Evidence for temporal regulation of polyprotein processing in vivo. *EMBO J.* 9, 2631–2638.

De la Fuente, J., Almazán, C., Blouin, E.F., Naranjo, V., and Kocan, K.M. (2006). Reduction of tick infections with Anaplasma marginale and A. phagocytophilum by targeting the tick protective antigen subolesin. Parasitol. Res. 100, 85–91.

De la Fuente, J., Blouin, E.F., Manzano-Roman, R., Naranjo, V., Almazán, C., Pérez de la Lastra, J.M., Zivkovic, Z., Jongejan, F., and Kocan, K.M. (2007a). Functional genomic

studies of tick cells in response to infection with the cattle pathogen, Anaplasma marginale. Genomics 90, 712–722.

De la Fuente, J., Kocan, K.M., Almazán, C., and Blouin, E.F. (2007b). RNA interference for the study and genetic manipulation of ticks. Trends Parasitol. 23, 427–433.

De la Fuente, J., Estrada-Pena, A., Venzal, J.M., Kocan, K.M., and Sonenshine, D.E. (2008a). Overview: Ticks as vectors of pathogens that cause disease in humans and animals. Front. Biosci. 13, 6938–6946.

De la Fuente, J., Maritz-Olivier, Christine, Naranjo, V., Ayoubi, P., Nijhof, A.M., Almazán, C., Canales, M., Pérez de la Lastra, J.M., Galindo, R.C., Blouin, E.F., Gortazar, C., Jongejan, F., Kocan, K.M. (2008b). Evidence of the role of tick subolesin in gene expression. BMC Genomics 9, 372.

De la Fuente, J., Blouin, E.F., Manzano-Roman, R., Naranjo, V., Almazán, C., Pérez de la Lastra, J.M., Zivkovic, Z., Massung, R.F., Jongejan, F., and Kocan, K.M. (2008c). Differential expression of the tick protective antigen subolesin in Anaplasma marginale- and A. phagocytophilum-infected host cells. Ann. N. Y. Acad. Sci. 1149, 27–35.

De la Fuente, J., Kocan, K.M., Blouin, E.F., Zivkovic, Z., Naranjo, V., Almazán, C., Esteves, E., Jongejan, F., Daffre, S., and Mangold, A.J. (2010). Functional genomics and evolution of tick-Anaplasma interactions and vaccine development. Vet. Parasitol. 167, 175–186.

De Madrid, A.T., and Porterfield, J.S. (1969). A simple micro-culture method for the study of group B arboviruses. *Bull. WHO* 40, 113–121.

Deprez, P., Gautschi, M., and Helenius, A. (2005). More than one glycan is needed for ER glucosidase II to allow entry of glycoproteins into the calnexin/calreticulin cycle. *Mol. Cell* 19, 183–195.

De Tulleo, L., and Kirchhausen, T. (1998). The clathrin endocytic pathway in viral infection. *EMBO J.* 17, 4585–4593.

Devonshire, A.S., Sanders, R., Wilkes, T.M., Taylor, M.S., Foy, C.A., and Huggett, J.F. (2013). Application of next generation qPCR and sequencing platforms to mRNA biomarker analysis. *Methods* 59, 89–100.

Ding, S.-W. (2010). RNA-based antiviral immunity. *Nat. Rev. Immunol.* 10, 632–644.

Ding, M.X., and Schlesinger, M.J. (1989). Evidence that Sindbis virus NSP2 is an autoprotease which processes the virus nonstructural polyprotein. *Virology* 171, 280–284.

Ding, S.-W., and Voinnet, O. (2007). Antiviral immunity directed by small RNAs. *Cell* 130, 413–426.

Dixon, L.K., Alonso, C., Escribano, J.M., Martins, J.M., Revilla, Y., Salas, M.L., and Takamatsu, H. (2012). Virus Taxonomy. In Virus Taxonomy: Ninth Report of the International Committee on Taxonomy of Viruses, A.M.Q. King, E. Lefkowitz, M.J. Adams, and E.B. Carstens, eds. (San Diego: Elsevier), pp. 153–162.

Dobler, G. (2010). Zoonotic tick-borne flaviviruses. *Vet. Microbiol.* 140, 221–228.

Dobler, G., Gniel, D., Petermann, R., and Pfeffer, M. (2012). Epidemiology and distribution of tick-borne encephalitis. *Wiener Medizinische Wochenschrift* 162, 230–238.

Donald, C.L., Kohl, A., and Schnettler, E. (2012). New insights into control of arbovirus replication and spread by insect RNA interference pathways. *Insects* 3, 511–531.

Dong, Y., Taylor, H.E., and Dimopoulos, G. (2006). AgDscam, a hypervariable immunoglobulin domain-containing receptor of the *Anopheles gambiae* innate immune system. *PLoS Biol.* 4, e229.

Donohue, K. V, Khalil, S.M.S., Ross, E., Grozinger, C.M., Sonenshine, D.E., and Michael Roe, R. (2010). Neuropeptide signaling sequences identified by pyrosequencing of the American dog tick synganglion transcriptome during blood feeding and reproduction. *Insect Biochem. Mol. Biol.* 40, 79–90.

Doolittle, J.M., and Gomez, S.M. (2011). Mapping protein interactions between Dengue virus and its human and insect hosts. *PLoS Negl. Trop. Dis.* 5, e954.

Dostert, C., Jouanguy, E., Irving, P., Troxler, L., Galiana-Arnoux, D., Hetru, C., Hoffmann, J. A, and Imler, J.-L. (2005). The Jak-STAT signaling pathway is required but not sufficient for the antiviral response of *Drosophila*. *Nat. Immunol.* 6, 946–953.

Du, Z.-Q., Ren, Q., Huang, A.-M., Fang, W.-H., Zhou, J.-F., Gao, L.-J., and Li, X.-C. (2013). A novel peroxinectin involved in antiviral and antibacterial immunity of mud crab, *Scylla paramamosain*. *Mol. Biol. Rep.*40, 6873-6881

Dumpis, U., Crook, D., and Oksi, J. (1999). Tick-borne encephalitis. *Clin. Infect. Dis.* 28, 882–890.

Duvic, B., Hoffmann, J.A., Meister, M., and Royet, J. (2002). Notch signaling controls lineage specification during *Drosophila* larval hematopoiesis. *Curr. Biol.* 12, 1923–1927.

Eggenberger, L.R., Lamoreaux, W.J., and Coons, L.B. (1990). Hemocytic encapsulation of implants in the tick *Dermacentor variabilis*. *Exp. Appl. Acarol.* 9, 279–287.

Egloff, M.-P., Benarroch, D., Selisko, B., Romette, J.-L., and Canard, B. (2002). An RNA cap (nucleoside-2'-O-)-methyltransferase in the flavivirus RNA polymerase NS5: crystal structure and functional characterization. *EMBO J.* 21, 2757–2768.

Emara, M.M., and Brinton, M.A. (2007). Interaction of TIA-1/TIAR with West Nile and dengue virus products in infected cells interferes with stress granule formation and processing body assembly. *Proc. Natl. Acad. Sci. U. S. A.* 104, 9041–9046.

Enders, J.F. (1954). Cytopathology of virus infections. *Ann. Rev. Microbiol.* 8, 473–502.

Enserink, M. (2006). Massive outbreak draws fresh attention to little-known virus. *Science* 311, 1085.

Esteves, E., Lara, F.A., Lorenzini, D.M., Costa, G.H.N., Fukuzawa, A.H., Pressinotti, L.N., Silva, J.R.M.C., Ferro, J.A., Kurtti, T.J., Munderloh, U.G., and Daffre, S. (2008). Cellular and molecular characterization of an embryonic cell line (BME26) from the tick *Rhipicephalus (Boophilus) microplus*. *Insect Biochem. Mol. Biol.* 38, 568–580.

Estrada-Peña, A., Bouattour, J.-L., Camicas, J.-L., and Walker, A. (2004). Ticks of domestic animals in the Mediterranean Region (San Francisco: University of Zaragoza).

Ewald, S.E., Lee, B.L., Lau, L., Wickliffe, K.E., Shi, G.-P., Chapman, H.A., and Barton, G.M. (2008). The ectodomain of Toll-like receptor 9 is cleaved to generate a functional receptor. *Nature* 456, 658–662.

Favoreel, H.W. (2003). Virus complement evasion strategies. *J. Gen. Virol.* 84, 1–15.

Fazakerley, J.K. (2002). Pathogenesis of Semliki Forest virus encephalitis. *J. Neurovirol.* 8 (Suppl. 2), 66–74.

Fernandez-Garcia, M.-D., Meertens, L., Bonazzi, M., Cossart, P., Arenzana-Seisdedos, F., and Amara, A. (2011). Appraising the roles of CBLL1 and the ubiquitin/proteasome system for flavivirus entry and replication. *J. Virol.* 85, 2980–2989.

Ferrandon, D., Imler, J.-L., Hetru, C., and Hoffmann, J.A. (2007). The *Drosophila* systemic immune response: sensing and signalling during bacterial and fungal infections. *Nat. Rev. Immunol.* 7, 862–874.

Figueiredo, M.B., Genta, F.A., Garcia, E.S., and Azambuja, P. (2008). Lipid mediators and vector infection: *Trypanosoma rangeli* inhibits *Rhodnius prolixus* hemocyte phagocytosis by modulation of phospholipase A2 and PAF-acetylhydrolase activities. *J. Insect Physiol.* 54, 1528–1537.

Finkelstein, Y., Faktor, O., Elroy-Stein, O., and Levi, B.Z. (1999). The use of bi-cistronic transfer vectors for the baculovirus expression system. *J. Biotechnol.* 75, 33–44.

Flannagan, R.S., Jaumouillé, V., and Grinstein, S. (2012). The cell biology of phagocytosis. *Annu. Rev. Pathol.* 7, 61–98.

Flenniken, M.L., and Andino, R. (2013). Non-specific dsRNA-mediated antiviral response in the honey bee. *PLoS One* 8, e77263.

Fogaça, A.C., da Silva, P.I.Jr, Miranda, M.T.M., Bianchi, A.G., Miranda, A., Ribolla, P.E. M., Daffre, S. (1999). Antimicrobial activity of a bovine hemoglobin fragment in the tick *Boophilus microplus*. *J. Biol. Chem.* 274, 25330–25334.

Fogaça, A.C., Lorenzini, D.M., Kaku, L.M., Esteves, E., Bulet, P., and Daffre, S. (2004). Cysteine-rich antimicrobial peptides of the cattle tick *Boophilus microplus*: isolation, structural characterization and tissue expression profile. *Dev. Comp. Immunol.* 28, 191–200.

Fogaça, A.C., Almeida, I.C., Eberlin, M.N., Tanaka, A.S., Bulet, P., and Daffre, S. (2006). Ixodidin, a novel antimicrobial peptide from the hemocytes of the cattle tick *Boophilus microplus* with inhibitory activity against serine proteinases. *Peptides* 27, 667–674.

Fortini, M.E., and Artavanis-Tsakonas, S. (1994). The suppressor of hairless protein participates in notch receptor signaling. *Cell* 79, 273–282.

Fragkoudis, R., Breakwell, L., McKimmie, C., Boyd, A., Barry, G., Kohl, A., Merits, A., and Fazakerley, J.K. (2007). The type I interferon system protects mice from Semliki Forest virus by preventing widespread virus dissemination in extraneural tissues, but does not mediate the restricted replication of avirulent virus in central nervous system neurons. *J. Gen. Virol.* 88, 3373–3384.

Fragkoudis, R., Chi, Y., Siu, R.W.C., Barry, G., Attarzadeh-Yazdi, G., Merits, A., Nash, A.A., Fazakerley, J.K., and Kohl, A. (2008). Semliki Forest virus strongly reduces mosquito host defence signaling. *Insect Mol. Biol.* 17, 647–656.

Fragkoudis, R., Attarzadeh-Yazdi, G., Nash, A.A., Fazakerley, J.K., and Kohl, A. (2009). Advances in dissecting mosquito innate immune responses to arbovirus infection. *J. Gen. Virol.* 90, 2061–2072.

Francischetti, I.M.B., Sá-Nunes, A., Mans, B.J., Santos, I.M., Ribeiro, J.M.C. (2009). The role of saliva in tick feeding. *Front. Biosci.* 2051–2088.

Franke, J., Fritzsch, J., Tomaso, H., Straube, E., Dorn, W., and Hildebrandt, A. (2010). Coexistence of pathogens in host-seeking and feeding ticks within a single natural habitat in Central Germany. *Appl. Environ. Microbiol.* 76, 6829–6836.

Fric, J., Zelante, T., Wong, A.Y.W., Mertes, A., Yu, H.-B., and Ricciardi-Castagnoli, P. (2012). NFAT control of innate immunity. *Blood* 120, 1380–1389.

Friedman, R., Levin, J., Grimley, P., and Berezesky, I.K. (1972). Membrane-associated replication complex in arbovirus infection. *J. Virol.* 10, 504–515.

Froshauer, S., Kartenbeck, J., and Helenius, A. (1988). Alphavirus RNA replicase is located on the cytoplasmic surface of endosomes and lysosomes. *J. Cell Biol.* 107, 2075–2086.

Fullaondo, A., and Lee, S.Y. (2012). Regulation of *Drosophila*-virus interaction. *Dev. Comp. Immunol.* 36, 262–266.

Galiana-Arnoux, D., Dostert, C., Schneemann, A., Hoffmann, J.A., and Imler, J.-L. (2006). Essential function in vivo for Dicer-2 in host defense against RNA viruses in *Drosophila*. *Nat. Immunol.* 7, 590–597.

Galindo, R.C., Doncel-Pérez, E., Zivkovic, Z., Naranjo, V., Gortazar, C., Mangold, A.J., Martín-Hernando, M.P., Kocan, K.M., and de la Fuente, J. (2009). Tick subolesin is an ortholog of the akirins described in insects and vertebrates. *Dev. Comp. Immunol.* 33, 612–617.

Garbuzov, A., and Tatar, M. (2010). Hormonal regulation of *Drosophila* microRNA let-7 and miR-125 that target innate immunity. *Fly (Austin).* 4, 306–311.

Garcia, E.S., Castro, D.P., Figueiredo, M.B., Genta, F.A., and Azambuja, P. (2009). *Trypanosoma rangeli*: a new perspective for studying the modulation of immune reactions of *Rhodnius prolixus*. *Parasit. Vectors* 2, 33.

Garcia, S., Billecocq, A., Crance, J.-M., Munderloh, U., Garin, D., and Bouloy, M. (2005). Nairovirus RNA sequences expressed by a Semliki Forest virus replicon induce RNA interference in tick cells. *Society* 79, 8942–8947.

Garcia, S., Billecocq, A., Crance, J.-M., Prins, M., Garin, D., and Bouloy, M. (2006). Viral suppressors of RNA interference impair RNA silencing induced by a Semliki Forest virus replicon in tick cells. *J. Gen. Virol.* 87, 1985–1989.

Garmashova, N., Gorchakov, R., Frolova, E., and Frolov, I. (2006). Sindbis virus nonstructural protein nsP2 is cytotoxic and inhibits cellular transcription. *J. Virol.* 80, 5686–5696.

Gehrke, R., Ecker, M., Aberle, S.W., Allison, S.L., Heinz, F.X., and Mandl, C.W. (2003). Incorporation of tick-borne encephalitis virus replicons into virus-like particles by a packaging cell line. *J. Virol.* 77, 8924–8933.

Gehrke, R., Heinz, F.X., Davis, N.L., and Mandl, C.W. (2005). Heterologous gene expression by infectious and replicon vectors derived from tick-borne encephalitis virus and direct comparison of this flavivirus system with an alphavirus replicon. *J. Gen. Virol.* 86, 1045–1053.

Geigenmüller-Gnirke, U., Weiss, B., Wright, R., and Schlesinger, S. (1991). Complementation between Sindbis viral RNAs produces infectious particles with a bipartite genome. *Proc. Natl. Acad. Sci. U. S. A.* 88, 3253–3257.

Gibbons, D.L., Ahn, A., Chatterjee, P.K., and Kielian, M. (2000). Formation and characterization of the trimeric form of the fusion protein of Semliki Forest virus. *J. Virol.* 74, 7772–7780.

Gibbons, D.L., Erk, I., Reilly, B., Navaza, J., Kielian, M., Rey, F.A., and Lepault, J. (2003). Visualization of the target-membrane-inserted fusion protein of Semliki Forest virus by combined electron microscopy and crystallography. *Cell* 114, 573–583.

Gibson, A.K., Smith, Z., Fuqua, C., Clay, K., and Colbourne, J.K. (2013). Why so many unknown genes? Partitioning orphans from a representative transcriptome of the lone star tick *Amblyomma americanum*. *BMC Genomics* 14, 135.

Gillespie, L.K., Hoenen, A., Morgan, G., and Mackenzie, J.M. (2010). The endoplasmic reticulum provides the membrane platform for biogenesis of the flavivirus replication complex. *J. Virol.* 84, 10438–10447.

Glasgow, G.M., Sheahan, B.J., Atkins, G.J., Wahlberg, J.M., Salminen, A., and Liljeström, P. (1991). Two mutations in the envelope glycoprotein E2 of Semliki Forest virus affecting the maturation and entry patterns of the virus alter pathogenicity for mice. *Virology* 185, 741–748.

Go, Y.Y., Balasuriya, U.B.R., and Lee, C. (2014). Zoonotic encephalitides caused by arboviruses: transmission and epidemiology of alphaviruses and flaviviruses. *Clin. Exp. Vaccine Res.* 3, 58–77.

Goic, B., Vodovar, N., Mondotte, J. A, Monot, C., Frangeul, L., Blanc, H., Gausson, V., Vera-Otarola, J., Cristofari, G., and Saleh, M.-C. (2013). RNA-mediated interference and reverse transcription control the persistence of RNA viruses in the insect model *Drosophila*. *Nat. Immunol.* 14, 396–403.

Gollins, S.W., and Porterfield, J.S. (1985). Flavivirus infection enhancement in macrophages: an electron microscopic study of viral cellular entry. *J. Gen. Virol.* 66, 1969–1982.

Gorbalenya, A., Koonin, E., Donchenko, A.P., and Blinov, V.M. (1989). Two related superfamilies of putative helicases involved in replication, recombination, repair and expression of DNA and RNA genomes. *Nucleic Acids Res.* 17, 4713–4730.

Gould, E.A., and Solomon, T. (2008). Pathogenic flaviviruses. *Lancet* 371, 500–509.

Graef, I.A., Gastier, J.M., Francke, U., and Crabtree, G.R. (2001). Evolutionary relationships among Rel domains indicate functional diversification by recombination. *Proc. Natl. Acad. Sci. USA* 98, 5740–5745.

Gratz, N.G. (2004). Critical review of the vector status of *Aedes albopictus*. *Med. Vet. Entomol.* 18, 215–227.

Greber, U.F., and Way, M. (2006). A superhighway to virus infection. *Cell* 124, 741–754.

Greig, A. (1972). The localization of African swine fever virus in the tick *Ornithodoros moubata porcinus*. *Arch. Gesamte Virusforsch.* 39, 240–247.

Gresíková, M., Sekeyová, M., Stúpalová, S., and Necas, S. (1975). Sheep milk-borne epidemic of tick-borne encephalitis in Slovakia. *Intervirology* 5, 57–61.

Grimley, P.M., Berezesky, I.K., and Friedman, R.M. (1968). Cytoplasmic structures associated with an arbovirus infection: loci of viral ribonucleic acid synthesis. *J. Virol.* 2, 1326–1338.

Grimley, P.M., Levin, J.G., Berezesky, I.K., and Friedman, R.M. (1972). Specific membranous structures associated with the replication of group A arboviruses. *J. Virol.* 10, 492–503.

Gritsun, T.S., Nuttall, P.A., and Gould, E.A. (2003). Tick-borne flaviviruses. *Adv. Virus Res.* 61, 317–371.

Gritsun, T.S., Lashkevich, V.A., and Gould, E.A. (2003). Tick-borne encephalitis. *Antiviral Res.* 57, 129–146.

Grubhoffer, L., and Jindrák, L. (1998). Lectins and tick-pathogen interactions: a minireview. *Folia Parasitol. (Praha).* 45, 9–13.

Grubhoffer, L., Kovář, V., and Rudenko, N. (2004). Tick lectins: structural and functional properties. *Parasitology* 129, S113–S125.

Gubler, D.J. (1996). The global resurgence of arboviral diseases. *Trans. R. Soc. Trop. Med. Hyg.* 90, 449–451.

Gubler, D.J. (2007). The continuing spread of West Nile virus in the western hemisphere. *Clin. Infect. Dis.* 45, 1039–1046.

Guerbois, M., Volkova, E., Forrester, N.L., Rossi, S.L., Frolov, I., and Weaver, S.C. (2013). IRES-driven expression of the capsid protein of the Venezuelan equine encephalitis virus TC-83 vaccine strain increases its attenuation and safety. *PLoS Negl. Trop. Dis.* 7, e2197.

Guglielmone, A.A., Robbins, R.G., Apanaskevich, D.A., Petney, T.N., Estrada-Peña, A., Horak, I.G., Shao, R., and Barker, S.C. (2010). The Argasidae, Ixodidae and Nuttalliellidae (Acari: Ixodida) of the world: a list of valid species names. *Zootaxa* 2528, 1–28.

Guyatt, K.J., Westaway, E.G., and Khromykh, A.A. (2001). Expression and purification of enzymatically active recombinant RNA-dependent RNA polymerase (NS5) of the flavivirus Kunjin. *J. Virol. Methods* 92, 37–44.

Habjan, M., Penski, N., Spiegel, M., and Weber, F. (2008). T7 RNA polymerase-dependent and -independent systems for cDNA-based rescue of Rift Valley fever virus. *J. Gen. Virol.* 89, 2157–2166.

Hajdušek, O., Síma, R., Ayllón, N., Jalovecká, M., Perner, J., de la Fuente, J., and Kopáček, P. (2013). Interaction of the tick immune system with transmitted pathogens. *Front. Cell. Infect. Microbiol.* 3, 26.

Hall, A. (1998). Rho GTPases and the actin cytoskeleton. *Science (80-.).* 279, 509–514.

Hammar, L., Markarian, S., Haag, L., Lankinen, H., Salmi, A., and Cheng, R.H. (2003). Prefusion rearrangements resulting in fusion peptide exposure in Semliki Forest virus. *J. Biol. Chem.* 278, 7189–7198.

Handler, D., Meixner, K., Pizka, M., Lauss, K., Schmied, C., Gruber, F.S., and Brennecke, J. (2013). The genetic makeup of the *Drosophila* piRNA pathway. *Mol. Cell* 50, 762–777.

Hansen, J.D., Vojtech, L.N., and Laing, K.J. (2011). Sensing disease and danger: a survey of vertebrate PRRs and their origins. *Dev. Comp. Immunol.* 35, 886–897.

Hardy, J.L., Houk, E.J., Kramer, L.D., and Reeves, W.C. (1983). Intrinsic factors affecting vector competence of mosquitoes for arboviruses. *Ann. Rev. Entomol.* 28, 229–262.

Haridas, V., Rajgokul, K.S., Sadanandan, S., Agrawal, T., Sharvani, V., Gopalakrishna, M.V.S., Bijesh, M.B., Kumawat, K.L., Basu, A., and Medigeshi, G.R. (2013). Bispidine-amino acid conjugates act as a novel scaffold for the design of antivirals that block Japanese encephalitis virus replication. *PLoS Negl. Trop. Dis.* 7, e2005.

Hase, T., Summers, P.L., Eckels, K.H., and Baze, W.B. (1987). Maturation process of Japanese encephalitis virus in cultured mosquito cells in vitro and mouse brain cells in vivo. *Arch. Virol.* 2, 135–151.

Heekin, A.M., Guerrero, F.D., Bendele, K.G., Saldivar, L., Scoles, G.A., Dowd, S.E., Gondro, C., Nene, V., Djikeng, A., and Brayton, K.A. (2013). Gut transcriptome of replete adult female cattle ticks, *Rhipicephalus (Boophilus) microplus*, feeding upon a *Babesia bovis*-infected bovine host. *Parasitol. Res.* 112, 3075–3090.

Hegedus, Z., Zakrzewska, A., Agoston, V.C., Ordas, A., Rácz, P., Mink, M., Spaink, H.P., and Meijer, A.H. (2009). Deep sequencing of the zebrafish transcriptome response to mycobacterium infection. *Mol. Immunol.* 46, 2918–2930.

Heinz, F.X., Mandl, C.W., and Holzmann, H., Kunz, C., Harris, B.A., Rey, F., Harrison, S.C. (1991). The flavivirus envelope protein E: isolation of a soluble form from tick-borne encephalitis virus and its crystallization. *J. Virol.* 65, 5579–5583.

Heinz, F.X., Auer, G., Stiasny, K., Holzmann, H., Mandl, C.W., Guirakhoo, F., and Kunz, C. (1994). The interactions of the flavivirus envelope proteins: implications for virus entry and release. *Arch. Virol. Suppl.* 9, 339–348.

Helenius, A., Kartenbeck, J., Simons, K., and Fries, E. (1980). On the entry of Semliki forest virus into BHK-21 cells. *J. Cell Biol.* 84, 404–420.

Helenius, A., Marsh, M., and White, J. (1982). Inhibition of Semliki forest virus penetration by lysosomotropic weak bases. *J. Gen. Virol.* 58 Pt 1, 47–61.

Henchal, E.A., Gentry, M.K., McCown, J.M., and Brandt, W.E. (1982). Dengue virus-specific and flavivirus group determinants identified with monoclonal antibodies by indirect immunofluorescence. *Am. J. Trop. Med. Hyg.* 31, 830–836.

Hess, A.M., Prasad, A.N., Ptitsyn, A., Ebel, G.D., Olson, K.E., Barbacioru, C., Monighetti, C., and Campbell, C.L. (2011). Small RNA profiling of Dengue virus-mosquito interactions implicates the PIWI RNA pathway in anti-viral defense. *BMC Microbiol.* 11, 45.

Hetz, C., Martinon, F., Rodriguez, D., and Glimcher, L.H. (2011). The Unfolded Protein Response: Integrating stress signals through the stress sensor IRE1 . *Physiol. Rev.* 91, 1219–1243.

Hirsch, R.L. (1982). The complement system: its importance in the host response to viral infection. *Microbiol. Rev.* 46, 71–85.

Hoenen, A., Liu, W., Kochs, G., Khromykh, A.A., and Mackenzie, J.M. (2007). West Nile virus-induced cytoplasmic membrane structures provide partial protection against the interferon-induced antiviral MxA protein. *J. Gen. Virol.* 88, 3013–3017.

Hoenninger, V.M., Rouha, H., Orlinger, K.K., Miorin, L., Marcello, A., Kofler, R.M., and Mandl, C.W. (2008). Analysis of the effects of alterations in the tick-borne encephalitis virus 3'-noncoding region on translation and RNA replication using reporter replicons. *Virology* 377, 419–430.

Holbrook, M.R. (2012). Kyasanur forest disease. *Antiviral Res.* 96, 353–362.

Holland, J., and Domingo, E. (1998). Origin and evolution of viruses. *Virus Genes* 16, 13–21.

Hollidge, B.S., González-Scarano, F., and Soldan, S.S. (2010). Arboviral encephalitides: transmission, emergence, and pathogenesis. *J. Neuroimmune Pharmacol.* 5, 428–442.

Hollinshead, M., Johns, H.L., Sayers, C.L., Gonzalez-Lopez, C., Smith, G.L., and Elliott, G. (2012). Endocytotic tubules regulated by Rab GTPases 5 and 11 are used for envelopment of herpes simplex virus. *EMBO J.* 31, 4204-4220.

Holzmann, H., Aberle, S.W., Stiasny, K., Werner, P., Mischak, A., Zainer, B., Netzer, M., Koppi, S., Bechter, E., and Heinz, F.X. (2009). Tick-borne encephalitis from eating goat cheese in a mountain region of Austria. *Emerg. Infect. Dis.* 15, 1671–1673.

Horn, M., Nussbaumerová, M., Sanda, M., Kovárová, Z., Srba, J., Franta, Z., Sojka, D., Bogyo, M., Caffrey, C.R., Kopácek, P., and Mares, M. (2009). Hemoglobin digestion in blood-feeding ticks: mapping a multipeptidase pathway by functional proteomics. *Chem. Biol.* 16, 1053–1063.

Huang, X.-D., Yin, Z.-X., Liao, J.-X., Wang, P.-H., Yang, L.-S., Ai, H.-S., Gu, Z.-H., Jia, X.-T., Weng, S.-P., Yu, X.-Q., and He, J.-G. (2009). Identification and functional study of a shrimp Relish homologue. *Fish Shellfish Immunol.* 27, 230–238.

Huang, Z., Kingsolver, M.B., Avadhanula, V., and Hardy, R.W. (2013). An antiviral role for antimicrobial peptides during the arthropod response to alphavirus replication. *J. Virol.* 87, 4272–4280.

Hubálek, Z., and Rudolf, I. (2012). Tick-borne viruses in Europe. *Parasitol. Res.* 111, 9–36.

Hudopisk, N., Korva, M., Janet, E., Simetinger, M., Grgič-Vitek, M., Gubenšek, J., Natek, V., Kraigher, A., Strle, F., and Avšič-Županc, T. (2013). Tick-borne encephalitis associated with consumption of raw goat milk, Slovenia, 2012. *Emerg. Infect. Dis.* 19, 806–808.

Hung, J.-J., Chung, C.-S., and Chang, W. (2002). Molecular chaperone Hsp90 is important for vaccinia virus growth in cells. *J. Virol.* 76, 1379–1390.

Hussain, M., Torres, S., Schnettler, E., Funk, A., Grundhoff, A., Pijlman, G.P., Khromykh, A.A., and Asgari, S. (2012). West Nile virus encodes a microRNA-like small RNA in the 3'

untranslated region which up-regulates GATA4 mRNA and facilitates virus replication in mosquito cells. *Nucleic Acids Res.* 40, 2210–2223.

Hussain, M., Walker, T., O'Neill, S.L., and Asgari, S. (2013). Blood meal induced microRNA regulates development and immune associated genes in the Dengue mosquito vector, *Aedes aegypti*. *Insect Biochem. Mol. Biol.* 43, 146–152.

Iacono-Connors, L.C., Smith, J.F., Ksiazek, T.G., Kelley, C.L., and Schmaljohn, C.S. (1996). Characterization of Langat virus antigenic determinants defined by monoclonal antibodies to E, NS1 and preM and identification of a protective, non-neutralizing preM. *Virus Res.* 43, 125–136.

Inoue, N., Hanada, K., Tsuji, N., Igarashi, I., Nagasawa, H., and Fujisaki, K. (2001). Characterization of phagocytic hemocytes in *Ornithodoros moubata* (Acari : Ixodidae). *J. Med. Entomol.* 38, 514–519.

Ishimine, T., Tadano, M., Fukunaga, T., and Okuno, Y. (1987). An improved micromethod for infectivity assays and neutralization tests of dengue viruses. *Biken J.* 30, 39–44.

Ishizu, H., Siomi, H., and Siomi, M.C. (2012). Biology of PIWI-interacting RNAs: new insights into biogenesis and function inside and outside of germlines. *Genes Dev.* 26, 2361–2373.

Iwanaga, S., and Lee, B.L. (2005). Recent advances in the innate immunity of invertebrate animals. *J. Biochem. Mol. Biol.* 38, 128–150.

Iwasaki, S., Kobayashi, M., Yoda, M., Sakaguchi, Y., Katsuma, S., Suzuki, T., and Tomari, Y. (2010). Hsc70/Hsp90 chaperone machinery mediates ATP-dependent RISC loading of small RNA duplexes. *Mol. Cell* 39, 292–299.

Jaenson, T.G.T., Hjertqvist, M., Bergström, T., and Lundkvist, A. (2012). Why is tick-borne encephalitis increasing? A review of the key factors causing the increasing incidence of human TBE in Sweden. *Parasit. Vectors* 5, 184.

Jiang, X., and Chen, Z.J. (2012). The role of ubiquitylation in immune defence and pathogen evasion. *Nat. Rev. Immunol.* 12, 35–48.

Jin, L.H., Choi, J.K., Kim, B., Cho, H.S., Kim, J., Kim-Ha, J., and Kim, Y.-J. (2009). Requirement of Split ends for epigenetic regulation of Notch signal-dependent genes during infection-induced hemocyte differentiation. *Mol. Cell. Biol.* 29, 1515–1525.

Johansson, M.W. (1999). Cell adhesion molecules in invertebrate immunity. *Dev. Comp. Immunol.* 23, 303–315.

Johansson, M.W., and Söderhäll, K. (1988). Isolation and purification of a cell adhesion factor from crayfish blood cells. *J. Cell Biol.* 106, 1795–1803.

Johansson, M.W., Lind, M.I., Holmblad, T., Thörnqvist, P.-O., and Söderhäll, K. (1995). Peroxinectin, a novel cell adhesion protein from crayfish blood. *Biochem. Biophys. Res. Commun.* 216, 1079–1089.

Johansson, M., Brooks, A.J., Jans, D.A., and Vasudevan, S.G. (2001). A small region of the dengue virus-encoded RNA-dependent RNA polymerase, NS5, confers interaction with both the nuclear transport receptor importin-beta and the viral helicase, NS3. *J. Gen. Virol.* 82, 735–745.

Johns, R., Sonenshine, D.E., and Hynes, W.L. (2000). Response of the tick *Dermacentor variabilis* (Acari: Ixodidae) to hemocoelic inoculation of *Borrelia burgdorferi* (Spirochetales). *J. Med. Entomol.* 37, 265–270.

Johns, R., Ohnishi, J., Broadwater, D.E., Sonenshine, D.E., De Silva, A.M., and Hynes, W.L. (2001). Contrast in tick innate immune responses to *Borrelia burgdorferi* challenge: immunotolerance in *Ixodes scapularis* versus immunocompetence in *Dermacentor variabilis* (Acari: Ixodidae). *J. Med. Entomol.* 38, 99–107.

Jones, L.D., Davies, C.R., Steel, G.M., and Nuttall, P.A. (1989). Vector capacity of *Rhipicephalus appendiculatus* and *Amblyomma variegatum* for Thogoto and Dhori viruses. *Med. Vet. Entomol.* 3, 195–202.

Jongejan, F., and Uilenberg, G. (2004). The global importance of ticks. *Parasitology* 129, S3.

Jose, J., Snyder, J.E., and Kuhn, R.J. (2009). A structural and functional perspective of alphavirus replication and assembly. *Future Microbiol.* 837–856.

Kääriäinen, L., Takkinen, K., Keränen, S., and Söderlund, H. (1987). Replication of the genome of alphaviruses. *J. Cell Sci. Suppl.* 7, 231–250.

Kadota, K., Satoh, E., Ochiai, M., Inoue, N., Tsuji, N., Igarashi, I., Nagasawa, H., Mikami, T., Claveria, F.G., and Fujisaki, K. (2002). Existence of phenol oxidase in the argasid tick *Ornithodoros moubata*. *Parasitol. Res.* 88, 781–784.

Kakumani, P.K., Ponia, S.S., Rajgokul, K.S., Sood, V., Chinnappan, M., Banerjea, A.C., Medigeshi, G.R., Malhotra, P., Mukherjee, S.K., and Bhatnagar, R.K. (2013). Role of RNA interference (RNAi) in dengue virus replication and identification of NS4B as an RNAi suppressor. *J. Virol.* 87, 8870–8883.

Karim, S., Troiano, E., and Mather, T.N. (2010). Functional genomics tool: gene silencing in *Ixodes scapularis* eggs and nymphs by electroporated dsRNA. *BMC Biotechnol.* 10, 1.

Karim, S., Singh, P., and Ribeiro, J.M.C. (2011). A deep insight into the sialotranscriptome of the gulf coast tick, *Amblyomma maculatum*. *PLoS One* 6, e28525.

Karlikow, M., Goic, B., and Saleh, M.-C. (2014). RNAi and antiviral defense in *Drosophila*: Setting up a systemic immune response. *Dev. Comp. Immunol.* 42, 85–92.

Kaufman, W.R. (2004). Assuring paternity in a promiscuous world: are there lessons for ticks among the insects? *Parasitology* 129, S145–S160.

Kawabata, S., and Muta, T. (2010). Sadaaki Iwanaga: Discovery of the lipopolysaccharide- and beta-1,3-D-glucan-mediated proteolytic cascade and unique proteins in invertebrate immunity. *J. Biochem.* 147, 611–618.

Keene, K.M., Foy, B.D., Sanchez-Vargas, I., Beaty, B.J., Blair, C.D., and Olson, K.E. (2004). RNA interference acts as a natural antiviral response to O'nyong-nyong virus (*Alphavirus*; *Togaviridae*) infection of *Anopheles gambiae*. *Proc. Natl. Acad. Sci. USA.* 101, 17240–17245.

Kemp, C., and Imler, J.-L. (2009). Antiviral immunity in *Drosophila*. *Curr. Opin. Immunol.* 21, 3–9.

Keränen, S., and Kääriäinen, L. (1979). Functional defects of RNA-negative temperature-sensitive mutants of Sindbis and Semliki Forest viruses. *J. Virol.* 32, 19–29.

Kerbo, N., Donchenko, I., Kutsar, K., and Vasilenko, V. (2005). Tick-borne encephalitis outbreak in Estonia linked to raw goat milk, May-June 2005. *Eurosurveillance* 10, 2730.

Keyser, P., Borge-Renberg, K., and Hultmark, D. (2007). The *Drosophila* NFAT homolog is involved in salt stress tolerance. *Insect Biochem. Mol. Biol.* 37, 356–362.

Khasnatinov, M.A., Ustanikova, K., Frolova, T.V, Pogodina, V.V, Bochkova, N.G., Levina, L.S., Slovak, M., Kazimirova, M., Labuda, M., Klempa, B., Eleckova, E., Gould, E.A., and Gritsun, T.S. (2009). Non-hemagglutinating flaviviruses: molecular mechanisms for the emergence of new strains via adaptation to European ticks. *PLoS One* 4, e7295.

Kiiver, K., Tagen, I., Zusinaite, E., Tamberg, N., Fazakerley, J.K., and Merits, A. (2008). Properties of non-structural protein 1 of Semliki Forest virus and its interference with virus replication. *J. Gen. Virol.* 89, 1457–1466.

Kim, D., Pertea, G., Trapnell, C., Pimentel, H., Kelley, R., and Salzberg, S.L. (2013). TopHat2: accurate alignment of transcriptomes in the presence of insertions, deletions and gene fusions. *Genome Biol.* 14, R36.

Kim, K.H., Rümenapf, T., Strauss, E.G., and Strauss, J.H. (2004). Regulation of Semliki Forest virus RNA replication: a model for the control of alphavirus pathogenesis in invertebrate hosts. *Virology* 323, 153–163.

Kim, R., Emi, M., Tanabe, K., and Murakami, S. (2006). Role of the unfolded protein response in cell death. *Apoptosis* 11, 5–13.

Kimble, J., and Simpson, P. (1997). The LIN-12/Notch signaling pathway and its regulation. *Annu. Rev. Cell Dev. Biol.* 13, 333–361.

Kingsolver, M.B., Huang, Z., and Hardy, R.W. (2013). Insect antiviral innate immunity: pathways, effectors, and connections. *J. Mol. Biol.* 425, 4921-4936

Ko, M.S., Lee, U.H., Kim, S.I., Kim, H.J., Park, J.J., Cha, S.J., Kim, S.B., Song, H., Chung, D.K., Han, I.S., Kwack, K., Park, J.-W. (2004). Overexpression of DRG2 suppresses the

growth of Jurkat T cells but does not induce apoptosis. *Arch. Biochem. Biophys.* 422, 137–144.

Kobayashi, M., Johansson, M., and Söderhäll, K. (1990). The 76 kDa cell-adhesion factor from crayfish haemocytes promotes encapsulation in vitro. *Cell Tissue Res.* 260, 113–118.

Kocan, K.M., Manzano-Roman, R., and de la Fuente, J. (2007). Transovarial silencing of the subolesin gene in three-host ixodid tick species after injection of replete females with subolesin dsRNA. *Parasitol. Res.* 100, 1411–1415.

Kocan, K.M., de la Fuente, J., Manzano-Roman, R., Naranjo, V., Hynes, W.L., and Sonenshine, D.E. (2008). Silencing expression of the defensin, varisin, in male *Dermacentor variabilis* by RNA interference results in reduced *Anaplasma marginale* infections. *Exp. Appl. Acarol.* 46, 17–28.

Kocan, K.M., Zivkovic, Z., Blouin, E.F., Naranjo, V., Almazán, C., Mitra, R., and de la Fuente, J. (2009). Silencing of genes involved in *Anaplasma marginale*-tick interactions affects the pathogen developmental cycle in *Dermacentor variabilis*. *BMC Dev. Biol.* 9, 42.

Koonin, E.V (1993). Computer-assisted identification of a putative methyltransferase domain in NS5 protein of flaviviruses and lambda 2 protein of reovirus. *J. Gen. Virol.* 74 (Pt 4), 733–740.

Kopacek, P., Hajdusek, O., and Buresova, V. (2012). Tick as a model for the study of a primitive complement system. In Recent Advances on Model Hosts, E. Mylonakis, F.M. Ausubel, M. Gilmore, and A. Casadevall, eds. (New York, NY: Springer New York), pp. 83–93.

Kopácek, P., Hajdusek, O., Buresová, V., and Daffre, S. (2010). Tick innate immunity. *Adv Exp Med Biol.* 708, 137–162.

Kopecký, J., and Stanková, I. (1998). Interaction of virulent and attenuated tick-borne encephalitis virus strains in ticks and a tick cell line. *Folia Parasitol. (Praha).* 45, 245–250.

Kopek, B.G., Perkins, G., Miller, D.J., Ellisman, M.H., and Ahlquist, P. (2007). Alphavirus RNA replicase is located is located on the cytoplasmic surface of endosomes and lysosomes. *PLoS Biol.* 5, e220.

Kozuch, O., and Mayer, V. (1975). Pig kidney epithelial (PS) cells: a perfect tool for the study of flaviviruses and some other arboviruses. *Acta Virol.* 19, 498.

Krishnan, M.N., Sukumaran, B., Pal, U., Agaisse, H., Murray, J.L., Hodge, T.W., and Fikrig, E. (2007). Rab 5 is required for the cellular entry of dengue and West Nile viruses. *J. Virol.* 81, 4881–4885.

Kudelko, M., Brault, J.-B., Kwok, K., Li, M.Y., Pardigon, N., Peiris, J.S.M., Bruzzone, R., Desprès, P., Nal, B., and Wang, P.G. (2012). Class II ADP-ribosylation factors are required for efficient secretion of dengue viruses. *J. Biol. Chem.* 287, 767–777.

Kuhn, R.J. (2007). *Togaviridae*: The viruses and their replication. In Field's Virology, M.D. Knipe, and M.H. Howley, eds. (Lippincott Williams & Wilkins), pp. 1001–1022.

Kuhn, K.H., and Haug, T. (1994). Ultrastructural, cytochemical, and immunocytochemical characterization of haemocytes of the hard tick *Ixodes ricinus* (Acari; Chelicerata). *Cell Tissue Res.* 277, 493–504.

Kujala, P., Ikäheimonen, A., Ehsani, N., Vihinen, H., Auvinene, P., Kääriäinen, L. (2001). Biogenesis of the Semliki Forest virus RNA replication complex. *J. Virol.* 75, 3873-3884.

Kuma, A., Hatano, M., Matsui, M., Yamamoto, A., Nakaya, H., Yoshimori, T., Ohsumi, Y., Tokuhisa, T., and Mizushima, N. (2004). The role of autophagy during the early neonatal starvation period. *Nature* 432, 1032–1036.

Kuno, G., Chang, G.-J.J., Tsuchiya, K.R., Karbatsos, N., and Cropp, C.B. (1998). Phylogeny of the genus *Flavivirus*. *J. Virol. Methods* 72, 72–83.

Kurata, S., Ariki, S., and Kawabata, S. (2006). Recognition of pathogens and activation of immune responses in *Drosophila* and horseshoe crab innate immunity. *Immunobiology* 211, 237–249.

Kurscheid, S., Lew-Tabor, A.E., Rodriguez Valle, M., Bruyeres, A.G., Doogan, V.J., Munderloh, U.G., Guerrero, F.D., Barrero, R.A., and Bellgard, M.I. (2009). Evidence of a tick

RNAi pathway by comparative genomics and reverse genetics screen of targets with known loss-of-function phenotypes in *Drosophila*. *BMC Mol. Biol.* 10, 1–21.

Kurth, P., Preiss, A., Kovall, R.A., and Maier, D. (2011). Molecular analysis of the notch repressor-complex in *Drosophila*: characterization of potential hairless binding sites on suppressor of hairless. *PLoS One* 6, e27986.

Kurtti, T.J., and Keyhani, N.O. (2008). Intracellular infection of tick cell lines by the entomopathogenic fungus *Metarhizium anisopliae*. *Microbiology* 154, 1700–1709.

Kurtti, T.J, Mattila, J.T., Herron, M.J., Felsheim, R.F., Baldridge, G.D., Burkhardt, N.Y., Blazar, Bruce R., Hackett, P.B., Meyer, J.M., and Munderloh, U.G. (2008). Transgene expression and silencing in a tick cell line: a model system for functional tick genomics. *Insect Biochem Mol Biol* 38, 963–968.

Kurtti, T.J., Munderloh, U.G., and Ahlstrand, G.G. (1988). Tick tissue and cell culture in vector research. *Adv. Dis. Vector Res.* 5, 87–109.

Kurtti, T.J., Munderloh, U.G., Andreadis, T.G., Magnarelli, L.A., and Mather, T.N. (1996). Tick cell culture isolation of an intracellular prokaryote from the tick *Ixodes scapularis*. *J. Invertebr. Pathol.* 67, 318–321.

Labreuche, Y., O'Leary, N.A., de la Vega, E., Veloso, A., Gross, P.S., Chapman, R.W., Browdy, C.L., and Warr, G.W. (2009). Lack of evidence for *Litopenaeus vannamei* Toll receptor (lToll) involvement in activation of sequence-independent antiviral immunity in shrimp. *Dev. Comp. Immunol.* 33, 806–810.

Labuda, M., and Nuttall, P.A. (2004). Tick-borne viruses. *Parasitology* 129, S221–S245.

Labuda, M., Jones, L.D., Williams, T., Danielova, V., and Nuttall, P.A. (1993a). Efficient transmission of tick-borne encephalitis virus between cofeeding ticks. *J. Med. Entomol.* 30, 295–299.

Labuda, M., Jones, L.D., Williams, T., and Nuttall, P.A. (1993b). Enhancement of tick-borne encephalitis virus transmission by tick salivary gland extracts. *Med. Vet. Entomol.* 7, 193–196.

Labuda, M., Nuttall, P.A., Kozuch, O., Elecková, E., Williams, T., Zuffová, E., and Sabó, A. (1993c). Non-viraemic transmission of tick-borne encephalitis virus: a mechanism for arbovirus survival in nature. *Experientia* 49, 802–805.

Labuda, M., Austyn, J.M., Zuffova, E., Kozuch, O., Fuchsberger, N., Lysy, J., and Nuttall, P.A. (1996). Importance of localized skin infection in tick-borne encephalitis virus transmission. *Virology* 219, 357–366.

Labuda, M., Kozuch, O., Zuffová, E., Elecková, E., Hails, R.S., and Nuttall, P.A. (1997). Tick-borne encephalitis virus transmission between ticks cofeeding on specific immune natural rodent hosts. *Virology* 235, 138–143.

Lachmann, P.J., and Davies, A. (1997). Complement and immunity to viruses. *Immunol. Rev.* 159, 69–77.

Lai, R., Takeuchi, H., Lomas, L.O., Jonczy, J., Rigden, D.J., Rees, H.H., and Turner, P.C. (2004). A new type of antimicrobial protein with multiple histidines from the hard tick, *Amblyomma hebraeum*. *FASEB J.* 18, 1447-1449

LaStarza, M.W., Lemm, J.A., and Rice, C.M. (1994). Genetic analysis of the nsP3 region of Sindbis virus: evidence for roles in minus-strand and subgenomic RNA synthesis. *J. Virol.* 68, 5781–5791.

Lavine, M.D., and Strand, M.R. (2002). Insect hemocytes and their role in immunity. *Insect Biochem. Mol. Biol.* 32, 1295–1309.

Lawrie, C.H., Uzcátegui, N.Y., Armesto, M., Bell-Sakyi, L., and Gould, E.A. (2004). Susceptibility of mosquito and tick cell lines to infection with various flaviviruses. *Med. Vet. Entomol.* 18, 268–274.

Leake, C.E. (1987). Comparative growth of arboviruses in cell lines derived from *Aedes* and *Anopheles* mosquitoes and from the tick *Boophilus microplus*. In Arboviruses in Arthropod Cells in Vitro, C.E. Yunker, ed. (Boca Raton: CRC Press), pp. 25–42.

Leake, C.J., Pudney, M., and Varma, M. (1980). Studies on arboviruses in established tick cell lines. In Invertebrate Systems In Vitro, E. Kurstak, K. Maramorosch, and A. Dubendorfer, eds. (Amsterdam: Elsevier/North Holland Biomedical Press), pp. 327–335.

Leary, K., and Blair, C.D. (1980). Sequential events in the morphogenesis of Japanese encephalitis virus. *J. Ultrastruct. Res.* 72, 123–129.

Lebestky, T., Jung, S.-H., and Banerjee, U. (2003). A Serrate-expressing signaling center controls *Drosophila* hematopoiesis. *Genes Dev.* 17, 348–353.

Lee, Y.S., Nakahara, K., Pham, J.W., Kim, K., He, Z., Sontheimer, E.J., and Carthew, R.W. (2004). Distinct Roles for *Drosophila* Dicer-1 and Dicer-2 in the siRNA/miRNA Silencing Pathways. *Cell* 117, 69–81.

Léger, P., Lara, E., Jagla, B., Sismeiro, O., Mansuroglu, Z., Coppée, J.Y., Bonnefoy, E., and Bouloy, M. (2013). Dicer-2- and Piwi-mediated RNA interference in Rift Valley fever virus-infected mosquito cells. *J. Virol.* 87, 1631–1648.

Lescar, J., Roussel, a, Wien, M.W., Navaza, J., Fuller, S.D., Wengler, G., and Rey, F.A. (2001). The fusion glycoprotein shell of Semliki Forest virus: an icosahedral assembly primed for fusogenic activation at endosomal pH. *Cell* 105, 137–148.

Levin, M.L., and Fish, D. (2000). Acquisition of coinfection and simultaneous transmission of *Borrelia burgdorferi* and *Ehrlichia phagocytophila* by *Ixodes scapularis* ticks. *Infect. Immun.* 68, 2183–2186.

Li, F., and Xiang, J. (2013a). Recent advances in researches on the innate immunity of shrimp in China. *Dev. Comp. Immunol.* 39, 11–26.

Li, F., and Xiang, J. (2013b). Signaling pathways regulating innate immune responses in shrimp. *Fish Shellfish Immunol.* 34, 973–980.

Li, G., and Rice, C.M. (1993). The signal for translational readthrough of a UGA codon in Sindbis virus RNA involves a single cytidine residue immediately downstream of the termination codon. *J. Virol.* 67, 5062–5067.

Li, H., and Durbin, R. (2009). Fast and accurate short read alignment with Burrows-Wheeler transform. *Bioinformatics* 25, 1754–1760.

Li, F., Yan, H., Wang, D., Priya, T.A.J., Li, S., Wang, B., Zhang, J., and Xiang, J. (2009a). Identification of a novel relish homolog in Chinese shrimp *Fenneropenaeus chinensis* and its function in regulating the transcription of antimicrobial peptides. *Dev. Comp. Immunol.* 33, 1093–1101.

Li, F., Wang, D., Li, S., Yan, H., Zhang, J., Wang, B., Zhang, J., and Xiang, J. (2010). A Dorsal homolog (FcDorsal) in the Chinese shrimp *Fenneropenaeus chinensis* is responsive to both bacteria and WSSV challenge. *Dev. Comp. Immunol.* 34, 874–883.

Li, S., Mead, E.A., Liang, S., and Tu, Z. (2009b). Direct sequencing and expression analysis of a large number of miRNAs in *Aedes aegypti* and a multi-species survey of novel mosquito miRNAs. *BMC Genomics* 10, 581.

Li, W., Li, Y., Kedersha, N., Anderson, P., Emara, M., Swiderek, K., Moreno, G., and Brinton, M. (2002). Cell proteins TIA-1 and TIAR interact with the 3′ stem-loop of the West Nile virus complementary minus-strand RNA and facilitate virus replication. *J. Virol.* 76, 11989–12000.

Ligoxygakis, P., Pelte, N., Hoffmann, J.A., and Reichhart, J.-M. (2002). Activation of *Drosophila* Toll during fungal infection by a blood serine protease. *Science* 297, 114–116.

Liljestrom, P., Lusa, S., Huylebroeck, D., and Garoff, H. (1991). In vitro mutagenesis of a full-length cDNA clone of Semliki Forest virus: the small 6,000-molecular-weight membrane protein modulates virus release. *J. Virol.* 65, 4107–4113.

Liljeström, P., and Garoff, H. (1991). A new generation of animal cell expression vectors based on the Semliki Forest virus replicon. *Nat. Biotechnol.* 9, 1356–1361.

Lilley, K., and Friedman, D. (2004). All about DIGE: quantification technology for differential-display 2D-gel proteomics. *Expert Rev. Proteomics* 1, 1–9.

Limjindaporn, T., Wongwiwat, W., Noisakran, S., Srisawat, C., Netsawang, J., Puttikhunt, C., Kasinrerk, W., Avirutnan, P., Thiemmeca, S., Sriburi, R., Sittisombut, N., Malasit, P., and Yenchitsomanus, P. (2009). Interaction of dengue virus envelope protein with endoplasmic

reticulum-resident chaperones facilitates dengue virus production. *Biochem. Biophys. Res. Comm.* 379, 196–200.

Lin, X., Cerenius, L., Lee, B.L., and Söderhäll, K. (2007). Purification of properoxinectin, a myeloperoxidase homologue and its activation to a cell adhesion molecule. *Biochim. Biophys. Acta* 1770, 87–93.

Lindenbach, B.D., and Rice, C.M. (1997). Trans-Complementation of yellow fever virus NS1 reveals a role in early RNA replication. *J. Virol.* 71, 9608–9617.

Lindenbach, B.D., Thiel, H.-J., and Rice, C.M. (2007). *Flaviviridae*: The Viruses and Their Replication. In Fields Virology, D.M. Knipe, and P.M. Howley, eds. (Philadelphia: Lippincott-Raven), pp. 1101–1152.

Lindgren, E., and Gustafson, R. (2001). Tick-borne encephalitis in Sweden and climate change. *Lancet* 358, 16–18.

Lindquist, L., and Vapalahti, O. (2008). Tick-borne encephalitis. *Lancet* 371, 1861–1871.

Linn, M.L., Gardner, J., Warrilow, D., Darnell, G.A., McMahon, C.R., Field, I., Hyatt, A.D., Slade, R.W., and Suhrbier, A. (2001). Arbovirus of marine mammals: a new alphavirus isolated from the elephant seal louse, *Lepidophthirus macrorhini*. *J. Virol.* 75, 4103–4109.

Lipardi, C., and Paterson, B.M. (2011). Retraction for Lipardi and Paterson, “Identification of an RNA-dependent RNA polymerase in *Drosophila* involved in RNAi and transposon suppression”. *Proc. Natl. Acad. Sci. USA* 108, 15010.

Little, T.J., and Kraaijeveld, A.R. (2004). Ecological and evolutionary implications of immunological priming in invertebrates. *Trends Ecol. Evol.* 19, 58–60.

Liu, H., Sadygov, R.G., and Yates, J.R. (2004). A model for random sampling and estimation of relative protein abundance in shotgun proteomics. *Anal. Chem.* 76, 4193–4201.

Liu, H., Söderhäll, K., and Jiravanichpaisal, P. (2009). Antiviral immunity in crustaceans. *Fish Shellfish Immunol.* 27, 79–88.

Liu, H., Li, Y., Gao, M., Wen, K., Jia, Y., Liu, X., Zhang, W., Ma, B., and Wang, J. (2012a). Complete genome sequence of a bovine viral diarrhea virus 2 from commercial fetal bovine serum. *J. Virol.* 86, 10233.

Liu, J., Smagghe, G., and Swevers, L. (2013). Transcriptional response of BmToll9-1 and RNAi machinery genes to exogenous dsRNA in the midgut of *Bombyx mori*. *J. Insect Physiol.* 59, 646–654.

Liu, L., Narasimhan, S., Dai, J., Zhang, L., Cheng, G., and Fikrig, E. (2011). *Ixodes scapularis* salivary gland protein P11 facilitates migration of *Anaplasma phagocytophilum* from the tick gut to salivary glands. *EMBO Rep.* 12, 1196–1203.

Liu, L., Dai, J., Zhao, Y.O., Narasimhan, S., Yang, Y., Zhang, L., and Fikrig, E. (2012b). *Ixodes scapularis* JAK-STAT pathway regulates tick antimicrobial peptides, thereby controlling the agent of human granulocytic anaplasmosis. *J. Infect. Dis.* 206, 1233–1241.

Liu, L., Li, Y., Li, S., Hu, N., He, Y., Pong, R., Lin, D., Lu, L., and Law, M. (2012c). Comparison of next-generation sequencing systems. *J. Biomed. Biotechnol.* 2012, 251364.

Liu, Q., Rand, T.A., Kalidas, S., Du, F., Kim, H.-E., Smith, D.P., and Wang, X. (2003). R2D2, a bridge between the initiation and effector steps of the *Drosophila* RNAi pathway. *Science* 301, 1921–1925.

Liu, W.-J., Chang, Y.-S., Wang, A.H.-J., Kou, G.-H., and Lo, C.-F. (2007). White spot syndrome virus annexes a shrimp STAT to enhance expression of the immediate-early gene *ie1*. *J. Virol.* 81, 1461–1471.

Liu, Y., Ye, X., Jiang, F., Liang, C., Chen, D., Peng, J., Kinch, L.N., Grishin, N. V, and Liu, Q. (2009). C3PO, an endoribonuclease that promotes RNAi by facilitating RISC activation. *Science* 325, 750–753.

Liu, Z., Liu, H., Liu, X., and Wu, X. (2008). Purification and cloning of a novel antimicrobial peptide from salivary glands of the hard tick, *Ixodes sinensis*. *Comp. Biochem. Physiol. B. Biochem. Mol. Biol.* 149, 557–561.

Livak, K.J., and Schmittgen, T.D. (2001). Analysis of relative gene expression data using real-time quantitative PCR and the $2^{-\Delta\Delta C}{}_{T}$ Method. *Methods* 25, 402–408.

Lloyd, R.E. (2013). Regulation of stress granules and P-bodies during RNA virus infection. *WIREs RNA* 4, 317–331.

Loosová, G., Jindrák, L., and Kopácek, P. (2001). Mortality caused by experimental infection with the yeast *Candida haemulonii* in the adults of *Ornithodoros moubata* (Acarina: Argasidae). *Folia Parasitol. (Praha).* 48, 149–153.

Lopez, S., Yao, J.S., Kuhn, R.J., Strauss, E.G., and Strauss, J.H. (1994). Nucleocapsid-glycoprotein interactions required for assembly of alphaviruses. *J. Virol.* 68, 1316–1323.

Lucas, K., and Raikhel, A.S. (2013). Insect microRNAs: biogenesis, expression profiling and biological functions. *Insect Biochem. Mol. Biol.* 43, 24–38.

Lwande, O.W., Lutomiah, J., Obanda, V., Gakuya, F., Mutisya, J., Mulwa, F., Michuki, G., Chepkorir, E., Fischer, A., Venter, M., and Sang, R. (2013). Isolation of tick and mosquito-borne arboviruses from ticks sampled from livestock and wild animal hosts in Ijara District, Kenya. *Vector-borne Zoonot. Dis.* 13, 637–642.

Machado, A., Sforca, M., Miranda, A., Daffre, S., Pertinhez, T.A., Spisni, A., and Miranda, M.T.M. (2007). Truncation of amidated fragment 33–61 of bovine α-hemoglobin: Effects on the structure and anticandidal activity. *Pept. Sci.* 88, 413–426.

Mackenzie, J. (2005). Wrapping things up about virus RNA replication. *Traffic* 6, 967–977.

Mackenzie, J.M., Jones, M.K., and Young, P.R. (1996). Immunolocalization of the dengue virus nonstructural glycoprotein NS1 suggests a role in viral RNA replication. *Virology* 220, 232–240.

Mackenzie, J.M., Khromykh, A.A., and Parton, R.G. (2007). Cholesterol manipulation by West Nile virus perturbs the cellular immune response. *Cell Host Microbe* 2, 229–239.

Madani, T.A. (2005). Alkhumra virus infection, a new viral hemorrhagic fever in Saudi Arabia. *J. Infect.* 51, 91–97.

Maier, D., Kurth, P., Schulz, A., Russell, A., Yuan, Z., Gruber, K., Kovall, R.A., and Preiss, A. (2011). Structural and functional analysis of the repressor complex in the Notch signaling pathway of *Drosophila melanogaster*. *Mol. Biol. Cell* 22, 3242–3252.

Makou, E., Herbert, A.P., and Barlow, P.N. (2013). Functional anatomy of complement factor H. *Biochemistry* 52, 3949–3962.

Mandl, C.W. (2005). Steps of the tick-borne encephalitis virus replication cycle that affect neuropathogenesis. *Virus Res.* 111, 161–174.

Mandl, C.W., Heinz, F.X., Stöckl, E., and Kunz, C. (1989). Genome sequence of tick-borne encephalitis virus (Western subtype) and comparative analysis of nonstructural proteins with other flaviviruses. *Virology* 173, 291–301.

Mandl, C.W., Ecker, M., Holzmann, H., Kunz, C., and Heinz, F.X. (1997). Infectious cDNA clones of tick-borne encephalitis virus European subtype prototypic strain Neudoerfl and high virulence strain Hypr. *J. Gen. Virol.* 78 (Pt 5), 1049–1057.

Mandl, C.W., Kroschewski, H., Allison, S.L., Kofler, R., Holzmann, H., Meixner, T., and Heinz, F.X. (2001). Adaptation of tick-borne encephalitis virus to BHK-21 cells results in the formation of multiple heparan sulfate binding sites in the envelope protein and attenuation *in vivo J. Virol*. 75, 5627-5637

Mangold, A.J., Galindo, R.C., and de la Fuente, J. (2009). Response to the commentary of D. Macqueen on: Galindo RC, Doncel-Pérez E, Zivkovic Z, Naranjo V, Gortazar C, Mangold AJ, et al. Tick subolesin is an ortholog of the akirins described in insects and vertebrates [Dev. Comp. Immunol. 33 (2009) 612–617]. *Dev. Comp. Immunol.* 33, 878–879.

Mansfield, K.L., Johnson, N., Phipps, L.P., Stephenson, J.R., Fooks, A.R., and Solomon, T. (2009). Tick-borne encephalitis virus - a review of an emerging zoonosis. *J. Gen. Virol.* 90, 1781–1794.

Mardis, E.R. (2008). Next-generation DNA sequencing methods. *Annu. Rev. Genomics Hum. Genet.* 9, 387–402.

Markoff, L. (2003). 5′- and 3′-noncoding regions in flavivirus RNA. *Adv. Virus Res.* 59, 177–228.

Marmaras, V.J., and Lampropoulou, M. (2009). Regulators and signalling in insect haemocyte immunity. *Cell. Signal.* 21, 186–195.

Marsh, M., and Helenius, A. (1980). Adsorptive endocytosis of Semliki Forest virus. *J. Mol. Biol.* 142, 439–454.

Marsh, M., Bolzau, E., and Helenius, A. (1983). Penetration of Semliki Forest virus from acidic prelysosomal vacuoles. *Cell* 32, 931–940.

Martinez, O., and Goud, B. (1998). Rab proteins. *Biochim. Biophys. Acta* 1404, 101–112.

Mathiot, C.C., Grimaud, G., Garry, P., Bouquety, J.C., Mada, A., Daguisy, A.M., and Georges, A.J. (1990). An outbreak of human Semliki Forest virus infections in Central African Republic. *Am. J. Trop. Med. Hyg.* 42, 386–393.

Matrosovich, M., Matrosovich, T., Garten, W., and Klenk, H.-D. (2006). New low-viscosity overlay medium for viral plaque assays. *Virol. J.* 3, 63.

Matsumoto, F., Saitoh, S.-I., Fukui, R., Kobayashi, T., Tanimura, N., Konno, K., Kusumoto, Y., Akashi-Takamura, S., and Miyake, K. (2008). Cathepsins are required for Toll-like receptor 9 responses. *Biochem. Biophys. Res. Commun.* 367, 693–699.

Mattila, J.T., Burkhardt, N.Y., Hutcheson, H.J., Munderloh, U.G., and Kurtti, T.J. (2007). Isolation of cell lines and a rickettsial endosymbiont from the soft tick *Carios capensis* (Acari: Argasidae: Ornithodorinae). *J. Med. Entomol.* 44, 1091–1101.

Mattila, J.T., Munderloh, U.G., and Kurtti, T.J. (2007). Phagocytosis of the Lyme disease spirochete, *Borrelia burgdorferi*, by cells from the ticks, *Ixodes scapularis* and *Dermacentor andersoni*, infected with an endosymbiont, *Rickettsia peacockii*. *J. Insect Sci.* 7, 58.

McInerney, G.M., Smit, J.M., Liljeström, P., and Wilschut, J. (2004). Semliki Forest virus produced in the absence of the 6K protein has an altered spike structure as revealed by decreased membrane fusion capacity. *Virology* 325, 200–206.

McIntyre, T.M., Prescott, S.M., and Stafforini, D.M. (2009). The emerging roles of PAF acetylhydrolase. *J. Lipid Res.* 50 Suppl, S255–9.

McLoughlin, M.F., and Graham, D.A. (2007). Alphavirus infections in salmonids--a review. *J. Fish Dis.* 30, 511–531.

McNally, K.L., Mitzel, D.N., Anderson, J.M., Ribeiro, J.M.C., Valenzuela, J.G., Myers, T.G., Godinez, A., Wolfinbarger, J.B., Best, S.M., and Bloom, M.E. (2012). Differential salivary gland transcript expression profile in *Ixodes scapularis* nymphs upon feeding or flavivirus infection. *Ticks Tick-borne. Dis.* 3, 18–26.

Megy, K., Emrich, S.J., Lawson, D., Campbell, D., Dialynas, E., Hughes, D.S.T., Koscielny, G., Louis, C., Maccallum, R.M., Redmond, S.N., et al. (2012). VectorBase: improvements to a bioinformatics resource for invertebrate vector genomics. *Nucleic Acids Res.* 40, D729–34.

Melancon, P., and Garoff, H. (1986). Reinitiation of translocation in the Semliki Forest virus structural polyprotein: identification of the signal for the E1 glycoprotein. *EMBO J.* 5, 1551–1560.

Mendes, N.D., Freitas, A.T., Vasconcelos, A.T., and Sagot, M.-F. (2010). Combination of measures distinguishes pre-miRNAs from other stem-loops in the genome of the newly sequenced *Anopheles darlingi*. *BMC Genomics* 11, 529.

Mercado-Curiel, R.F., Palmer, G.H., Guerrero, F.D., and Brayton, K. a (2011). Temporal characterisation of the organ-specific *Rhipicephalus microplus* transcriptional response to *Anaplasma marginale* infection. *Int. J. Parasitol.* 41, 851–860.

Merits, A., Vasiljeva, L., Ahola, T., Kääriäinen, L., and Auvinen, P. (2001). Proteolytic processing of Semliki Forest virus-specific non-structural polyprotein by nsP2 protease. *J. Gen. Virol.* 82, 765–773.

Merkling, S.H., and van Rij, R.P. (2012). Beyond RNAi: Antiviral defense strategies in *Drosophila* and mosquito. *J. Insect Physiol.*

Metzker, M.L. (2010). Sequencing technologies - the next generation. *Nat. Rev. Genet.* 11, 31–46.

Michalak, M., Corbett, E.F., Mesaeli, N., Nakamura, K., and Opas, M. (1999). Calreticulin: one protein, one gene, many functions. *Biochem. J.* 344 Pt 2, 281–292.

Miller, S., and Krijnse-Locker, J. (2008). Modification of intracellular membrane structures for virus replication. *Nat. Rev. Microbiol.* 6, 363–374.

Miyoshi, T., Takeuchi, A., Siomi, H., and Siomi, M.C. (2010). A direct role for Hsp90 in pre-RISC formation in *Drosophila*. *Nat. Struct. Mol. Biol.* 17, 1024–1026.

Mizushima, N., Yamamoto, A., Matsui, M., Yoshimori, T., and Ohsumi, Y. (2004). *In vivo* analysis of autophagy in response to nutrient starvation using transgenic mice expressing a fluorescent autophagosome marker. *Mol. Biol. Cell* 15, 1101–1111.

Morais, A.T., Terzian, A.C., Duarte, D.V., Bronzoni, R.V., Madrid, M.C., Gavioli, A.F., Gil, L.H., Oliveira, A.G., Zanelli, C.F., Valentini, S.R., Rahal, P., and Nogueira, M.L. (2013). The eukaryotic translation initiation factor 3 subunit L protein interacts with *Flavivirus* NS5 and may modulate yellow fever virus replication. *Virol. J.* 10, 205.

Morales, C., Wu, S., Yang, Y., Hao, B., and Li, Z. (2009). *Drosophila* glycoprotein 93 is an ortholog of mammalian heat shock protein gp96 (grp94, HSP90b1, HSPC4) and retains disulfide bond-independent chaperone function for TLRs and integrins. *J. Immunol.* 183, 5121–5128.

Morazzani, E.M., Wiley, M.R., Murreddu, M.G., Adelman, Z.N., and Myles, K.M. (2012). Production of virus-derived ping-pong-dependent piRNA-like small RNAs in the mosquito soma. *PLoS Pathog.* 8, e1002470.

Moshkin, M.P., Novikov, E.A., Tkachev, S.E., and Vlasov, V.V (2009). Epidemiology of a tick-borne viral infection: theoretical insights and practical implications for public health. *Bioessays* 31, 620–628.

Mosso, C., Galván-Mendoza, I.J., Ludert, J.E., and del Angel, R.M. (2008). Endocytic pathway followed by dengue virus to infect the mosquito cell line C6/36 HT. *Virology* 378, 193–199.

Mulenga, A., Macaluso, K.R., Simser, J.A., and Azad, A.F. (2003). Dynamics of *Rickettsia*-tick interactions: identification and characterization of differentially expressed mRNAs in uninfected and infected *Dermacentor variabilis*. *Insect Mol. Biol.* 12, 185–193.

Mulenga, A., Simser, J.A., Macaluso, K.R., and Azad, A.F. (2004). Stress and transcriptional regulation of tick ferritin HC. *Insect Mol. Biol.* 13, 423–433.

Munderloh, U.G., and Kurtti, T.J. (1989). Formulation of medium for tick cell culture. *Exp. Appl. Acarol.* 7, 219–229.

Munderloh, U.G., Liu, Y., Wang, M., Chen, C., and Kurtti, T.J. (1994). Establishment, maintenance and description of cell lines from the tick *Ixodes scapularis*. *J. Parasitol.* 80, 533–543.

Munz, E., Reimann, M., and Mahnel, H. (1987). Nairobi sheep disease virus and Reovirus-like particles in the tick cell line TTC-243 from *Rhipicephalus appendiculatus*: experiences with the handling of the tick cells, immunoperoxidase, and ultrahistological studies. In Arboviruses in Arthropod Cells in Vitro, C.E. Yunker, ed. (Boca Raton: CRC Press), pp. 133–147.

Murray, C.L., Jones, C.T., and Rice, C.M. (2008). Architects of assembly: roles of *Flaviviridae* non-structural proteins in virion morphogenesis. *Nat. Rev. Microbiol.* 6, 699–708.

Muta, T., and Iwanaga, S. (1996). The role of hemolymph coagulation in innate immunity. *Curr. Opin. Immunol.* 8, 41–47.

Muylaert, I.R., Chambers, T.J., Galler, R., and Rice, C.M. (1996). Mutagenesis of the N-linked glycosylation sites of the yellow fever virus NS1 protein: effects on virus replication and mouse neurovirulence. *Virology* 222, 159–168.

Myles, K.M., Wiley, M.R., Morazzani, E.M., and Adelman, Z.N. (2008). Alphavirus-derived small RNAs modulate pathogenesis in disease vector mosquitoes. *Proc. Natl. Acad. Sci. USA* 105, 19938–19943.

Nagy, P.D., Wang, R.Y., Pogany, J., Hafren, A., and Makinen, K. (2011). Emerging picture of host chaperone and cyclophilin roles in RNA virus replication. *Virology* 411, 374–382.

Najm, N.-A., Silaghi, C., Bell-Sakyi, L., Pfister, K., and Passos, L.M.F. (2012). Detection of bacteria related to *Candidatus* Midichloria mitochondrii in tick cell lines. *Parasitol. Res.* 110, 437–442.

Nakajima, Y., Ishibashi, J., Yukuhiro, F., Asaoka, A., Taylor, D., and Yamakawa, M. (2003a). Antibacterial activity and mechanism of action of tick defensin against Gram-positive bacteria. *Biochim. Biophys. Acta - Gen. Subj.* 1624, 125–130.

Nakajima, Y., Ogihara, K., Taylor, D., and Yamakawa, M. (2003b). Antibacterial hemoglobin fragments from the midgut of the soft tick, *Ornithodoros moubata* (Acari: Argasidae). *J. Med. Entomol.* 40, 78–81.

Nakamoto, M., Moy, R.H., Xu, J., Bambina, S., Yasunaga, A., Shelly, S.S., Gold, B., and Cherry, S. (2012). Virus recognition by Toll-7 activates antiviral autophagy in *Drosophila*. *Immunity* 36, 658–667.

Naranjo, V., Ayllón, N., Pérez de la Lastra, J.M., Galindo, R.C., Kocan, K.M., Blouin, E.F., Mitra, R., Alberdi, P., Villar, M., and de la Fuente, J. (2013). Reciprocal regulation of NF-kB (Relish) and Subolesin in the tick vector, *Ixodes scapularis*. *PLoS One* 8, e65915.

Nava, S., Guglielmone, A.A., and Mangold, A.J. (2009). An overview of systematics and evolution of ticks. *Front. Biosci.* 14, 2857–2877.

Nene, V., Lee, D., Kang'a, S., Skilton, R., Shah, T., de Villiers, E., Mwaura, S., Taylor, D., Quackenbush, J., and Bishop, R. (2004). Genes transcribed in the salivary glands of female *Rhipicephalus appendiculatus* ticks infected with *Theileria parva*. *Insect Biochem. Mol. Biol.* 34, 1117–1128.

Nesvizhskii, A.i., and Aebersold, R. (2004). Analysis, statistical validation and dissemination of large-scale proteomics datasets generated by tandem MS. *Drug Discov. Today* 9, 173–181.

Ng, M.L., Tan, S.H., and Chu, J.J.H. (2001). Transport and budding at two distinct sites of visible nucleocapsids of West Nile (Sarafend) virus. *J. Med. Virol.* 65, 758–764.

Nijhof, A.M., Taoufik, A., de la Fuente, J., Kocan, K.M., de Vries, E., and Jongejan, F. (2007). Gene silencing of the tick protective antigens, *Bm86*, *Bm91* and *subolesin*, in the one-host tick *Boophilus microplus* by RNA interference. *Int. J. Parasitol.* 37, 653–662.

Nuttall, P.A. (2009). Molecular characterization of tick-virus interactions. *Front. Biosci.* 14, 2466–2483.

Nuttall, P.A., and Labuda, M. (2004). Tick–host interactions: saliva-activated transmission. *Parasitology* 129, S177–S189.

Odorizzi, G. (2006). The multiple personalities of Alix. *J. Cell Sci.* 119, 3025–3032.

Offerdahl, D.K., Dorward, D.W., Hansen, B.T., and Bloom, M.E. (2012). A three-dimensional comparison of tick-borne *flavivirus* infection in mammalian and tick cell lines. *PLoS One* 7, e47912.

Okamura, K., Ishizuka, A., Siomi, H., and Siomi, M.C. (2004). Distinct roles for Argonaute proteins in small RNA-directed RNA cleavage pathways. *Genes Dev.* 18, 1655–1666.

Ong, S.T., Ho, J.Z.S., Ho, B., and Ding, J.L. (2006). Iron-withholding strategy in innate immunity. *Immunobiology* 211, 295–314.

Osborne, B., and Miele, L. (1999). Notch and the immune system. *Immunity* 11, 653–663.

Otsuki, K., Maeda, J., Yamamoto, H., and Tsubokura, M. (1978). Studies on avian infectious bronchitis virus (IBV). III. Interferon induction by and sensitivity to interferon of IBV. *Arch. Virol.* 255, 249–255.

Överby, A.K., Popov, V.L., Niedrig, M., and Weber, F. (2010). Tick-borne encephalitis virus delays interferon induction and hides its double-stranded RNA in intracellular membrane vesicles. *J. Virol.* 84, 8470–8483.

Paingankar, M.S., Gokhale, M.D., and Deobagkar, D.N. (2010). Dengue-2-virus-interacting polypeptides involved in mosquito cell infection. *Arch. Virol.* 155, 1453–1461.

Pal, S., and Wu, L.P. (2009). Pattern recognition receptors in the fly. *Fly* 3, 121–129.

Panaretou, B., Prodromou, C., Roe, S.M., O'Brien, R., Ladbury, J.E., Piper, P.W., and Pearl, L.H. (1998). ATP binding and hydrolysis are essential to the function of the Hsp90 molecular chaperone in vivo. *EMBO J.* 17, 4829–4836.

Paradkar, P.N., Trinidad, L., Voysey, R., Duchemin, J.-B., and Walker, P.J. (2012). Secreted Vago restricts West Nile virus infection in *Culex* mosquito cells by activating the Jak-STAT pathway. *Proc. Natl. Acad. Sci. USA* 109, 18915–18920.

Park, B., Brinkmann, M.M., Spooner, E., Lee, C.C., Kim, Y.-M., and Ploegh, H.L. (2008). Proteolytic cleavage in an endolysosomal compartment is required for activation of Toll-like receptor 9. *Nat. Immunol.* 9, 1407–1414.

Pastorino, B., Boucomont-Chapeaublanc, E., Peyrefitte, C.N., Belghazi, M., Fusaï, T., Rogier, C., Tolou, H.J., and Almeras, L. (2009). Identification of cellular proteome modifications in response to West Nile virus infection. *Mol. Cell. Proteomics* 8, 1623–1637.

Pastorino, B., Nougairède, A., Wurtz, N., Gould, E., and de Lamballerie, X. (2010). Role of host cell factors in *flavivirus* infection: Implications for pathogenesis and development of antiviral drugs. *Antiviral Res.* 87, 281–294.

Patel, R.K., and Hardy, R.W. (2012). Role for the phosphatidylinositol 3-kinase-Akt-TOR pathway during sindbis virus replication in arthropods. *J. Virol.* 86, 3595–3604.

Pathak, S., Webb, H.E., Oaten, S.W., and Bateman, S. (1976). An electron-microscopic study of the development of virulent and avirulent strains of Semliki Forest virus in mouse brain. *J. Neurol. Sci.* 28, 289–300.

Pattanakitsakul, S., Rungrojcharoenkit, K., Kanlaya, R., Sinchaikul, S., Noisakran, S., Chen, S.-T., Malasit, P., and Visith, T. (2007). Proteomic analysis of host responses in HepG2 cells during dengue virus infection. *J. Proteome Res.* 6, 4592–4600.

Patterson, S.D., and Aebersold, R.H. (2003). Proteomics: the first decade and beyond. *Nat. Genet.* 33 Suppl, 311–323.

Pedra, J.H.F., Narasimhan, S., Rendić, D., DePonte, K., Bell-Sakyi, L., Wilson, I.B.H., and Fikrig, E. (2010). Fucosylation enhances colonization of ticks by *Anaplasma phagocytophilum*. *Cell. Microbiol.* 12, 1222–1234.

Peleg, J. (1969). Behaviour of infectious RNA from four different viruses in continuously subcultured *Aedes aegypti* mosquito embryo cells. *Nature* 221, 193–194.

Peña, J., and Harris, E. (2011). Dengue virus modulates the unfolded protein response in a time-dependent manner. *J. Biol. Chem.* 286, 14226–14236.

Peränen, J., and Kääriäinen, L. (1991). Biogenesis of type I cytopathic vacuoles in Semliki Forest virus-infected BHK cells. *J. Virol.* 65, 1623–1627.

Pereira, L.S., Oliveira, P.L., Barja-Fidalgo, C., and Daffre, S. (2001). Production of reactive oxygen species by hemocytes from the cattle tick *Boophilus microplus*. *Exp. Parasitol.* 99, 66–72.

Perera, R., Riley, C., Isaac, G., Hopf-Jannasch, A.S., Moore, R.J., Weitz, K.W., Pasa-Tolic, L., Metz, T.O., Adamec, J., and Kuhn, R.J. (2012). Dengue virus infection perturbs lipid homeostasis in infected mosquito cells. *PLoS Pathog.* 8, e1002584.

Pfeffer, M., and Dobler, G. (2011). Tick-borne encephalitis virus in dogs – is this an issue? *Parasit. Vectors* 4, 59.

Pialoux, G., Gaüzère, B.-A., Jauréguiberry, S., and Strobel, M. (2007). Chikungunya, an epidemic arbovirosis. *Lancet Infect. Dis.* 7, 319–327.

Pichu, S., Ribeiro, J.M.C., and Mather, T.N. (2009). Purification and characterization of a novel salivary antimicrobial peptide from the tick, *Ixodes scapularis*. *Biochem. Biophys. Res. Comm.* 390, 511–515.

Pieren, M., Galli, C., Denzel, A., and Molinari, M. (2005). The use of calnexin and calreticulin by cellular and viral glycoproteins. *J. Biol. Chem.* 280, 28265–28271.

Pitaluga, A.N., Mason, P.W., and Traub-Cseko, Y.M. (2008). Non-specific antiviral response detected in RNA-treated cultured cells of the sandfly, *Lutzomyia longipalpis*. *Dev. Comp. Immunol.* 32, 191–197.

Plekhova, N.G., Somova, L.M., Lyapun, I.N., Kondrashova, N.M., Krylova, N. V., Leonova, G.N., and Pustovalov, E. V. (2011). The cells of innate systems in tick-borne encephalitis. In Flavivirus Encephalitis, D. Ruzek, ed. (Rijeka: InTech), pp. 167–194.

Pletnev, A.G., Bray, M., and Hanley, K. (2001). Tick-borne Langat/mosquito-borne dengue *flavivirus* chimera, a candidate live attenuated vaccine for protection against disease caused by members of the tick-borne. *J. Virol.* 75, 8259–8267.

Pockley, A.G. (2003). Heat shock proteins as regulators of the immune response. *Lancet* 362, 469–476.

Pohl, P.C., Klafke, G.M., Júnior, J.R., Martins, J.R., da Silva Vaz, I., and Masuda, A. (2012). ABC transporters as a multidrug detoxification mechanism in *Rhipicephalus (Boophilus) microplus*. *Parasitol. Res.* 111, 2345–2351.

Popara, M., Villar, M., Mateos-Hernández, L., de Mera, I.G.F., Marina, A., del Valle, M., Almazán, C., Domingos, A., and de la Fuente, J. (2013). Lesser protein degradation machinery correlates with higher BM86 tick vaccine efficacy in *Rhipicephalus annulatus* when compared to *Rhipicephalus microplus*. *Vaccine* 31, 4728–4735.

Powers, A., Huang, H., Roehrig, J., Strauss, E., and Weaver, S. (2012). Virus Taxonomy. In Virus Taxonomy: Ninth Report of the International Committee on Taxonomy of Viruses, A.M.Q. King, E. Lefkowitz, M.J. Adams, and E.B. Carstens, eds. (San Diego: Elsevier), pp. 1103–1110.

Pratt, W.B., and Toft, D.O. (2003). Regulation of signaling protein function and trafficking by the hsp90/hsp70-based chaperone machinery. *Exp. Biol. Med.* 228, 111–133.

Premachandra, H.K.A., De Zoysa, M., Nikapitiya, C., Lee, Y., Wickramaarachchi, W.D.N., Whang, I., and Lee, J. (2013). Molluskan fasciclin-1 domain-containing protein: molecular characterizationand gene expression analysis of fasciclin 1-like protein from disk abalone (*Haliotis discus discus*). *Gene* 522, 219–225.

Prescott, S.M., Zimmerman, G.A., Stafforini, D.M., and McIntyre, T.M. (2000). Platelet-activating factor and related lipid mediators. *Ann. Rev. Bio* 69, 419–445.

Price, W.H., and Thind, I.S. (1973). Immunization of mice against Russian spring-summer virus complex and monkeys against Powassan virus with attenuated Langat E5 virus. *Am. J. Trop. Med. Hyg.* 22, 100–108.

Price, W.H., Parks, J.J., Ganaway, J., O'Leary, W., and Lee, R. (1963). The ability of an attenuated isolate of Langat virus to protect primates and mice against other members of the Russian spring-summer virus complex. *Am. J. Trop. Med. Hyg.* 12, 787–799.

Price, W.H., Thind, I.S., Teasdall, R.D., and O'Leary, W. (1970). Vaccination of human volunteers against Russian spring-summer (RSS) virus complex with attenuated Langat E5 virus. *Bull. WHO* 42, 89–94.

Pryor, M.J., Rawlinson, S.M., Butcher, R.E., Barton, C.L., Waterhouse, T.A., Vasudevan, S.G., Bardin, P.G., Wright, P.J., Jans, D.A., and Davidson, A.D. (2007). Nuclear localization of dengue virus nonstructural protein 5 through its importin α/β-recognized nuclear localization sequences is integral to viral infection. *Traffic* 8, 795–807.

Pudney, M. (1987). Tick cell lines for the isolation and assay of arboviruses. In Arboviruses in Arthropod Cells in Vitro, C.E. Yunker, ed. (Boca Raton: CRC Press), pp. 87–101.

Pudney, M., Varma, M., and Leake, C.J. (1979). Replication of arboviruses in arthropod in vitro systems. In Tick-Borne Diseases and Their Vectors, J. Wilde, ed. (Edinburgh: Centre for Tropical Veterniary Medicine), pp. 490–496.

Quintin, J., Cheng, S.-C., van der Meer, J.W., and Netea, M.G. (2014). Innate immune memory: towards a better understanding of host defense mechanisms. *Curr. Opin. Immunol.* 29, 1–7.

Rachinsky, A., Guerrero, F.D., and Scoles, G.A. (2007). Differential protein expression in ovaries of uninfected and *Babesia*-infected southern cattle ticks, *Rhipicephalus (Boophilus) microplus*. *Insect Biochem. Mol. Biol.* 37, 1291–1308.

Rachinsky, A., Guerrero, F.D., and Scoles, G.A. (2008). Proteomic profiling of *Rhipicephalus (Boophilus) microplus* midgut responses to infection with *Babesia bovis*. *Vet. Parasitol.* 152, 294–313.

Radtke, F., MacDonald, H.R., and Tacchini-Cottier, F. (2013). Regulation of innate and adaptive immunity by Notch. *Nat. Rev. Immunol.* 13, 427–437.

Rahman, S., Matsumura, T., Masuda, K., Kanemura, K., and Fukunaga, T. (1998). Maturation site of dengue type 2 virus in cultured mosquito C6/36 cells and Vero cells. *Kobe J. Med. Sci.* 44, 65–79.

Ramirez, J.L., and Dimopoulos, G. (2010). The Toll immune signaling pathway control conserved anti-dengue defenses across diverse *Ae. aegypti* strains and against multiple dengue virus serotypes. *Dev. Comp. Immunol.* 34, 625–629.

Rand, T.A., Ginalski, K., Grishin, N. V, and Wang, X. (2004). Biochemical identification of Argonaute 2 as the sole protein required for RNA-induced silencing complex activity. *Proc. Natl. Acad. Sci. USA* 101, 14385–14389.

Randolph, S.E. (2004). Evidence that climate change has caused “emergence” of tick-borne diseases in Europe? *Int. J. Med. Microbiol. Suppl.* 293, 5–15.

Randow, F., and Seed, B. (2001). Endoplasmic reticulum chaperone gp96 is required for innate immunity but not cell viability. *Nat. Cell Biol.* 3, 891–896.

Rao, A., Luo, C., and Hogan, P.G. (1997). Transcription factors of the NFAT family: regulation and function. *Ann. Rev. Immunol.* 15, 707–747.

Rehacek, J. (1964). Comparison of the susceptibility of primary tick and chick embryo cell cultures to small amounts of tick-borne encephalitis virus. *Acta Virol.* 8, 470–471.

Rehacek, J. (1965). Cultivation of different viruses in tick tissue cultures. *Acta Virol.* 9, 332-337.

Rehacek, J. (1973). Maintaining of tick-borne encephalitis (TBE) virus, Western subtype, in tick cells in vitro. In Proceedings of the Third International Colloquium on Invertebrate Tissue Culture, J. Rehacek, D. Blaskovic, and W.F. Hink, eds. (Bratislava: Slovak Academy of Sciences), pp. 439–443.

Rehacek, J. (1987). Arthropod cell cultures in studies of tick-borne togaviruses and orbiviruses in Central Europe. In Arboviruses in Arthropod Cells in Vitro, C.E. Yunker, ed. (Boca Raton: CRC Press), pp. 115 –132.

Rey, F., Heinz, F.X., Mandl, C.W., Kunz, C., and Harrison, S.C. (1995). The envelope glycoprotein from tick-borne encephalitis virus at 2 Å resolution. *Nature* 375, 291–298.

Rezza, G., Nicoletti, L., Angelini, R., Romi, R., Finarelli, A.C., Panning, M., Cordioli, P., Fortuna, C., Boros, S., Magurano, F., Silvi, G., Angelini, P., Dottori, M., Ciufolini, M.G., Majori, G.C., and Cassone, A. (2007). Infection with chikungunya virus in Italy: an outbreak in a temperate region. *Lancet* 370, 1840–1846.

Rice, C.M, Lenches, E.M., Eddy, S.R., Shin, S.J., Sheets, R.L., and Strauss, J.H. (1985). Nucleotide sequence of yellow fever virus: implications for flavivirus gene expression and evolution. *Science.* 229, 726–733.

Van Rij, R.P., Saleh, M.-C., Berry, B., Foo, C., Houk, A., Antoniewski, C., and Andino, R. (2006). The RNA silencing endonuclease Argonaute 2 mediates specific antiviral immunity in *Drosophila melanogaster*. *Genes Dev.* 20, 2985–2995.

Rikkonen, M. (1996). Functional significance of the nuclear-targeting and NTP-binding motifs of Semliki Forest virus nonstructural protein nsP2. *Virology* 218, 352–361.

Rikkonen, M., Peränen, J., and Kääriäinen, L. (1994). ATPase and GTPase activities associated with Semliki Forest virus nonstructural protein nsP2. *J. Virol.* 68, 5804–5810.

Rittig, M.G., Kuhn, K.H., Dechant, C.A., Gauckler, A., Modolell, M., Ricciardi-Castagnoli, P., Krause, A., and Burmester, G.R. (1996). Phagocytes from both vertebrate and invertebrate species use “coiling” phagocytosis. *Dev. Comp. Immunol.* 20, 393–406.

Robalino, J., Bartlett, T.C., Chapman, R.W., Gross, P.S., Browdy, C.L., and Warr, G.W. (2007). Double-stranded RNA and antiviral immunity in marine shrimp: inducible host mechanisms and evidence for the evolution of viral counter-responses. *Dev. Comp. Immunol.* 31, 539–547.

Robertson, S.J., Mitzel, D.N., Taylor, R.T., Best, S.M., and Bloom, M.E. (2009). Tick-borne flaviviruses: dissecting host immune responses and virus countermeasures. *Immunol. Res.* 43, 172–186.

Robin, S., Ramful, D., Le Seach, F., Jaffar-Bandjee, M.-C., Rigou, G., and Alessandri, J.-L. (2008). Neurologic manifestations of pediatric chikungunya infection. *J. Child Neurol.* 23, 1028–1035.

Rodriguez, J. (2012). Semliki Forest virus infection of mosquito cells novel insights into host responses and antiviral immunity. PhD thesis, University of Edinburgh.

Rodriguez-Andres, J., Rani, S., Varjak, M., Chase-Topping, M.E., Beck, M.H., Ferguson, M.C., Schnettler, E., Fragkoudis, R., Barry, G., Merits, A., Fazakerley, J.K., Strand, M.R.,

Kohl, A. (2012). Phenoloxidase activity acts as a mosquito innate immune response against infection with Semliki Forest virus. *PLoS Pathog.* 8, e1002977.

Rosà, R., Pugliese, A., Norman, R., and Hudson, P.J. (2003). Thresholds for disease persistence in models for tick-borne infections including non-viraemic transmission, extended feeding and tick aggregation. *J. Theor. Biol.* 224, 359–376.

Rückert, C., Bell-Sakyi, L., Fazakerley, J., and Fragkoudis, R. (accepted for publication 2014). Antiviral responses of arthropod vectors: an update on recent advances. *VirusDisease*.

Rupper, A., and Cardelli, J. (2001). Regulation of phagocytosis and endo-phagosomal trafficking pathways in *Dictyostelium discoideum*. *Biochim. Biophys. Acta* 1525, 205–216.

Růzek, D., Bell-Sakyi, L., Kopecký, J., and Grubhoffer, L. (2008). Growth of tick-borne encephalitis virus (European subtype) in cell lines from vector and non-vector ticks. *Virus Res.* 137, 142–146.

Růžek, D., Yakimenko, V.V, Karan, L.S., and Tkachev, S.E. (2010). Omsk haemorrhagic fever. *Lancet* 376, 2104–2113.

Sabin, L.R., Hanna, S.L., and Cherry, S. (2010). Innate antiviral immunity in *Drosophila*. *Curr. Opin. Immunol.* 22, 4–9.

Saleh, M.-C., Tassetto, M., van Rij, R.P., Goic, B., Gausson, V., Berry, B., Jacquier, C., Antoniewski, C., and Andino, R. (2009). Antiviral immunity in *Drosophila* requires systemic RNA interference spread. *Nature* 458, 346–350.

Sambrook, J., Fritsch, E., and Maniatis, T. (1989). Molecular Cloning: A Laboratory Manual (Cold Spring Harbor, NY: Cold Spring Harbor Laboratory Press).

Sanders, H.R., Foy, B.D., Evans, A.M., Ross, L.S., Beaty, B.J., Olson, K.E., and Gill, S.S. (2005). Sindbis virus induces transport processes and alters expression of innate immunity pathway genes in the midgut of the disease vector, *Aedes aegypti*. *Insect Biochem. Mol. Biol.* 35, 1293–1307.

Sangsuriya, P., Rojtinnakorn, J., Senapin, S., and Flegel, T.W. (2010). Identification and characterization of Alix/AIP1 interacting proteins from the black tiger shrimp, *Penaeus monodon*. *J. Fish Dis.* 33, 571–581.

Scadden, A.D.J. (2005). The RISC subunit Tudor-SN binds to hyper-edited double-stranded RNA and promotes its cleavage. *Nat. Struct. Mol. Biol.* 12, 489–496.

Schmittgen, T.D., and Livak, K.J. (2008). Analyzing real-time PCR data by the comparative C_T method. *Nat. Protoc.* 3, 1101–1108.

Schneider, H. (1931). Über epidemische Meningitis serosa. *Wien. Klin. Wochenschr.* 44, 350–352.

Schnettler, E., Sterken, M.G., Leung, J.Y., Metz, S.W., Geertsema, C., Goldbach, R.W., Vlak, J.M., Kohl, A., Khromykh, A.A., and Pijlman, G.P. (2012). Noncoding flavivirus RNA displays RNA interference suppressor activity in insect and mammalian cells. *J. Virol.* 86, 13486–13500.

Schnettler, E., Donald, C.L., Human, S., Watson, M., Siu, R.W.C., McFarlane, M., Fazakerley, J.K., Kohl, A., and Fragkoudis, R. (2013a). Knockdown of piRNA pathway proteins results in enhanced Semliki Forest virus production in mosquito cells. *J. Gen. Virol.* 94, 1680–1689.

Schnettler, E., Ratinier, M., Watson, M., Shaw, A.E., McFarlane, M., Varela, M., Elliott, R.M., Palmarini, M., and Kohl, A. (2013b). RNA interference targets arbovirus replication in *Culicoides* cells. *J. Virol.* 87, 2441–2454.

Schnettler, E., Tykalová, H., Watson, M., Sharma, M., Sterken, M.G., Obbard, D.J., Lewis, S.H., McFarlane, M., Bell-Sakyi, L., Barry, G., Weisheit, S., Best, S.M., Kuhn, R.J., Pijlman, G.P., Chase-Topping, M.E., Gould, E.A., Grubhoffer, L., Fazakerley, J.K., and Kohl A. (2014). Induction and suppression of tick cell antiviral RNAi responses by tick-borne flaviviruses. *Nucleic Acids Res.* doi: 10.1093/nar/gku657

Schrauf, S., Mandl, C.W., Bell-Sakyi, L., and Skern, T. (2009). Extension of flavivirus protein C differentially affects early RNA synthesis and growth in mammalian and arthropod host cells. *J. Virol.* 83, 11201–11210.

Schroeder, A., Mueller, O., Stocker, S., Salowsky, R., Leiber, M., Gassmann, M., Lightfoot, S., Menzel, W., Granzow, M., and Ragg, T. (2006). The RIN: an RNA integrity number for assigning integrity values to RNA measurements. *BMC Mol. Biol.* 7, 3.

Schwarz, A., von Reumont, B.M., Erhart, J., Chagas, A.C., Ribeiro, J.M.C., and Kotsyfakis, M. (2013). *De novo Ixodes ricinus* salivary gland transcriptome analysis using two next-generation sequencing methodologies. *FASEB J.* 27, 4745–4756.

Schweitzer, B.K., Chapman, N.M., and Iwen, P.C. (2009). Overview of the *Flaviviridae* with an emphasis on the Japanese Encephalitis group viruses. *Lab. Med.* 40, 493–499.

Scott, J.C., Brackney, D.E., Campbell, C.L., Bondu-Hawkins, V., Hjelle, B., Ebel, G.D., Olson, K.E., and Blair, C.D. (2010). Comparison of dengue virus type 2-specific small RNAs from RNA interference-competent and -incompetent mosquito cells. *PLoS Negl. Trop. Dis.* 4, e848.

Senigl, F., Kopecký, J., and Grubhoffer, L. (2004). Distribution of E and NS1 proteins of TBE virus in mammalian and tick cells. *Folia Microbiol. (Praha).* 49, 213–216.

Senigl, F., Grubhoffer, L., and Kopecký, J. (2006). Differences in maturation of tick-borne encephalitis virus in mammalian and tick cell line. *Intervirology* 49, 239–248.

Severo, M.S., Sakhon, O.S., Choy, A., Stephens, K.D., and Pedra, J.H.F. (2013a). The “ubiquitous” reality of vector immunology. *Cell. Microbiol.* 15, 1070-1078.

Severo, M.S., Choy, A., Stephens, K.D., Sakhon, O.S., Chen, G., Chung, D.-W.D., Le Roch, K.G., Blaha, G., and Pedra, J.H.F. (2013b). The E3 ubiquitin ligase XIAP restricts *Anaplasma phagocytophilum* colonization of *Ixodes scapularis* ticks. *J. Infect. Dis.* 208, 1830–1840.

Sforça, M.L., Machado, A., Figueredo, R.C.R., Oyama, S., Silva, F.D., Miranda, A., Daffre, S., Miranda, M.T.M., Spisni, A., and Pertinhez, T.A. (2005). The micelle-bound structure of an antimicrobial peptide derived from the alpha-chain of bovine hemoglobin isolated from the tick *Boophilus microplus*. *Biochemistry* 44, 6440–6451.

Shelly, S., Lukinova, N., Bambina, S., Berman, A., and Cherry, S. (2009). Autophagy is an essential component of *Drosophila* immunity against vesicular stomatitis virus. *Immunity* 30, 588–598.

Shevchenko, A., Tomas, H., Havlis, J., Olsen, J. V, and Mann, M. (2006). In-gel digestion for mass spectrometric characterization of proteins and proteomes. *Nat. Protoc.* 1, 2856–2860.

Shi, Y. (2003). Mammalian RNAi for the masses. *Trends Genet.* 19, 9–12.

Shin, S.W., Kokoza, V., Ahmed, A., and Raikhel, A.S. (2002). Characterization of three alternatively spliced isoforms of the Rel/NF-κB transcription factor Relish from the mosquito *Aedes aegypti*. *Proc. Natl. Acad. Sci. USA* 99, 9978–9983.

Shin, S.W., Kokoza, V., Bian, G., Cheon, H.-M., Kim, Y.J., and Raikhel, A.S. (2005). REL1, a homologue of *Drosophila* dorsal, regulates toll antifungal immune pathway in the female mosquito *Aedes aegypti*. *J. Biol. Chem.* 280, 16499–16507.

Shirako, Y., and Strauss, J.H. (1994). Regulation of Sindbis virus RNA replication: uncleaved P123 and nsP4 function in minus-strand RNA synthesis, whereas cleaved products from P123 are required for efficient plus-strand RNA synthesis. *J. Virol.* 68, 1874–1885.

Shirako, Y., Strauss, E.G., and Strauss, J.H. (2000). Suppressor mutations that allow sindbis virus RNA polymerase to function with nonaromatic amino acids at the N-terminus: evidence for interaction between nsP1 and nsP4 in minus-strand RNA synthesis. *Virology* 276, 148–160.

Silva, F.D., Rezende, C.A., Rossi, D.C.P., Esteves, E., Dyszy, F.H., Schreier, S., Gueiros-Filho, F., Campos, C.B., Pires, J.R., and Daffre, S. (2009). Structure and mode of action of microplusin, a copper II-chelating antimicrobial peptide from the cattle tick *Rhipicephalus (Boophilus) microplus*. *J. Biol. Chem.* 284, 34735–34746.

Sim, S., and Dimopoulos, G. (2010). Dengue virus inhibits immune responses in *Aedes aegypti* cells. *PLoS One* 5, e10678.

Sim, C., Hong, Y.S., Tsetsarkin, K.A., Vanlandingham, D.L., Higgs, S., and Collins, F.H. (2007). *Anopheles gambiae* heat shock protein cognate 70B impedes O’nyong-nyong virus replication. *BMC Genomics* 8, 231.

Sim, S., Ramirez, J.L., and Dimopoulos, G. (2012). Dengue virus infection of the *Aedes aegypti* salivary gland and chemosensory apparatus induces genes that modulate infection and blood-feeding behavior. *PLoS Pathog.* 8, e1002631.

Simser, J.A., Mulenga, A., Macaluso, K.R., and Azad, A.F. (2004). An immune responsive factor D-like serine proteinase homologue identified from the American dog tick, *Dermacentor variabilis*. *Insect Mol. Biol.* 13, 25–35.

Simser, J.A., Palmer, A.N.N.T., Munderloh, U.G., and Kurtti, T.J. (2001). Isolation of a spotted fever group *Rickettsia* , *Rickettsia peacockii* , in a Rocky Mountain wood tick , *Dermacentor andersoni*, cell line. *Appl. Environ. Microbiol.* 67, 546–552.

Singh, S.K., and Unni, S.K. (2011). Chikungunya virus: host pathogen interaction. *Rev. Med. Virol.* 21, 78–88.

Siomi, M.C., Sato, K., Pezic, D., and Aravin, A.A. (2011). PIWI-interacting small RNAs: the vanguard of genome defence. *Nat. Rev. Mol. Cell Biol.* 12, 246–258.

Skalsky, R.L., Vanlandingham, D.L., Scholle, F., Higgs, S., and Cullen, B.R. (2010). Identification of microRNAs expressed in two mosquito vectors, *Aedes albopictus* and *Culex quinquefasciatus*. *BMC Genomics* 11, 119.

Smith, C.E.G. (1956). A virus resembling Russian spring–summer encephalitis virus from an Ixodid tick in Malaya. *Nature* 178, 581–582.

Smithburn, K.C., Haddow, A.J., and Mahaffy, A.F. (1946). A neurotropic virus isolated from *Aedes* mosquitoes caught in the Semliki Forest. *Am. J. Trop. Med. Hyg.* 26, 189–208.

Smorodincev, A.A., and Dubov, A. V. (1986). Live vaccines against tick-borne encephalitis. In Tick-Borne Encephalitis and Its Vaccine Prophylaxis, A.A. Smorodincev, ed. (Leningrad, Russia: Meditsina), pp. 190–211.

Sonenshine, D.E., Hynes, W.L., Ceraul, S.M., Mitchell, R., and Benzine, T. (2005). Host blood proteins and peptides in the midgut of the tick *Dermacentor variabilis* contribute to bacterial control. *Exp. Appl. Acarol.* 36, 207–223.

Sonenshine, D.E., Bissinger, B.W., Egekwu, N., Donohue, K. V, Khalil, S.M., and Roe, R.M. (2011). First transcriptome of the testis-vas deferens-male accessory gland and proteome of the spermatophore from *Dermacentor variabilis* (Acari: Ixodidae). *PLoS One* 6, e24711.

Song, H., Kim, S., Ko, M.S., Kim, H.J., Heo, J.C., Lee, H.J., Lee, H.S., Han, I.S., Kwack, K., Park, J.W. (2004). Overexpression of DRG2 Increases G_2/M phase cells and decreases sensitivity to Nocodazole-induced apoptosis. *J. Biochem.* 135, 331–335.

Song, X., Hu, J., Jin, P., Chen, L., and Ma, F. (2013). Identification and evolution of an *NFAT* gene involving *Branchiostoma belcheri* innate immunity. *Genomics* 102, 355–362.

Souza-Neto, J.A., Sim, S., and Dimopoulos, G. (2009). An evolutionary conserved function of the JAK-STAT pathway in anti-dengue defense. *Proc. Natl. Acad. Sci. USA* 106, 17841–17846.

Spuul, P., Salonen, A., Merits, A., Jokitalo, E., Kääriäinen, L., and Ahola, T. (2007). Role of the amphipathic peptide of Semliki Forest virus replicase protein nsP1 in membrane association and virus replication. *J. Virol.* 81, 872–883.

Spuul, P., Balistreri, G., Hellström, K., Golubtsov, A. V, Jokitalo, E., and Ahola, T. (2011). Assembly of alphavirus replication complexes from RNA and protein components in a novel *trans*-replication system in mammalian cells. *J. Virol.* 85, 4739–4751.

Sritunyalucksana, K., Wongsuebsantati, K., Johansson, M.W., and Söderhäll, K. (2001). Peroxinectin, a cell adhesive protein associated with the proPO system from the black tiger shrimp, *Penaeus monodon*. *Dev. Comp. Immunol.* 25, 353–363.

Srivastava, P. (2002). Roles of heat-shock proteins in innate and adaptive immunity. *Nat. Rev. Immunol.* 2, 185–194.

Stadler, K., Allison, S.L., Schalich, J., and Heinz, F.X. (1997). Proteolytic activation of tick-borne encephalitis virus by furin. *J. Virol.* 71, 8475–8481.

Stafforini, D.M., McIntyre, T.M., Zimmerman, G.A., Prescott, S.M. (1997). Platelet-activating factor acetylhydrolases. *J. Biol. Chem.* 272, 17895–17898.

Stapleton, J.T., Foung, S., Muerhoff, A.S., Bukh, J., and Simmonds, P. (2011). The GB viruses: a review and proposed classification of GBV-A, GBV-C (HGV), and GBV-D in genus *Pegivirus* within the family *Flaviviridae*. *J. Gen. Virol.* 92, 233–246.

Steele, G.M., and Nuttall, P.A. (1989). Difference in vector competence of two species of sympatric ticks, *Amblyomma variegatum* and *Rhipicephalus appendiculatus*, for Dugbe virus (*Nairovirus*, *Bunyaviridae*). *Virus Res.* 14, 74–84.

Stiasny, K., and Heinz, F.X. (2006). *Flavivirus* membrane fusion. *J. Gen. Virol.* 87, 2755–2766.

Stopforth, E., Neitz, A.W.H., and Gaspar, A.R.M. (2010). A proteomics approach for the analysis of hemolymph proteins involved in the immediate defense response of the soft tick, *Ornithodoros savignyi*, when challenged with *Candida albicans*. *Exp. Appl. Acarol.* 51, 309–325.

Strauss, J.H., and Strauss, E.G. (1994). The alphaviruses: gene expression, replication, and evolution. *Microbiol. Rev.* 58, 491–562.

Strauss, E.G., Rice, C.M., and Strauss, J.H. (1983). Sequence coding for the alphavirus nonstructural proteins is interrupted by an opal termination codon. *Proc. Natl. Acad. Sci. USA* 80, 5271–5275.

Strauss, J.H., Wang, K.S., Schmaljohn, A.L., Kuhn, R.J., and Strauss, E.G. (1994). Host cell receptors for Sindbis virus. *Arch. Virol.* 9, 473–484.

Stroschein-Stevenson, S.L., Foley, E., O'Farrell, P.H., and Johnson, A.D. (2005). Identification of *Drosophila* gene products required for phagocytosis of *Candida albicans*. *PLoS Biol.* 4, 87–99.

Strous, G.J., and Govers, R. (1999). The ubiquitin-proteasome system and endocytosis. *J. Cell Sci.* 112 (Pt 1, 1417–1423.

Stump, W.T., and Hall, K.B. (1993). SP6 RNA polymerase efficiently synthesizes RNA from short double-stranded DNA templates. *Nucleic Acids Res.* 21, 5480–5484.

Su, H.-L., Liao, C.-L., and Lin, Y.-L. (2002). Japanese encephalitis virus infection initiates endoplasmic reticulum stress and an unfolded protein response. *J. Virol.* 76.

Subauste, M.C., Pertz, O., Adamson, E.D., Turner, C.E., Junger, S., and Hahn, K.M. (2004). Vinculin modulation of paxillin-FAK interactions regulates ERK to control survival and motility. *J. Cell Biol.* 165, 371–381.

Sun, C., Shao, H.-L., Zhang, X.-W., Zhao, X.-F., and Wang, J.-X. (2011). Molecular cloning and expression analysis of signal transducer and activator of transcription (STAT) from the Chinese white shrimp *Fenneropenaeus chinensis*. *Mol. Biol. Rep.* 38, 5313–5319.

Suomalainen, M., Liljeström, P., and Garoff, H. (1992). Spike protein-nucleocapsid interactions drive the budding of alphaviruses. *J. Virol.* 66, 4737–4747.

Suopanki, J., Sawicki, D.L., Sawicki, S.G., and Kääriäinen, L. (1998). Regulation of alphavirus 26S mRNA transcription by replicase component nsP2. *J. Gen. Virol.* 79 (Pt 2), 309–319.

Süss, J. (2008). Tick-borne encephalitis in Europe and beyond – The epidemiological situation as of 2007. *Eurosurveillance* 13, 1–8.

Süss, J. (2003). Epidemiology and ecology of TBE relevant to the production of effective vaccines. *Vaccine* 21, S19–S35.

Takkinen, K. (1986). Complete nucleotide sequence of the nonstructural protein genes of Semliki Forest virus. *Nucleic Acids Res.* 14, 5667–5682.

Takkinen, K., Peränen, J., Keränen, S., Söderlund, H., and Kääriäinen, L. (1990). The Semliki-Forest-virus-specific nonstructural protein nsP4 is an autoproteinase. *Eur. J. Biochem.* 189, 33–38.

Tamang, D., Tseng, S.M., Huang, C.Y., Tsao, I.Y., Chou, S.Z., Higgs, S., Christensen, B.M., and Chen, C.C. (2004). The use of a double subgenomic Sindbis virus expression system to study mosquito gene function: effects of antisense nucleotide number and duration of viral infection on gene silencing efficiency. *Insect Mol. Biol.* 13, 595–602.

Tamberg, N., Lulla, V., Fragkoudis, R., Lulla, A., Fazakerley, J.K., and Merits, A. (2007). Insertion of EGFP into the replicase gene of *Semliki Forest virus* results in a novel, genetically stable marker virus. *J. Gen. Virol.* 88, 1225–1230.

Tan, B.H., Fu, J., Sugrue, R.J., Yap, E.H., Chan, Y.C., and Tan, Y.H. (1996). Recombinant dengue type 1 virus NS5 protein expressed in *Escherichia coli* exhibits RNA-dependent RNA polymerase activity. *Virology* 216, 317–325.

Taylor, D. (2006). Innate immunity in ticks : A review. *Acarol. Soc Japan* 15, 109–127.

Terenius, O., Papanicolaou, A., Garbutt, J.S., Eleftherianos, I., Huvenne, H., Kanginakudru, S., Albrechtsen, M., An, C., Aymeric, J.-L., Barthel, A., Bebas, P., Bitra, K., Bravo, A., Chevalier, F., Collinge, D.P., Crava, C.M., de Maagd, R.A., Duvic, B., Erlandson, M., Faye, I., Felföldi, G., Fujiwara, H., Futahashi, R., Gandhe, A.S., Gatehouse, H.S., Gatehouse, L.N., Giebultowicz, J.M., Gómez, I., Grimmelikhuijzen, C.J.P., Groot, A.T., Hauser, F., Heckel, D.G., Hegedus, D.D., Hrycaj, S., Huang, L., Hull, J.J., Iatrou, K., Iga, M., Kanost, M.R., Kotwica, J., Li, C., Li, J., Liu, J., Lundmark, M., Matsumoto, S., Meyering-Vos, M., Millichap, P.J., Monteiro, A., Mrinal, N., Niimi, T., Nowara, D., Ohnishi, A., Oostra, V., Ozaki, K., Papakonstantinou, M., Popadic, A., Rajam, M.V., Saenko, S., Simpson, R.M., Soberón, M., Strand, M.R., Tomita, S., Toprak, U., Wang, P., Wee, C.W., Whyard, S., Zhang, W., Nagaraju, J., Ffrench-Constant, R.H., Herrero, S., Gordon, K., Swevers, L., and Smagghe, G. (2011). RNA interference in Lepidoptera: an overview of successful and unsuccessful studies and implications for experimental design. *J. Insect Physiol.* 57, 231–245.

Thirugnanasambantham, K., Hairul-Islam, V.I., Saravanan, S., Subasri, S., and Subastri, A. (2013). Computational approach for identification of *Anopheles gambiae* miRNA involved in modulation of host immune response. *Appl. Biochem. Biotechnol.* 170, 281–291.

Thörnqvist, P., Johansson, M.W., and Söderhäll, K. (1994). Opsonic activity of cell adhesion proteins and β-1,3-glucan binding proteins from two crustaceans. *Dev. Comp. Immunol.* 18, 3–12.

Thurner, C., Witwer, C., Hofacker, I.L., and Stadler, P.F. (2004). Conserved RNA secondary structures in *Flaviviridae* genomes. *J. Gen. Virol.* 85, 1113–1124.

Tonteri, E., Jääskeläinen, A.E., Tikkakoski, T., Voutilainen, L., Niemimaa, J., Henttonen, H., Vaheri, A., and Vapalahti, O. (2011). Tick-borne encephalitis virus in wild rodents in winter, Finland, 2008–2009. *Emerg. Infect. Dis.* 1.

Trapnell, C., Hendrickson, D.G., Sauvageau, M., Goff, L., Rinn, J.L., and Pachter, L. (2013). Differential analysis of gene regulation at transcript resolution with RNA-seq. *Nat. Biotechnol.* 31, 46–53.

Trombetta, E.S. (2003). The contribution of N-glycans and their processing in the endoplasmic reticulum to glycoprotein biosynthesis. *Glycobiology* 13, 77R–91R.

Tsai, C.W., McGraw, E.A., Ammar, E.-D., Dietzgen, R.G., and Hogenhout, S.A. (2008). *Drosophila melanogaster* mounts a unique immune response to the Rhabdovirus sigma virus. *Appl. Environ. Microbiol.* 74, 3251–3256.

Tsuji, N., Miyoshi, T., Battsetseg, B., Matsuo, T., Xuan, X., and Fujisaki, K. (2008). A cysteine protease is critical for *Babesia* spp. transmission in *Haemaphysalis* ticks. *PLoS Pathog.* 4, e1000062.

Tucker, T., Marra, M., and Friedman, J.M. (2009). Massively parallel sequencing: the next big thing in genetic medicine. *Am. J. Hum. Genet.* 85, 142–154.

Uchil, P.D., Kumar, A.V.A., and Satchidanandam, V. (2006). Nuclear localization of *flavivirus* RNA synthesis in infected cells. *J. Virol.* 80, 5451–5464.

Vagin, V. V, Sigova, A., Li, C., Seitz, H., Gvozdev, V., and Zamore, P.D. (2006). A distinct small RNA pathway silences selfish genetic elements in the germline. *Science* 313, 320–324.

Valiente-Echeverría, F., Melnychuk, L., and Mouland, A.J. (2012). Viral modulation of stress granules. *Virus Res.* 169, 430–437.

Van den Hurk, A.F., Ritchie, S.A., and Mackenzie, J.S. (2009). Ecology and geographical expansion of Japanese encephalitis virus. *Ann. Rev. Entomol.* 54, 17–35.

Varich, N.L., Petrík, Y., Farashyan, V.R., and Kaverin, N.V. (1981). Virus-specific and cell-specific RNA transcripts in influenza virus-infected cells: The rate of synthesis and the content in the nuclei. *Arch. Virol.* 284, 279–284.

Varma, M.G. (1989). Progress in the study of human and animal pathogens in primary and established tick cell lines. In Invertebrate Cell System Applications, J. Mitsuhashi, ed. (Boca Raton, Florida: CRC Press), pp. 119–128.

Varma, M.G., Pudney, M., and Leake, C.J. (1975). The establishment of three cell lines from the tick *Rhipicephalus appendiculatus* (Acari: Ixodidae) and their infection with some arboviruses. *J. Med. Entomol.* 11, 698–706.

Vasiljeva, L., Merits, A., Auvinen, P., and Kääriäinen, L. (2000). Identification of a novel function of the *alphavirus* capping apparatus. RNA 5'-triphosphatase activity of Nsp2. *J. Biol. Chem.* 275, 17281–17287.

Vazeille, M., Moutailler, S., Coudrier, D., Rousseaux, C., Khun, H., Huerre, M., Thiria, J., Dehecq, J.-S., Fontenille, D., Schuffenecker, I., Despres, P., Failloux, A.-B. (2007). Two Chikungunya isolates from the outbreak of La Reunion (Indian Ocean) exhibit different patterns of infection in the mosquito, *Aedes albopictus*. *PLoS One* 2, e1168.

Vereta, L.A., Skorobrekha, V.Z., Nikolaeva, S.P., Aleksandrov, V.I., Tolstonogova, V.I., Zakharycheva, T.A., Red'ko, A.P., Lev, M.I., and Savel'eva, N.A. (1991). The transmission of the tick-borne encephalitis virus via cow's milk. *Med. Parazitol. (Mosk).* 3, 54–56.

Vijayendran, D., Airs, P.M., Dolezal, K., and Bonning, B.C. (2013). Arthropod viruses and small RNAs. *J. Invertebr. Pathol.* 114, 186-195

Villar, M., Ayllón, N., Busby, A.T., Galindo, R.C., Blouin, E.F., Kocan, K.M., Bonzón-Kulichenko, E., Zivkovic, Z., Almazán, C., Torina, A., Vázquez, J., and de la Fuente, J. (2010a). Expression of heat shock and other stress response proteins in ticks and cultured tick cells in response to *Anaplasma* spp. infection and heat shock. *Int. J. Proteomics* 2010, 1–11.

Villar, M., Torina, A., Nuñez, Y., Zivkovic, Z., Marina, A., Alongi, A., Scimeca, S., La Barbera, G., Caracappa, S., Vázquez, J., and Fuente, J. (2010b). Application of highly sensitive saturation labeling to the analysis of differential protein expression in infected ticks from limited samples. *Proteome Sci.* 8, 43.

Villar, M., Popara, M., Bonzón-Kulichenko, E., Ayllón, N., Vázquez, J., and de la Fuente, J. (2012). Characterization of the tick-pathogen interface by quantitative proteomics. *Ticks Tick-borne. Dis.* 3, 154–158.

Villar, M., Popara, M., Mangold, A.J., and de la Fuente, J. (2013). Comparative proteomics for the characterization of the most relevant *Amblyomma* tick species as vectors of zoonotic pathogens worldwide. *J. Proteomics*.

Villar, M., Popara, M., Ayllón, N., Fernández de Mera, I.G., Mateos-Hernández, L., Galindo, R.C., Manrique, M., Tobes, R., and de la Fuente, J. (2014). A systems biology approach to the characterization of stress response in *Dermacentor reticulatus* tick unfed larvae. *PLoS One* 9, e89564.

Virtanen, I., and Wartiovaara, J. (1974). Semliki Forest virus-induced cytoplasmic membrane structures associated with Semliki Forest virus infection studied by the freeze-etching method. *J. Virol.* 13, 222–225.

Vlachou, D., Schlegelmilch, T., Christophides, G.K., and Kafatos, F.C. (2005). Functional genomic analysis of midgut epithelial responses in *Anopheles* during *Plasmodium* invasion. *Curr. Biol.* 15, 1185–1195.

Vodovar, N., Bronkhorst, A.W., van Cleef, K.W.R., Miesen, P., Blanc, H., van Rij, R.P., and Saleh, M.-C. (2012). Arbovirus-derived piRNAs exhibit a ping-pong signature in mosquito cells. *PLoS One* 7, e30861.

Voinnet, O. (2005). Non-cell autonomous RNA silencing. *FEBS Lett.* 579, 5858–5871.

Volkova, E., Frolova, E., Darwin, J.R., Forrester, N.L., Weaver, S.C., and Frolov, I. (2008). IRES-dependent replication of Venezuelan equine encephalitis virus makes it highly attenuated and incapable of replicating in mosquito cells. *Virology* 377, 160–169.

Wahlberg, J.M., Bron, R., Wilschut, J., and Garoff, H. (1992). Membrane fusion of Semliki Forest virus involves homotrimers of the fusion protein. *J. Virol.* 66, 7309–7318.

Waldock, J., Olson, K.E., and Christophides, G.K. (2012). *Anopheles gambiae* antiviral immune response to systemic O'nyong-nyong infection. *PLoS Negl. Trop. Dis.* 6, e1565.

Walker, A., Bouattour, J.-L., Camicas, A., Estrada-Peña, A., Horak, I.G., Latif, A.A., Pegram, R.G., and Preston, P.M. (2003). Ticks of domestic animals in Africa: A guide to identification of species (Edinburgh: Bioscience Reports).

Wallner, G., Mandl, C.W., Kunz, C., and Heinz, F.X. (1995). The flavivirus 3′-noncoding region: extensive size heterogeneity independent of evolutionary relationships among strains of tick-borne encephalitis virus. *Virology*.

Wan, L., Molloy, S.S., Thomas, L., Liu, G., Xiang, Y., Rybak, S.L., and Thomas, G. (1998). PACS-1 defines a novel gene family of cytosolic sorting proteins required for *trans*-Golgi network localization. *Cell* 94, 205–216.

Wang, W., and Shakes, D.C. (1996). Molecular evolution of the 14-3-3 protein family. *J. Mol. Evol.* 43, 384–398.

Wang, W., and Zhang, X. (2008). Comparison of antiviral efficiency of immune responses in shrimp. *Fish Shellfish Immunol.* 25, 522–527.

Wang, X.-W., and Wang, J.-X. (2013). Pattern recognition receptors acting in innate immune system of shrimp against pathogen infections. *Fish Shellfish Immunol.* 34, 981–989.

Wang, Y., and Zhu, S. (2011). The defensin gene family expansion in the tick *Ixodes scapularis*. *Dev. Comp. Immunol.* 35, 1128–1134.

Wang, K.S., Kuhn, R.J., Strauss, E.G., Ou, S., and Strauss, J.H. (1992). High-affinity laminin receptor is a receptor for Sindbis virus in mammalian cells. *J. Virol.* 66, 4992–5001.

Wang, P.-H., Gu, Z.-H., Huang, X.-D., Liu, B.-D., Deng, X., Ai, H.-S., Wang, J., Yin, Z.-X., Weng, S.-P., Yu, X.-Q., and He, J.-G. (2009). An immune deficiency homolog from the white shrimp, *Litopenaeus vannamei*, activates antimicrobial peptide genes. *Mol. Immunol.* 46, 1897–1904.

Wang, P.-H., Liang, J.-P., Gu, Z.-H., Wan, D.-H., Weng, S.-P., Yu, X.-Q., and He, J.-G. (2012). Molecular cloning, characterization and expression analysis of two novel Tolls (LvToll2 and LvToll3) and three putative Spätzle-like Toll ligands (LvSpz1-3) from *Litopenaeus vannamei*. *Dev. Comp. Immunol.* 36, 359–371.

Wang, W.-A., Groenendyk, J., and Michalak, M. (2012). Calreticulin signaling in health and disease. *Int. J. Biochem. Cell Biol.* 44, 842–846.

Wang, X., Aliyari, R., Li, W.-X., Li, H.-W., Kim, K., Carthew, R., Atkinson, P., and Ding, S. (2006). RNA interference directs innate immunity against viruses in adult *Drosophila*. *Science (80-.).* 312, 452–454.

Wang, Y.F., Sawicki, S.G., and Sawicki, D.L. (1994). Alphavirus nsP3 functions to form replication complexes transcribing negative-strand RNA. *J. Virol.* 68, 6466–6475.

Wang, Y.F., Sawicki, S.G., and Sawicki, D.L. (1991). Sindbis virus nsP1 functions in negative-strand RNA synthesis. *J. Virol.* 65, 985–988.

Warrener, P., Tamura, J.K., and Collett, M.S. (1993). RNA-stimulated NTPase activity associated with yellow fever virus NS3 protein expressed in bacteria. *J. Virol.* 67, 989–996.

Washburn, M.P., Wolters, D., and Yates, J.R. (2001). Large-scale analysis of the yeast proteome by multidimensional protein identification technology. *Nat. Biotechnol.* 19, 242–247.

Waterhouse, R.M., Kriventseva, E. V., Meister, S., Xi, Z., Alvarez, K.S., Bartholomay, L.C., Barillas-Mury, C., Bian, G., Blandin, S., Christensen, B.M., Dong, Y., Jiang, H., Kanost, M.R., Koutsos, A.C., Levashina, E.A., Li, J., Ligoxygakis, P., MacCallum, R.M., Mayhew, G.F., Mendes, A., Michel, K., Osta, M.A., Paskewitz, S., Shin, S.W., Vlachou, D., Wang, L., Wei, W., Zheng, L., Zou, Z., Severson, D.W., Raikhel, A.S., Kafatos, F.C., Dimopoulos, G., Zdobnov, E.M., and Christophides, G.K. (2007). Evolutionary dynamics of immune-related genes and pathways in disease-vector mosquitoes. *Science* 316, 1738–1743.

Watson, F.L., Püttmann-Holgado, R., Thomas, F., Lamar, D.L., Hughes, M., Kondo, M., Rebel, V.I., and Schmucker, D. (2005). Extensive diversity of Ig-superfamily proteins in the immune system of insects. *Science* 309, 1874–1878.

Weaver, S.C. (1997). Vector biology in viral pathogenesis. In Viral Pathogenesis, N. Nathanson, ed. (New York, NY: Lippincott-Raven), pp. 329–352.

Weaver, S.C., and Barrett, A.D.T. (2004). Transmission cycles, host range, evolution and emergence of arboviral disease. *Nat. Rev. Microbiol.* 2, 789–801.

Weaver, S.C., and Reisen, W.K. (2010). Present and future arboviral threats. *Antiviral Res.* 85, 328–345.

Weaver, S.C., Powers, A.M., Brault, A.C., and Barrett, A.D.T. (1999). Molecular epidemiological studies of veterinary arboviral encephalitides. *Vet. J.* 157, 123–138.

Weaver, S.C., Salas, R., Rico-Hesse, R., Ludwig, G. V, Oberste, M.S., Boshell, J., and Tesh, R.B. (1996). Re-emergence of epidemic Venezuelan equine encephalomyelitis in South America. *Lancet* 348, 436–440.

Webb, H.E., Wetherley-Mein, G., Gordon Smith, C.E., and McMahon, D. (1966). Leukaemia and neoplastic processes treated with Langat and Kyasanur Forest disease viruses: a clinical and laboratory study of 28 patients. *Brit. Med. J.* 1, 258–266.

Weber, A.N.R., Tauszig-Delamasure, S., Hoffmann, J.A., Lelièvre, E., Gascan, H., Ray, K.P., Morse, M.A., Imler, J.-L., and Gay, N.J. (2003). Binding of the *Drosophila* cytokine Spätzle to Toll is direct and establishes signaling. *Nat. Immunol.* 4, 794–800.

Wei, H., and Zhou, M.-M. (2010). Viral-encoded enzymes that target host chromatin functions. *Biochim. Biophys. Acta* 1799, 296–301.

Weiss, B., Nitschko, H., Ghattas, I., Wright, R., and Schlesinger, S. (1989). Evidence for specificity in the encapsidation of Sindbis virus RNAs. *J. Virol.* 63, 5310–5318.

Weissenböck, H., Hubálek, Z., Bakonyi, T., and Nowotny, N. (2010). Zoonotic mosquito-borne flaviviruses: worldwide presence of agents with proven pathogenicity and potential candidates of future emerging diseases. *Vet. Microbiol.* 140, 271–280.

Welsch, S., Miller, S., Romero-Brey, I., Merz, A., Bleck, C.K.E., Walther, P., Fuller, S.D., Antony, C., Krijnse-Locker, J., and Bartenschlager, R. (2009). Composition and three-dimensional architecture of the dengue virus replication and assembly sites. *Cell Host Microbe* 5, 365–375.

Wengler, G., and Wengler, G. (1991). The carboxy-terminal part of the NS 3 protein of the West Nile flavivirus can be isolated as a soluble protein after proteolytic cleavage and represents an RNA-stimulated NTPase. *Virology* 184, 707–715.

Wengler, G., and Wengler, G. (1993). The NS 3 nonstructural protein of flaviviruses contains an RNA triphosphatase activity. *Virology* 197, 265–273.

Wengler, G., Wengler, G., and Gross, H.J. (1978). Studies on virus-specific nucleic acids synthesized in vertebrate and mosquito cells infected with flaviviruses. *Virology* 89, 423–437.

Werme, K., Wigerius, M., and Johansson, M. (2008). Tick-borne encephalitis virus NS5 associates with membrane protein scribble and impairs interferon-stimulated JAK-STAT signalling. *Cell. Microbiol.* 10, 696–712.

Willems, W.R., Kaluza, G., Boschek, C.B., Bauer, H., Hager, H., Schütz, H.-J., and Feistner, H. (1979). Semliki Forest virus: cause of a fatal case of human encephalitis. *Science* 203, 1127–1129.

Winnebeck, E.C., Millar, C.D., and Warman, G.R. (2010). Why does insect RNA look degraded? *J. Insect Sci.* 10, 159.

Woolaway, K.E., Lazaridis, K., Belsham, G.J., Carter, M.J., and Roberts, L.O. (2001). 5′ untranslated region of *Rhopalosiphum padi* virus contains an internal ribosome entry site which functions efficiently in mammalian, plant, and insect translation. *J. Virol.* 75, 10244–10249.

Worby, C.A., and Dixon, J.E. (2002). Sorting out the cellular functions of sorting nexins. *Nat. Rev. Mol. Cell Biol.* 3, 919–931.

Wu, H., Peisley, A., Graef, I.A., and Crabtree, G.R. (2007). NFAT signaling and the invention of vertebrates. *Trends Cell Biol.* 17, 251–260.

Wu, Q., Luo, Y., Lu, R., Lau, N., Lai, E.C., Li, W.-X., and Ding, S.-W. (2010). Virus discovery by deep sequencing and assembly of virus-derived small silencing RNAs. *Proc. Natl. Acad. Sci. USA* 107, 1606–1611.

Wu, Y., Teng, C., Chen, Y., Chen, S., Chen, Y., Lin, Y., and Wu, T. (2008). Internal ribosome entry site of *Rhopalosiphum padi* virus is functional in mammalian cells and has cryptic promoter activity in baculovirus-infected Sf21 cells. *Acta Pharmacol. Sin.* 29, 965–974.

Xi, Z., Ramirez, J.L., and Dimopoulos, G. (2008). The *Aedes aegypti* toll pathway controls dengue virus infection. *PLoS Pathog.* 4, e1000098.

Yang, G., Yang, L., Zhao, Z., Wang, J., and Zhang, X. (2012). Signature miRNAs involved in the innate immunity of invertebrates. *PLoS One* 7, e39015.

Yang, W., Chendrimada, T.P., Wang, Q., Higuchi, M., Seeburg, P.H., Shiekhattar, R., and Nishikura, K. (2006). Modulation of microRNA processing and expression through RNA editing by ADAR deaminases. *Nat. Struct. Mol. Biol.* 13, 13–21.

Ye, T., Tang, W., and Zhang, X. (2012). Involvement of Rab6 in the regulation of phagocytosis against virus infection in invertebrates. *J. Proteome Res.* 11, 4834–4846.

Yoshii, K., Yanagihara, N., Ishizuka, M., Sakai, M., and Kariwa, H. (2013). N-linked glycan in tick-borne encephalitis virus envelope protein affects viral secretion in mammalian cells, but not in tick cells. *J. Gen. Virol.* 94, 2249–2258.

Yu, D., Sheng, Z., Xu, X., Li, J., Yang, H., Liu, Z., Rees, H.H., and Lai, R. (2006). A novel antimicrobial peptide from salivary glands of the hard tick, *Ixodes sinensis*. *Peptides* 27, 31–35.

Yu, I.-M., Zhang, W., Holdaway, H.A., Li, L., Kostyuchenko, V.A., Chipman, P.R., Kuhn, R.J., Rossmann, M.G., and Chen, J. (2008). Structure of the immature dengue virus at low pH primes proteolytic maturation. *Science* 319, 1834–1837.

Yu, S.-W., Wang, H., Poitras, M.F., Coombs, C., Bowers, W.J., Federoff, H.J., Poirier, G.G., Dawson, T.M., and Dawson, V.L. (2002). Mediation of poly(ADP-ribose) polymerase-1-dependent cell death by apoptosis-inducing factor. *Science* 297, 259–263.

Yunker, C.E. (1987). Preparation and maintenance of arthropod cell cultures: Acari, with emphasis on ticks. In Arboviruses in Arthropod Cells in Vitro, C.E. Yunker, ed. (Boca Raton: CRC Press), pp. 35–51.

Yunker, C.E., Cory, J., and Meibos, H. (1981). Continous cell lines from embryonic tissues of ticks (Acari: Ixodidae). *In Vitro* 17, 139–142.

Zacks, M.A., and Paessler, S. (2010). Encephalitic alphaviruses. *Vet. Microbiol.* 140, 281–286.

Zambon, R.A., Vakharia, V.N., and Wu, L.P. (2006). RNAi is an antiviral immune response against a dsRNA virus in *Drosophila melanogaster*. *Cell. Microbiol.* 8, 880–889.

Zanoni, I., and Granucci, F. (2012). Regulation and dysregulation of innate immunity by NFAT signaling downstream of pattern recognition receptors (PRRs). *Eur. J. Immunol.* 42, 1924–1931.

Zeng, D., Chen, X., Xie, D., Zhao, Y., Yang, C., Li, Y., Ma, N., Peng, M., Yang, Q., Liao, Z., Wang, H., and Chen, X. (2013). Transcriptome analysis of Pacific white shrimp (*Litopenaeus vannamei*) hepatopancreas in response to Taura syndrome Virus (TSV) experimental infection. *PLoS One* 8, e57515.

Zhang, M., Zheng, X., Wu, Y., Gan, M., He, A., Li, Z., Zhang, D., Wu, X., and Zhan, X. (2013). Differential proteomics of *Aedes albopictus* salivary gland, midgut and C6/36 cell induced by dengue virus infection. *Virology* 444, 109–118.

Zhao, L., and Jones, W. (2012). Expression of heat shock protein genes in insect stress responses. *Invertebr. Surviv. J.* 93–101.

Zhioua, E., Yeh, M.T., and LeBrun, A. (1997). Assay for phenoloxidase activity in *Amblyomma americanum* , *Dermacentor variabilis* , and *Ixodes scapularis*. *J. Parasitol.* 83, 553–554.

Zhou, J., Ueda, M., Umemiya, R., Battsetseg, B., Boldbaatar, D., Xuan, X., and Fujisaki, K. (2006). A secreted cystatin from the tick *Haemaphysalis longicornis* and its distinct expression patterns in relation to innate immunity. *Insect Biochem. Mol. Biol.* 36, 527–535.

Zhu, J.-Y., Yang, P., Zhang, Z., Wu, G.-X., and Yang, B. (2013). Transcriptomic immune response of *Tenebrio molitor* pupae to parasitization by *Scleroderma guani*. *PLoS One* 8, e54411.

Zhu, W., Smith, J.W., and Huang, C.-M. (2010). Mass spectrometry-based label-free quantitative proteomics. *J. Biomed. Biotechnol.* 2010, 1–6.

Zilber, L.A. (1939). Spring-summer tick-borne encephalitis (in Russian). *Arkhiv Biol. Nauk* 56, 255–261.

Zivkovic, Z., Torina, A., Mitra, R., Alongi, A., Scimeca, S., Kocan, K.M., Galindo, R.C., Almazán, C., Blouin, E.F., Villar, M., Nijhof, A.M., Mani, R., La Barbera, G., Caracappa, S., Jongejan, F., and de la Fuente, J. (2010a). Subolesin expression in response to pathogen infection in ticks. *BMC Immunol.* 11, 7.

Zivkovic, Z., Esteves, E., Almazán, C., Daffre, S., Nijhof, A.M., Kocan, K.M., Jongejan, F., and de la Fuente, J. (2010b). Differential expression of genes in salivary glands of male *Rhipicephalus (Boophilus) microplus* in response to infection with *Anaplasma marginale*. *BMC Genomics* 11, 186.

Appendix

6.1 Preparation of L-15B medium

The preparation of L-15B medium was done according to the recipe of Munderloh and Kurtti (1989). In brief, trace mineral stock solutions A, B and C are prepared and 1ml of each is used to make up stock solution D (Table A.6.1). The vitamin stock solution (Table A.6.2) is mixed and dissolved, as for all stock solutions, in deionised water, in the order listed, to a final volume of 100 ml.

Table A.6.1 Ingredients and recipe for trace Mineral Stock solution D

Ingredient	Weight (mg/100ml)
Stock solution A	
$CoCl \times 6H_2O$	20
$CuSO_4 \times 5H_2O$	20
$MnSO_4 \times H_2O$	160
$ZnSO_4 \times 7H_2O$	200
Stock solution B	
$NaMoO_4 \times 2H_2O$	20
Stock solution C	
Na_2SeO_3	20
Stock solution D	
Glutathione (reduced)	1000
Asorbic acid	1000
$FeSO_4 \times 7H_2O$	50
Stock solution A	1ml
Stock solution B	1ml
Stock solution C	1ml

Table A.6.2 Ingredients and recipe for Vitamin Stock

Ingredient	Weight (mg/100ml)
p-aminobenzoic acid	100
Cyanocobalamine (B_{12})	50
d- Biotin	10

Aliquots of mineral stock solutions A, B, C and D and vitamin stock solution were frozen at -20˚C. All ingredients can be obtained from Sigma.

To make up L-15B medium, L-15 (Leibovitz) powder (Invitrogen) for 1 litre is dissolved in 900 ml deionised water and supplemented with ingredients, as listed in Table A.6.3. After addition of these ingredients deionised water is added to reach a

final volume of 1l. Medium is sterilised by filtration (0.22 µm) and can be stored at 4˚C up to 4 months or at -20˚C.

Table A.6.3 Ingredients and recipe for L-15B medium

Ingredient	
Aspartic acid	299 mg
Glutamic acid	500 mg
Proline	300 mg
α-ketoglutaric acid	299 mg
D-glucose	2239 mg
Mineral stock D	1ml
Vitamin stock	1ml

Before the addition of supplements, such as TPB and FCS, the pH of the L15B-medium was adjusted with sterile 1N NaOH to approximately pH 6.8.